NASA CR-72984
16402-6012-RO-00

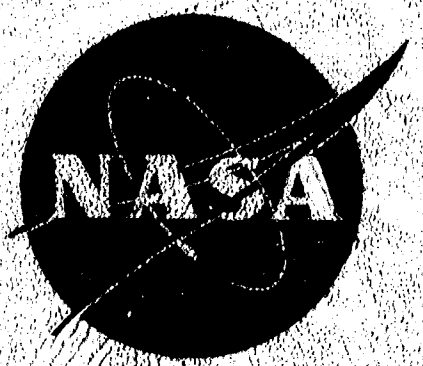

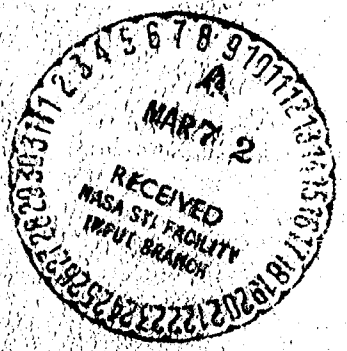


# THERMALLY STABLE LAMINATING RESINS

by

R. J. Jones, R. W. Vaughan and E. A. Burns

TRW
SYSTEMS GROUP



prepared for

NATIONAL AERONAUTICS AND SPACE ADMINISTRATION



NASA Lewis Research Center
Contract NAS3-13489

Tito T. Serafini, Project Manager

Requests for copies of this report should be referred to

National Aeronautics and Space Administration
Scientific and Technical Information Facility
P. O. Box 33
College Park, Md. 20740

| 1. Report No. | 2. Government Accession No. | 3. Recipient's Catalog No. |
|---|---|---|
| NASA CR-72984 | | |

| 4. Title and Subtitle | 5. Report Date |
|---|---|
| Thermally Stable Laminating Resins | February 7, 1972 |
| | 6. Performing Organization Code |

| 7. Author(s) | 8. Performing Organization Report No. |
|---|---|
| R. J. Jones, R. W. Vaughan and E. A. Burns | 16402-6012-R0-00 |
| | 10. Work Unit No. |

| 9. Performing Organization Name and Address | 11. Contract or Grant No. |
|---|---|
| TRW Systems Group<br>Redondo Beach, California 90278 | NAS3-13489 |
| | 13. Type of Report and Period Covered |
| 12. Sponsoring Agency Name and Address | Contractor Report |
| National Aeronautics and Space Administration<br>Washington, D. C. 20546 | 14. Sponsoring Agency Code |

15. Supplementary Notes

Project Manager, Tito T. Serafini, Materials and Structures Division,
NASA Lewis Research Center, Cleveland, Ohio

16. Abstract

Improved thermally stable laminating resins have been developed based on the addition-type pyrolytic polymerization. Detailed monomer and polymer synthesis and characterization studies have identified formulations which facilitate press molding processing and autoclave fabrication of glass and graphite fiber reinforced composites. A specific resin formulation, termed PIOP was utilized to prepare a Courtaulds HMS reinforced simulated air foil demonstration part by an autoclave molding process.

| 17. Key Words (Suggested by Author(s)) | 18. Distribution Statement |
|---|---|
| Laminating Resins<br>Autoclave Processing<br>Addition Cured Polyimides | Unclassified - unlimited |

| 19. Security Classif. (of this report) | 20. Security Classif. (of this page) | 21. No. of Pages | 22. Price* |
|---|---|---|---|
| Unclassified | Unclassified | 196 | $3.00 |

* For sale by the National Technical Information Service, Springfield, Virginia 22151

NASA CR-72984
16402-6012-RO-00

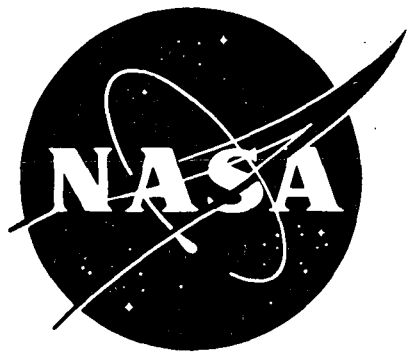

# THERMALLY STABLE LAMINATING RESINS

by

R. J. Jones, R. W. Vaughan and E. A. Burns

TRW
SYSTEMS GROUP

ONE SPACE PARK • REDONDO BEACH • CALIFORNIA

prepared for

NATIONAL AERONAUTICS AND SPACE ADMINISTRATION

NASA Lewis Research Center
Contract NAS3-13489

Tito T. Serafini, Project Manager

## FOREWORD

This document constitutes the final report for the work accomplished between 13 April 1970 and 13 June 1971 by TRW Systems for the National Aeronautics and Space Administration, Lewis Research Center, under Contract NAS3-13489 on Thermally Stable Laminating Resins.

This work was conducted under the technical direction of Dr. Tito T. Serafini of the Lewis Research Center, Cleveland, Ohio.

The Applied Chemistry Department of the Chemistry and Chemical Engineering Laboratory, Applied Technology Division was responsible for the work performed on this program. Mr. B. Dubrow, Manager, Chemistry and Chemical Engineering Laboratory provided overall program supervision and Dr. E. A. Burns, Manager, Applied Chemistry Department was Program Manager. The Principal Investigator responsibilities for the program were performed by Dr. R. J. Jones. Major technical contributions throughout the program were provided by Mr. R. W. Vaughan and Dr. C. A. Flegal. Acknowledgment is made of the technical assistance provided during the program by the following TRW Systems personnel.

Members of the Professional Staff

| | |
|---|---|
| J. F. Clausen | Applied Chemistry Department |
| A. Grunt | Applied Chemistry Department |
| J. F. Jones | Applied Chemistry Department |
| W. P. Kendrick | Applied Chemistry Department |
| M. L. Kraft | Applied Chemistry Department |
| W. D. Lusk | Chemical Engineering Department |
| C. A. Sheppard | Applied Chemistry Department |

Technical Support

| | |
|---|---|
| J. Arce | Applied Chemistry Department |
| J. N. Kennedy | Applied Chemistry Department |
| D. B. Kilday | Applied Chemistry Department |
| R. S. Thorpe | Applied Chemistry Department |
| K. K. Ueda | Applied Chemistry Department |
| L. G. Van Wijngaerde | Applied Chemistry Department |
| W. F. Wright | Applied Chemistry Department |

NASA CR-72984
16402-6012-R0-00

# THERMALLY STABLE LAMINATING RESINS

by

R. J. Jones, R. W. Vaughan and E. A. Burns

## SUMMARY

This report is the final program report describing work performed by TRW Systems for the National Aeronautics and Space Administration, Lewis Research Center, under Contract NAS3-13489. The objective of this program was to improve the processability of the pyromellitic anhydride containing addition-type polyimide laminating resins developed in Contract NAS3-12412. This objective was accomplished with 1) support of further studies of model compound pyrolysis parameters and pyrolysis product characterization, 2) polymer synthesis and characterization investigations, 3) laminating process optimization and post curing studies, 4) oxidative degradation investigations and 5) development of autoclave molding process and fabrication of a complex simulated air foil section.

The first phase of the work involved further synthesis and characterization of model compounds using the results of the previous program (Contract NAS3-12412) as the basis for chemical modifications to characterize the pyrolytical polymerization cure reaction of the A-type polyimides and establish reduced processing conditions. The past studies suggested that partial completion of the reverse Diels-Alder reaction of the A-type polyimide model compound, N-phenyl nadimide, was a necessary step in the addition-type cure reaction and hence, studies were conducted with blends of N-phenyl nadimide and N-phenyl maleimide to determine the extent of cure at a temperature lower than that required for initiation of the reverse Diels-Alder reaction. In addition, studies were undertaken using Lewis acid catalysts (for promotion of the addition-type cure reaction) and applied pressure to determine the time-temperature dependency of these parameters toward achieving coreaction of the model compounds. It was shown that Lewis acids, specifically tin tetrachloride, were the most effective means to reduce cure temperature and time requirements.

The second phase of the program consisted of investigations involving blends of maleic and nadic anhydride capped prepolymers containing methylene dianiline and pyromellitic dianhydride in the presence and absence of tin tetrachloride. These studies showed that 1% w/w catalyst concentrations reduced molding powder cure time to 10 minutes (from 30 minutes) while yielding a product possessing good 589°K (600°F) thermo-oxidative stability.

Concurrently with the model compound and polymer synthesis and characterization studies, laminate process optimization studies were conducted to establish conditions required to prepare sound Courtaulds HMS graphite fiber reinforced laminates from P10P, the A-type polyimide resin identified in Contract NAS3-12412 as possessing improved thermo-oxidative stability. Candidate prepreg preparation methods were screened using resin solids, solvent mixtures, and imidization temperature and time as process variables. Imidized preforms were prepared from prepregs using the two most promising imidizing cycles to identify the most effective combination of imidization and molding processing conditions. The best combination of processing conditions consisted of an imidizing cycle of two hours at 478°K (400°F), a final molding pressure of 3.45 $MN/m^2$ (500 psi) for 60 minutes at 589°K (600°F). A two-hour 616°K (650°F) cycle was useful in developing maximum initial and isothermally aged properties.

Graphite fiber reinforced P10P polyimide laminates prepared in the fashion developed above were examined for their thermo-oxidative stability. This study consisted of determining the influence of oxygen content (20, 60, 100% v/v), temperature (505°K and 589°K) and applied mechanical load (0 and 50% of flexural failure). These studies showed that for unstressed specimens the degradation (weight loss as a function of time) was more sensitive to temperature than oxygen content variation although at constant temperature the degradation was related to oxygen content. In addition, it was observed that stressing the specimens caused a marked increase in thermo-oxidative degradation. The stressed specimens underwent stress relaxation and permanent set in the test environment. The observation of visco-elastic behavior for these laminates has identified an important material property which must be considered in designing load-bearing structural composites.

The last phase of the program consisted of developing an autoclave moldable version of the P10P polyimide resin. A study of formulation variations showed that resin flow could be retained over a wide temperature range by incorporation of thiodianiline in the prepolymer backbone. Prepreg flow studies were conducted using glass reinforcements which identified specific conditions for obtaining low void, high strength laminates. Supporting studies were undertaken to identify key processing conditions, such as bagging materials, sealants and operational procedures. Typically, the glass reinforced autoclave composites had flexural strengths of over 550 $MN/m^2$ at room temperature with retention greater than 60% at 589°K. Shear strength retention at 589°K was greater than 60% and modulus retention was greater than 85%.

Studies using the identical formulation and processing procedures for graphite reinforced composites gave lower than desired properties. Cursory investigations have identified that sizing the graphite fiber is a key step towards enhancing the overall graphite reinforced autoclave laminate properties. It is believed that optimization of the processing techniques for graphite reinforced composites can be accomplished and is recommended for future studies.

A complex graphite fiber reinforced demonstration component (simulated air foil) was designed together with requisite tooling. Processing for autoclave molding the demonstration part was developed and a display model was fabricated.

CONTENTS

CONTENTS (CONTINUED)

CONTENTS (CONTINUED)

TABLES

TABLES (CONTINUED)

TABLES (CONTINUED)

# ILLUSTRATIONS

ILLUSTRATIONS (CONTINUED)

ILLUSTRATIONS (CONTINUED)

# 1. INTRODUCTION

This final report presents the work accomplished by TRW Systems for the National Aeronautics and Space Administration, Lewis Research Center, under Contract NAS3-13489 during the period 1 May 1970 through 13 August 1971. This program consisted of experimental studies aimed toward the continued development of thermally stable laminating resins investigated in Contract NAS3-12412 (Reference 1). The effort was aimed toward further improving the processability and thermo-oxidative stability of the resin. The underlying motivation for conducting this program is the development of high performance resin-fiber composites for use in air breathing engine systems which would permit significant system advantages (high strength-to-density ratios, high modulus-to-density ratios, excellent damping characteristics and low cost).

The thermally stable laminating resins investigated in this program were based on the A-type polyimide resin system which was conceived and first examined during Contract NAS3-7949 (Reference 2) for use as an ablative material. This resin system is formed by a curing mechanism which is believed to be unique in polymer art, namely, pyrolytic polymerization. Specifically, the technique involves the preparation of soluble low molecular weight polyamide-acid prepolymers having reactive alicyclic rings at the terminal positions. It was found that pyrolysis of the imidized prepolymers resulted in the formation of macromolecules *in situ*. The polymerization of these prepolymers was found to meet the properties delineated above and fabric-reinforced laminates were processed with relative ease.

The A-type polyimide resin system was carried to a further degree of advancement by TRW Systems through extensive development studies with the aim of determining the commercial potential of one specific formulation called P13N. This material has been accepted throughout the industry and has been selected to fabricate high performance composites for use in air breathing engine systems by several government contractors.

In an effort aimed towards further improvement of the A-type resin system under Contract NAS3-12412 (Reference 1), a new formulation (termed P10P) was identified having significantly enhanced thermo-oxidative stability which could be processed by standard press molding methods. This finding was

accomplished through basic investigations on the mechanism of the pyrolytic polymerization reaction through model imide compounds. The information obtained from the model compound studies was utilized to guide the synthesis of prepolymers and polymers. The ease of conversion of the polyimide precursor (amide-acid) to form the fully cured imide was studied together with the conditions necessary for the subsequent conversion to cured polyimide polymer.

Critical process variables were investigated to determine the degree of improvement imparted by the chemical backbone used in the preparation of the new polyimide polymers. Glass reinforced composites were prepared using prepolymers which offered promise of further improvement in processing and thermo-oxidative stability. Mechanical properties of glass and graphite fiber reinforced composites were determined at room and elevated temperatures and the results of these studies were assessed in terms of operational properties and processing conditions.

The key experimental findings of Contract NAS3-12412 (Reference 1) provided recommendations for further processing and product improvements to which this current program was addressed. Specifically, investigations were carried out aimed toward 1) improving the processability and thermo-oxidative stability of resin identified in Contract NAS3-12412 (Reference 1), 2) elucidating the mechanism of oxidative degradation, 3) improving the 589°K (600°F) strength retention of polyimide-resin/graphite fiber composites, and 4) developing an autoclavable polyimide resin.

In the program reported here the pyrolytic polymerization reaction was investigated through model imide compounds to determine the effect of mixed blends of reactive alicyclic groups, catalyst and pressure. The results of these studies were used to guide further polymer synthesis investigations for improving the processability of the resin. Process optimization and post curing studies were undertaken to define the best conditions for preparing thermally stable Courtaulds HM graphite reinforced composites. Oxidative degradation studies were performed on graphite fiber laminates under various load conditions as a function of oxygen content and temperature in an effort to elucidate the mechanism of oxidative degradation and to provide a basis for future chemical tailoring to eliminate the most labile chemical sites.

Finally, detailed studies were conducted which resulted in the development of an autoclavable polyimide resin. These studies involved resin synthesis and flow characterization of candidate formulations, evaluation of bagging materials, investigation of fiber sizing methods, and development of processing conditions for preparing both glass and graphite fiber reinforced autoclave molded composites which resulted in the feasibility demonstration of preparing a simulated air frame part of complex shape.

This report is divided into five principal sections covering the program tasks: 1) Task I - Synthesis and Characterization of Model Compounds, 2) Task II - Polymer Synthesis and Characterization, 3) Task III - Process Optimization and Post Curing Studies, 4) Task IV - Oxidative Degradation Studies, and 5) Task V - Autoclave Molding Studies.

The significant conclusions reached from evaluation and assessment from the results are listed together with recommendations for activities that warrant further investigations. This report identifies in a separate section new technology originating from the program. The information presented in the main body of this report is supplemented by appendices covering detailed descriptions of procedures, equipment and raw test data.

## 2. TASK I - SYNTHESIS AND CHARACTERIZATION OF MODEL COMPOUNDS

The objective of this task was to obtain insight into further processing improvements of the polyimide resin developed under Contract NAS3-12412 (Reference 1). This objective was achieved by obtaining additional understanding of the environmental conditions which govern the pyrolytic polymerization reaction for model compounds which allowed selection of conditions for investigation in actual A-type prepolymers in Task II. It was necessary to conduct the mechanistic studies with model compounds because of the inherent intractability of the cured products from pyrolytic polymerization of A-type prepolymers.

Model compound studies conducted in Contract NAS3-12412 showed that the pyrolytic polymerization reaction of N-phenyl nadimide consisted of at least two main reactions:

- First - a partial reverse Diels-Alder reaction of nadic anhydride end caps on the prepolymers requiring temperature of 543°K (500°F) at onset, and
- Second - a chain extension terpolymerization involving the products of the reverse Diels-Alder reaction as maleimide, cyclopentadiene and unreacted nadimide precursor.

It was evident from the pyrolytic polymerization studies conducted in Contract NAS3-12412 (Reference 1) that three areas of investigation were warranted to characterize the reaction more completely and establish reduced processing conditions. These areas are: 1) end capped polymer blends, 2) applied pressure, and 3) use of catalysts.

The rate limiting step in the pyrolytic polymerization is the initial reverse Diels-Alder reaction. Prior vacuum pyrolyses of the model N-phenyl nadimide showed that 5%-20% of available cyclopentadiene did not participate in the polymerization. It was conjectured that if maleic capped precursors were already available at the onset of the cure reaction, the chain extension polymerization would be facilitated. A study was conducted that determined the effect of compensating for the loss of cyclopentadiene through the use of nadimide and maleimide blends. Additional vacuum pyrolyses were conducted as a preliminary study to correlate data with those obtained in NAS3-12412 (Reference 1).

The time-temperature parameters established in the vacuum pyrolysis study were utilized for the applied pressure investigation. It was shown that cyclopentadiene initially evolved during the reverse Diels-Alder reaction was incorporated into the model polymer structure to give a product of similar thermo-oxidative stability and structure to those obtained in vacuum studies. Polymers resulting from a 95:5 w/w blend of nadimide/maleimide were almost identical in nature to those prepared from nadimide alone.

The most promising processing conditions identified in pressure pyrolysis experimentation were selectively screened in the presence of catalysts known to promote polymerization of the nadic, maleic, and/or cyclopentadiene components active in A-type polyimide cure. It was shown that Lewis acids, specifically tin tetrachloride, were the most effective means to effect an improvement of required temperature and time cure parameters.

Details of each pyrolysis study as well as a mechanistic interpretation of data and correlation with preliminary studies conducted in NAS3-12412 (Reference 1) are provided below.

## 2.1 SYNTHESIS AND PYROLYSIS STUDIES OF MODEL COMPOUNDS

Model compounds studies were conducted in four integral subtask experimental phases:

- Synthesis of model compounds,
- Vacuum pyrolysis experimentation conducted to obtain baseline data for correlation of the current study with prior NAS3-12412 methodology,
- Pressure pyrolysis experimentation to simulate the realistic processing conditions which actually occur in A-type polyimide cure, and
- Catalyst screening studies conducted on most promising model polymers obtained under vacuum and pressure to improve further improved polymer processing/property relationships.

Each of these studies are described individually below. A mechanistic interpretation summary of all model compound studies is provided as the final discussion (Section 2.2).

### 2.1.1 Synthesis of Model Compounds

The effectiveness of N-phenyl nadimide (I) as a model for A-type polyimide polymers was demonstrated in Contract NAS3-12412 (Reference 1). This compound and N-phenyl maleimide (II), useful as polymer caps in pyrolytic polymerization, were selected as key ingredients for conducting a model compound investigation for the reduction of cure parameters and catalyst identification applicable to actual A-type polyimide polymers.

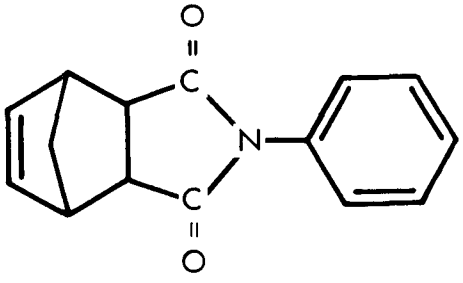

N-phenyl Nadimide (I)

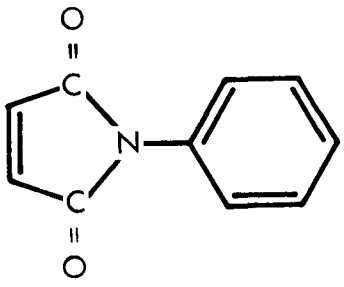

N-phenyl Maleimide (II)

Quantities of (I) and (II) sufficient to undertake and complete pyrolytic polymerization studies were prepared. Experimental details of the synthesis and characterization conducted on the model compound products are provided in Appendix A.

### 2.1.2 Vacuum Pyrolysis Experimentation

A vacuum (reduced pressure) pyrolysis apparatus identical to that utilized in Contract NAS3-12412 was assembled and employed to conduct nine key experiments on model compound (I) and blends of (II) in (I). The apparatus is shown in Figure 1 and its operation is described below. In this description, sections of the apparatus are identified by reference to Figure 1 by letter designation.

> A weighed sample of model imide is placed in the sample tube (A) and the entire system is purged with nitrogen. After purging, the system is evacuated to ~1 torr with an efficient vacuum pump (B-vacuum line) and the system is closed. A crucible furnace (C) is preheated to test temperature and is then put into place so that it completely envelops the sample tube containing the sample to initiate the pyrolysis experiment. The temperature inside the sample tube is monitored by a thermometer (D). The sample temperature and the time from reaction initiation are recorded at frequent

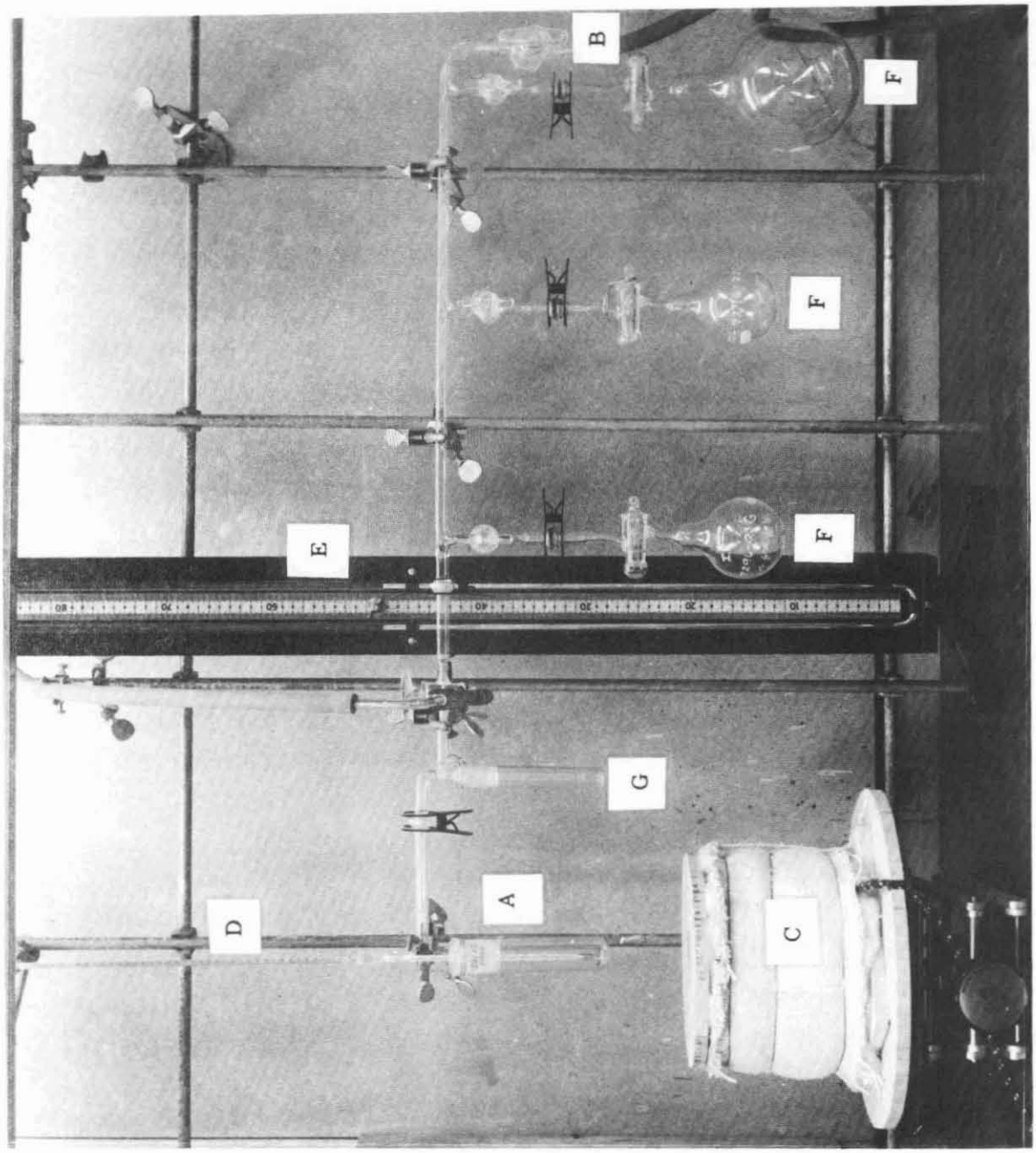


Figure 1. Apparatus Employed for Model Compound Pyrolysis Studies (See Pages 7 and 9 for description of lettered components)

intervals during the experiment along with the system pressure (measured by manometer E). At the end of a predetermined time period, the stopcocks to the gas collection bulbs (F) are closed, the tube furnace is removed, and the system is allowed to slowly cool. When the temperature has reached 298-303°K in the sample tube, the pressure in the system is adjusted to atmospheric pressure with a nitrogen purge. The solid pyrolysis residue and any sublimed material are then isolated separately as well as any liquid material trapped in a cold trap (G) and all samples are numbered for characterization. The equation employed for calculation of gas quantities is given in Appendix B.

A total of nine pyrolyses experiments were completed on N-phenyl nadimide (I) and blends of (I) and N-phenyl maleimide (II). Details of the pyrolyses are summarized in Table I. In all cases the pulverized model imide samples were observed to undergo initial melt and flow phases, followed by gradual consolidation to give a glassy, tan polymeric residue. The degree of color developed during pyrolysis varied according to temperature and time with the higher temperatures and two-hour experiments giving a darker product.

It was necessary to adjust the reduced pressure during the course of the experiments in order to substantially reduce the quantities of sublimate that arose in similar studies in NAS3-12412 (Reference 1). This technique reduced sublimate of the total mass isolated to approximately 5% w/w or less.

The vacuum pyrolysis residues listed in Table I were characterized for apparent structure by infrared and nuclear magnetic resonance analyses. Details of these studies are provided in Appendix B, and summarized mechanisticly in Section 2.2. No significant differences were noted for residues from current pyrolyses of (I) over those isolated in NAS3-12412.

The most important result arising from the vacuum pyrolysis studies was establishment of which processing parameters (i.e., temperature and time) gave the polymeric residue of highest initial thermo-oxidative stability. This was accomplished by thermogravimetric analysis (TGA) of each material as detailed in Appendix B. The TGA characterization showed that vacuum pyrolysis conditions of 589°K (600°F) temperature for a pyrolyses duration of at least one hour gave the most promising samples. The vacuum pyrolysis work gave no finite resolution of whether a nadic species alone or a blend of maleic in nadic provided the most promising polymer product.

TABLE I

SUMMARY OF MODEL IMIDE REDUCED PRESSURE PYROLYSIS EXPERIMENTATION

| Code | Blend Level of N-phenyl Maleimide in N-phenyl Nadimide (% w/w) | Pyrolysis Duration (Hrs) | Pyrolysis Conditions Temperature/Pressure[a] (°K/kN/m$^2$) | Mass Isolated Total Yield (% w/w) |
|---|---|---|---|---|
| 1 | 0.0 | 1.0 | 566/16-21 | 94.8 |
| 2 | 0.0 | 1.0 | 589/74-81 | 100.6 |
| 3 | 0.0 | 1.0 | 623/54-72 | 100.0 |
| 4 | 0.0 | 2.0 | 566/17-20 | 93.8 |
| 5 | 0.0 | 2.0 | 589/28-37 | 96.4 |
| 6 | 5.0 | 1.0 | 589/22-48 | 97.1 |
| 7 | 5.0 | 2.0 | 566/ 7-15 | 95.6 |
| 8 | 20.0 | 1.0 | 589/38-50 | 100.7 |
| 9 | 20.0 | 2.0 | 566/34-54 | 102.3 |

[a]The pressures given are the initial pressure and the final pressure at the end of the pyrolysis run (1 atmosphere = 101 kN/m$^2$)

The results of the vacuum pyrolysis study correlated well in regards to requisite processing parameters with pressure experimentation as is described below.

### 2.1.3 Pressure Pyrolysis Experimentation

The influence of pressure on model imide pyrolysis reactions was a key parameter assessed during Task I studies. Utilization of pressure during pyrolysis more closely simulates the curing conditions employed for A-type polyimide polymers to effect proper consolidation to nil-low void laminates. The study of pressure effects on model compound cure showed that apparently an identical mechanism occurs in either vacuum or pressure environments. The results from this study allowed definition of a catalyst type for A-type polyimides to be identified.

A total of 25 pyrolysis experiments were completed under pressure on N-phenyl nadimide (I) and blends of (I) and N-phenyl maleimide (II) employing the pressure device shown in Figure 2. The device, although simple in design, performed without problems throughout the study. Because of its small dimensions, the apparatus provided the advantages of rapid heat-up rates and ease of handling. The pressure chamber was utilized for pressure pyrolysis systems by incorporation into the set-up shown in Figure 3.

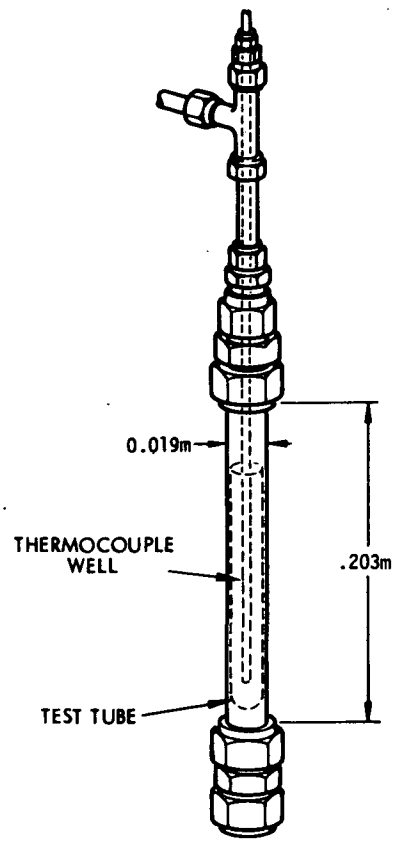


Figure 2. Pressure Chamber Used for Pyrolysis Experimentation

The system employed for the experimentation as shown in Figure 3 possesses the desired features of 1) a thermocouple well in direct contact with the sample in the test tube, 2) a relief valve for releasing pressure in case of a non-anticipated pressure build-up occurred at the highest temperatures and pressures studied (623°K and 1.48 $KN/m^2$, and 3) a means for recording the pressure and temperature simultaneously.

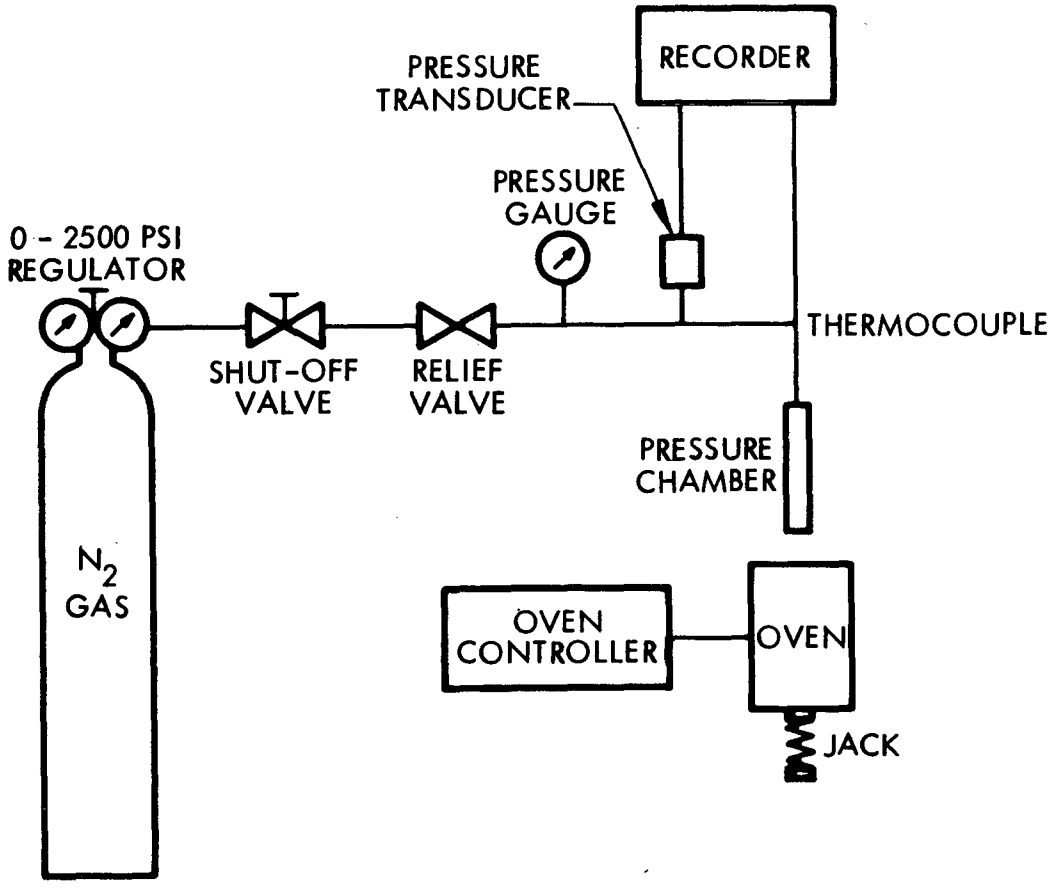


Figure 3. Schematic Pressure Pyrolysis Experimentation Set-up

The pressure experiments were conducted according to the methodology described in Appendix B.

Although the set-up described above did not allow visual observation of phenomena occurring during pyrolysis, the strip-chart recorder utilized printed out a temperature/time profile which showed melting of the sample at 415°K (289°F). Phases associated with reverse Diels-Alder and *in situ* polymerization of the post reverse Diels-Alder products did not appear in the profile. However, the samples obtained from the experiments were identical in appearance to those described previously from vacuum pyrolysis.

The total experiments conducted under pressure are summarized in Table II. An identical procedure was employed for characterization of these residues as was used for the model polymers obtained in vacuum experimentation.

TABLE II

MODEL COMPOUND PYROLYSIS RUNS CONDUCTED UNDER APPLIED PRESSURE[a]

| Blend Level of N-phenyl Maleimide in N-phenyl Nadimide (% w/w) | Pyrolysis Duration (Hrs) | Temperature (°K) | | | | | | | |
|---|---|---|---|---|---|---|---|---|---|
| | | 544 | | 566 | | 589 | | 623 | |
| | | Pressure ($MN/m^2$) 0.45 | 1.48 | Pressure ($MN/m^2$) 0.45 | 1.48 | Pressure ($MN/m^2$) 0.45 | 1.48 | Pressure ($MN/m^2$) 0.45 | 1.48 |
| 0.0 | 0.5 | | | | | | X | X | X |
| | 1.0 | | | X | X | X | X | | |
| | 2.0 | | X | | | | | | |
| 5.0 | 0.5 | | | | | | X | X | |
| | 1.0 | | | X | X | X | X | | |
| | 2.0 | | X | | X | | X | | |
| 20.0 | 0.5 | | | | | | X | X | |
| | 1.0 | | | | X | X | X | | |
| | 2.0 | | X | | X | | X | | |

[a]Absolute pressure

Each residue was routinely screened for gross structure by infrared analysis and for thermo-oxidative stability (TOS) by TGA. In all cases the infrared spectra were very similar to those obtained in vacuum studies. TGA screening established that the requisite of 589°K temperature for adequate cure during pyrolysis was necessary for pressure pyrolysis as was also the case for vacuum experiments. These data also demonstrated that 1.48 $MN/m^2$ (200 psig) gave a product of higher TOS than a lower pressure of 0.45 $MN/m^2$ (50 psig). A complete documentation of polymeric residue characterization is provided in Appendix B.

The pressure pyrolysis studies aided definition of the effect of N-phenyl maleimide (II) blends in N-phenyl nadimide (I) on polymer properties. It was determined that a 20% w/w blend of (II) in (I) gave products of diminished TOS over products from (I) alone or a 5% w/w blend of (II) in (I). However, it was impossible to define or select the most promising end cap configuration between (I) or the 5% w/w blend of (II) in (I) on the basis of this study. Consequently, it was necessary to investigate both end cap candidates in A-type polyimide polymers to show that (I) alone leads to the most favorable neat resin product (see Section 3).

Details of all characterization methods employed and data determined on the residues produced pyrolytically under pressure are provided in Appendix B. Included in Appendix B are both infrared and TGA screening data as well as nmr, vapor phase osmometry (VPO) and bromine absorption results on key (most promising) samples.

The experimental parameters defined (i.e., 589°K, 1.48 $MN/m^2$, two hours) to give the model polymer residues of highest TOS in the pressure studies were employed to conduct a catalyst screening study on model compound (I) as described in Section 2.1.4. A mechanistic interpretation of cure phenomena occurring during model compound pyrolysis under pressure is provided in Section 2.2.

### 2.1.4 Catalyst Studies

The adaptability of the A-type polyimide polymer concept to give polymers of varying processability/property trade-offs because of ingredient and prepolymer formulated molecular weight modifications has been described previously in NAS3-12412 (Reference 1) and herein in Section 6. However,

prior to this program, no systematic attempt had been made to study the effect of catalysts on A-type polyimide processability/property relationships. This section describes an investigation which led to the identification of a catalyst class having high potential for providing polymers of enhanced processability/property trade-offs.

The results of pressure-pyrolysis studies described in Section 2.1.3 showed that relatively severe processing conditions of a 589°K cure temperature for two hours duration were required to give model polymers of the most promising (highest) degree of initial TOS at a reasonable cure pressure of 1.48 $MN/m^2$. Consequently, an experimental study was designed and implemented to reduce the cure temperature and/or the cure duration requirements. In order to utilize previously documented data, a literature search was conducted on catalysts of the 1) Lewis acid, 2) Lewis base, and 3) peroxide (free radical) types which have been shown to promote polymerization of the norbornene (nadic) and cyclopentadiene entities shown in NAS3-12412 (Reference 1) to be present in the initial stages of polymerization (reverse Diels-Alder) of A-type polyimides. Since maleic derivatives polymerize under the influence of all of these catalysts the search was concentrated on the two olefin compounds. The predominantly mentioned catalysts, were of the Lewis acid-(metal halide) type as shown in Table III.

TABLE III

MOST PROMISING CATALYSTS IDENTIFIED IN LITERATURE STUDIES

| Olefin | Catalyst Type | Reference |
|---|---|---|
| Cyclopentadiene | $SnCl_4$, plus other Lewis acids including $AlCl_3$ and $TiCl_4$ | 3 |
| | $TiCl_4$-triisobutyl aluminum complex | 4 |
| | $SnCl_4$ | 5 |
| | $SnCl_4$, $TiCl_4$, $AlBr_3$ and $BF_3OEt_2$ | 6 |
| Norbornene (nadic) | $TiCl_4$-lithium aluminum tetraheptyl | 7 |

Representative simple compounds from each of the three catalyst categories were studied in preliminary pyrolyses experiments. For preliminary screening of the three catalysts types, it was decided to fix the cure temperature and the pressure at 589°K and 1.48 $MN/m^2$, respectively, and investigate the effect of catalysts on cure time required to produce model polymers of TOS equivalent to that occurring in non-catalyzed studies (see Section 2.1.3). The model compound selected for study was N-phenyl nadimide (I), since at the time of the catalyst screening, the value of N-phenyl maleimide (II) blends in (I) was not yet defined.

The catalysts screened and experimental results from these studies are given in Table IV. The most significant phenomenon shown to occur

TABLE IV

PRELIMINARY CATALYZED PYROLYSIS DATA[a]

| Catalysts Screened Type/Compound | Catalyst Level (w/w %) | Experimental Results |
|---|---|---|
| Lewis acid - $SnCl_4$ | 1<br>3 | Strong exotherm occurred when model compound reached 561°K-589°K. Polymer product thermal stability (TGA in $N_2$ was $\geq$589°K (600°F) at both levels. |
| $TiCl_4$ | 1<br>3 | Exotherm occurred as described above, but polymer products at both levels only demonstrated 523°K (480°F) stability |
| $AlCl_3$ | 3 | Exotherm occurred, but polymer residue degraded at temperatures >523°K. |
| Lewis base- Triethylamine | 3 | No exotherm occurred during pyrolysis. |
| Free Radical - Benzoyl Peroxide | 3 | No exotherm occurred during pyrolysis. |

[a]All experiments run at 589°K and for 0.5 hour in the pressure apparatus shown in Figure 2.

initially in the pyrolysis cycle was a large and uncontrollable exotherm. This phenomenon was shown to occur only when catalysts of the Lewis acid metal halide type were employed. The characterization parameter employed

to define the effect of the catalyst was TGA. These analyses showed that products of the highest TOS were produced using tin tetrachloride as the Lewis acid catalyst.

Based upon these initial screening data, an experimental matrix study was devised to investigate systematically the utility of $SnCl_4$ to reduce requisite cure temperature and/or cure duration of model compound polymerization. This study was implemented using a partial factorial experimental design for parameters of cure time, cure temperature and catalyst concentration and determining the incipient thermal decomposition temperature of the polymerized product.

The results of the study are summarized in Table V. During the experiments, it was observed that a very strong exothermic reaction occurred at pyrolyses conducted at 575°K and 589°K which raised the pyrolysis temperature recorded to an initial 605°K and 644°K, respectively. This phenomenon was observed for both 1% and 3% w/w $SnCl_4$ levels. A representative curve of the temperature profile is shown in Figure 4 for the pyrolysis conducted at 589°K for one hour employing 1% w/w $SnCl_4$. As can be seen in Table V, the exothermic reaction that gave the high incipient decomposition temperature evidently caused degradation of the product *in situ* and yielded products of initial thermo-oxidative stability inferior to those obtained for uncatalyzed reactions at 589°K. The results show that 1% w/w $SnCl_4$ is sufficient to cause a pronounced effect on polymerization of (I). The $SnCl_4$ appears to be a suitable catalyst for both lowering the required pyrolysis temperature to give a high TOS polymer residue in the normal cure period of 1.5 to 2.0 hours or lowering the cure temperature and cure duration required as evidenced by attainment of a high TOS product at 575°K in a minimum of 45 minutes. As described in Section 3, these findings were applied to the actual synthesis of A-type polyimide polymers with significant results.

In addition to the TGA measurements, each of the pyrolysis residues listed in Table V were characterized for structure by infrared spectroscopy. Also, further characterization, in terms of nmr, VPO and bromine absorption determinations, were carried out on key samples. All of these data are described in Appendix B. A mechanistic interpretation of these findings is given in the following section.

TABLE V
RESULTS OF CATALYSIS STUDY

| Pyrolysis Temperature Imposed/ Temperature Observed (°K/°K) | $SnCl_4$ Catalyst Level (% w/w) | | | | | | | Initial Thermal Stability by TGA (°K/°F) |
|---|---|---|---|---|---|---|---|---|
| | 1% Duration (min.) | | | | | 3% Duration (min.) | | |
| | 30 | 45 | 60 | 90 | 120 | 30 | 60 | |
| 561/561 | X | | | | | | | 472/390 |
| | | X | | | | | | 472/390 |
| | | | X | | | | | 589/600 |
| | | | | X | | | | 589/600 |
| | | | | | X | | | 589/600 |
| | | | | | | X | | 589/600 |
| | | | | | | | X | 578/580 |
| 575/605 | X | | | | | | | 572/570 |
| | | X | | | | | | 583/590 |
| | | | X | | | | | 589/600 |
| | | | | | | X | | 561/550 |
| | | | | | | | X | 547/525 |
| 589/644 | | X | | | | | | 523/485 |
| | | | X | | | | | 533/500 |

## 2.2 MECHANISTIC INTERPRETATION OF TASK I - PYROLYSES EXPERIMENTATION

This section provides interpretation of the pyrolysis experiments reported in Section 2.1 in terms of probable chemical mechanistic processes. The pyrolytic residues used in the mechanistic interpretation were those selected as most promising and/or representative as based upon favorable thermo-oxidative stability (ca., 589°K) under minimum processing requirements. Specific data used in this theoretical interpretation are compiled in tabular or graphic form in Appendix B. Frequent reference is made to the findings of the initial mechanism study reported under Contract NAS3-12412 (Reference 1).

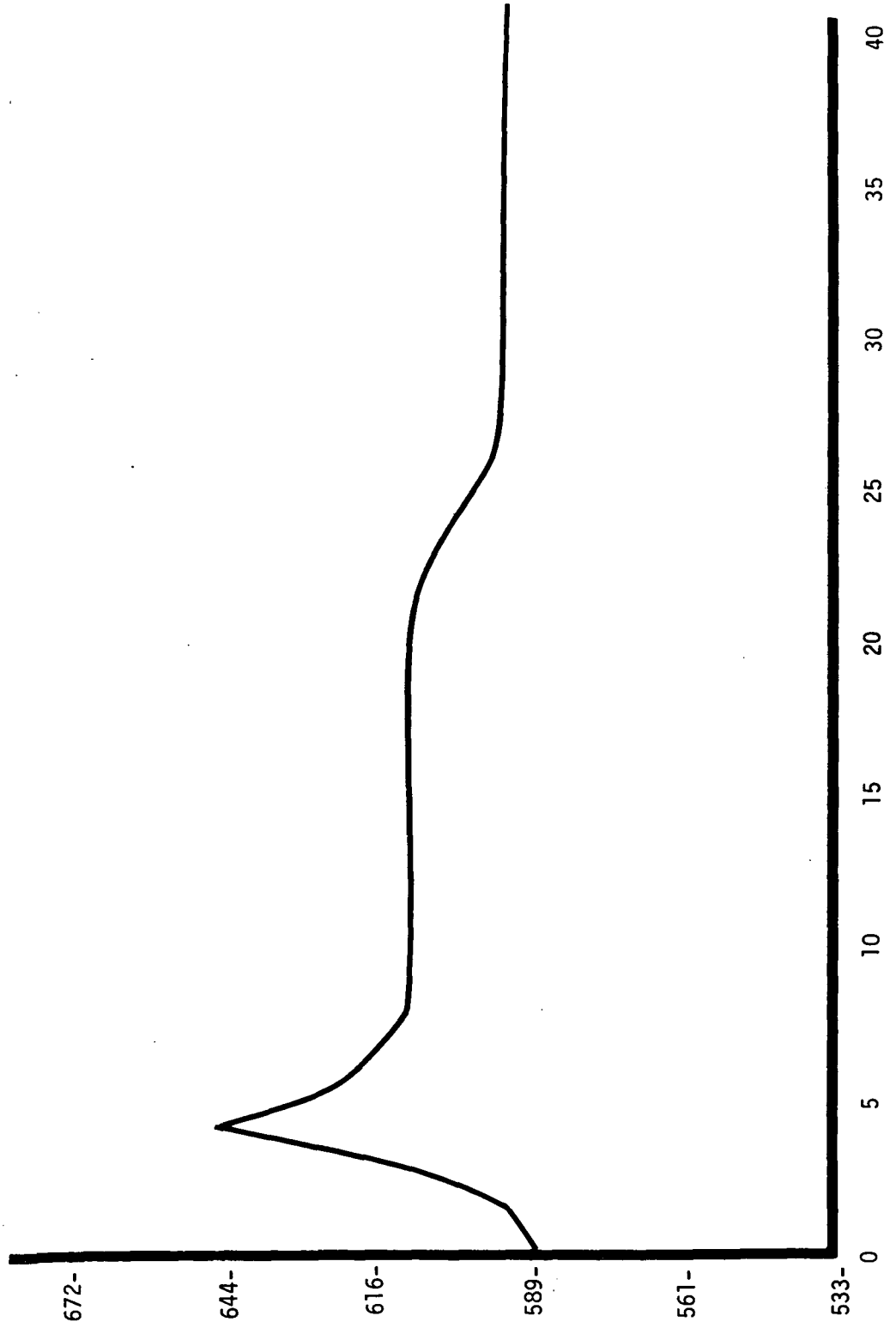


Figure 4. Actual Temperature/Time Plot of N-phenyl Nadimide Pyrolysis Conducted at 589°K and 1.48 MN/m$^2$ Employing 1% w/w $SnCl_4$ Catalyst

### 2.2.1 Mechanistic Interpretation of Vacuum Pyrolyses Experimentation

An integral portion of the pyrolyses experiments conducted previously in NAS3-12412 were performed in a reduced pressure environment. During these prior studies performed at an initial pressure of approximately 21 $N/m^2$ on N-phenyl nadimide (I), no attempt was made to regulate escape of cyclopentadiene (III) generated from the initial reverse Diels-Alder unzipping of (I). To facilitate discussion of the polymerization mechanism the compounds involved are shown as follows:

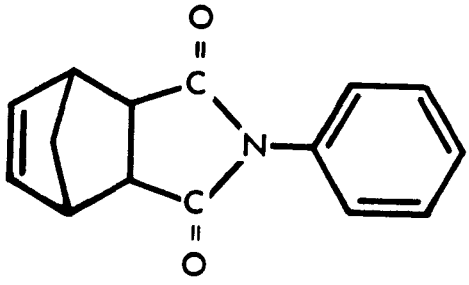

N-phenyl Nadimide (I)

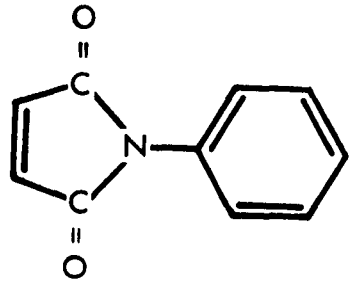

N-phenyl Maleimide (II)

Cyclopentadiene (III)

As stated previously in NAS3-12412 (Reference 1), it was postulated that the following pyrolysis step occurs initially

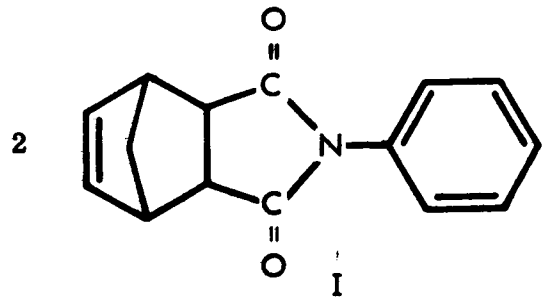

I

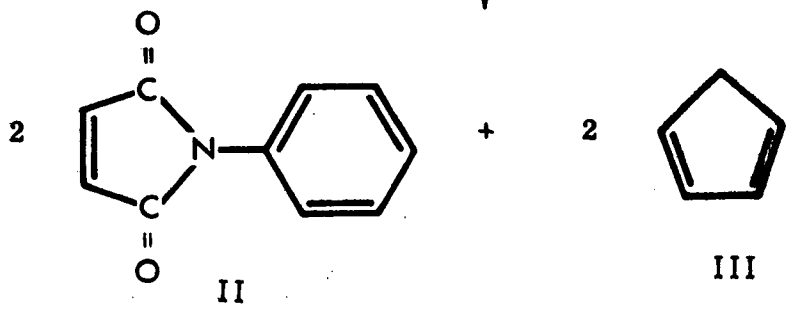

II III

(1)

and that (II) linearly consumes (III) in a 2:1 ratio according to Equation 2. This reaction gives an activated species which was presumed

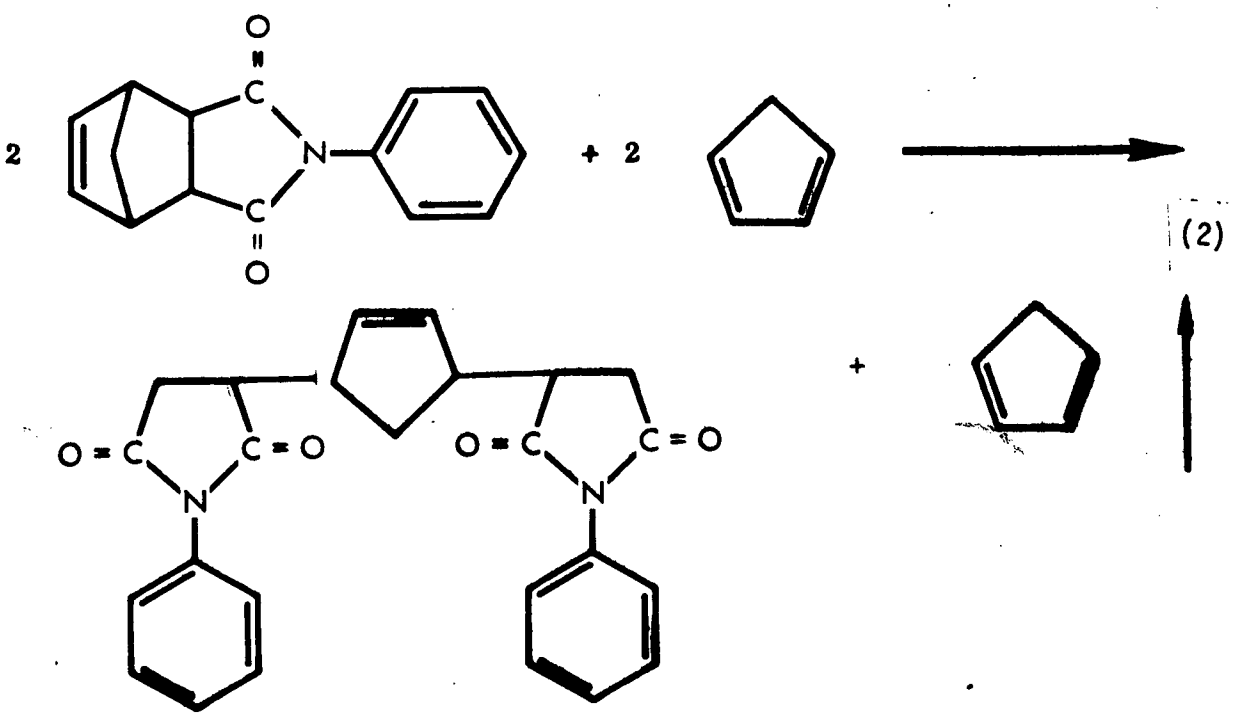

(2)

to initiate further polymerization via co- or terpolymerization involving all three unsaturated species, namely, N-phenyl nadimide (I), N-phenyl maleimide (II), and cyclopentadiene (III). The species from Equation 1 react further from continual reverse Diels-Alder reaction to give the possible backbone structure given in Equation 3.

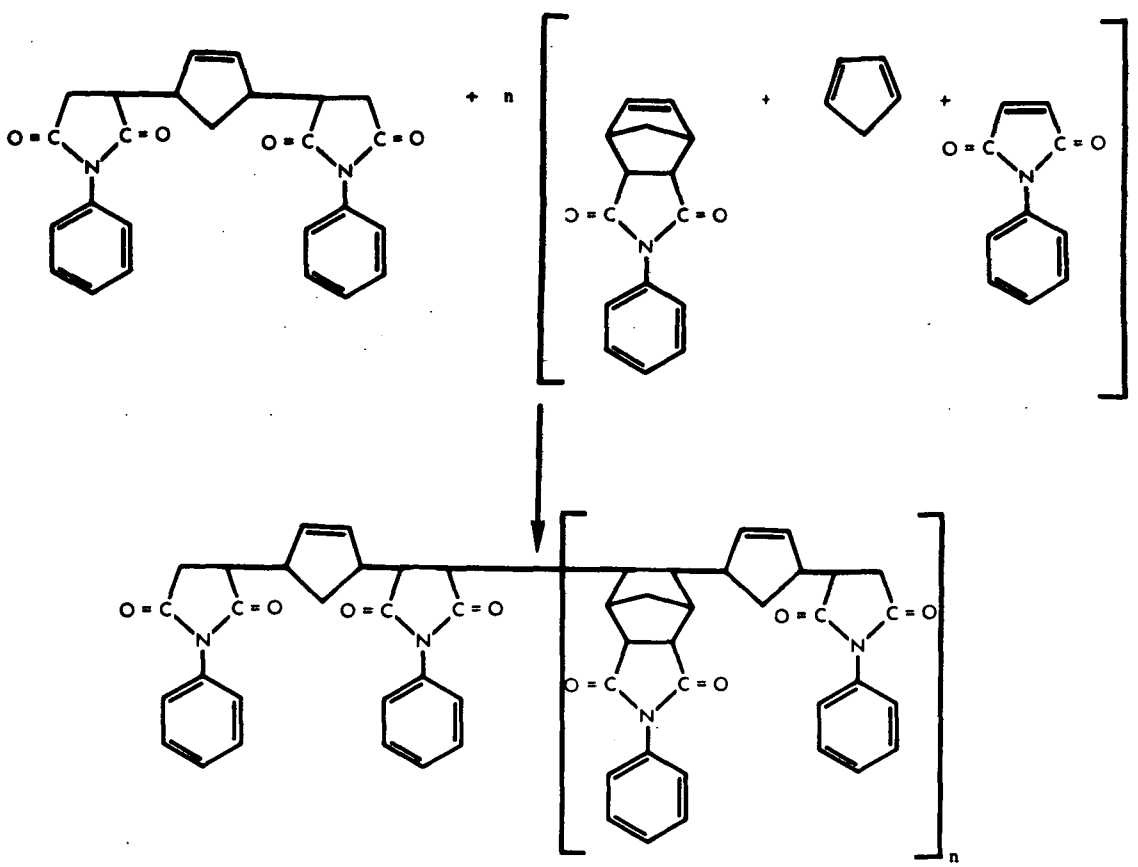

However, in current studies during which the pressure was regulated to approximately 6.3 $MN/m^2$, excess (III) did not volatilize off and nearly quantitative amounts (ca., 98-100%) of pyrolysis residues were recovered. In the present study, all experimental spectral data suggest that the same gross structure results as those determined in NAS3-12412. The number average molecular weight ($\overline{M}_n$) for these samples were ~900 g/mol and an unsaturation of titratable double bonds of approximately one per 3000 g of pyrolysis residue (see Appendix B). These results suggest that the mechanism shown in Equations 4 and 5 predominates.

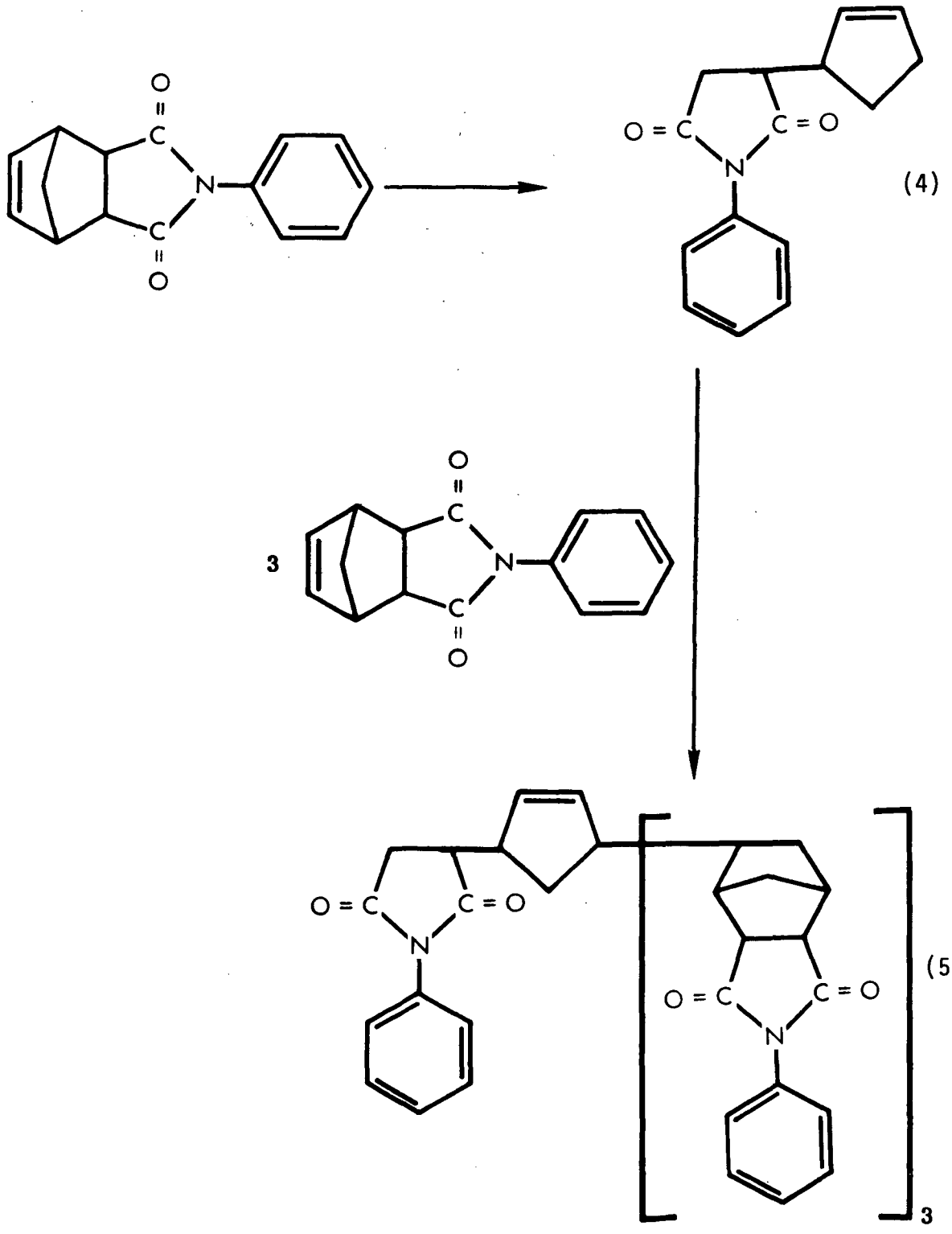

(4)

(5)

$\overline{M}_n$ = 956

and since activation of the pyrolysis mass has occurred, the above reaction is accompanied by the homopolymerization of further model compound species present as follows:

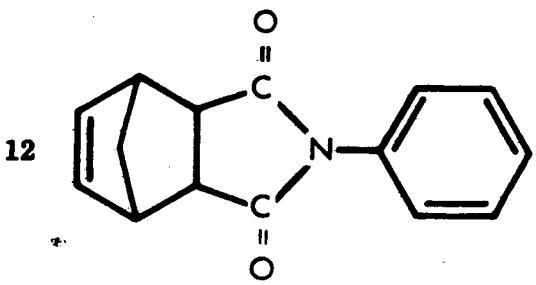

12



(6)

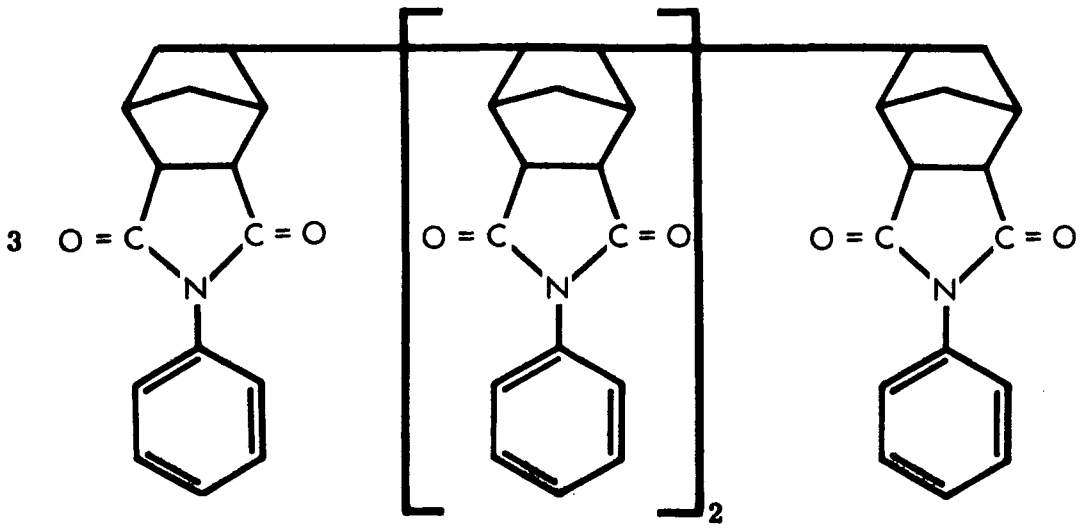

3

2

$\overline{M}_n = 956$

Completion of reactions 5 and 6 in the indicated proportion accounts for the $\overline{M}_n$ and bromine absorption data, as well as infrared and nuclear magnetic resonance spectral evidence presented in Appendix B, which are identical for the presenceof the same gross structure for the current pyrolysis residues as those determined in NAS3-12412 (Reference 1).

A plausible mechanistic incorporation of N-phenyl maleimide into the model polymers is considered in Section 2.2.1.1.

### 2.2.2 Mechanistic Interpretation of Pressure Pyrolyses Experimentation

The area of model compound pyrolyses which received prime emphasis during this program experimentation was that conducted under applied pressure. Details of the experimentation conducted in the absence of catalysts and those in the presence of catalysts were provided previously in Sections 2.1.2 and 2.1.3, respectively. Characterization data on key (most promising) pyrolysis residues are provided in Appendix B. Mechanistic interpretations of the non-catalyzed and catalyzed pyrolyses studies are provided below.

#### 2.2.2.1 Non-catalyzed Pressure Experiments

The pyrolysis studies of N-phenyl nadimide (I) and blends of N-phenyl maleimide (II) in (I) were described in Section 2.1. Characterization of the most promising pyrolysis residues (those demonstrating highest initial thermo-oxidative stability) by infrared and nmr structural analysis (see Appendix B) indicated the same gross structure results from pyrolysis at 1.38 $MN/m^2$ as to that which results from vacuum pyrolysis experiments. However, the $\overline{M}_n$ of the residues produced employing pressure methodology were slightly higher on the average (ca., $\overline{M}_n$ = 1050) than those obtained in vacuum, while bromine absorption for titratable double bonds remained relatively constant at approximately one per 2400-3000 g/mol of polymeric residue. Taking these characterization results into account, the following mechanistic interpretation appears plausible.

In order to give the same gross structure of the pyrolysis residues utilizing a 100% N-phenyl nadimide (I) starting material, it is assumed that some reverse Diels-Alder reaction of (I) occurs to give N-phenyl maleimide (II) and cyclopentadiene (III) which then recombine and rapidly consume unreacted (I) as is the same case for pyrolyses conducted under vacuum (see Section 2.2.1, Equation 4). Pressure pyrolysis residues from (I) possessing higher molecular weight are best accounted for by the simple addition of one more nadimide molecule in the polymer structure of the polymer equations (5) and (6) in Section 2.2.1, which gives $\overline{M}_n$ = 1195, which approximates the $\overline{M}_n$ average of ∿1100 determined experimentally.

In detailed analysis of polymeric residues arising from the pressure pyrolyses of blends of (I) containing 5% w/w N-phenyl maleimide (II), the same gross structure occurred (see Section 2.2.2 and Appendix B) as in the case for 100% (I) pyrolyzed in vacuum and pressure environments. The bromine titration data for the blend of (II) in (I) were equivalent to that observed for 100% (I), but the $\overline{M}_n$'s measured for the blend averaged approximately 70 g/mol less than for 100% (I). The molecular weight difference is almost identical to the molecular weight of cyclopentadiene (III), which was expected if (II) is incorporated into the polymeric structure by the mechanism postulated in NAS3-12412 (Reference 1) and further established herein. The structure of the polymers incorporating a 5% w/w blend of (II) in (I) is most probably that shown below.

First, the activated reverse Diels-Alder species of (I) is formed as before. It then either reacts with the added (II) from the blend as below as was postulated in NAS3-12412 (Reference 1).

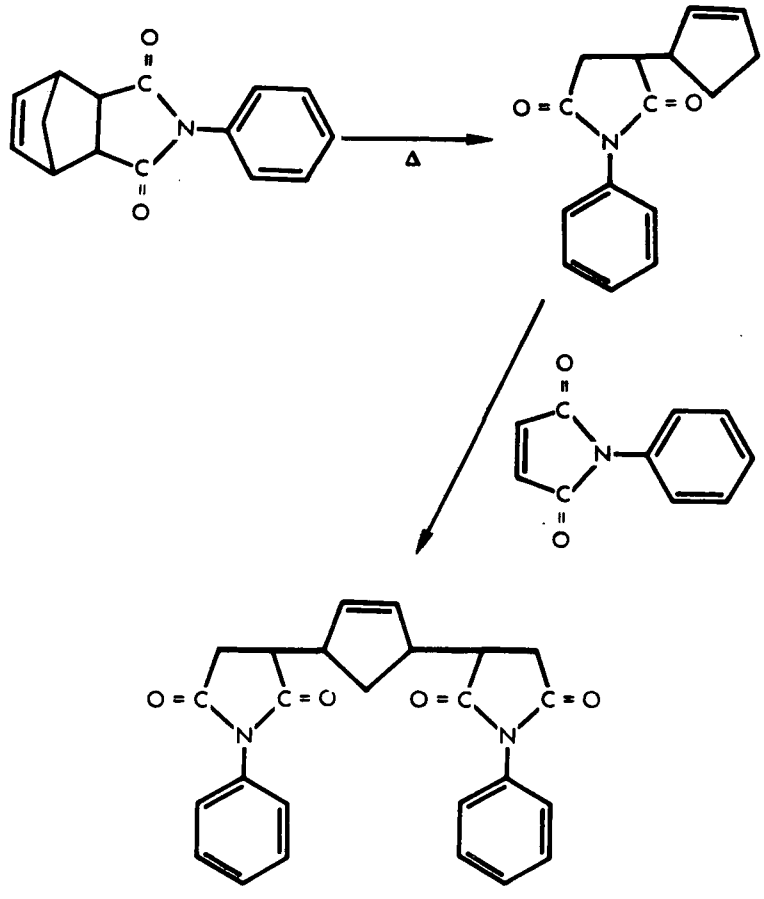

(4)

(7)

which in turn consumes (I) as follows:

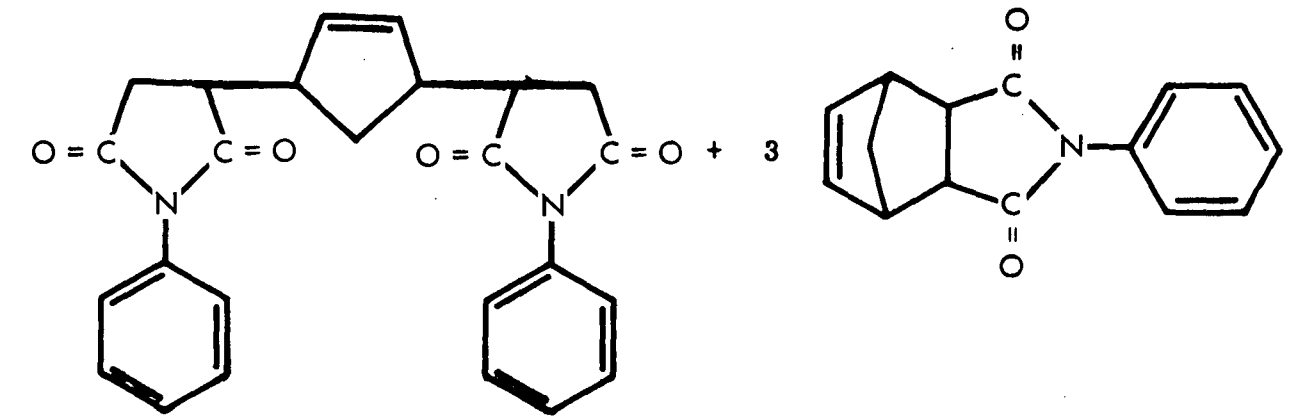

(8)

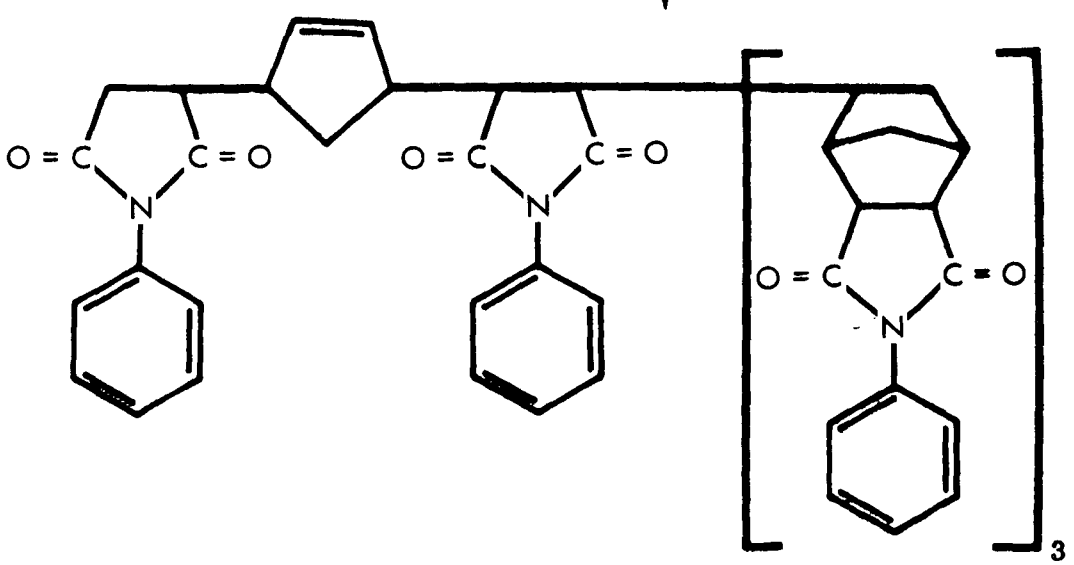

$\overline{M}_n$ = 1129

or the initially formed reverse Diels-Alder species shown in Equation 7 reacts randomly with both (I) and (II) as follows:

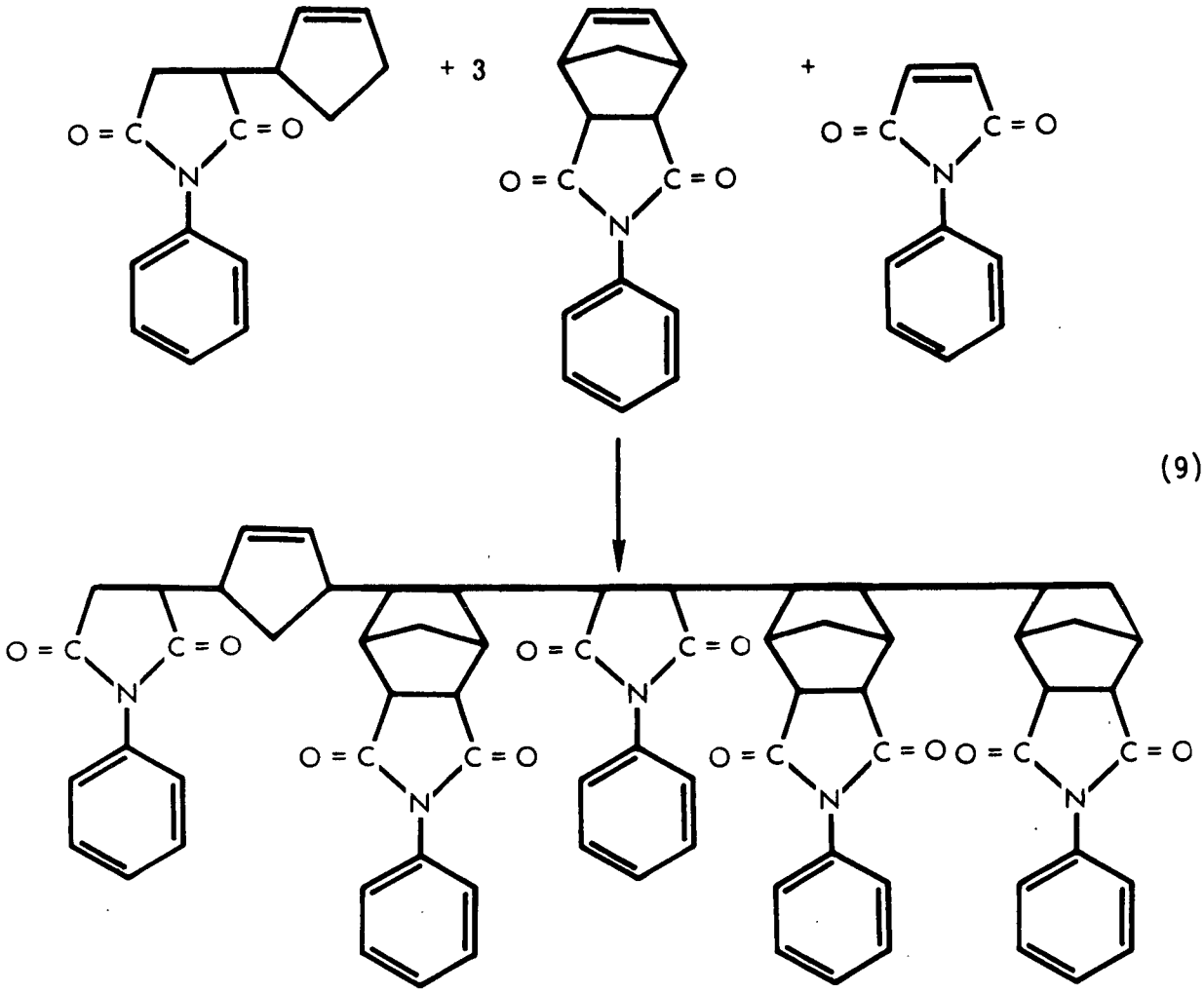

(9)

$\overline{M}_n$ = 1195

or an equivalent random structure.

The bromine absorption measurements infer that one double bond occurs per approximately every 2500 g/mol of pyrolysis residue and once again indicates that the above structure is accompanied by homopolymerization of (I) or (I) and (II) as was shown in Equation 4.

2.2.2.2 Catalyzed Pressure Pyrolysis Experimentation - The uncatalyzed experimentation conducted under pressure, as described in Section 2.2.2,

could not discern any advantage between the use of a total nadic end cap structure or a blend of maleic and nadic end caps. Because characterization of pyrolysis residues from both end cap species gave strong indication that the same gross structure (within the detectability of characterization methods employed and polymer thermo-oxidative stability) occurred employing both end cap options, it was elected to investigate the efficacy of catalysts in model compounds by employing one end cap species in order to maximize information arising from such a study. Consequently, N-phenyl nadimide (I) was selected, since the nadic species had received considerable development work in Contract NAS3-12412 (Reference 1) and Contract NAS3-13203 (Reference 8) and therefore, would provide data for ultimate direct comparison in cured polymers with those investigated in the previous work (see Section 3).

Catalyst screening studies on (I) in model compound studies as described in Section 2.1.3 identified tin tetrachloride ($SnCl_4$) to be the most promising of those investigated. During model compound pyrolysis studies conducted on (I) in the presence of $SnCl_4$, the catalytic power of $SnCl_4$ to lower both required pyrolysis temperature and time was identified. The most promising polymer residues were selected by TGA screening of thermo-oxidative stability as was the procedure employed for selection of all residues characterized in detail in Task I. The detailed characterization of several most promising samples produced in the presence of $SnCl_4$ under various pyrolysis parameter environments once again indicated that the gross model polymer structure was the same as those occurring in vacuum and pressure studies employing no catalyst (see Appendix B for details). However, as was the case for uncatalyzed vacuum and pressure data described in Sections 2.3.1 and 2.2.2.1, $\overline{M}_n$'s and/or bromine absorption data were different from each of the other environments studies. In the presence of $SnCl_4$, all samples studied gave an average value of $\overline{M}_n$ ~730 which corresponds almost exactly to incorporation of the elements of three moles of N-phenyl nadimide into the polymer structures (three moles of (I) = 717g). The bromine absorption values determined for the catalyzed pyrolysis residues were the lowest of any produced in the environments studied and showed that only one double bond occurred for each $\geq$3500 g/mol of polymer.

The data strong suggest that in the presence of $SnCl_4$ some (∿15%) of (I) undergoes the normal reverse Diels-Alder reaction, linear recombination and polymerization as follows:

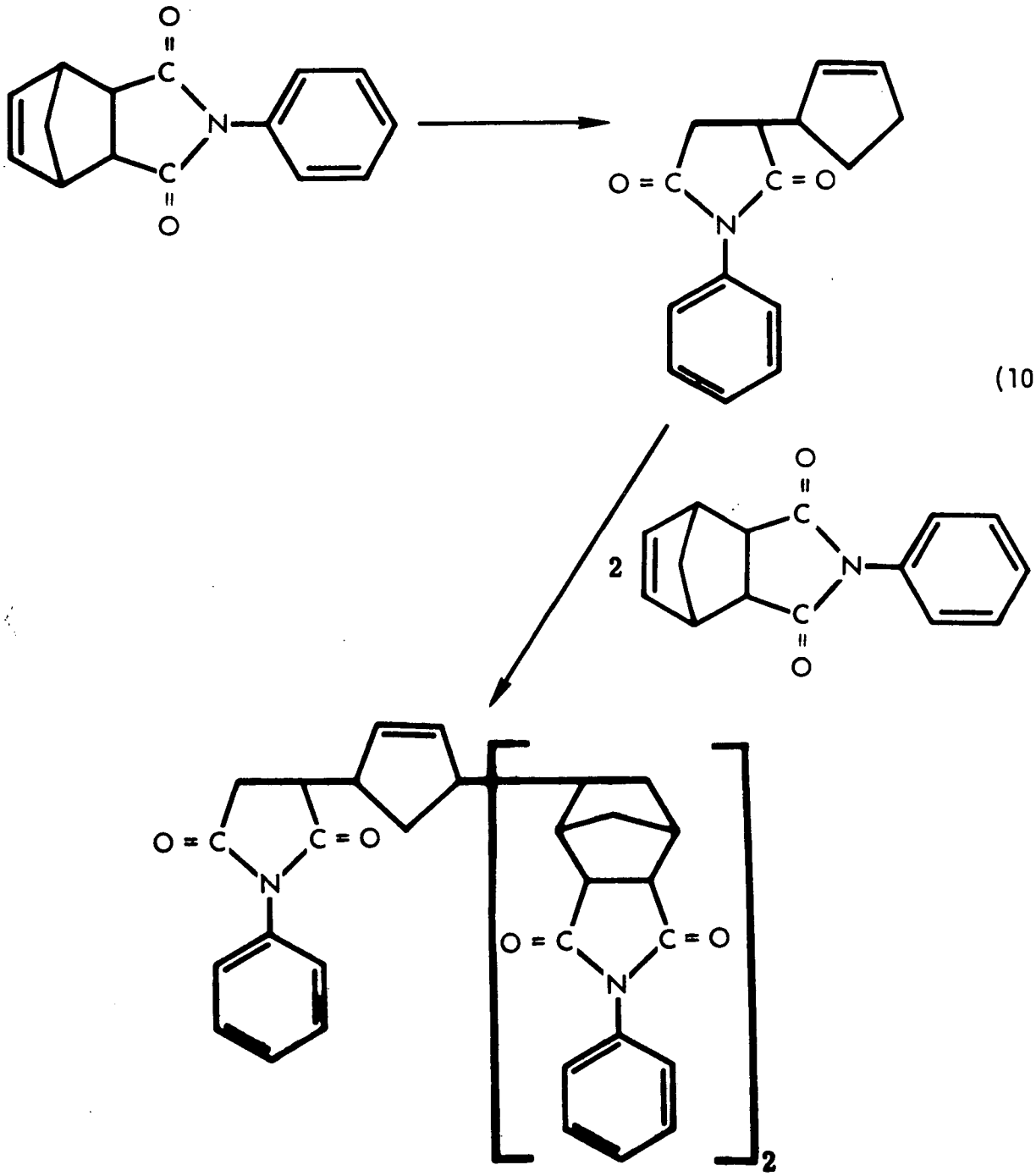

(10)

$\overline{M}_n$ = 717

but the predominant polymerization reaction occurring is homopolymerization of (I) in the presence of $SnCl_4$ as follows:

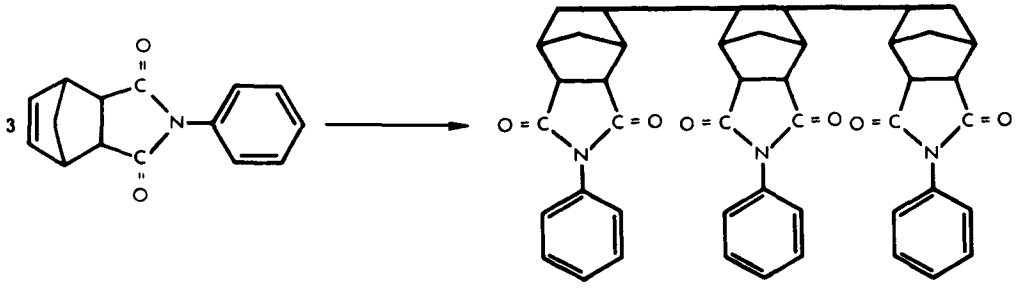

(11)

$$\overline{M}_n = 717$$

The predominance of the trimer of (I) which contains no cyclopentadiene entity or weak link from a double bond is an explanation why the catalyzed pyrolysis residues demonstrate equivalent TGA stability to the higher $\overline{M}_n$ products obtained in uncatalyzed vacuum and pressure environments which contain more double bond character from the cyclopentene polymer linkage.

### 2.2.3 Summary of Task I - Pyrolyses Conducted in Various Environments

It is strongly believed that the current model compound study described in this report reinforces the model compound polymerization mechanism originally postulated in NAS3-12412 (Reference 1). The same gross polymer structure results from pyrolysis studies conducted under vacuum, pressure or pressure plus catalyst environments which gives strong evidence that the reverse Diels-Alder reaction occurs initially to promote pyrolytic polymerization involving a maleic-cyclopentadiene adduct shown in Section 2.2 as Equation 4. The various environments only seem to affect degree of polymerization ($\overline{M}_n$) and apparent homopolymerization of the nadic capped species or nadic/maleic blends. In all environments studied, polymeric structures of

high initial thermo-oxidative stability ($\geq$589°K) were produced which is very similar in nature to that observed for actual A-type polymer formulations (see Sections 3 and 6).

The relative value of model compound studies has been clearly demonstrated in this program and has contributed significantly to identification and clarification of processing parameters and catalysts as follows:

- Requirement of 1.44 MN/m$^2$ pressure for adequate polymerization of nadic capped species.
- Requirement of 589°K polymerization temperature for polymerization to most promising nadic capped polymers.
- Non-requirement or significance of nadic/maleic end cap blends.
- Effectiveness of $SnCl_4$ catalyst for lowering required A-type polymer temperature and/or time processing parameters.

The model compound studies allowed rapid assessment of many alternative processing parameters and potential catalysts to be made, which would be impossible to duplicate in depth and scope if such experimentation were attempted on actual A-type polymer configurations. The direct use of the most promising processing/catalyst conditions for advancing the value of A-type polymers as neat resins and composite matrices is described in detail throughout the remainder of this report and particularly in Section 3.

The characterization information acquired from the most promising pyrolysis residues is tabularized and/or presented in graphic form in Appendix B. This information is described, presented and compared to provide clarification for both the experiments and their mechanistic interpretation.

The model studies discussed here provided much useful information on the requisite processing requirementsof nadic capped polymers. Further processing improvements using a new, but similar end cap were identified in Task V studies described in Section 6. Consequently, further work appears warranted in which new end caps designed specifically to lower required polymer processing parameters (e.g., cure temperature) are screened in model structures utilizing catalyst technology developed in this program.

# 3. TASK II - POLYMER SYNTHESIS AND CHARACTERIZATION

The objective of this task was to utilize the findings of Task I in A-type polyimide configurations; namely, investigate:

- The potential of employing nadic anhydride and maleic anhydride end cap blends to increase resin thermo-oxidative stability, and
- The effectiveness of the tin tetrachloride catalyst for improving processability/thermo-oxidative stability properties of A-type polymers.

The logical choice for an A-type polyimide backbone ingredients for study (see below) was a combination of pyromellitic dianhydride ($R_1$)

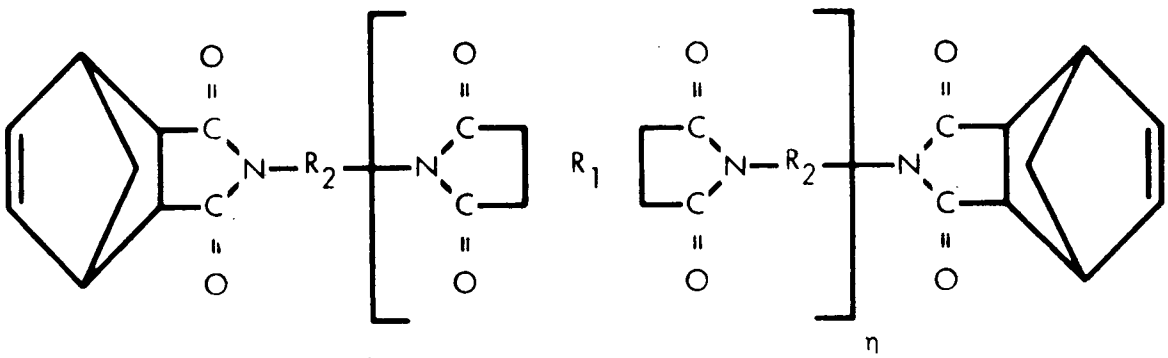

and methylene dianiline ($R_2$), formulated at stoichiometry to give a value of n equal to 1.4, thus providing a polyimide backbone identical to that of P10P. The P10P resin, denoting a 1000 formulated molecular weight (FMW) combination of NA, MDA and PMDA (1000 FMW NA/MDA/PMDA) was shown to possess highly promising thermo-mechanical properties and processing ease in both neat and press fabricated composite configurations in Contract NAS3-12412 (Reference 1) and NAS3-13203 (Reference 8). Further investigations of P10P were conducted in this program as discussed in Sections 4 - 6. These studies have identified areas for resin/composite improvement. It is anticipated such improvements will be achieved by the end cap blend/catalyst screening study described below.

## 3.1 PREPOLYMER SYNTHESIS STUDIES

The two A-type polyimide candidates selected for catalyst/molding studies as described above were prepared as amide-acid (A-A) varnishes in dimethyl formamide (DMF) at a 40% w/w solids loading employing standard procedures defined and described in Contract NAS3-13203 (Reference 8) from recrystallized MDA, PMDA, NA and/or MA ingredients. The A-A prepolymer

varnishes were converted to their corresponding imidized prepolymer form by first, thermal evaporation of the DMF followed by imidization under vacuum. Details of the varnish and imidized prepolymer synthesis methodology as well as appropriate chemical and structural characterization completed are provided in Appendix C.

## 3.2 POLYMER MOLDING (CURE) STUDIES

The conditions required for molding (curing) the neat 1000 FMW NA/MDA/PMDA and 95NA:5MA/MDA/PMDA prepolymer powders into highly consolidated cured specimens were studied in the presence and absence of tin tetrachloride catalyst. Studies conducted on each of the two A-type polyimide prepolymer formulations are described separately below.

### 3.2.1 Attempted Molding of 95NA:5MA/MDA/PMDA

The model compound studies which defined the apparently equivalent pyrolytic polymerization behavior and thermal properties of a 95:5 (w/w) blend of a nadic/maleic end cap to a 100% nadic end cap have been discussed in detail in Section 2. Because no distinct advantage for the blend over a homo-nadic capped species could be found in the model compound investigation, it was a necessary and logical step to study the fabrication behavior and subsequent property relationship of the 95NA:5MA blend in the realistic domain of actual A-type polymers.

The 95NA:5MA/MDA/PMDA powder was subjected to a neat resin plug fabrication screening study employing a fixed molding pressure of 3.44 $MN/m^2$ (500 psig) shown in all previous work, as well as the P10P composite studies (see Sections 4 and 5), to give a highly consolidated, acceptably cured specimen. The powder was repeatedly subjected to molding efforts at 3.44 $MN/m^2$ in a temperature range of 533°K-589°K (500°F-600°F) for time periods in the range of 0.5 to 1.0 hour employing 0 to 30 seconds dwell times, all shown to be effective for molding P10P. In no instance was a consolidated specimen produced of a quality on which a Barcol hardness measurement could be performed. Each specimen either crumbled during an attempted Barcol determination or was not consolidated to such an extent that removal from the mold was not possible. Because model compound studies showed no distinct advantage on this 95NA:5MA configuration over 100% NA, work was discontinued on the blend approach to allow additional effort on P10P. The highly

promising results of the PlOP/catalyst molding investigation is described in the following discussion.

3.2.2 Molding of PlOP Powder

As stated before, the high thermo-oxidative stability of the neat molded PlOP A-type polyimide formulation was established in Contracts NAS3-12412 (Reference 1) and NAS3-13203 (Reference 8). This fact and the failure of the 95NA:5MA/MDA/PMDA formulation to demonstrate any advantage over PlOP, made the latter a logical candidate for evaluation of the tin tetrachloride catalyst identified to be highly promising in the model compound studies described in Section 2.1.3.

Samples of PlOP prepolymer molding powder were subjected to a screening study in which neat resin plugs were fabricated in both the presence and absence of $SnCl_4$. The objective of this study was to investigate the efficacy of the catalyst to lower cure temperature and/or cure time, since the model studies gave evidence that both fabrication parameters could be lowered. Because the limited scope of this task and the previously defined performance of PlOP molded at low pressures (see Section 6) a molding pressure of 3.44 $KN/m^2$ (500 psi) was again selected as a fixed variable. During initial screening of molding parameter variations, the following observations were readily apparent employing either uncatalyzed PlOP powder or samples containing 1% (w/w) added $SnCl_4$:

- Highly consolidated specimens deemed adequately cured (i.e., Barcol hardness $\geq$50) could not be molded at a temperature below 589°K (600°F) either catalyzed or uncatalyzed.
- Highly consolidated specimens could not be molded from uncatalyzed PlOP in cure periods at 589°K of less than 0.5 hour.

The first observation was not unexpected, since prior studies on neat and reinforced specimens of PlOP showed that a molding temperature of 589°K was the minimum that gave acceptable products reproducibly. This temperature is evidently required to obtain melt and flow of the MDA/PMDA backbone in PlOP, even though model studies showed effective pyrolytic polymerization cure through the NA end cap at 561°K (550°F) in the presence of the $SnCl_4$ catalyst. Hence, molding temperature as a variable for investigation was eliminated, allowing the remainder of the study to screen the effect of $SnCl_4$

on reducing the cure time required at 589°K and 3.44 $MN/m^2$ to produce a highly consolidated P10P plug which possessed the high thermo-oxidative stability of this system demonstrated in Contracts NAS3-12412 (Reference 1) and NAS3-13203 (Reference 8).

A total of nine products were molded to investigate the potential of the $SnCl_4$ catalyst and compare performance with uncatalyzed specimens. The results of this investigation are presented in Table VI.

TABLE VI

RESULTS OF UNCATALYZED AND CATALYZED P10P MOLDING STUDIES[a]

| Sample Code | $SnCl_4$ Catalyst Level (% w/w) | Cure Time (Hr) | Product Barcol Hardness |
|---|---|---|---|
| 1 | 0.0 | 0.50 | 52 |
| 2 | 0.0 | 1.00 | 51 |
| 3 | 1.0 | 0.17 | 52 |
| 4 | 1.0 | 0.33 | 52 |
| 5 | 1.0 | 0.50 | 54 |
| 6 | 1.0 | 0.75 | 52 |
| 7 | 1.0 | 1.00 | 52 |
| 8 | 2.5 | 0.50 | 52 |
| 9 | 2.5 | 1.00 | 54 |

[a]Processed at a 589°K (600°F) cure temperature and a 3.44 $MN/m^2$ (500 psi) pressure

The following attributes of the $SnCl_4$ catalyst were apparent:

- The dispersion of catalyst in the powder (see Appendix C for details) caused no difficulty in fabrication methodology
- All specimens molded from P10P either catalyzed or uncatalyzed were of very high consolidation character as evidenced by Barcol hardness
- Catalyzed P10P powder could be molded in acceptable plugs for a cure duration of less than 0.5 hour

The final evidence that demonstrated the utility of the $SnCl_4$ catalyst was shown in isothermal aging studies performed on each of the nine PIOP samples. The aging study is discussed in Section 3.2.4. Other pertinent data on the specimens are provided in Appendix C, which includes structural assessment of the cured products.

### 3.2.3 Isothermal Aging Study on Molded PIOP Products

The efficacy of the $SnCl_4$ catalyst to promote rapid cure of the PIOP powder when molded at 589°K and 3.44 $MN/m^2$ into highly consolidated plugs was discussed in the previous section. However, rapid cure only demonstrated feasibility to reduce cure time and gave no insight as to the effect of decreased cure periods on the very important property of thermo-oxidative stability. Consequently, each of the nine plugs described in Table VI were isothermally aged in air at 589°K for a period of 500 hours. The results of this study are summarized in Table VII and displayed graphically in Figure 5. The data show several very interesting trends, some of which have been verified previously in Contracts NAS3-12412 (Reference 1) and NAS3-13203 (Reference 8), as well as other resin screening studies described herein (see Section 6). The most significant findings of this study are as follows:

- Uncatalyzed PIOP requires at least a one-hour cure duration to produce thermo-oxidative stable polymer.
- A 1% w/w $SnCl_4$ catalyst level is sufficient to promote cure rate enhancement of PIOP.
- Cure durations of >0.5 hours in the presence of $SnCl_4$ provide a less favorable product than shorter cure durations.
- All PIOP samples tested demonstrated excellent to acceptable stability in flowing air at 589°K (600°F).

Each of these findings are elaborated on below.

The uncatalyzed PIOP neat resin aging study conducted in this task has vividly demonstrated the high inherent thermo-oxidative stability of this A-type polyimide formulation when processed under a favorable set of conditions. The uncatalyzed PIOP specimen processed at 589°K cure temperature at a pressure of 3.44 $MN/m^2$ for one hour has once again demonstrated

TABLE VII

ISOTHERMAL AGING RESULTS AT 589°K CONDUCTED ON PIOP NEAT RESIN PLUGS[a]

| Sample[b] Code | Cure Time (Hr) | % $SnCl_4$ Catalyst Employed for Fabrication (w/w) | % Resin Weight Loss at Experimental Duration Points (Hr) | | | | | |
|---|---|---|---|---|---|---|---|---|
| | | | 68 | 118 | 161 | 257 | 330 | 500 |
| 1 | 0.5 | 0.0 | 5.1 | 7.5 | 9.6 | 14.0 | 16.9 | 24.0 |
| 2 | 1.0 | 0.0 | 1.9 | 2.4 | 2.7 | 3.4 | 3.8 | 4.8 |
| 3 | 0.17 | 1.0 | 2.2 | 3.0 | 3.4 | 4.7 | 5.7 | 7.9 |
| 4 | 0.33 | 1.0 | 2.3 | 3.0 | 3.5 | 4.7 | 5.8 | 8.3 |
| 5 | 0.50 | 1.0 | 2.7 | 3.5 | 4.1 | 5.2 | 6.1 | 8.4 |
| 6 | 0.75 | 1.0 | 2.7 | 3.6 | 4.4 | 6.0 | 7.4 | 11.0 |
| 7 | 1.0 | 1.0 | 2.2 | 3.5 | 4.2 | 5.9 | 7.6 | 11.8 |
| 8 | 0.5 | 2.5 | 3.6 | 5.3 | 6.3 | 9.5 | 12.3 | 20.7 |
| 9 | 1.0 | 2.5 | 3.9 | 4.9 | 5.7 | 7.3 | 8.7 | 24.0 |

[a]Isothermally aged in air (100 $cm^3$/min flow) in an apparatus and using methodology described in Appendix C.

[b]See Table VI for further description and sample data

the excellent thermo-oxidative stability established for this resin in Contracts NAS3-12412 and NAS3-13203. The total weight loss observed here of 4.8% compares favorably with the 2-6% observed in the prior programs under identical conditions. The requirement for a one-hour cure duration without catalyst is vividly shown by comparison of the 4.8% weight loss under this cure duration with the much greater (24%) measured for the uncatalyzed PIOP cured for 0.5-hour. A similar requirement for a cure pressure of 3.44 $MN/m^2$ can be readily seen by referring to Section 6, where in a similar effort conducted in screening of autoclavable A-type polyimide candidates, PIOP when processed at the same 589°K cure temperature and one-hour cure, but at 40% of the pressure (1.38 $MN/m^2$) demonstrated an unacceptable weight loss of 28% when aged under identical conditions. These findings also show that the high inherent thermo-oxidative stability at 589°K of neat molded PIOP resin is adversely affected by high modulus

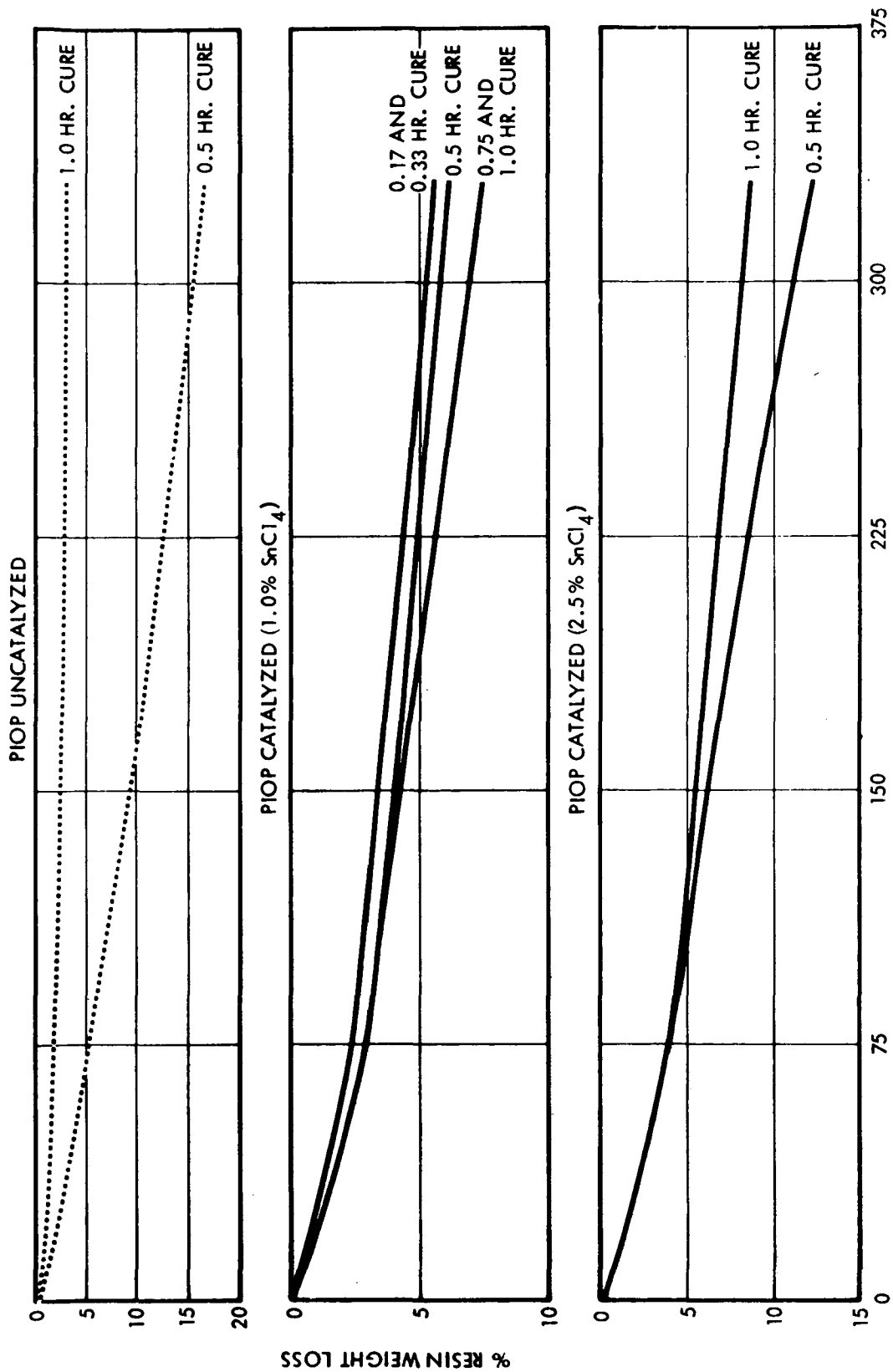


Figure 5. Isothermal Weight Loss of PIOP Resin Molded in the Presence and Absence of $SnCl_4$ Catalyst as a Function of Aging at 589°K in Air (100 $cm^3$/min flow)

graphite reinforcement as shown by similar aging studies conducted on P10P/Courtaulds HMS fiber reinforced composites as discussed in Section 4.

The result of the aging studies on P10P resin processed in the presence of $SnCl_4$ catalyst has definitely demonstrated that a 1% w/w level is sufficient to reduce significantly the cure time required to define a thermo-oxidatively stable neat resin specimen. This particular level of catalyst was selected for study because of model compound work (see Section 2.1.3), and although certainly a significant advancement in A-type polyimide processing art, further work is definitely needed for optimization of catalyst levels and tin catalysts derivatives (e.g., metal alkyls) in order to define the optimum trade-off between thermo-oxidative stability and processability. Similar investigations should be conducted on autoclavable A-type polyimide formulations (see Section 6) where the prepolymers will melt and flow below the 589°K required for P10P, consequently the effect of the catalyst to lower cure temperature shown in the model compound work appears to be significant. In the autoclave processing area, the reduction of required cure temperatures could be of greater significance than lowering of cure times for molding powder or press laminate applications.

The observation of reduced resin thermo-oxidative stability in the presence of catalysts during 0.5-hour cure durations is most probably associated with the large exothermic reaction observed at 589°K pyrolysis temperature for the model compound studies (see Section 2.1.3, Table IV and Figure 4). Because the rapid internal exotherm reaches a temperature of 644°K (700°F) sufficiently high to cause rapid thermally degradation of the aliphatic portion of the molecule, prolonged (ca., $\geq$0.5-hour) cure at the 589°K temperature required for P10P would of necessity cause *in situ* degradation as a function of excess cure time.

# 4. TASK III - PROCESS OPTIMIZATION STUDIES

The objective of this task was to optimize composite processing techniques developed during Contracts NAS3-12412 and NAS3-13203 (References 1 and 8) for PIOP varnish and Courtaulds HMS graphite fiber reinforcement. These studies included variations in press molding cycles as well as molding thicker laminates (3.18-mm) than that evaluated previously. Post-cure cycles of the resultant composites in a nitrogen atmosphere also were evaluated.

The most promising combinations of processing conditions was selected and employed to prepare composites for detailed evaluation in Task IV.

## 4.1 PRELIMINARY PROCESSING STUDIES

During the preliminary processing studies, techniques were developed which provided good fiber collimation and wetting while preparing prepreg tapes utilizing the Courtaulds HMS high modulus graphite fiber tows with the PIOP amide-acid varnish. Molding and imidizing cycles were screened to provide a limited number of variables for examination during the process optimization studies. Details of these experimental activities are provided in the following narrative.

### 4.1.1 Prepareg Preparation and Characterization

Courtaulds HMS* high modulus graphite fiber tows were impregnated with PIOP amide-acid varnish and collimated by drum winding at 31 to 32 tows/meter. Impregnation of the fibers was performed using a spray-gum mounted on the drum winding equipment. Resin content control was maintained by monitoring the quantity of resin deposited by the spray gun. Winding rate was 12.7 cm/sec on a 76.2 cm diameter drum.

It was observed that the prepregs prepared for the first study (imidization process study) appeared to possess dry fibers in the center of the bundles (tow). This was confirmed upon examination of broken cured composites prepared from these prepregs where there appeared to be a mixture of

*Courtaulds HMS tows are high modulus fibers ($\sim$35-40 GN/m$^2$) Tensile Modulus, 10,000 filaments per tow, pretreated to provide good fiber adhesion but without any organic (resin) size.

well and poorly wetted fibers. In order to enhance fiber wetting during impregnation, it was decided to evaluate solvent blends in the varnishes. Varnishes prepared utilizing solvent blends are detailed in Table VIII.

TABLE VIII
IMPREGNATING VARNISHES

| Constituent | Parts by Weight | | |
|---|---|---|---|
| | A | B | C |
| P10P (36% wt. Resin Solid in DMF) | 100 | 70 | 70 |
| DMF | 44 | 20 | 20 |
| Methanol | --- | 20 | 10 |
| MEK | --- | 10 | 20 |
| Total Resin Solids, % w/w | 25 | 21 | 21 |

Properties of prepregs prepared from these varnishes are provided in Table IX. It was observed during the preparation of subsequent batches of prepregs (reported in Table IX) that the fiber wetting was dependent upon the total amount of resin in the prepreg rather than upon the solvents used. The varnishes prepared using solvent blends provided equivalent properties in prepregs and composites as those varnishes using a single solvent system (DMF). Prepregs having resin solids contents less than 35% w/w contained poorly wetted fibers and had poor handling characteristics (e.g., low tack and poor tape integrity). Therefore, for the purpose of this task, it was concluded that the solvent blend varnishes offer no advantages.

Characterization of these prepregs consisted of volatile matter and resin solids content determinations. The volatile matter contents were determined by weight loss after exposure of 0.5 g prepreg sample in an air circulating oven at 589°K for 30 minutes. Resin solids contents were determined by acid digestion of the retained, cured, volatiles content specimen. Details of the characterization procedures are given in Appendix F.

### 4.1.2 Imidization Process Studies

Prepregs were cut into 7.61-cm square panels and stacked 12 plies high. A flat steel plate 0.318-cm thick, was laid on top of the stacked prepreg

TABLE IX

PHYSICAL PROPERTIES OF P10P/HMS PREPREG TAPES

| | Prepreg Batch Number | | | | | | | | | | | | | | | | |
|---|---|---|---|---|---|---|---|---|---|---|---|---|---|---|---|---|---|
| | 43 | 57 | 58 | 59 | 60 | 61 | 64 | 67 | 68 | 69 | 70 | 77 | 79 | 81 | 87 | 89 | 91 |
| P10P Varnish Batch No. | 15 | 25 | 25 | 25 | 25 | 25 | 25 | 25 | 25 | 25 | 25 | 55 | 55 | 55 | 55 | 61 | 61 |
| Varnish Dilution Formulation[a] | (b) | A | A | A | A | A | A | A | A | A | A | B | B | C | A | A | A |
| Drying Cycle °K/mins | 394/15 | 394/15 | 394/15 | 394/10 | 394/15 | 394/15 | 394/15 | 394/15 | 394/15 | 394/5 | 394/10 | 394/15 | 394/15 | 394/5 | 366/10 | 366/10 | 366/10 |
| Volatile Content % w/w | 20.9 | 12.0 | 19.3 | 22.8 | 18.1 | 15.7 | 9.2 | 8.5 | 23.4 | 13.2 | 17.9 | 15.3 | 7.9 | 25.2 | 21.3 | 24.5 | 24.3 |
| Resin Solids Content % w/w | 50.2 | 40.3 | 39.7 | 41.8 | 42.4 | 44.3 | 37.1 | 33.7 | 36.6 | 38.4 | 35.0 | 29.7 | 49.7 | 34.8 | 24.6 | 37.1 | 35.9 |

[a]See Table VIII

[b]Not diluted - as received 36% w/w resin solids

[approximately equivalent to 1.4 kN/m$^2$ (0.2 psi) pressure] to maintain the fibers in a flat and well-collimated condition. These prepreg stacks then were imidized in an air-circulating oven in accordance with a test matrix prescribed in Figure 6.

| Imidizing Time, Hours | Imidizing Temperature (°K) 422 | 436 | 450 | 464 | 478 |
|---|---|---|---|---|---|
| 1 | | | | X | X |
| 2 | | | X | X | X |
| 4 | | X | X | X | X |
| 8 | | X | X | X | |
| 16 | X | X | X | | |
| 40 | X | X | | | X |

X = Condition to be investigated

Figure 6. Imidizing Screening Matrix

The resultant imidized preforms were molded into 7.6 x 7.6 x 0.32-cm composite panels as follows:

> A 10.2 x 7.6-cm cavity mold was preheated to 589°K (600°F) on the electrically heated platens of a hydraulic press. The preforms were dropped into the open cavity of the preheated mold and the mold then was closed at a controlled rate so that the total time elapsed from when the preform first contacted the surface of the female mold to when pressure build-up commenced was between 15 to 30 seconds. A molding pressure of 3.45 MN/m$^2$ (500 psig) was applied and the composites were cured for 60 minutes. Upon completion of the cure cycle, pressure was released and the composites were cooled to <366°K (200°F) in the mold under light restraint (approximately 1.4 kN/m$^2$).
>
> The cured composites were machined into short-beam shear specimens 0.63 x 1.78-cm and tested in flexure at room temperature using a 4:1 span-to-depth ratio.

It was concluded from the results presented in Table X that the two most promising imidizing cycles worthy of further evaluation during the process variation studies were two hours at 478°K (400°F) and eight hours at 464°K (375°F). These selections were based upon the higher shear



20

TABLE X

PROPERTIES FROM IMIDIZING STUDIES

| Imidizing Cycle °K/Hr | Preform Weight Loss %[a] | Preform Resin Flow % w/w[b] | Shear Strength | | Composite Density g/cm$^3$ | Composite Resin Content % w/w | Composite Void Content % v/v | Composite Fiber Content % v/v |
|---|---|---|---|---|---|---|---|---|
| | | | Value[c] MN/m$^2$ | Std.Dev. MN/m$^2$ | | | | |
| 478/1 | 26.3 | 10.6 | 38.5 | 14.2 | 1.56 | 45.4 | 0.7 | 44.8 |
| 478/2 | 20.8 | 2.4 | 59.1 | 2.3 | 1.59 | 41.9 | 0.1 | 48.6 |
| 478/4 | 22.5 | <0.1 | 51.8 | 3.1 | 1.56 | 46.2 | 0.3 | 44.2 |
| 478/40 | 17.4 | 0.8 | (d) | (d) | 1.47 | 45.6 | 6.4 | 42.1 |
| 464/1 | 21.2 | 21.6 | 36.9 | 7.9 | 1.31 | 31.6 | 21.0 | 47.2 |
| 464/2 | 33.9 | 12.9 | 47.2 | 3.4 | 1.62 | 36.7 | 0.3 | 54.0 |
| 464/4 | 20.5 | 10.1 | 46.6 | 2.1 | 1.61 | 38.4 | 0.3 | 52.2 |
| 464/8 | 17.5 | 1.4 | 62.9 | 4.5 | 1.56 | 45.8 | 0.5 | 44.5 |
| 450/2 | 19.1 | 15.2 | 44.6 | 2.8 | 1.62 | 35.4 | 0.8 | 55.1 |
| 450/4 | 16.9 | 19.4 | 44.8 | 1.7 | 1.44 | 46.4 | 8.0 | 40.6 |
| 450/8 | 21.2 | 3.9 | 52.8 | 2.8 | 1.57 | 46.5 | -0.4 | 44.2 |
| 450/16 | 17.0 | 6.2 | 35.6 | 2.9 | 1.58 | 33.2 | 4.1 | 55.6 |
| 436/4 | 16.6 | 19.2 | 29.0 | 0.8 | 1.63 | 29.7 | 2.5 | 60.3 |
| 436/8 | 22.3 | 4.6 | 49.0 | 2.9 | 1.58 | 45.3 | -0.5 | 45.5 |
| 436/16 | 16.8 | 16.0 | 31.2 | 4.1 | 1.64 | 35.5 | -0.5 | 55.7 |
| 436/40 | 15.6 | 14.2 | 20.0 | 0.4 | 1.63 | 35.6 | 0.1 | 55.2 |
| 422/16 | 17.8 | 11.8 | 37.4 | 0.6 | 1.66 | 39.9 | 3.5 | 52.5 |
| 422/40 | 16.7 | 11.9 | 23.3 | 2.1 | 1.58 | 42.4 | 0.6 | 47.9 |

[a]Weight loss during imidizing cycle

[b]Determined on cured composite test panel

[c]Tested in quintuplicate

[d]Delaminated during machining

strengths 59.3 MN/m$^2$ (8.6 Ksi) and 63.4 MN/m$^2$ (9.2 Ksi), respectively, in combination with low void contents (∿0.1 and ∿0.5% v/v, respectively), obtained when using these cycles. Graphical presentation of the effects of imidizing cycles upon shear strengths is provided in Figure 7.

It is of interest to note that cycles of two hours at 478°K and forty hours at 422°K (300°F) produced composites of similar fiber volume (48.6 and 47.9% v/v) and with similar void contents (0.1 and 0.6% v/v) but with great differences in shear strengths 59.2 MN/m$^2$ (8.6 Ksi) and 23.4 MN/m$^2$ (3.4 Ksi). In general, these data indicate (Figure 7) that prepregs exposed to prolonged thermal treatments in the 422°K to 478°K temperature range produce low shear strength composites. Furthermore, it appears that at 478°K, the imidizing time cycle becomes quite critical and is probably optimum at some time between one to four hours. The 63.4 MN/m$^2$ (9.2 Ksi) shear strength obtained through the eight hours at 464°K cycle is considered acceptable since this shear strength is at the same level as the best reported for epoxy/HMS graphite composites.

### 4.1.3 Process Variation Studies

Imidized preforms were prepared from prepreg tapes in the same manner as described in Section 4.1.2 and using the two selected imidizing cycles (2 hours at 478°K and 8 hours at 464°K). A cascading fractional factorial screening study was performed in order to define the most effective combination of processing conditions (imidizing and molding). The first step in this study explored combinations of the two imidizing cycles, two cure temperatures (561°K and 589°K), and two molding pressures (1.38 MN/m$^2$ and 3.45 MN/m$^2$). Details of this matrix are provided in Figure 8. Composites were molded in the same manner as described in Section 4.1.2 and evaluated for shear strength by the short beam flexural method at room temperature. Results of this screening matrix are reported in Table XI and the least squares statistical analysis of the results of shear strength data is presented in Table XII. It is seen that the cure temperature is the most significant variable in affecting the shear strength. From Table XI it is seen that the 589°K cure temperature had the most influence in providing the best properties for this study. Furthermore, it is assumed that low molding pressures (e.g., 1.38 MN/m$^2$) are unsatisfactory because all of the

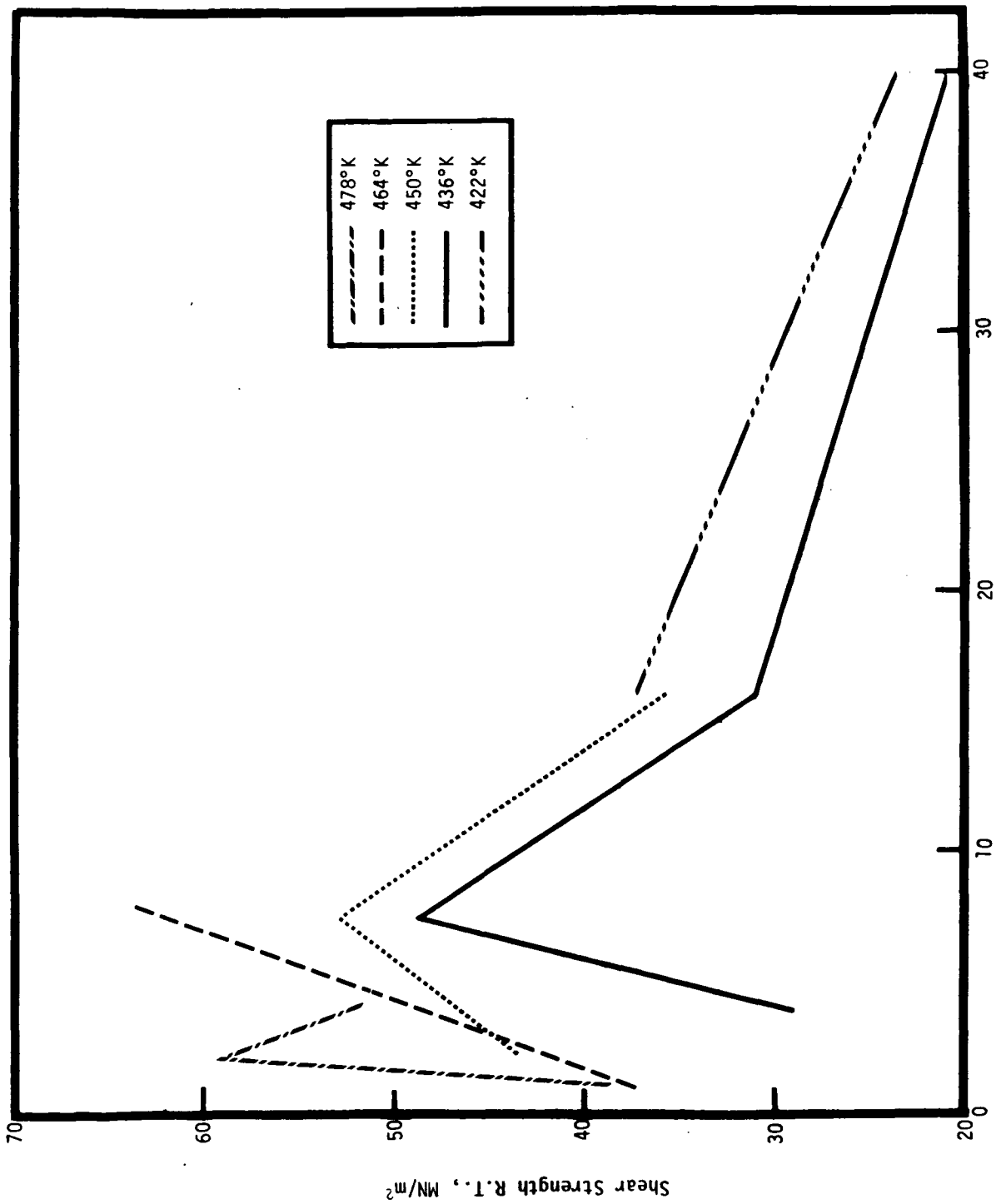


Figure 7. Effect of Imidizing Cycles Upon Shear Strength

| Experiment | Factors/Condition[a] | | | |
|---|---|---|---|---|
| | A | B | C | D |
| 1 | - | - | - | - |
| 2 | + | - | - | + |
| 3 | - | + | - | + |
| 4 | + | + | - | - |
| 5 | - | - | + | + |
| 6 | + | - | + | - |
| 7 | - | + | + | - |
| 8 | + | + | + | + |

Figure 8. Processing Studies Matrix

[a]Code for Factors/Conditions Matrix

| Factor | Condition | Step 1 | | Step 2 | |
|---|---|---|---|---|---|
| | | + | - | + | - |
| A | Cure temperature (°K) | 589 | 561 | 603 | 589 |
| B | Cure time, mins. | 60 | 30 | 60 | 30 |
| C | Molding pressure ($MN/m^2$) | 3.45 | 1.38 | 6.89 | 3.45 |
| D | Imidizing cycle, °K/Hrs | 478/2 | 464/8 | 478/2 | 464/8 |

shear strengths reported in Table XI are considerably lower than those reported in Table X where 6.89 $MN/m^2$ (1000 Psi) molding pressure was employed.

In Step 2 of the cascading fractional factorial screening study, it was decided to investigate a higher molding temperature and pressure than in Step 1 while keeping the cure times and imidizing cycles the same. Processing condition details of this second step also are provided in Figure 3. The composites again were molded in the same manner as in 4.1.2 and room temperature shear strengths were determined. Data from this step in the processing study are provided in Table XIII and the results of a statistical analysis are presented in Table XIV. It is seen from these data that no one factor has a statistically significant effect on the shear strength although the imidizing cycle is the most sensitive variable. The higher fiber contents obtained in these composites (~60% v/v) compared with those in the imidizing study (~50% v/v) appear to result (as expected) in lower shear strengths

TABLE XI

PROPERTIES FROM PROCESSING STUDIES - STEP 1

| Imidizing Cycle °K/Hr. | Prepreg Batch[a] | Preform Weight Loss[b] %w/w | Cure Temperature °K | Cure Time, Min | Molding Pressure $MN/m^2$ | Resin Flow[c] % w/w | Composite Shear Strength | |
|---|---|---|---|---|---|---|---|---|
| | | | | | | | Value $MN/m^2$ | Std. Dev. $MN/m^2$ |
| 464/8 | Mixtures of Batches 57, 58 & 61 | 14.2 | 561 | 30 | 1.38 | 0.6 | 27.3 | 0.8 |
| 478/2 | | 15.5 | 589 | 30 | 1.38 | 2.0 | 38.2 | 1.4 |
| 478/2 | | 16.1 | 561 | 60 | 1.38 | 4.3 | 36.3 | 1.4 |
| 464/8 | | 14.7 | 589 | 60 | 1.38 | 1.1 | 40.4 | 1.7 |
| 478/2 | | 13.8 | 561 | 30 | 3.45 | 5.0 | 33.4 | 2.8 |
| 464/8 | | 16.4 | 589 | 30 | 3.45 | 1.5 | 42.3 | 1.0 |
| 464/8 | | 13.6 | 561 | 60 | 3.45 | 3.2 | 32.2 | 1.3 |
| 478/2 | | 15.3 | 589 | 60 | 3.45 | 1.3 | 36.1 | 1.2 |

[a]See Table VIII

[b]Weight loss during imidizing cycle

[c]Determined on cured composite test panel

[d]Determined in quintuplicate

TABLE XII

STATISTICAL ANALYSIS[a] OF TABLE V SHEAR STRENGTH DATA

| Comparison | Total | Effect | Degrees of Freedom | Sum of Squares | "F" Test Ratio |
|---|---|---|---|---|---|
| A | 4030 | 1007.5 | 1 | 2030112 | 4.73[b] |
| B | 570 | 142.5 | 1 | 40612 | 0.096 |
| C | 230 | 57.5 | 1 | 6612 | 0.016 |
| D | 250 | 62.5 | 1 | 7812 | 0.018 |
| AB, CD | -1710 | -365.0 | 1 | 365512 | - |
| AC, BD | -310 | -77.5 | 1 | 12012 | - |
| AD, BC | -2710 | -677.5 | 1 | 918012 | - |

[a]"F" Test, Ref. 9.

[b]A value of F = 5.54 is significant at the 90% confidence level

It was decided, therefore, that the conditions to be examined in the following process optimization studies would consist of:

- Imidizing cycles - 8 hours at 464°K (375°F) and 2 hours at 478°K (400°F)
- Curing cycle - 1 hour at 589°K (600°F)
- Molding pressures - 3.45 $MN/m^2$ (500 psi) and 6.89 $MN/m^2$ (1000 psi)
- Composite fiber contents - ∿50 and 60% v/v

TABLE XIII

PROPERTIES FROM PROCESSING STUDIES - STEP 2

| Imidizing Cycle °K/Hrs | Preform Weight Loss,[a] % w/w | Molding Cycle | | | Resin Flow, % w/w[b] | Composite Shear Strength | | Composite | | | |
|---|---|---|---|---|---|---|---|---|---|---|---|
| | | Temperature °K | Time, Min | Pressure MN/m$^2$ | | Value MN/m$^2$[c] | Std. Dev. MN/m$^2$ | Density g/cm$^3$ | Resin Content % w/w | Void Content % v/v | Fiber Content % v/v |
| 464/8 | 12.9 | 589 | 30 | 3.45 | 2.2 | 59.6 | 0.8 | 1.65 | 32.8 | 0.01 | 58.4 |
| 478/2 | 11.9 | 603 | 30 | 3.45 | 4.7 | 52.1 | 1.6 | 1.62 | 33.5 | 1.55 | 56.7 |
| 478/2 | 11.6 | 589 | 60 | 3.45 | 3.6 | 45.7 | 2.3 | 1.63 | 32.8 | 1.23 | 57.7 |
| 464/8 | 12.4 | 603 | 60 | 3.45 | 2.4 | 53.6 | 4.7 | 1.65 | 31.3 | 0.62 | 59.7 |
| 478/2 | 11.6 | 589 | 30 | 6.89 | 6.9 | 50.7 | 2.8 | 1.65 | 29.5 | 1.34 | 61.2 |
| 464/8 | 11.1 | 603 | 30 | 6.89 | 5.2 | 54.2 | 3.5 | 1.64 | 32.2 | 0.86 | 58.5 |
| 464/8 | 11.6 | 589 | 60 | 6.89 | 3.1 | 54.8 | 1.1 | 1.66 | 32.5 | -0.47 | 59.0 |
| 478/2 | 13.1 | 603 | 60 | 6.89 | 5.5 | 52.3 | 3.5 | 1.64 | 29.1 | 2.09 | 61.2 |

[a]Weight loss during imidizing cycle

[b]Determined on cured composite test panels

[c]Determined in quintuplicate



CR 72984
16402-6012-RO-00

TABLE XIV

STATISTICAL ANALYSIS[a] OF SHEAR STRENGTH DATA

| Comparison | Total | Effect | Degrees of Freedom | Sum of Squares | "F" Test Ratio |
|---|---|---|---|---|---|
| A | 180 | 45 | 1 | 4050 | 0.016 |
| B | -1480 | -370 | 1 | 273800 | 1.049 |
| C | 120 | 50 | 1 | 1800 | 0.007 |
| D | -3140 | -785 | 1 | 1232450 | 4.721[b] |
| AB, CD | 1360 | 340 | 1 | 231200 | - |
| AC, BD | 80 | 20 | 1 | 800 | - |
| AD, BC | 2100 | 52.5 | 1 | 551250 | - |

[a]"F" Test, Ref. 9.

[b]A value of F = 5.54 is significant at the 90% confidence level

## 4.2 PROCESS OPTIMIZATION STUDIES

Six panels were molded from prepreg Batches 77, 79, 81, 87, 89 and 91 using the same techniques as discussed in Section 4.2. These panels were 13-cm long x 23-cm wide and 12-ply thick (0.32-cm thick), the mold cavity in this case was 20-cm long x 23-cm wide. Ten flexural specimens 1.3-cm wide x 13-cm long and 10 short-beam shear specimens 0.64-cm wide x 2.54-cm long were machined from the cured panels. Half of the number of specimens were tested at room temperature and the remainder were tested at 589°K. Shear strengths were determined using a 32:1 span-to-depth ratio. Fiber volumes of the composites ranged between 51.5 and 60.6% which approximate the target values (50 to 60%).

The resultant mechanical properties presented in Table XV, indicated that the two hours/478°K imidizing cycle, one hour/589°K cure cycle and 3.45 $MN/m^2$ molding pressure was the most promising process. Highest room temperature and 589°K shear strength values were obtained with this process. Flexural strengths at room temperature and 589°K were not significantly different to show any influence from processing and the flexural moduli appeared

TABLE XV
RESULTS OF PROCESS OPTIMIZATION STUDIES

| | | Panel Number | | | | | |
|---|---|---|---|---|---|---|---|
| | | 1 | 2 | 3 | 4 | 5 | 6 |
| Processing Conditions | Imidizing Cycle (°K) Hr | 464/8 | 464/8 | 478/2 | 478/2 | 478/2 | 478/2 |
| | Molding Pressure $MN/m^2$ | 3.45 | 6.89 | 3.45 | 6.89 | 3.45 | 6.89 |
| Physical Properties | Resin Content, % 2/2 | 35.1 | 30.6 | 33.2 | 33.3 | 38.8 | 38.3 |
| | Density, $g/cm^3$ | 1.56 | 1.66 | 1.65 | 1.65 | 1.60 | 1.56 |
| | Void Content, % v/v | 4.6 | 0.3 | 0.1 | 0.2 | 0.7 | 0.3 |
| | Fiber Volume, % v/v | 53.3 | 60.6 | 58.0 | 57.9 | 51.5 | 52.3 |
| Shear Properties | Strength at 297°K $MN/m^2$ | 54.1 | 53.0 | 63.9 | 62.9 | 63.5 | 54.0 |
| | Std. Dev. 297°K $MN/m^2$ | 1.41 | 4.8 | 0.6 | 1.3 | 3.5 | 1.3 |
| | Strength at 589°K $MN/m^2$ | 38.5 | 35.5 | 39.9 | 35.2 | 45.4 | 37.1 |
| | Std. Dev. 589°K $MN/m^2$ | 0.5 | 0.9 | 2.6 | 6.6 | 6.0 | 1.4 |
| Flexural Properties[b] | Strength at 297°K $MN/m^2$ | 728 | 721 | 730 | 694 | 752 | 769 |
| | Std. Dev. 297°K | 67 | 16 | 50 | 43 | 50 | 37 |
| | Strength at 589°K $MN/m^2$ | 653 | 665 | 691 | 645 | 738 | 689 |
| | Std. Dev. 297°K | 56 | 37 | 49 | 21 | 36 | 49 |
| | Modulus at 589°K $GN/m^2$ | 163 | 168 | 168 | 169 | 160 | 159 |
| | Std. Dev. 297°K | 10 | 10 | 12 | 11 | 10 | 6 |
| | Modulus at 589°K $GN/m^2$ | 161 | 180 | 172 | 183 | 163 | 154 |
| | Std. Dev. 297°K | 5 | 6 | 11 | 5 | 6 | 6 |

[a]Molded for 60 minutes at 589°K

[b]Quintruplicate replication

to be influenced mainly by differences in fiber volumes. Void contents for most of the panels were low (<1.0%) except in one case where 4% v/v was measured.

Based upon these findings, the following processing conditions for the post cure studies were selected:

- o Imidizing cycle two hours at 478°K
- o Molding pressure 3.45 $MN/m^2$
- o Cure cycle 60 minutes at 589°K

## 4.3 POST CURE STUDIES

Five 13-cm long x 23-cm wide x 12-ply thick (0.32-cm thick) panels were molded from prepreg prepared in accordance with the selected conditions: a) imidizing cycle of two hours at 478°K in an air-circulating oven, and b) molding cycle of one hour at 589°K under 3.45 $MN/m^2$ positive pressure. Flexural properties at room temperature were determined in triplicate and shear strengths at room temperature were determined in quintruplicate on each panel prior to post cure. These results, together with resin contents, fiber volumes and void contents from the fractured specimens are presented in Table XVI. Four panels then were post cured in a flowing nitrogen atmosphere (0.084 $m^3/hr$) in accordance with the matrix provided in Table XVII. All four panels were weighed before and after post cure but in all cases displayed no weight loss during post cure. Each panel then was machined into six flexural test specimens and ten short-beam shear specimens.

TABLE XVI
INITIAL PROPERTIES OF PANELS FOR POST CURE SCREENING

| Panel Number | 1 | 2 | 3 | 4 |
|---|---|---|---|---|
| Resin Content, % w/w | 42.1 | 43.2 | 40.0 | 39.7 |
| Fiber Volume, % v/v | 47.8 | 47.4 | 51.1 | 50.2 |
| Void Content, % v/v | -2.02 | -0.05 | -0.90 | 1.42 |
| Flexural Strength, $MN/m^2$ | 578 | 669 | 672 | 675 |
| Flexural Modulus, $GN/m^2$ | 150 | 160 | 158 | 157 |
| Shear Strength, $MN/m^2$ | 54 | 57 | 54 | 53 |

Specimens of each configuration (3 flexural and 5 shear) from each panel including the non-post cured panels, were isothermally aged for 336 hours in a 589°K air circulating oven having an air velocity of 127 cm/sec and an air change rate of 0.19 $m^3$/sec.

TABLE XVII
POST CURE SCREENING MATRIX[a]

| Post Cure Temperature, (°K) | Post Cure Time, Hours | |
|---|---|---|
| | 8 | 16 |
| 589 | x | x |
| 616 | x | x |

[a]All post cure cycles were performed in a nitrogen atmosphere

Properties of these specimens were determined after the above aging period and are compared with the properties of unaged specimens in Table XVII. It is seen from these data that the eight hours post cure cycle at 616°K (650°F) had the greatest influence in improving composite 589°K (600°F) shear and flexural strengths.

These findings led to the selection of this post cure cycle for inclusion in the extended press cure cycle evaluation. Subsequently, a 12.7-cm long x 22.9-cm wide x 12-ply thick panel was molded using a press cycle of one hour at 589°K under 3.45 $MN/m^2$ pressure followed immediately by eight hours at 616°K under 3.45 $MN/m^2$ pressure. Final properties for this panel are included in Table XVIII.

The results reported in Table XVIII were assessed together with findings obtained by TRW Equipment Laboratories under Contract NAS3-13203 (Reference 8) to ascertain the desirability of post cure. Table XVIII shows that an 8-hour 616°K post cure gave a marginal improvement in properties over that which might be attributed to inherent experimental variations and that a longer (16 hours) 616°K post cure cycle significantly degraded the properties on aging. In

# TABLE XVIII
## POST CURE STUDY RESULTS

| Properties | Post Cure Cycle: NONE | | 8/589[a] | | 16/589[a] | | 8/616[a] | | 16/616[a] | | 8/616[b] | |
|---|---|---|---|---|---|---|---|---|---|---|---|---|
| | Unaged | Aged[c] | Unaged | Aged[c] | Unaged | Aged[c] | Unaged | Aged[c] | Unaged | Aged[c] | Unaged [j] | Aged[c] |
| Resin Content, % w/w | 39.0 | 38.0 | 43.2 | 40.0 | 42.1 | 40.6 | 39.7 | 35.4 | 40.0 | 38.3 | 39.6 | 37.8 |
| Density, g/cm$^3$ | 1.61 | 1.63 | 1.59 | 1.62 | 1.63 | 1.61 | 1.58 | 1.63 | 1.62 | 1.63 | 1.60 | 1.63 |
| Fiber Volume, % v/v | 51.7 | 53.2 | 47.4 | 51.2 | 47.8 | 50.3 | 50.2 | 55.4 | 51.2 | 52.9 | 51.0 | 53.5 |
| Void Content, % v/v | 0.01 | -0.83 | -0.36 | -1.00 | -2.45 | -0.61 | 1.61 | 0.20 | -1.00 | -0.8 | 0.21 | -1.0 |
| SHEAR STRENGTH | | | | | | | | | | | | |
| at 298°K, MN/m$^2$ | 61.6 [j] | -- | 57.2 | -- | 54.4 | -- | 53.1 | -- | 53.7 | -- | 53.2 [j] | -- |
| at 589°K, MN/m$^2$ | 40.8 | 30.8 | 42.3 | 27.4 | 41.2 | 31.3 | 45.5 | 34.5 | 30.0 | 27.6 | 31.9 [j] | 38.5 |
| Retention, % [d] | 66 | 50 | 74. | 48. | 76. | 57. | 86. | 65. | 56. | 52. | 60. | 72. |
| Type of Failure | g | f | g | f | g | f | g | f | g | f | g | f |
| Weight Loss, % w/w [e] | 0 | 5.0 | 0 | 7.1 | 0 | 6.5 | 0 | 5.4 | 0 | 7.7 | 0 | 4.9 |
| FLEXURAL STRENGTH | | | | | | | | | | | | |
| at 298°K, MN/m$^2$ | 747 [j] | -- | 669 | -- | 578 | -- | 675 | -- | 672 | -- | 679 [j] | -- |
| at 589°K, MN/m$^2$ | 679 | 609 | 677 | 606 | 707 | 584 | 706 | 650 | 606 | 384 | 447 | 577 |
| Retention, % [d] | 90 | 81 | 101 | 90. | 121. | 104. | 105. | 97. | 90. | 57. | 66. | 85. |
| Weight Loss, % w/w [e] | 0 | 3.7 | 0 | 4.3 | 0 | 4.6 | 0 | 3.9 | 0 | 4.9 | 0 | 3.2 |
| FLEXURAL MODULUS | | | | | | | | | | | | |
| at 298°K, GN/m$^2$ | 146 [j] | -- | 160 | -- | 150 | -- | 157 | -- | 158 | -- | 168 [j] | -- |
| at 589°K, GN/m$^2$ | 173 | 143 | 162 | 139 | 167 | 136 | 157 | 143 | 132 | 134 | 133 [j] | 150 |
| Retention, % [d] | 119 | 97 | 100 | 87 | 111 | 91 | 100 | 91 | 83 | 85. | 79. | 89. |

[a] Post cured in a flowing nitrogen atmosphere (24 cm$^3$/sec)

[b] Post cured under molding pressure (3.45 MN/m$^2$) in a press

[c] Aged specimens were exposed to a 589°K flowing air atmosphere (127cm/sec) for 336 hours

[d] Calculated 100 . $\frac{\text{Property at 589°K}}{\text{Property at 298°K (as molded)}}$

[e] Calculated 100 . $\frac{\text{Weight after aging}}{\text{Weight as molded}}$

[f] Shear failure - delamination at ends of specimen

[g] Tensile failure - tensile failure in outer fibers of specimen

[h] Compound failure - delamination in center of specimen

[j] Tested on Cal-Tester

Contract NAS3-13203 it was determined that a 2-hour 616°K (650°F) inert environment post cure of graphite reinforced laminates molded at 616°K provided a statistically significant enhancement of properties. Consequently, it was decided mutually by the NASA and TRW Project Managers to use a 2-hour 616°K nitrogen environment post cure cycle for Task IV studies.

# 5. TASK IV - OXIDATIVE DEGRADATION STUDIES

The objective of this task was to gain insight into the chemical mechanisms operative in the thermo-oxidative degradation of the A-type polyimide polymer. Studies were conducted to determine the thermo-mechanical stability of Courtaulds HMS graphite fiber reinforced PlOP composites in the form of flexural strength and modulus as a function of oxidative environment, temperature and applied load. During the course of the study, a significant stress relaxation was observed and originally planned activities for correlating mechanical property determinations with specific chemical mechanisms were eliminated in order to concentrate on defining the limits of the thermal creep phenomena. Details of the oxidative degradation studies are presented below.

## 5.1 PREPARATION OF TEST SPECIMENS

Twelve graphite composite panels consisting of Courtaulds HMS graphite fiber tows and PlOP polyimide resin were prepared by the process selected during the Task III studies as described in the preceding section.

Courtaulds HMS graphite fiber tow was impregnated with PlOP amide-acid solution and collimated to 31 to 32 tows/meter by drum winding. The prepreg tape then was dried initially by rotating on the winding drum under heat lamps for thirty minutes after which it was removed and treated in an air-circulating oven for twenty minutes at 364°K (200°F). Nominal properties of these tapes were 35% w/w resin solids and 25% w/w volatile matter contents. These prepreg tapes then were cut and stacked 12.7-cm long by 22.9-cm wide by 11-ply (0.32-cm thick). Each stack consisted of a random selection of prepreg tapes. The stacked material was imidized in an air-circulating oven by a two-hour cycle at 478°K (400°F). Molding of the imidized preforms was performed by dropping the stack into a mold preheated to 589°K (600°F) and applying 3.45 $MN/m^2$ (500 psig) pressure within 15 to 20 seconds. The composites were cured for sixty minutes after which the pressure was released and the panel was cooled to below 450°K (350°F) under slight restraint before removal from the mold. These panels were post cured in a flowing nitrogen atmosphere [25-$cm^3$/sec at 616°K (650°F) for two hours].

## 5.2 PRE-AGING CHARACTERIZATION

Random sampling from the molded panels was made during this effort in order to check the shear strength, fiber content and void content. These findings are provided in Table XIX. All twelve panels were machined into flexural test coupons 1.27-cm wide by 12.7-cm long (15 coupons per panel) to provide a total of 180 coupons.

TABLE XIX

PROPERTIES OF RANDOMLY SAMPLED P10P COURTAULDS HMS GRAPHITE COMPOSITES

| Sample No. | Fiber Content % v/v | Void Content % v/v | Shear Strength | |
|---|---|---|---|---|
| | | | Avg. Value $MN/m^2$ | Std. Dev. $MN/m^2$ |
| 1 | 44.1 | 2.7 | 54 | 9 |
| 2 | 47.1 | 0.3 | 62 | 5 |
| 3 | 48.1 | 3.8 | 46 | 7 |
| 4 | 49.9 | 0.1 | 54 | 10 |
| 5 | 46.9 | 6.3 | 54 | 17 |

Room temperature flexural properties were determined in sextruplicate for three of the panels and in triplicate for the remaining nine panels. Data are summarized in Table XX. The raw detailed data are presented in Appendix E together with a flexural strength distribution curve.

## 5.3 STRESSED DEGRADATION STUDIES

It was originally planned to obtain the individual room temperature flexural strength of each specimen by interpolating and extrapolating from the data presented in Table XXI. However, because the plots of the data did not exhibit uniform trends, it was concluded that reliable interpolations and extrapolations could not be performed. Therefore, an alternative procedure was sought that would provide reliable base-line values.

During subsequent analysis of the available data, it was observed that 90% of all values obtained fell within three times the standard deviation for the properties of each panel. Therefore, it was decided that a reliable nominal flexural strength value could be obtained by using the average flexural strength of each panel minus three times the standard deviation for the flexural strength.

TABLE XX

SUMMARY OF FLEXURAL PROPERTIES FOR P10P/GRAPHITE PANELS

| Panel Number | Replicates | Strength | | Modulus | |
|---|---|---|---|---|---|
| | | Average $MN/m^2$ | Std. Dev. $MN/m^2$ | Average $GN/m^2$ | Std. Dev. $GN/m^2$ |
| 72-2 | 3 | 706 | 57 | 152 | 10 |
| 72-1 | 3 | 754 | 85 | 151 | 8 |
| 71 | 3 | 760 | 25 | 139 | 1 |
| 70-2 | 3 | 866 | 51 | 145 | 2 |
| 70-1 | 3 | 845 | 43 | 142 | 4 |
| 67 | 6 | 693 | 19 | 156 | 8 |
| 66 | 3 | 572 | 38 | 143 | 3 |
| 65 | 6 | 663 | 50 | 146 | 8 |
| 74-2 | 3 | 829 | 83 | 154 | 10 |
| 74-1 | 6 | 874 | 34 | 161 | 4 |
| 73-2 | 3 | 721 | 48 | 150 | 6 |
| 73-1 | 3 | 770 | 54 | 150 | 1 |
| Overall Avg. | 45 | 752 | 45[a] | 150 | 5.4[a] |

[a]Pooled Standard Deviation

TABLE XXI

PANEL RESIN CONTENT SUMMARY

| Coupon Code | Resin Content (% w/w) | Coupon Code | Resin Content (% w/w) |
|---|---|---|---|
| 65 | 43.2 | 72-1 | 43.9 |
| 66 | 47.2 | 72-2 | 43.0 |
| 67 | 45.7 | 73-1 | 42.6 |
| 70-1 | 47.3 | 73-2 | 39.6 |
| 70-2 | 43.2 | 74-1 | 39.7 |
| 71 | 40.4 | 74-2 | 43.4 |
| Average | 44.5 | Average | 43.0 |

$$\text{Nominal } F_u = \overline{X} - 3\sigma$$

Using this approach, the nominal flexural strengths for twelve specimens were defined (see Table XX). Flexural strengths at 589°K were assumed to be 80% of the above values and the stress/strain slope (M) was assumed to be constant over this temperature range (R.T. to 589°K).

The twelve selected specimens then were stressed to 50% of their calculated (589°K) ultimate strength (40% of the nominal flexural strength) by loading them into restraining jigs (illustrated in Figure 9). A Cal-tester

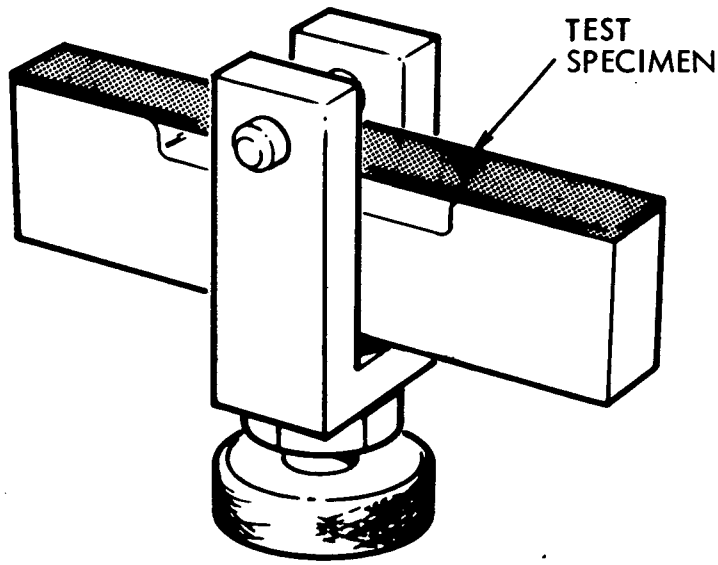


Figure 9. Restraining Jig

apparatus was employed to apply the desired load at room temperature (see Table XXII). The span-to-depth ratio for each loaded specimen was 32:1.

During the ensuing stressed degradation studies, stress relaxation was observed. The stressed specimens developed a permanent set after two days at 589°K. Stress relaxation occurred, which resulted in loosening of the specimen in the fixture upon cooling to room temperature. These specimens then were reloaded and again subjected to 589°K exposure. After two days exposure, further stress relaxation occurred. It was obvious from these results that specimens could not be maintained at a constant stress level by use of the present flexural jigs which were designed to clamp the specimens at a given fired deflection. Furthermore, the permanent set and

stress relaxation observed during these experiments indicated that the composites were visco-elastic. In some of the stressed specimens creasing of the composite occurred at the location where the loading bar contacted the specimen. This effect shown in Figure 10. It was decided that a screening study of the high temperature creep characteristics of these composites would provide valuable information. Subsequently, a brief

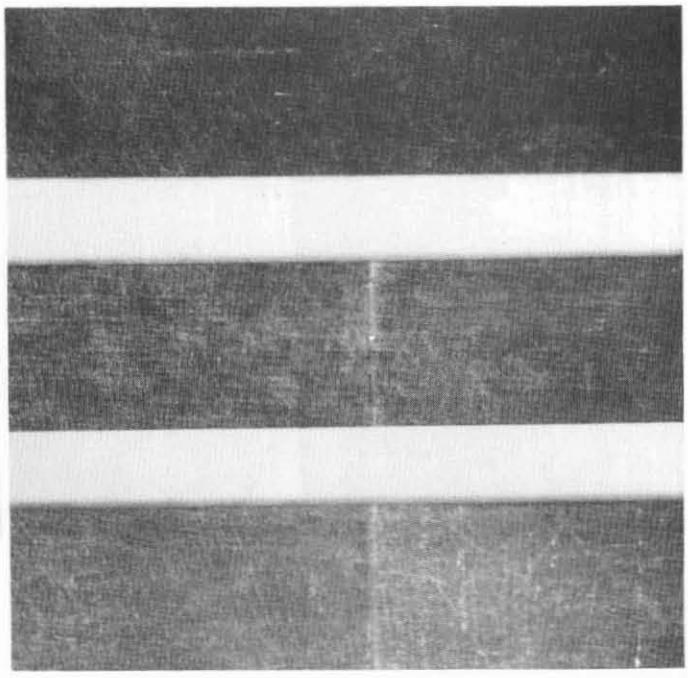


Figure 10. Thermoplastic Flow In Flexural Test Bars

screening study to provide preliminary information on the mechanical modes of creep for these composites was performed instead of continuing the stressed degradation studies. Details of this study are provided in Section 5.5.

TABLE XXII.

STRESSED DEGRADATION SPECIMENS

| Panel and Specimen Number | Average Flexural Strength For Panel ($\overline{X}$) $MN/m^2$ | Standard Deviation ($\sigma$) $MN/m^2$ | Nominal[a] Flexural Strength $MN/m^2$ | Specimen Width cm | Specimen Thickness cm | Applied[b] Load Newtons |
|---|---|---|---|---|---|---|
| 73-1-6 | 1032 | 76 | 804 | 1.260 | 0.325 | 207 |
| 73-1-8 | 1032 | 76 | 804 | 1.260 | 0.328 | 207 |
| 73-1-11 | 1032 | 76 | 804 | 1.260 | 0.328 | 207 |
| 73-2-11 | 963 | 77 | 732 | 1.270 | 0.323 | 194 |
| 74-2-15 | 1060 | 97 | 769 | 1.265 | 0.312 | 199 |
| 74-2-2 | 1060 | 97 | 769 | 1.268 | 0.315 | 199 |
| 67-4 | 889 | 47 | 748 | 1.255 | 0.317 | 193 |
| 71-6 | 988 | 42 | 862 | 1.265 | 0.315 | 223 |
| 71-7 | 988 | 42 | 862 | 1.268 | 0.323 | 223 |
| 72-1-4 | 986 | 108 | 662 | 1.265 | 0.317 | 171 |
| 72-1-6 | 986 | 108 | 662 | 1.263 | 0.315 | 171 |
| 72-2-2 | 936 | 52 | 780 | 1.268 | 0.320 | 201 |

[a]Nominal flexural strength = $\overline{X} - 3\sigma$

[b]40% of nominal flexural load

## 5.4 THERMO-OXIDATIVE DEGRADATION STUDIES

The unstressed thermo-oxidative aging studies were designed to provide the bulk of the data for elucidation of the chemical degradation mechanism. Much of this effort was diverted during the program for further studies of the high temperature creep under stress identified in Section 5.5 below. However, the effects of stress level, oxygen concentration and temperature on the oxidative aging have been quantified. All of the tested resin/composite coupons and the trapped degradation products have been retained for further detailed characterization at a later time if warranted.

A schematic diagram of the storage apparatus is shown in Figure 11. Details of the aging test procedures and raw data results are provided in Appendix D. Simply stated, the method consisted of utilizing three separate storage manifolds simultaneously in a single oven to permit

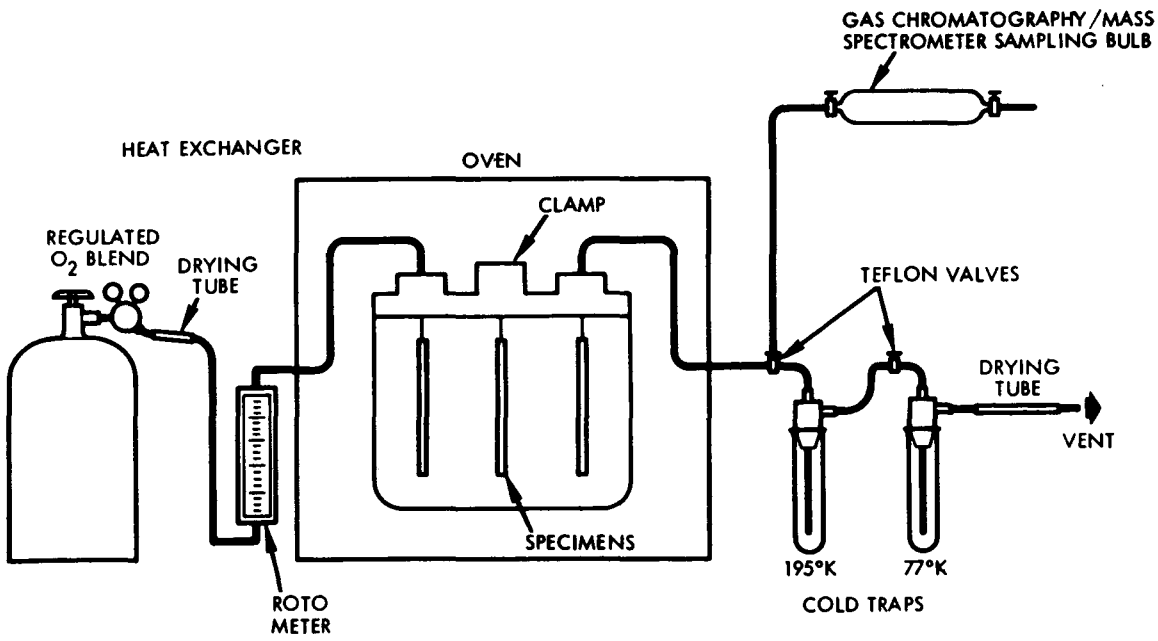


Figure 11. Aging Apparatus For Unstressed Specimens

concurrent testing. The specimens were aged at three different temperatures under three environmental conditions (20% v/v, 60% v/v, and 100% v/v oxygen) for storage durations sufficient to cause no more than 25% w/w of the resin weight loss. Samples were removed periodically under carefully controlled conditions to ensure no spurious deleterious reactions occurred and then weighed to monitor the weight retention as a function of time. Samples were removed and the flexural properties determined at different storage durations. It was hoped that a quantitative relationship between weight retention and percent of original property could be established.

Evaluation of the composite/resin weight retention summaries shows the effects of several parameters on the oxidative aging limitations (See Appendix D). The spread in the data for a single aging study indicates panel to panel variations. A statistical analysis of the data showed two populations of six panels each. Those panels which exhibited the best weight retention were 65, 66, 67, 70-1, 70-2, and 71 (panel group 1) while those which performed poorly were 72-1, 72-2, 73-1, 73-2, 74-1, and 74-2 (panel group 2). This conclusion is summarized in Figure 12 which shows the average performance of each group of panels unstressed at 505°K in 20% $O_2$ atmosphere.

Panel group 1 was prepared during a fifteen-day period using several lots of fiber and lots 5112-50 and 5112-51 of P10P. Panel group 2 was prepared in two days using a single lot of fiber and lot 5112-52 of P10P. Panel group 1 prepregs were prepared from 25% resin content varnish and panel group 2 from 18% resin content varnish. The resin content of panel group 1 averaged 44.5% (w/w) and that of panel group 2, 43.0% w/w (Table XXI). At this time the available information regarding these two panel groups does not appear to explain their apparent difference in thermo-oxidative stability.

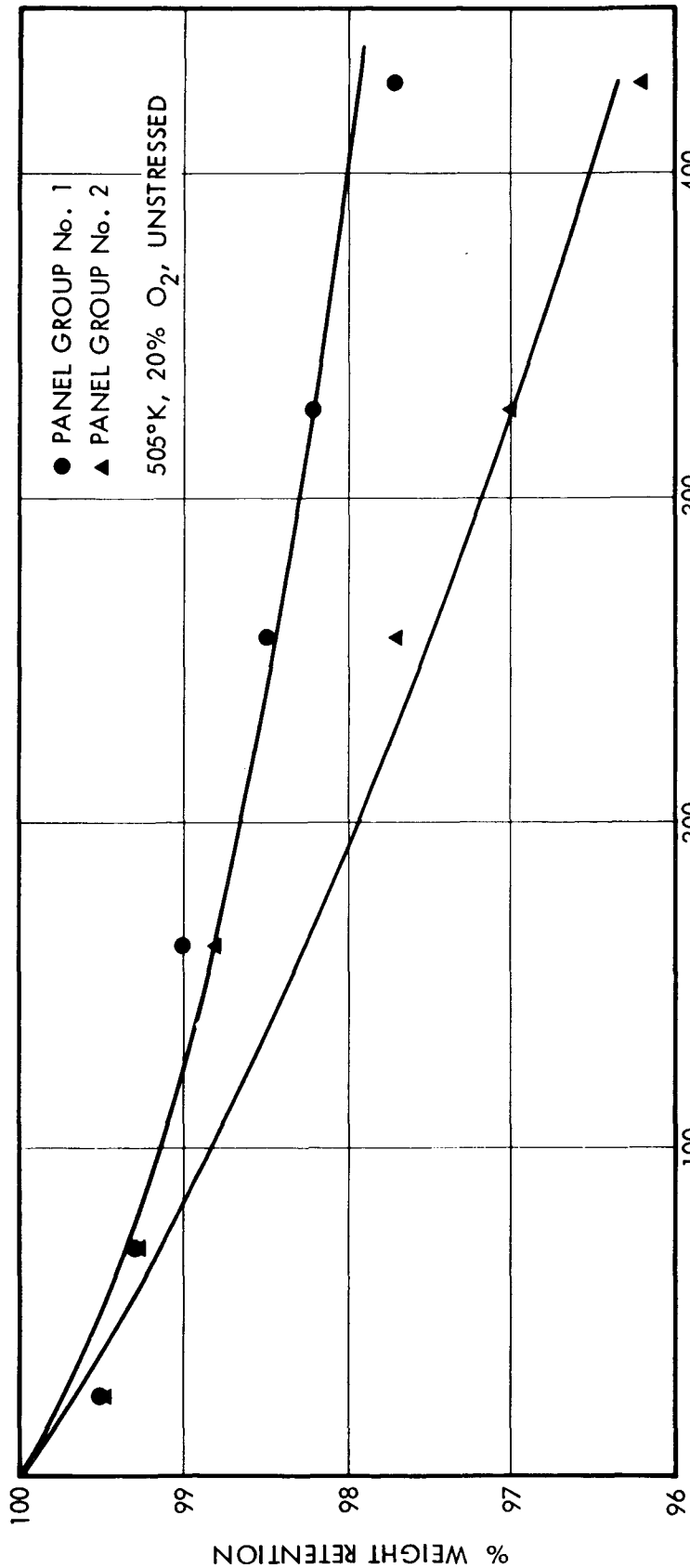


Figure 12. Weight Retention of Group 1 and Group 2 Panels

In order to assess properly the effects of oxygen level and temperature on the aging behavior only the data from Panel Group 1 were compared. These data are summarized in Figure 13. These data show that at 505°K with 20% v/v oxygen the unstressed specimens lost weight at about 3-5% per 1000 hours following an initial weight loss of 1% in 150 hours. The results for a 20% oxygen, 505°K, unstressed specimen show a slightly larger than expected overall weight loss after 1000 hours because of a 64-hour weekend period in the middle of the test when the temperature unexplainably averaged 547°K (525°F). This temperature variation, however, did not significantly affect the overall test results or conclusions.

The early test data at 589°K showed a negligible difference in rate of aging for samples in 60% v/v or 100% v/v oxygen environment. Therefore, tests with 60% oxygen were not continued. Specimens in 100% oxygen were noted to lose 5% of their weight three times faster than specimens in 20% v/v oxygen at the two temperatures. As discussed in Section 5.3, it was difficult to assess the effect of stress on degradation because of the high visco-elastic behavior of the composites. However, studies definitely indicated that weight loss was accelerated approximately two-fold at the 50% stress level.

A comparison of the trapped degradation product weights with the gas analyses for CO and $CO_2$ shows that >75% of the decomposition products were CO, $CO_2$ and $H_2O$. The planned detailed analysis of the trap residues by gas chromatography-mass spectroscopy was deleted to permit study of the observed visco-elasticity more closely. Similarly, the analysis of composite/resin structural changes by mass thermal analysis was postponed also. It is recommended that this study be conducted in the future because it appears some chemical changes would be measured in view of the fact that digestion of the specimens in $H_2SO_4$ for resin content seemed somewhat slower on the aged samples. Elemental analysis of the specimens for carbon hydrogen and nitrogen contents was postponed also. The attempted IR analyses of the composite panels were largely unsuccessful. It is recommended that further spectrochemical characterization of the aged and unaged specimens should be performed by laser Raman analysis.

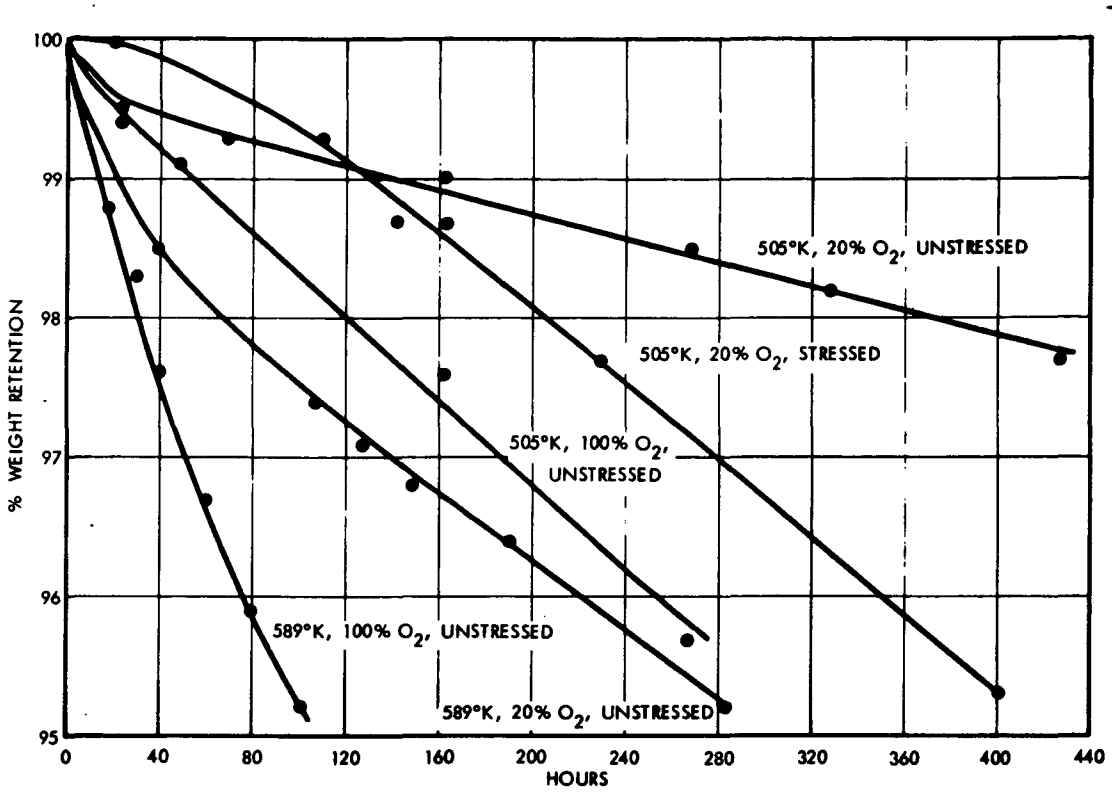


Figure 13. Weight Retention of Stressed And Unstressed Specimens

TABLE XXII
COMPOSITE RESIN WEIGHT AND RESIN RETENTION

| Coupon Code | Weight Retention, % w/w | Resin Retention, % w/w | |
|---|---|---|---|
| | | Actual | Calculated |
| 70-1-13 | 95.9 | 85 | 91 |
| 74-2-2 | 95.3 | 75 | 89 |
| 70-2-6 | 94.4 | 82 | 87 |
| 71-13 | 94.2 | 89 | 86 |
| 70-1-10 | 93.7 | 90 | 87 |
| 73-2-2 | 90.2 | 82 | 76 |
| 73-2-11 | 89.9 | 83 | 76 |
| 73-2-1 | 85.7 | 87 | 66 |
| 74-2-6 | 85.4 | 67 | 66 |
| 72-2-7 | 82.2 | 80 | 59 |
| 71-14 | 78.5 | 78 | 53 |

Four test specimens were aged deliberately to nearly 25% weight loss. Somewhat surprisingly these specimens while aged noticeably did not show any severe visual changes due to this aging (Figure 14). There was no apparent fiber fraying or large cracking. An analysis of the resin content of aged specimens indicates that both the resin and the fiber are the source of weight loss from the composite (Table XXII ). Data reported in Table XXII were generated based on a material balance of the specimens as conducted by the analysis of the resin content of the aged specimens. On the contrary, a separate aging study at 505°K in 20% v/v oxygen showed that the neat graphite fiber did not lose appreciable weight in 168 hours. These conflicting observations can be explained by two different means or their combinations: 1) errors in the resin analysis of the aged specimens, or 2) a synergistic effect of oxidation of the fiber when in the presence of resin. In view of the visual observations and the fairly well substantiated analyses methods, it appears the synergistic oxidation of the fiber is the more probable explanation.

Flexural strength and modulus at room temperature determinations were made on specimens upon completion of their aging cycles. The raw data are presented in detail in Appendix D, and are summarized in Table XXIII and in Figure 15. Summarized data are based upon the average values of the flexural strengths presented in the Appendix with all wild data expelled. General appearance of this graph suggests that the most significant influence in trend structure is aging time and not variations in temperature (within the range of 505°K to 589°K) nor variations in oxygen level. Also, it is seen from the raw data in the Appendix that generally the best strength retentions are found in panels from Group 1 thus substantiating the conclusions drawn from the thermo-oxidative degradation weight-loss data. However, it is seen that all the raw data presented in the Appendix is extremely scattered, therefore, making it difficult to draw valid conclusions.

## 5.5 FLEXURAL CREEP STUDIES

In order to define more clearly the visco-elastic behavior of the graphite polyimide composites first observed during the stressed degradation studies (see Section 5.3 ), a brief flexural creep study was initiated. Flexural test coupons were loaded at two stress levels (50 and 75%

TABLE XXIII.

SUMMARIZED FLEXURAL DATA FOR AGED SPECIMENS

| Aging Conditions | | | Average Flexural Properties | | |
|---|---|---|---|---|---|
| Temperature °K | Oxygen % w/w | Duration Hrs. | Strength $MN/m^2$ | Strength(a) Retention % | Modulus $GN/m^2$ |
| 589 | 20 | 127 | 697 | 71 | 153 |
| 589 | 20 | 284 | 616 | 61 | 146 |
| 589 | 20 | 375.5 | 696 | 72 | 139 |
| 589 | 60 | 107 | 819 | 83 | 146 |
| 589 | 60 | 191.5 | 621 | 63 | 147 |
| 589 | 100 | 101.5 | 730 | 77 | 155 |
| 505 | 20 | 521 | 624 | 66 | 145 |
| 505 | 100 | 257 | 572 | 63 | 153 |
| 505 | 100 | 427 | 495 | 60 | 147 |
| 505 | 100 | 585 | 543 | 60 | 156 |

(a) $\frac{\text{Average Flexural Strength of Aged Specimens at R.T.}}{\text{Initial Average Flexural Strength at R.T.}} \times 100$

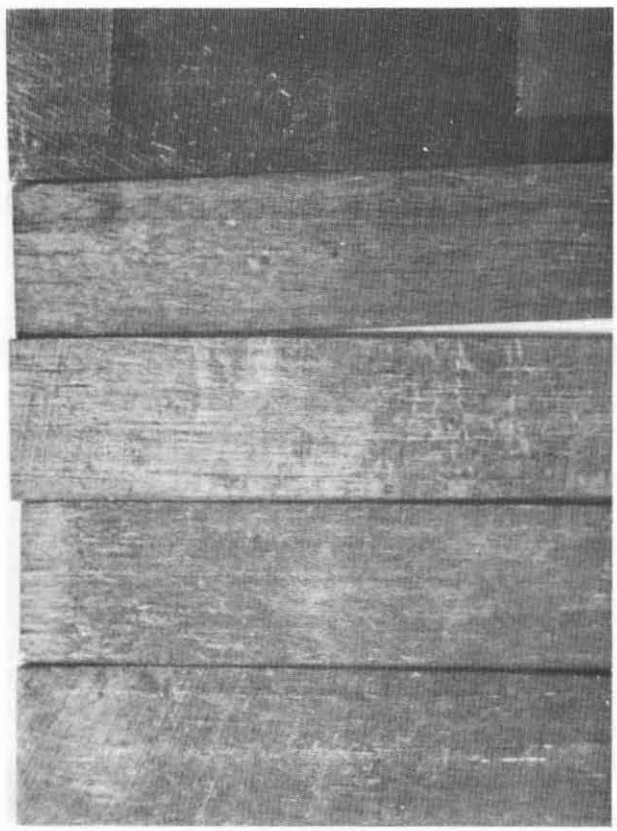

Exposure

70-2-9 - 296°K, unaged control

67-4 - 505°K, 20% v/v $O_2$
724 hrs., Unstressed

73-1-1 505°K, 100% v/v $O_2$
585 hrs., Unstressed

70-2-3 - 589°K, 60% v/v $O_2$
191.5 hrs., Unstressed

72-1-2 - 589°K, 100% v/v $O_2$
101.5 hrs., Unstressed

Figure 14. Thermally Aged Specimens with 25% Weight Loss

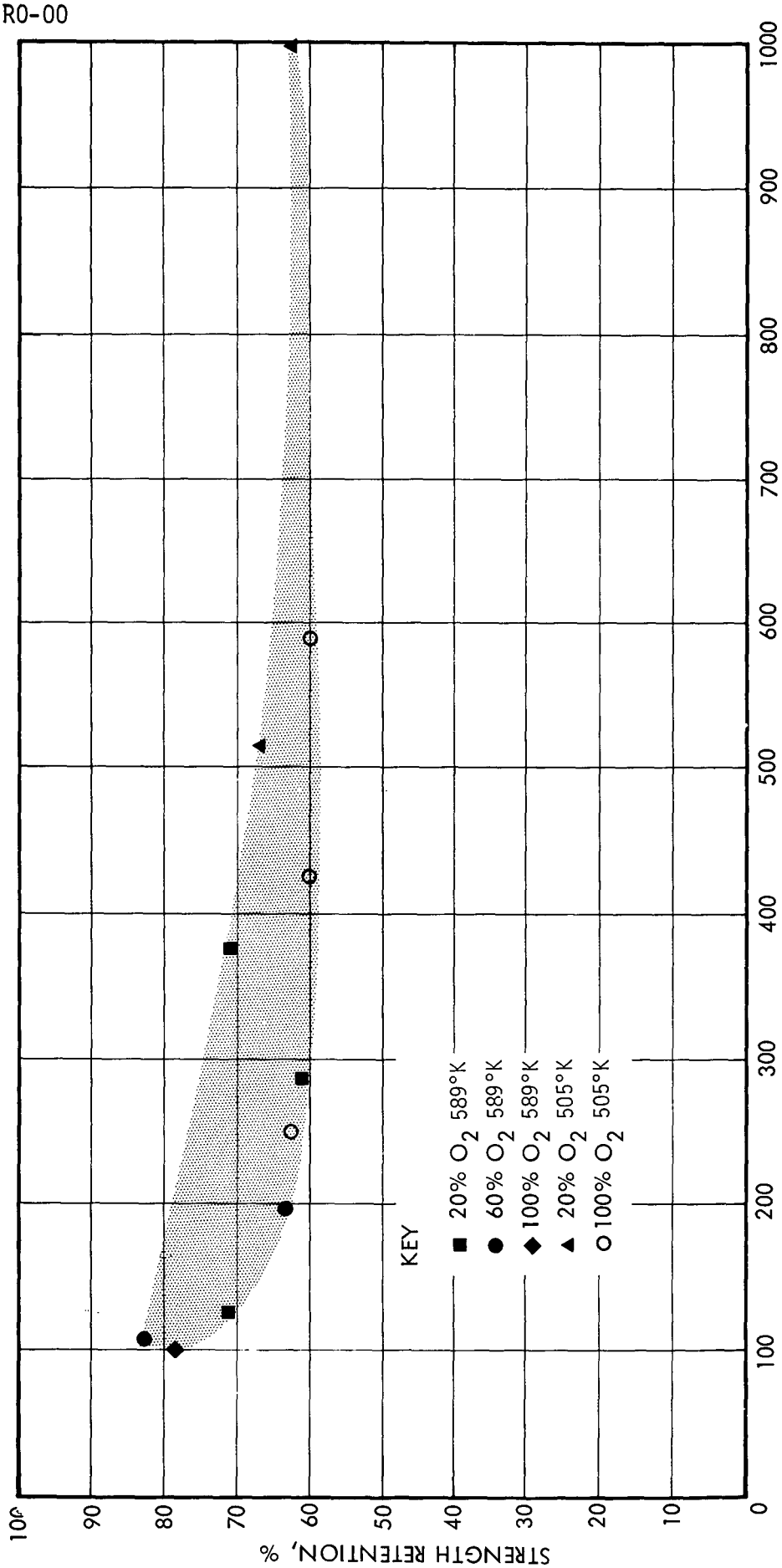


Figure 15. Flexural Strength of Aged Specimens

of ultimate) and held under constant stress at four air temperature environments (558°K, 566°K, 577°K, and 589°K). Changes in the specimens deflections were monitored under these conditions for up to 45 hours duration. The resultant data defined clear creep patterns that showed an initial creep rate for the first one to three hours (depending upon the applied stress level and air temperature) followed by a slower creep rate eventually to failure. It was observed that deflection prior to failure in several cases was considerably higher than is normally measured when performing flexural strength determinations. Calculations of the outer fiber strain in these cases provided higher values than reported for the fibers ultimate elongation at failure. This information substantiated that resin creep is occurring. Details of these studies are provided below.

### 5.5.1 Test Procedure

Using Courtaulds HMS graphite, P10P composite specimens remaining from the stress degradation studies, flexural strength and modulus determinations were performed in triplicate at each of the four selected temperatures, 558°K, 566°K, 577°K and 589°K. These data are provided in Table XXIV and Figure 16. A single flexural test coupon then was loaded in an Instron test machine using a standard flexural test jig at the desired stress level after normalizing the specimen to the test temperature by a 30-minute soak. Deflection was measured by a dial indicator indexing onto the Instron crosshead and the deflection was recorded at regular time intervals. Duration of the first test performed was 45 hours approximately but subsequent tests were terminated after approximately 24 hours. Specimens that did not fail during test were observed to have developed a permanent set after removal from the test jig.

TABLE XXIV.
FLEXURAL STRENGTH AT ELEVATED TEMPERATURE

| Test Temperature °K | Average Flexural Strength at Elevated Temperature, $MN/m^2$ |
|---|---|
| 588 | 620 |
| 566 | 582 |
| 577 | 531 |
| 589 | 476 |

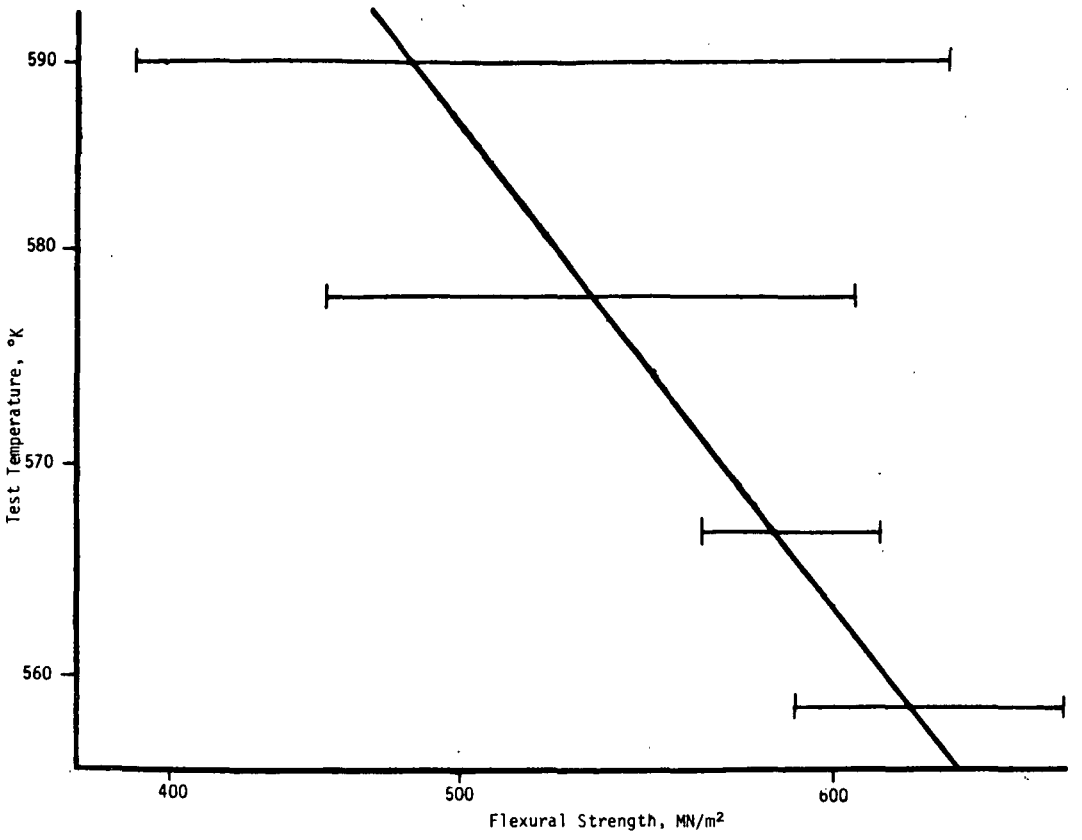


Figure 16. Flexural Strength at Elevated Temperature

### 5.5.2 Test Results

Test specimen deflections measured as a function of exposure time were normalized in accordance with Equation 12 to eliminate variations introduced by slightly different specimen geometry. The reference dimensions are 3.175-mm thickness, 12.7-mm width and 101.6-mm span. The normalized deflections, $D_n$, are presented in Table XXV and raw flexural creep data are provided in Appendix E.

For constant load and flexural modulus

$$D_n = D \left[ \frac{L_o^3}{b_o d_o^3} \right] \frac{bd^3}{L^3} \qquad (12)$$

or

$$D_n = 2580 \; D \cdot \frac{bd^3}{L^3} \qquad (13)$$

where D = measured deflection, mm
b = specimen width, mm
d = specimen thickness, mm
L = test span, mm
and the subscript represents reference

TABLE XXV

NORMALIZED FLEXURAL DEFLECTION

| Test Temperature °K | Flexural Load[a] % | Deflection, mm | | | | | |
|---|---|---|---|---|---|---|---|
| | | Time at Temperature, min | | | | | |
| | | 0 | 30 | 60 | 240 | 450 | 1350 |
| 558 | 50 | 1.199 | 1.321 | 1.372 | 1.40[a] | 1.422 | 1.486[b] |
| | 75 | 1.778 | 1.930 | 1.956 | 2.159 | 2.222 | 2.667 |
| 566 | 50 | 1.257 | 1.499 | 1.524 | 1.562 | 1.575 | 1.613 |
| | 75 | 1.801 | 1.854 | 1.879 | 1.905 | 1.928 | 1.969 |
| 577 | 50 | 1.422 | 1.892 | 1.994 | 2.083 | 2.134 | 2.197 |
| | 75 | 2.209 | 2.413 | 2.515 | 2.794 | 3.023 | 3.531 |
| 589 | 50 | 1.397 | 1.448 | 1.499 | 1.864 | 1.879 | 1.956 |
| | 75 | 1.702 | 2.039 | 2.098 | 2.311 | 2.718 | --[c] |

[a]Stress level, % of ultimate flexural strength at test temperature.

[b]1.499 mm deflection after 2700 minutes of test.

[c]4.089 mm deflection after 1600 minutes test; specimen failed at this time.

The specimen loaded at 75% stress level in a 589°K (600°F) air environment was the only specimen which failed during test. This failure occurred after approximately 24 hours of test (1465 minutes) and the mode of failure appeared to be compressive. Total measured deflection of this specimen immediately prior to failure was 0.160-mm which was approximately double the deflection at failure for the three control specimens tested at 589°K (See Table XXIV). A calculation was made to determine the theoretical maximum strain in the outer fibers of this specimen. The equation used was:

$$r = \frac{6\ Dd}{L^2}$$

Where:

r = Maximum strain in outer fibers, mm/mm

D = Measured deflection, mm

L = Span, mm

d = Specimen thickness, mm

This calculation provided a value of 0.0077-mm whereas published data for Courtaulds HMS fiber shows a maximum fiber strain in tension of 0.0047-mm to 0.0063-mm. It was concluded therefore, that there is definitely a movement of fibers occurring during flexural creep testing which can probably be attributed to creep of the resin matrix since the shear stress is not of sufficient magnitude to cause debonding.

Analysis of the remaining data indicated that there were considerable inconsistancies between many of the datum points although overall there appeared to be a progressive creep pattern resulting from increases in test temperature and stress. Therefore, in order to expel the wild data and to provide idealized flexural creep curves, best-fit curves were drawn depicting deflection as an effect of temperature for each of the deflection measurement intervals and also for each stress level (see Appendix E). From these plots, datum points were obtained for plotting flexural deflection creep curves. These curves are provided in Figure 17 for the 50% stress level tests and in Figure 18 for the 75% stress level tests. Because these curves are highly idealized and the tests were performed for relatively short durations, it is recommended that a more detailed study be made in order to establish reliable engineering information. Future studies should utilize multiple specimens for each datum point and the specimens should be subjected to test for longer durations, preferably to rupture. Also, additional stress levels would be of value in order to plot deflection as an effect of stress level as well as an effect of temperature.

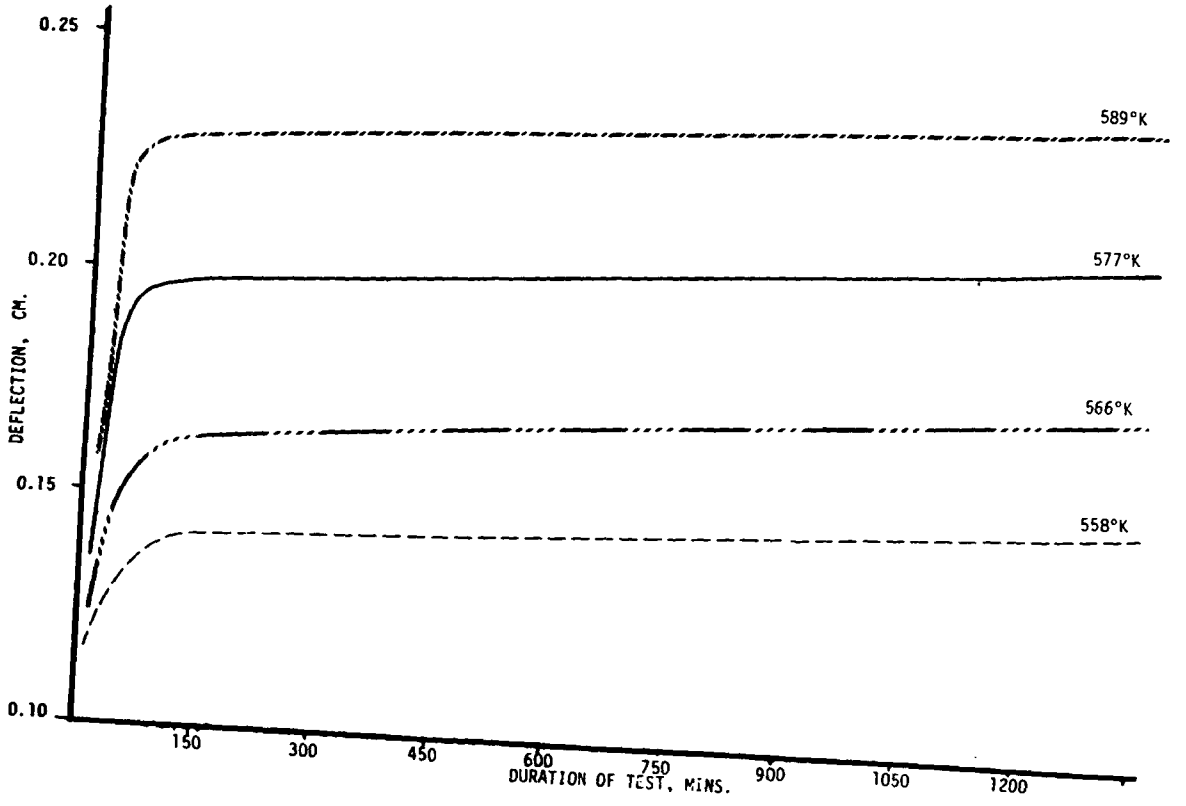


Figure 17. Flexural Creep *vs* Time at 50% Stress Level

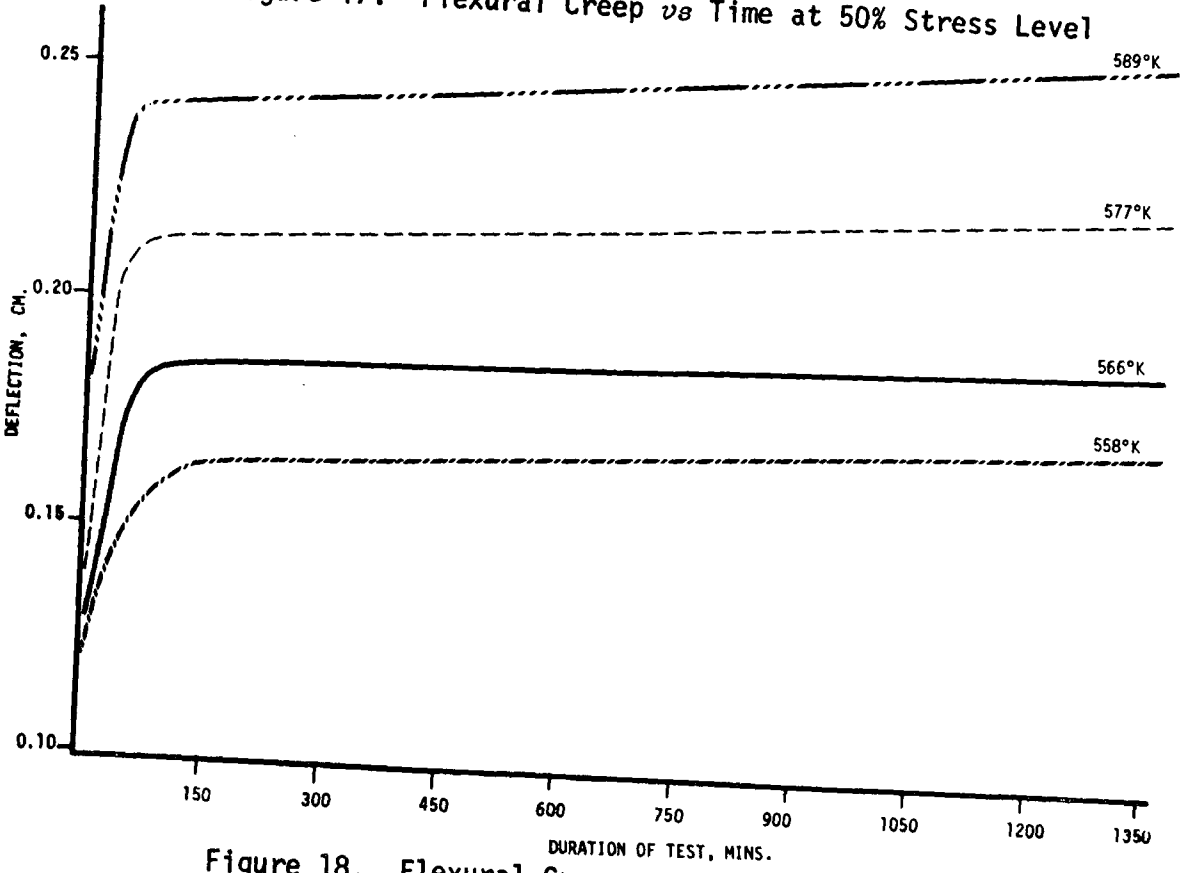


Figure 18. Flexural Creep *vs* Time at 75% Stress Level

# 6. TASK V - AUTOCLAVE MOLDING STUDIES

In Contract NAS 3-12412 several approaches were identified that had high potential to improve the processability of the A-type polyimide resin system to permit autoclave processing of fiber reinforced composites. The objective of this task was to implement development of formulation and processing procedures to effect autoclave fabrication of glass and graphite fiber reinforced composites.

Ingredient and prepolymer formulated molecular weight variations were selected based on their potential to impart a broad melt, flow and cure temperature range to A-type polyimide prepolymers. A total of eight combinations of ingredients and formulated molecular weights were prepared and screened for neat resin property and processing characteristics. Candidate resins then were screened for flow characteristics on glass fabric in a window flow-press through which visual polymer phase changes were observed during simulated autoclave molding cycles. Glass fiber and high modulus graphite fiber reinforced flat panel composites then were autoclave molded and evaluated. A complex graphite fiber reinforced demonstration component was designed together with the requisite tooling. Processing for autoclave molding a demonstration part was developed and a display model was fabricated. Detailed discussion of these activities is provided below.

## 6.1 VARNISH SYNTHESIS AND CHARACTERIZATION STUDIES

### 6.1.1 Selection of Autoclavable Candidates

This program task marked the first attempt to define a specific A-type polyimide formulation possessing the processing characteristics and resin thermo-mechanical properties making it suitable for autoclave fabrication into advanced graphite reinforced composites. After conceptual evaluation of possible ingredient and prepolymer formulated molecular weight (FMW) combinations, a total of eight specific A-type polyimide modifications were selected for their high potential to demonstrate facile autoclave processability and also retain the high mechanical properties and thermo-oxidative stability of PIOP-type resins.

The eight resin ingredient/FMW modifications selected for study are summarized in Table XXVI along with their inherent attributes as defined

TABLE XXVI

A-TYPE POLYIMIDE RESINS SELECTED
FOR STUDY AS AUTOCLAVABLE MATERIALS

| Formulation[a] | Formulated Molecular Weight (FMW) |
|---|---|
| NA/MDA/PMDA | 1000[b] |
| | 1150 |
| NA/80MDA:20TDA/PMDA | 1000 |
| | 1150 |
| MN/MDA/PMDA | 1000 |
| | 1150 |
| MN/80MDA:20TDA/PMDA | 1000 |
| | 1150 |

[a]Code/monomer attribute:

| | | |
|---|---|---|
| NA | = | Nadic anhydride/standard A-type end cap |
| MN | = | Methyl nadic anhydride/imparts longer gel time to A-type formulations than NA |
| MDA | = | Methylene dianiline/standard A-type diamine demonstrating excellent thermo-mechanical properties with PMDA |
| TDA | = | Thiodianiline/demonstrates excellent flow in A-type formulations as a co-diamine with MDA |
| PMDA | = | Pyromellitic diahydride/imparts excellent thermo-mechanical properties to A-type polyimide formulations. |

[b]Formulations chosen for detailed study as press-grade laminating varnishes in Contract NAS 3-13202; original ingredient combination identified in Contract NAS 3-12412.

in various polymer configurations in prior studies. Pyromellitic dianhydride (PMDA) was selected as the dianhydride for use in all formulations because of its contribution to improved thermo-oxidative stability to A-type polyimide polymers as demonstrated in Contracts NAS 3-12412 and NAS 3-13203. Formulated molecular weights of 1000 and 1150 for each ingredient combination were selected for investigation to optimize processing characteristics. The 1000 and 1150 FMW NA/MDA/PMDA formulations were identified for investigation due to their prior study as high performance press grade formulations, hence they could serve as standards as well as lend themselves for initial evaluation as autoclavable candidates. The attributes of other ingredients included in the study are given in the code at the bottom of Table XXVI.
at the bottom of Table XXVI.

### 6.1.2 Varnish Synthesis Studies

The eight autoclave candidates were prepared as amide-acid (A-A) varnishes in dimethyl formamide (DMF) at a 40% w/w solids loading according to standard A-type polyimide formulation technology. Each varnish possessed a relative viscosity in the expected range of 0.2 - 1.0 $Ns/m^2$.
Details of synthesis procedures and viscosities are provided in Appendix C.

### 6.1.3 Molding Powder Synthesis

The eight varnishes were converted to imidized prepolymer molding powders by vacuum evaporation of the DMF solvent and subsequent air drying. Details of the molding powder preparation and infrared confirmation of complete imidization are given in Appendix C.

### 6.1.4 Plug Molding Studies

The eight imidized prepolymer molding powders were subjected to a molding study employing simulated autoclave molding pressures and temperatures of 589°K (600°F). The Barcol hardness indicative of consolidated specimens for each candidate are summarized in Table XXVII. The intermediate hardness values (ca., 30-42) indicated that six resin formulations plus P13N (added as a standard), would undergo consolidation under the simulated autoclave processing conditions of 1.4 $MN/m^2$ and 589°K. The effect of higher pressures on consolidation were that 1000 and 1150

TABLE XXVII

MOLDING DATA ON AUTOCLAVABLE RESIN CANDIDATES[a]

| Formulation | Formulated Molecular Weight (FMW) | Molding Temperature ($^{o}K$) | Product Barcol Hardness |
|---|---|---|---|
| NA/MDA/PMDA | 1000 | 589 | 42 |
| | 1150 | 589 | 40 |
| MN/MDA/PMDA | 1000 | 589 | 34 |
| | 1150 | 589 | 32 |
| NA/80MDA:20TDA/PMDA | 1000 | 560 - 620 | -- |
| | 1150 | 589 | 41 |
| MN/80MDA:20TDA/PMDA | 1000 | 560 - 620 | -- |
| | 1150 | 589 | 32 |
| | | 620 | 34 |
| P13N | | 589 | 46 |

[a]All samples molded at constant dwell time of 15 seconds and 1 hour cure at 1.4 $MN/m^2$ .

FMW NA/MDA/PMDA as well as P13N all gave higher Barcol hardness values consistent with data obtained previously in NAS3-12412 and NAS3-13203. (Also, see Section 3).

The 1000 FMW NA/80MDA:20TDA/PMDA and MN/80MDA:20TDA/PMDA powders could not be molded into consolidated specimens in the range of temperatures (e.g., 560 - 620$^{o}K$) deemed reasonable for autoclavability at an applied pressure of 1.4 $MN/m^2$. However, as discussed in Section 6.2, the latter formulation demonstrated excellent autoclavable processing characteristics and was ultimately selected as the resin candidate of choice.

### 6.1.5 Isothermal Aging Characterization of Molded Plugs

Samples of the six molded plugs discussed above were isothermally aged in air (106 $cm^3$/min. flow) at elevated temperatures in a Lindberg Heavy Duty crucible furnace apparatus. Samples of the molded plugs were cut into a semi-circular configuration of dimensions 0.48-cm thick x 2.54-cm diameter.

The thermo-oxidative stability of the autoclave resin candidates was assessed by measuring plug weight loss as a function of time (weighings were taken every 48 to 72 hours) at temperatures of 616°K (650°F) and 589°K (600°F). The weight loss data are shown for each temperature in Figures 19 and 20, respectively.

The relatively rapid degradation in air at 616°K (Figure 19) was anticipated because of previous work on Contract NAS 3-13203 (Ref 8) which showed that more consolidated resin samples containing PMDA (eg, Barcol hardness $\geq$50) lost 25-50% w/w resin after aging for a 336-hour time period. The testing at 616°K was terminated after 285 hours because of the extreme (i.e., >40%) weight loss of all candidate samples. As had been found in similar studies under Contracts NAS 3-12412 and NAS 3-13203 (Refs 1 and 8), an accelerated weight loss was observed during the first 72 hours of aging. The aging data show that the useful life of the resin candidates on exposure to an oxidizing environment at 616°K appears to be limited to approximately 100 hours or less. This study did show a trend which was substantiated at 589°K, that TDA containing resins show the best stability of the six candidates suitable for the aging test.

The thermo-oxidative stability of the six candidates was much improved at 589°K as shown in Figure 20. The same trend for a more rapid resin weight loss up to 72 hours was observed also at this aging temperature. The aging data at 589°K have shown that TDA containing formulations are the most thermo-oxidatively stable resin candidates, particularly the 1150 FMW MN/80MDA:20TDA/PMDA resin. These data indicate that the neat resin matrices to be used for preparing high modulus graphite composites should demonstrate a useful property performance period of approximately 500 hours or more. The slopes in Figure 20 extrapolate to 50% resin weight loss, (deemed indicative of loss of useful properties) in the region of 500-700 hours. This information strongly suggests that the new PMDA/TDA containing resin candidates are more thermo-oxidatively stable than P13N when molded under identical processing conditions approximating autoclave molding temperatures and pressures.

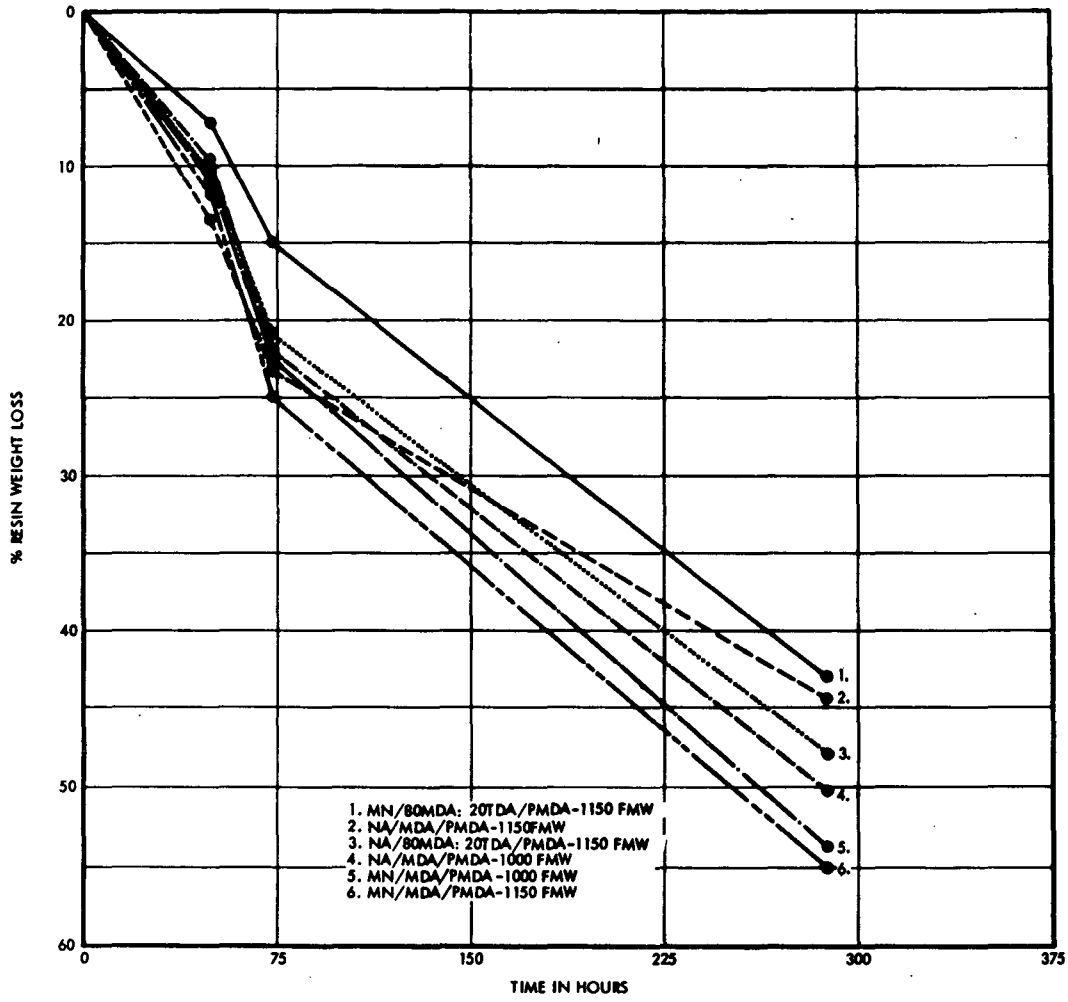


Figure 19. Plot of Resin Weight Loss as a Function of Isothermal Aging at 616°K in Air (100 $cm^3$/min. flow).

A significant improvement in the inherent thermo-oxidative stability of neat P10P (1000 FMW NA/MDA/PMDA) is effected by molding at higher pressures [eg., 3.55 $MN/m^2$ (500 psig)] as is discussed in Section 3. The influence of high modulus graphite fiber on thermo-oxidative stability is considered in Section 4.

Infrared analysis for structure was performed on all cured polymers. These data are described in Appendix C.

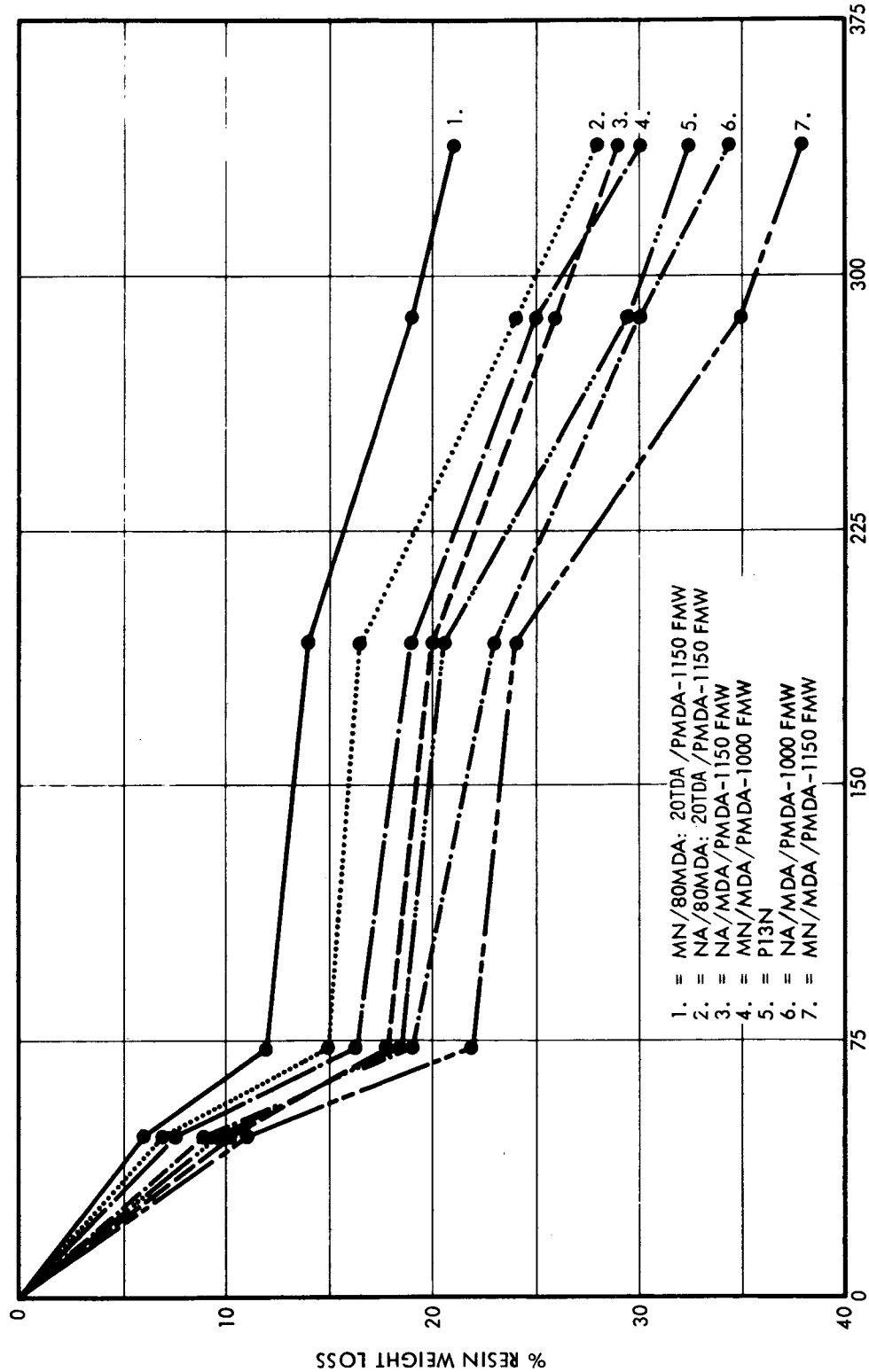


Figure 20. Plot of Resin Weight Loss as a Function of Isothermal Aging at 589°K in Air (100 $cm^3$/min. flow).

## 6.2 RESIN FLOW STUDIES

A special resin flow screening apparatus was designed and constructed that permitted precise visio-physical flow characterization of prepregs. Candidate A-type amide-acid varnishes were coated onto glass fabric and high modulus graphite fiber reinforcements and the resultant prepregs were screened in the resin flow screening apparatus (flow-press). Correlation of the visual observations with the flow-press studies was made by infrared analysis of resin samples taken from the prepregs at various stages of the flow-press cycle. These studies established that the NA/80MDA:20TDA/PMDA and MN/80MDA:20TDA/PMDA formulations, both at 1000 FMW, were the most promising resin candidates for autoclave molding. Feasibility of using autoclave molding cycles compatible with state of the art industrial equipment was established while using simulated autoclave conditions in the flow-press. Details of these studies are provided below.

### 6.2.1 Resin Flow Screening Apparatus

A special apparatus, shown in Figure 21, was designed and constructed that permitted a precise visio-physical characterization of resin flow in prepregs by screening:

- Visual observation of resin phase changes during molding cycles by means of an observation window located directly over the flow specimen
- Laminate consolidation by monitoring pressure drops through high precision pressure gauges
- Quantitative resin flow by use of standard SPI flow tests (Appendix A)

This equipment consists of a standard Pasadena Hydraulics, Inc. (PHI) 20-ton capacity bench press frame with a 12.7-cm x 12.7-cm milled hole located symmetrically about the center of the upper bolster plate. Standard PHI hydraulic equipment is installed on the frame and includes a two-stage hand operated pump, two-stage pressure dump valve, pressure cylinder and ram. Pressure build-up during molding cycles is prevented by means of a Sprague Engineering adjustable pressure release valve Model 79129 which is installed in the main hydraulic pressure line. This valve can be precisely set at any desired operating pressure in the range of 0.17 - 1.48 $MN/m^2$ (10 - 200 psig). Pressure is measured by a Helicord 15-cm dial instrument calibrated from

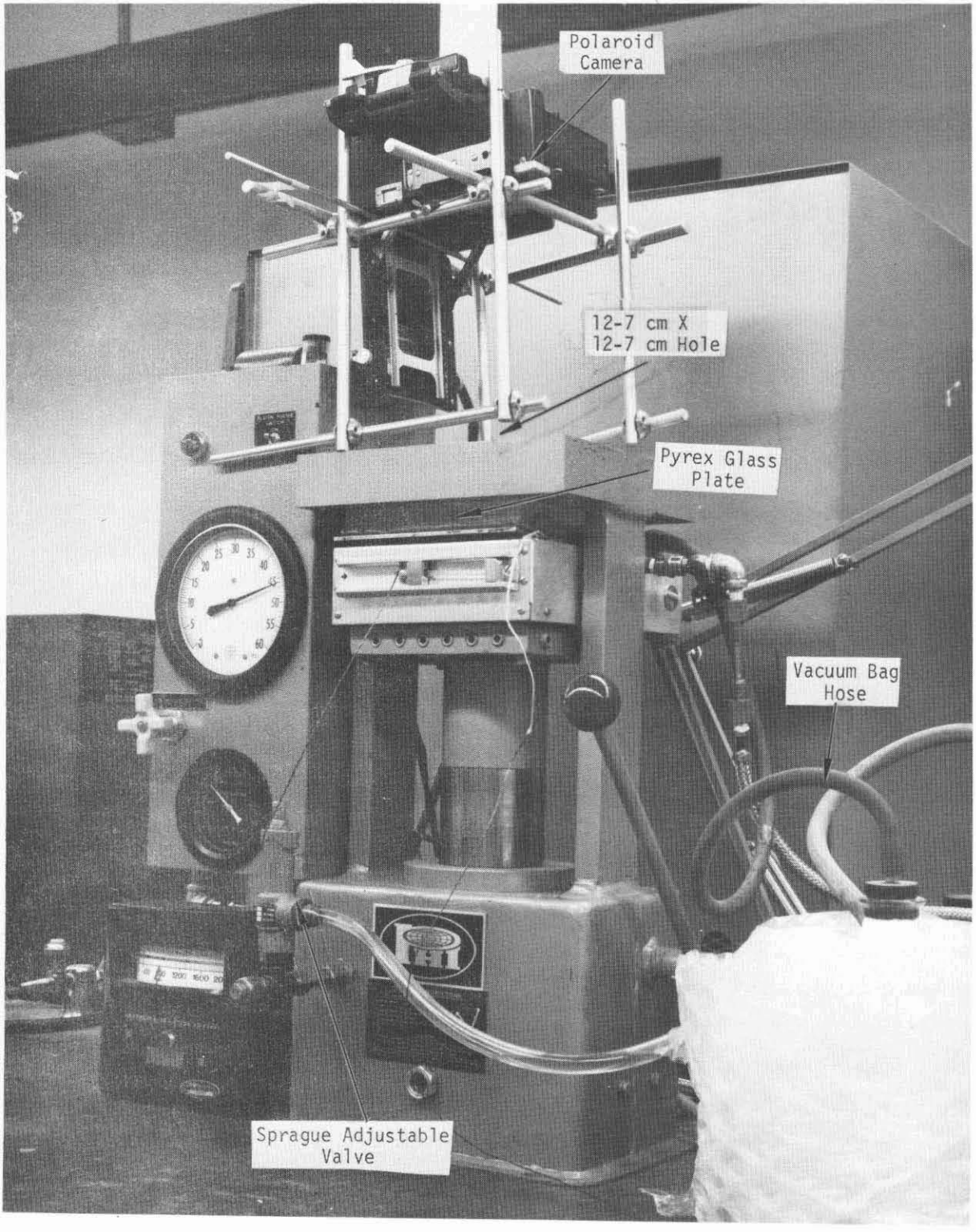


Figure 21. Resin Flow Screening Apparatus

0 - 2.2 kN (0 - 500 pounds) force. A single lower platen, electrically heated to 700°K (800°F), is installed together with a Barber Colman Model 293C temperature controller. The upper platen consists of a 2.5-cm thick piece of Pyrex glass. A Polaroid camera is mounted directly over the observation window to permit photographic documentation of the sequential visual changes occurring during the flow studies. Thermal recordings of the flow specimen cure cycles are provided by use of thermocouples installed in the specimens and connected to a standard Minneapolis Honeywell strip chart recorder.

6.2.2 Development of Characterization Procedures

Several experiments were run in order to develop laboratory techniques with the equipment described in 6.2.1. The two most significant experiments which led to final selection of a screening procedure are discussed below.

Prepreg was prepared consisting of Style 181 E-glass fabric, A1100 amino silane finish, and TRW P10P polyimide laminating varnish. These prepregs were dried at 366°K (200°F) for 30 minutes and consisted of approximately 38% w/w resin solids and 12% w/w volatiles content. These prepregs were cut into 10-cm x 10-cm squares with the fiber warp on a 45° bias and then stacked six-ply thick.

A stack of prepreg with a thermocouple imbedded between the central plies was loaded directly onto the cold lower press platen. The upper Pyrex glass platen, coated with Frekote 33 release agent, then was located on top of the prepreg, 0.45 $MN/m^2$ (50 psig) pressure was applied and then the prepreg was heated up at a rate of 3.3°K/min. Figure 22 shows a series of sequential photographs obtained during the heating cycle. When the prepreg temperature reached 337°K (138°F) (Figure 22b) the prepreg began to darken accompanied by the conversion from opaque to translucent. At 373°K (212°F) this change was complete (Figure 22c) and remained so until at 408°K (275°F) the edges started to lighten in color and again turn opaque (Figure 22d). Condensation was observed on the glass platen around the edges of the prepreg and a small resin flow bead was observed at the prepreg edges. This condition continued up to 419°K (294°F) (Figure 22e) where only a small dark section in the center of the panel remained; at 488°K (419°F) this also disappeared (Figure 22f). No further changes were observed until around 561°K (550°F) when a general color darkening became apparent.

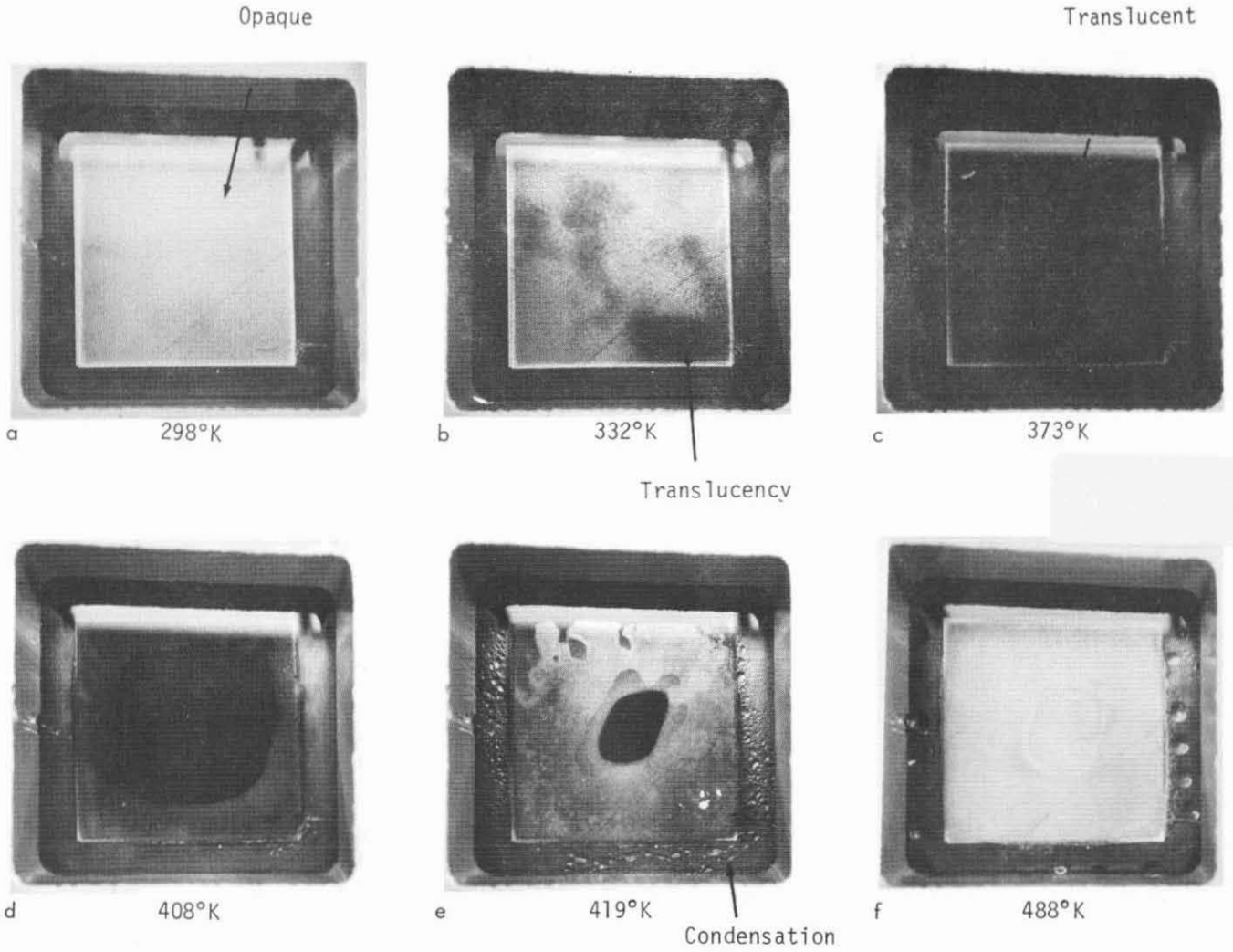


Figure 22. Sequential Photographs of Phenomena Occurring During Heat-up of 1000 FMW NA/MDA/PMDA in a Resin Flow Screening Apparatus from 337°K to 488°K

A duplicate experiment then was prepared except that the test was run with the prepreg contained within a vacuum bag. This was achieved by laying glass bleeder cloth and a Teflon impregnated glass fabric separator sheet onto an aluminum alloy plate on which the prepreg stack was placed. A thermocouple was located between the central plies and polyimide film (Kapton), 0.05-mm thick, was located over the prepreg. This was sealed to the base plate with uncatalyzed silicone rubber gum stock (Stauffer Wacker 7220). Adherence of the gumstock to the polyimide film was achieved by painting Stauffer Wacker Primer SWS-401 onto the faying surfaces. The vacuum bag was evacuated to provide a pressure of 4.8 $kN/m^2$ after which 0.4 $Mm/m^2$ gauge (50 psig) positive pressure was applied while using the Pyrex glass upper platen. The heat-up cycle at a rate of 3.3°K/min (6°F/min) then was started in the same manner as before.

Darkening of the prepreg accompanied by conversion to a translucent condition started at 366°K (200°F) (Figure 23) and spread over the entire surface by 380°K (225°F). At 408°K (275°F), resin flow was prevalent at the prepreg corners and edges (Figure 23b). Color change and return to the opaque condition started at 422°K (300°F) (Figure 23c) and was completed by 450°K (350°F). Again, no further change occurred until about 589°K (600°F) when general darkening of the prepreg was observed.

Upon completion of these experiments, it was concluded that the test method using the vacuum bag is preferred because it closely simulates an autoclave process as well as provides an excellent means of surveillance over the phase changes during cure of the prepreg resins. Consequently, this procedure was adopted for the resin flow screening studies.

### 6.2.3 Resin Flow Screening Studies - Glass

Prepreg panels were prepared consisting of Style 181 E-glass fabric, A1100 amino-silane finish and the candidate resin systems listed in Table XXVIII. The glass fabric was impregnated by laboratory hand-dipping procedures and then dried in an air-circulating oven for the drying cycle prescribed in Table XXVIII. Subsequently, the prepreg panels were cut into 101.6-mm (4-inch) squares with the fiber warp on a 45° bias and stacked 6-ply thick. The individual stacks then were assembled separately on an aluminum base plate, a vacuum bag was installed and resin flow tests were performed in the flow-press using the procedures described in Reference 1.

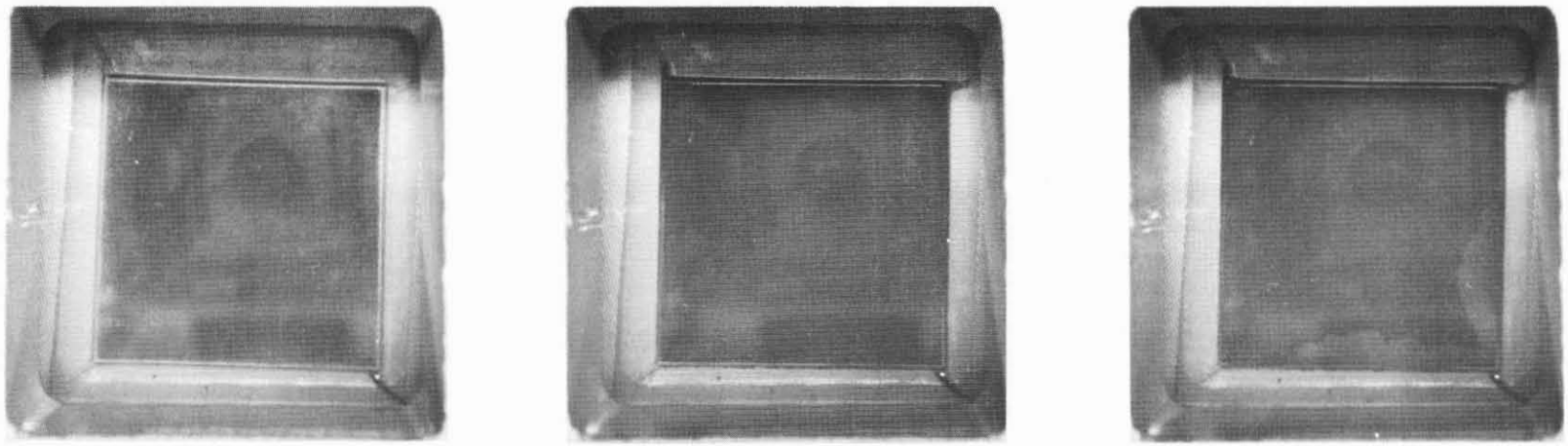

a 366°K b 408°K c 422°K

Figure 23. Sequential Photographs of Phenomena Occurring During Heat-up of 1000 FMW NA/MDA/PMDA in a Resin Flow Screening Apparatus from 366°K to 422°K

# TABLE XXVIII
## FLOW PRESS RESIN SCREENING

| Resin Formulation Constituents | FMW | Prepreg Drying Cycle | | Prepreg Properties | | Flow Test Characterizations | | | | | | Flow Specimen Properties | | | |
|---|---|---|---|---|---|---|---|---|---|---|---|---|---|---|---|
| | | °K | Min. | Volatiles % w/w | Resin Solids % w/w | Pressure $MN/m^2$ | Resin Wet Flow | Start of Resin Flow °K | End of Resin Flow °K | Duration of Resin Flow Min. | Resin Solids % w/w | Density $g/cm^3$ | Barcol Hardness | Void Content % v/v | Fiber Volume % v/v |
| NA/MDA/PMDA | 1000 | 355 | 30 | 14.4 | 32.8 | 0.45 | a | 416 | 444 | 5 | 30.9 | a | 30/35 | a | a |
| NA/MDA/PMDA | 1150 | 355<br>372 | 50<br>25 | 11.6 | 37.1 | 0.45 | 15.4 | 408 | 433 | 5 | 35.9 | a | 25/30 | a | a |
| MN/MDA/PMDA | 1000 | 378 | 45 | 10.7 | 38.0 | 0.45 | 10.2 | 411 | 430 | 4 | 39.3 | a | 35/40 | a | a |
| MN/MDA/PMDA | 1000 | 378 | 35 | 12.1 | 39.1 | 0.45 | 12.7 | 450 | 483 | 6 | 39.3 | a | 50/55 | a | a |
| MN/MDA/PMDA | 1000 | 378 | 35 | 12.1 | 39.1 | 0.79 | 12.7 | 450 | 494 | 17[b] | 38.3 | a | 55/60 | a | a |
| MN/MDA/PMDA | 1150 | 378 | 35 | 11.9 | 37.5 | 0.45 | 11.8 | 450 | 491 | 15[b] | 35.9 | a | 40/45 | a | a |
| MN/80MDA:20TDA/PMDA | 1000 | 378 | 30 | 11.9 | 32.2 | 0.79 | 11.4 | 422 | 455 | 8 | 34.8 | 1.86 | 65/70 | 2.46 | 47.7 |
| MN/80MDA:20TDA/PMDA | 1000 | 378 | 30 | 11.9 | 32.2 | 1.14 | a | 403 | 475 | 22[b] | 33.4 | 1.82 | 50/55 | 2.92 | 47.7 |
| MN/80MDA:20TDA/PMDA | 1000 | 378 | 20 | 12.8 | 33.6 | 0.79 | 10.4 | | 450 | 8 | 34.7 | 1.87 | 60/65 | 2.01 | 48.1 |
| MN/80MDA:20TDA/PMDA | 1150 | 378 | 55 | 12.2 | 40.4 | 0.45 | 12.4 | 436 | 478 | 7 | 39.5 | a | 40/45 | a | a |
| MN/80MDA:20TDA/PMDA | 1150 | 378 | 40 | 13.8 | 37.9 | 0.79 | 14.8 | 450 | 472 | 7 | 37.5 | a | 45/50 | a | a |
| NA/80MDA:20TDA/PMDA | 1000 | 378 | 30 | 11.8 | 38.8 | 0.79 | 13.9 | 444 | 486 | 12[b] | 37.8 | 1.79 | 55/60 | 4.12 | 43.8 |
| NA/80MDA:20TDA/PMDA | 1000 | 378 | 25 | 14.5 | 40.5 | 0.45 | 25.4 | 436 | 472 | 6 | 30.2 | a | 40/45 | a | a |
| NA/80MDA:20TDA/PMDA | 1000 | 378 | 20 | 13.4 | 33.7 | 0.79 | 26.6 | 378 | 408 | 2 | 19.4 | a | 50/55 | a | a |
| NA/80MDA:20TDA/PMDA | 1000 | 378 | 25 | 11.8 | 32.7 | 0.79 | 17.5 | 408 | 430 | 7 | 28.5 | 1.92 | 58 | 3.86 | 54.0 |
| NA/80MDA:20TDA/PMDA | 1150 | 378 | 35 | 14.1 | 39.3 | 0.45 | 14.6 | 450 | 478 | 7 | 34.0 | a | 20/25 | a | a |

a) Not suitable for test due to poor consolidation.

b) Longer reported flow time is result of localized central area of specimen which remained in fluid condition after remainder of panel had lost its translucency.

During the resin flow studies, it was observed that an initial period of fluidity occurred in the temperature range 311°K (100°F) to 361°K (190°F) which was followed later by a definite resin flow and laminate consolidation period in the temperature range of 389°K (240°F) to 500°K (440°F). At commencement of the fluidity and resin flow periods, the prepreg changed from an optically opaque condition to transluscent. A pressure drop occurred simultaneously with the start of the resin fluidity period which required continual adjustment of the hydraulic pressure until the prepreg reverted to the opaque condition. Upon completion of resin flow, the prepregs reverted to the opaque condition and remained so throughout the remainder of the molding cycle. A photographic recording of the sequence of visual phase changes throughout the flow-press cycle is provided in Figure 24. This particular photographic sequence does not show a condition occurring in certain panels (Table XXVIII) where the resin in a central area of the specimen remained fluid for a longer duration than the resin in the remainder of the panels. It is believed that this localized fluid area was prepolymer plasticized by entrapped DMF solvent.

In order to define whether amide-acid or polyimide resin flow was being observed during processing, infrared analysis was performed on resin samples taken from the prepregs at various stages of the flow-press cycle. It was established that amide-acid is present (although in decreasing quantities) throughout the visual resin flow period, which is finally completed at 478°K (400°F).

The visual observations were correlated with increasing imidization, as the temperature was raised, by monitoring increasing absorption of the imide functionality at 1700 and 1770 $cm^{-1}$ and the decreasing absorption of the amide-acid band at 1630 $^{-1}$. Using this IR scan interpretation, it was possible to discern that visual flow occurred up to <478°K (<400°F) while amide-acid still was present (Figures 25, 26, 27) but visual flow terminated upon complete imidization (Figure 28).

### 6.2.4 Flow-Press Process Screening Studies of Glass Prepregs

Style 181 A1100 E-glass fabric, prepregs containing the candidate resin systems prepared as described in Section 5.1 were used for a flow-press process screening study. Processing parameters investigated were molding pressures, heat-up rates and prepreg volatile matter content levels (Table XXIX).

Figure 24. Sequential Photographs of Phenomena Occurring During Heat-up of 1000 FMW NA/80MDA:20SDA/PMDA in a Resin Flow Screening Apparatus from 295°K to 575°K

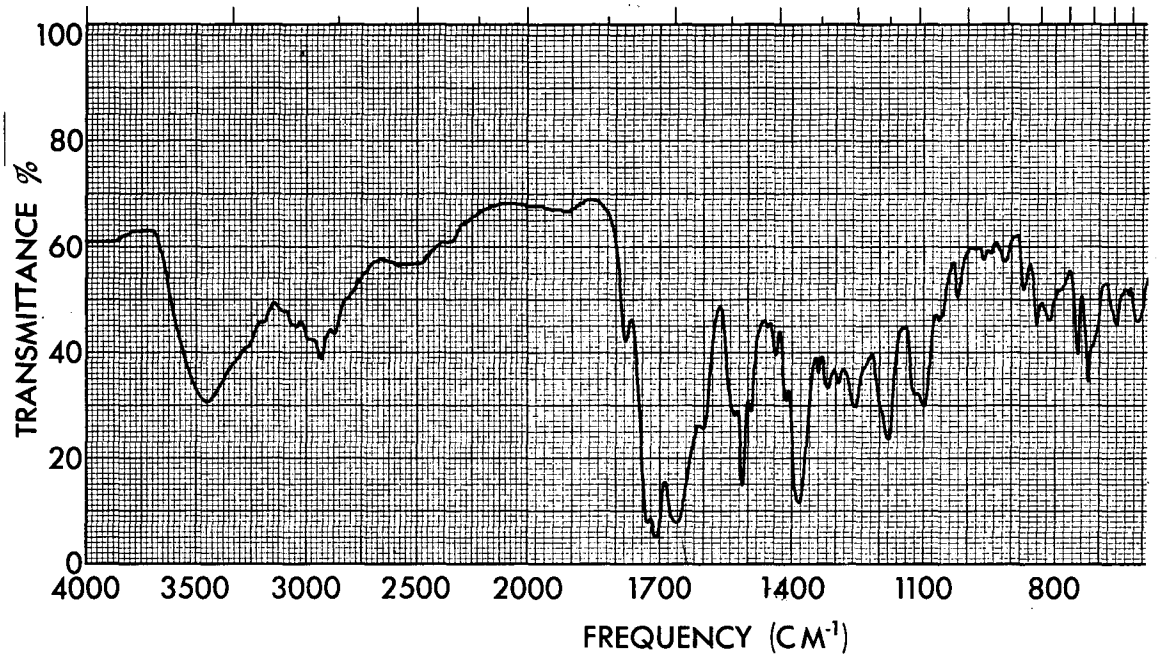


Figure 25. Infrared Spectrum of 1000 FMW NA/80MDA:20TDA/PMDA Resin Removed from Opaque Glass Prepreg Heated to <311°K (KBr) Concentration: 3.9 mg/g KBr

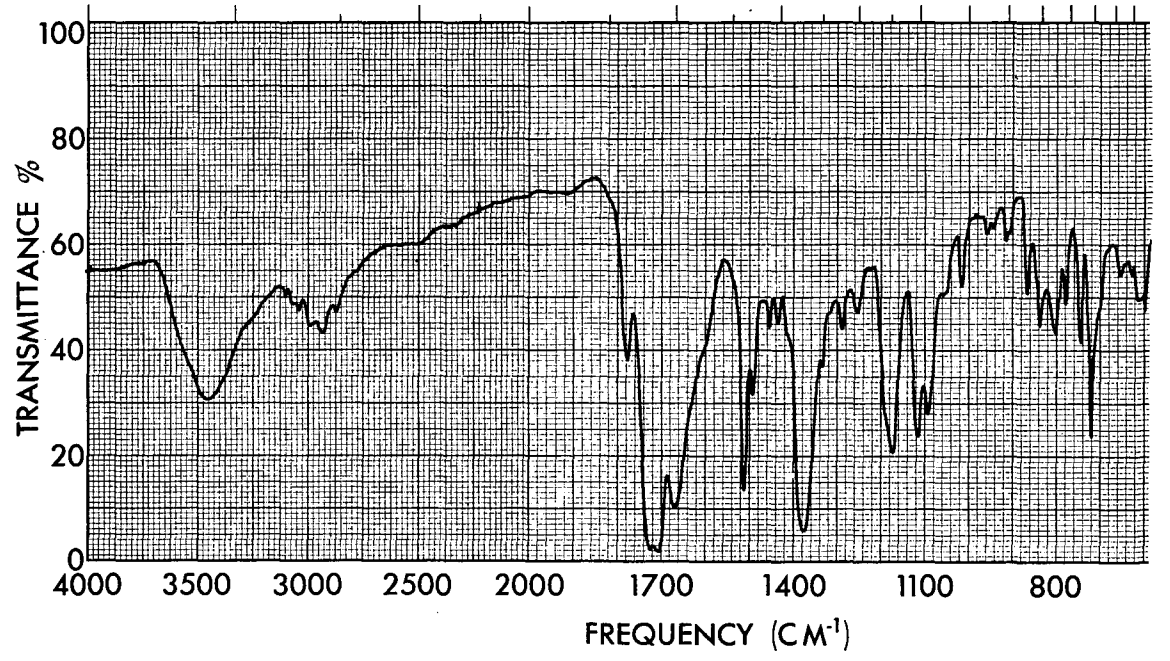


Figure 26. Infrared Spectrum of 1000 FMW NA/80MDA:20TDA/PMDA Resin Removed from One Quarter Clear Glass Prepreg Heated to 366°K (KBr) Concentration: 4.1 mg/g KBr

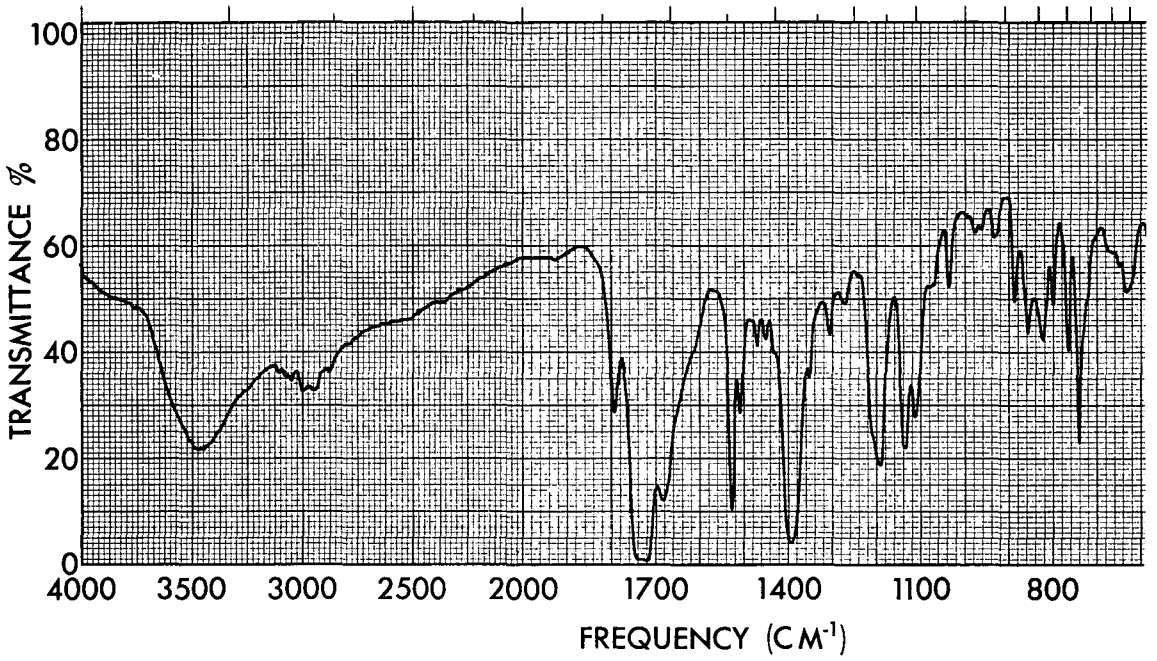


Figure 27. Infrared Spectrum of 1000 FMW NA/80MDA:20TDA/PMDA Resin Removed from One-Half Clear Glass Prepreg Heated to 422°K (KBr) Concentration: 3.3 mg/g KBr

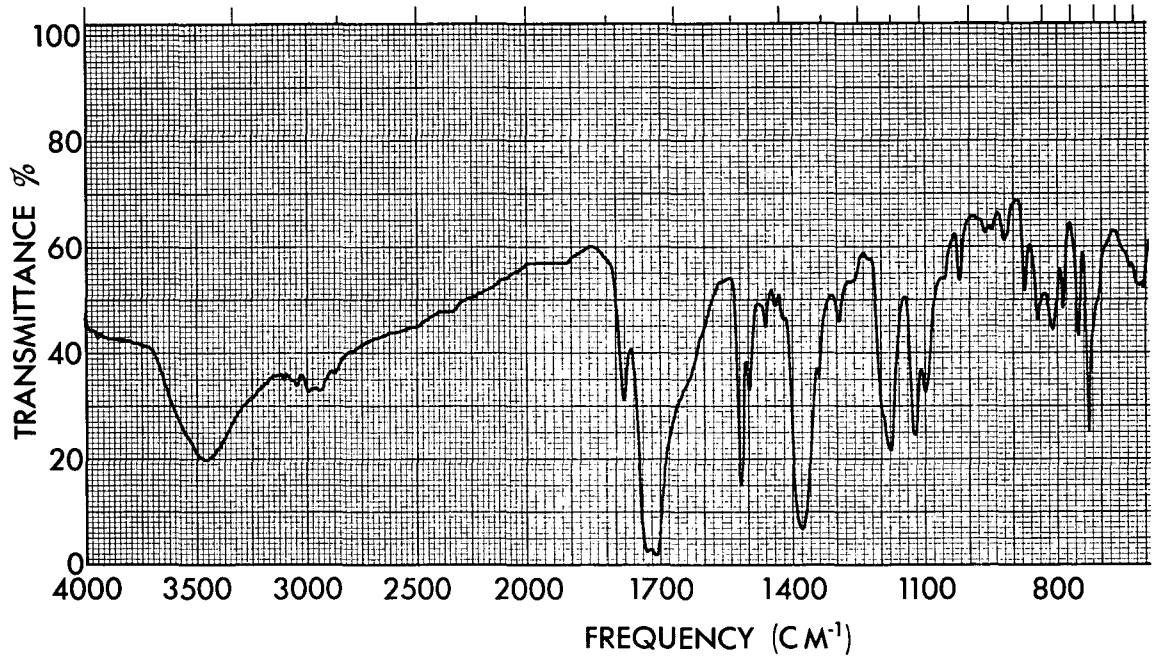


Figure 28. Infrared Spectrum of 1000 FMW NA/80MDA:20TDA/PMDA Resin Removed from Totally Clear Glass Prepreg Heated to 478°K (KBr) Concentration: 3.3 mg/g KBr

TABLE XXIX

FLOW PRESS PROCESS SCREENING

| Processing Conditions and Resultant Properties | Resin Type | | | | | | | | | |
|---|---|---|---|---|---|---|---|---|---|---|
| | MN/80MDA:20TDA/PMDA 1000 FMW | | | | | NA/80MDA:20TDA/PMDA 1000 FMW | | | | |
| FLOW PRESS CHARACTERIZATION | | | | | | | | | | |
| Molding Pressure, $MN/m^2$ | 345 | 345 | 689 | 689 | 689 | 345 | 345 | 689 | 689 | 689 |
| Heat-up Rate, °K/Min | 1.4 | 3.3 | 3.3 | 3.7 | 1.8 | 3.1 | 5.5 | 3.6 | 3.1 | 2.2 |
| Wet Resin Flow, % w/w | 12.1 | 12.7 | 11.4 | 10.4 | 10.4 | 11.7 | a | 13.9 | 10.9 | 9.3 |
| Start of Resin Flow, °K | 405 | 428 | 422 | 405 | 408 | 422 | 433 | 444 | 408 | 405 |
| End of Resin Flow, °K | 416 | 450 | 455 | 441 | 444 | 444 | 464 | 486 | 444 | 436 |
| Duration of Resin Flow, Min | 4. | 5. | 8. | 5. | 7. | 5. | 2. | 11. | 2. | 8. |
| PROPERTIES OF FLOW SPECIMEN | | | | | | | | | | |
| Flexural Strength, $MN/m^2$ | 182 | 169 | 383 | 336 | 262 | 142 | a | 292 | 217 | 240 |
| Density, $kg/m^3$ | 1.71 | 1.72 | 1.86 | 1.83 | 1.84 | 1.69 | a | 1.79 | 1.76 | 1.78 |
| Resin Content, % w/w | 37.1 | 38.2 | 34.8 | 36.8 | 35.6 | 38.8 | a | 37.8 | 38.2 | 38.5 |
| Void Content, % v/v | 9.1 | 7.5 | 2.5 | 2.7 | 3.2 | 8.7 | a | 4.1 | 5.6 | 4.3 |
| Fiber Content, % v/v | 42.2 | 41.9 | 47.7 | 45.5 | 46.6 | 40.8 | a | 43.8 | 42.3 | 43.1 |
| Barcol Hardness | 50. | 48. | 55/60 | 62. | 60. | 42. | a | 55/60 | 60. | 56. |

a) Poor consolidation in panel, not suitable for test.

b) Determined on 6-ply laminate 0.127-cm with warp at $\pm 45°$ orientation.

Results of this study indicate that good glass fabric laminates can be obtained by a combination of:

- 0.69 $MN/m^2$ (100 psi) molding pressure
- 3.3°K (6°F) to 3.9°K (7°F) per minute heat-up rate
- Prepreg volatile matter content level in the range of 10.4% w/w to 13.9% w/w

Effects of a temperature dwell cycle then were evaluated [30 minutes at 405°K (270°F)] on prepreg containing MN/80MDA:20TDA/PMDA resin. Properties of this panel (Table XXX) show no significant differences to properties

TABLE XXX

FLOW-PRESS DWELL CYCLE SCREENING

| Property | Value |
|---|---|
| Flow Press Characterization | |
| Dwell Cycle, Mins/°K | 35/408 |
| Molding Pressure, $MN/m^2$ | 0.79 |
| Heat-up Rate, °K/Mins | 1.8 |
| Resin Flow, % w/w | 9.4 |
| Resin Flow Start, °K | 408 |
| Resin Flow Complete, °K | 408 |
| Flow Duration, Mins | 18 |
| Flow Specimen Properties | |
| Flexural Strength, $kN/m^2$ | 299 |
| Density, $g/cm^3$ | 1.84 |
| Resin Content, % w/w | 36.4 |
| Void Content, % v/v | 2.3 |
| Fiber Content, % v/v | 46.1 |
| Barcol Hardness | 59 |

reported in Table XXIX for the same prepreg.

6.2.5 Flow-Press Graphite Prepreg Screening Studies

Prepreg tapes were prepared using Courtaulds HMS graphite fiber tow and MN/80MDA:20TDA/PMDA resin. These tapes were cut into 10-cm square panels, stacked unidirectionally 12-ply thick and evaluated in the flow-press using a simulated autoclave process as described in Section 6.2.2. This study

TABLE XXXI

FLOW-PRESS GRAPHITE/POLYIMIDE PREPREG[a] SCREENING

| Property | Values | |
|---|---|---|
| PREPREG CHARACTERIZATION | | |
| Resin Content, % w/w | 37.2 | 38.0 |
| Volatile Matter Content, % w/w | 11.5 | 13.3 |
| FLOW-PRESS CHARACTERIZATION | | |
| Molding Pressure, ($MN/m^2$) | 0.69 | 0.69 |
| Heat-up Rate, °K/Min | 4.9 | 3.9 |
| Resin Flow, % w/w | b | 20.9 |
| Resin Flow Start, °K | c | 419 |
| Resin Flow Complete, °K | c | 450 |
| Flow Duration, Mins. | c | 8 |
| FLOW SPECIMEN PROPERTIES | | |
| Flexural Strength, $MN/m^2$ | 757 | 564 |
| Flexural Modulus, $GN/m^2$ | 121 | 124 |
| Shear Strength, $MN/m^2$ | b | 27 |
| Type of Failure | b | Shear |
| Density, $g/cm^3$ | 1.39 | 1.49 |
| Resin Content, % w/w | 24.7 | 37.3 |
| Void Content, % v/v | 18.5 | 8.2 |
| Fiber Content, % v/v | 55.1 | 49.1 |

[a]Courtaulds HMS Graphite Fiber tow and MN/80MDA:20TDA/PMDA 1000 FMW resin
[b]Not evaluated because this panel was 6-ply thick
[c]Initial flow lasted from 311°K - 380°K. No second flow observed.

(Table XXXI) indicated that a higher volatile content level was necessary in graphite fiber prepregs than the nominal 12% w/w established earlier for glass fabric prepregs.

The overall results of this study indicated that only the MN or NA/80MDA: 20TDA/PMDA 1000 FMW resin formulations provided adequate ply consolidation

and laminate integrity when processed under simulated autoclave conditions. It is seen in Table XXVIII that the remaining six formulations did not provide specimens suitable for further characterization. Volatile content of the prepreg prior to start of the molding cycle was identified as being a major factor in producing consolidated laminates.

## 6.3 EVALUATION OF BAGGING MATERIALS

The only commercially available material found suitable for forming a pressure membrane (vacuum bag) for autoclave molding composites at 589°K cure temperatures was DuPont Kapton polyimide film. Other materials that will withstand the cure environment are either too stiff and brittle (e.g., stainless steel or aluminum alloy foil) or too weak (e.g., Teflon film). Developmental studies were performed in order to obtain satisfactory methods of sealing the Kapton film to the metal base plate and vacuum lines. Discussions of the evaluation of Kapton film thickness and vacuum bag sealants are provided below.

### 6.3.1 Kapton Film Evaluation

Kapton films in 0.05 and 0.075-mm thickness were evaluated. The 0.05-mm thick film was found to be the most satisfactory since the thicker film pulled away from the vacuum bag sealants at about 539°K (510°F) and caused a pressure leakage.

### 6.3.2 Vacuum Bag Sealants

The following sealant materials were evaluated for forming seals between the Kapton film, metal base plate and vacuum lines:

- High Temperature Vacuum Bag Sealant - Schnee, Moorehead Chemicals, Inc., Irving, Texas
- Uncatalyzed Silicon Rubber Gum Stock 7220, Stauffer Wacker, Inc. Adriaan, Michigan
- RTV 106 - General Electric, Waterford, New York

Use of these three sealants singly did not provide satisfactory seals at temperatures above 533°K, therefore, combinations of these sealants were evaluated. From these evaluations it was shown that a combination of RTV 106 sealant and Stauffer Wacker 7220 gum stock provided satisfactory seals at

589°K. It was found also necessary to apply Stauffer Wacker Primer SWS-401 to the Kapton film faying surfaces in order to obtain good adhesion.

### 6.3.3 Vacuum Bagging Technique

The following technique for vacuum bagging flat panel composites was developed and used throughout the studies discussed in Sections 6.4 and 6.5 (see Figure 29). Stauffer Wacker 7220 gum stock was applied as a 0.63-cm wide bead by a Semco Sealant air gun around the periphery of the aluminum alloy base plate and a bead of RTV 106 was laid around the outside of the 7220 gum-stock bead. Primer SWS-401 was coated onto the faying surfaces of the Kapton film and air dried. Four plies of Style 181 glass fabric were laid onto the base plate and porous Teflon-glass release fabric (Connecticut Hard Rubber Co.) was placed on top of the glass bleader fabric. The prepreg

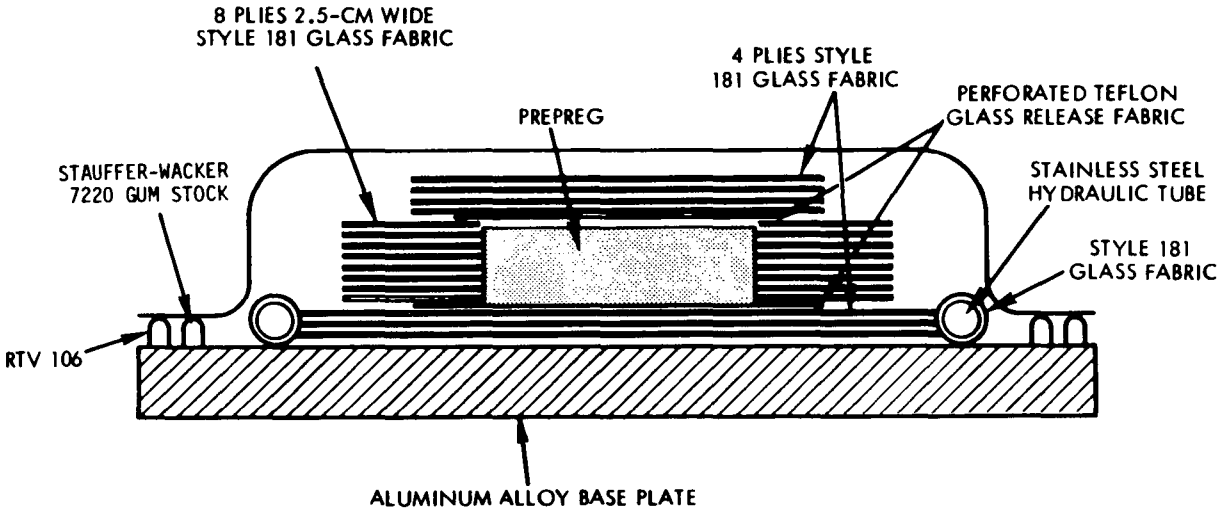


Figure 29. Schematic of Bagging System

stack was located on top of the Teflon fabric and eight plies of 2.5-cm wide Style 181 fabric were placed around the edge of the prepreg stack. A piece of porous Teflon glass release fabric and four plies of Style 181 glass bleader fabric were placed on top of the prepreg. Two pieces of 0.95-cm diameter stainless steel hydraulic tubing were wrapped in Style 181 glass fabric and located on the base plate. RTV 106 and 7220 gum stock sealants were applied around the tubes and the Kapton film was sealed over

the assembly. One tube was connected to a vacuum pump evacuation line and the other line to a vacuum gauge. Assemblies prepared in this manner then were ready for autoclave molding by the prescribed procedure.

## 6.4 AUTOCLAVE MOLDING OF GLASS PREPREGS

Prepregs were prepared from Style 181-A-1100 E glass fabric and the two candidate resin systems (1000 FMW NA/80MDA:20TDA/PMDA and MN/80MDA:20TDA/PMDA). These were subjected to a series of short processing studies to define the potential mechanical properties obtainable in flat panel laminates. After selection of the most promising process and resin system (MN/80MDA:20TDA/PMDA), brief reproducibility studies were performed. Details of these studies are described below.

### 6.4.1 Pressure/Heat-up Rate Study

A study was performed to define the effects of autoclave molding pressure and heat-up rate upon flat panel laminate end-properties. Details of this study are provided in Table XXXII. It was concluded from the data presented in Table XXXII that a 0.69 $MN/m^2$ molding pressure and 1.7 to 2.2°K/Min (3 to 4°F/min) heatup rate provided the most promising mechanical properties. The methyl nadic containing resin system (MN/80MDA:20TDA/PMDA) was selected at this point for the remainder of these studies based upon the overall higher properties obtained with this system under each processing condition.

### 6.4.2 Prepreg Volatile Matter Content

During the previous flow-press studies, it was established that the prepreg volatile matter content level is a key processing factor. Therefore, a study of varying volatile matter contents in prepregs was performed using the processing conditions selected in Section 6.4.1. Details of this study are provided in Table XXXIII. These studies showed that a volatile matter content in the range of 11 to 12% provided the desired resin flow with this process. High volatile matter contents produced excessive flow resulting in low resin and high void contents. Lower volatile matter contents did not provide sufficient resin flow resulting in high resin contents, poor consolidation and high void contents.

TABLE XXXII

PROPERTIES FROM AUTOCLAVE PROCESSING STUDIES

| Prepreg Drying Cycle | | | Prepreg Properties | | Processing Conditions | | | Laminate Properties | | | | |
|---|---|---|---|---|---|---|---|---|---|---|---|---|
| End[a] Cap | °K | Min | Volatile Matter %, w/w | Resin Solids Content %, w/w | Heat-up Rate °K/min | Pressure $MN/m^2$ | Flex. Str. $MN/m^2$ | Flex. Mod. $GN/m^2$ | Density $g/cm^3$ | Resin Solids Content % w/w | Void Content % v/v | Fiber Content % v/v |
| NA | 378 | 25 | 11.2 | 33.6 | 5.6 - 6.7 | 0.69 | 454 | 18.5 | 1.86 | 33.4 | 3.4 | 48.8 |
| MN | 378 | 25 | 11.4 | 35.6 | 5.6 - 6.7 | 0.69 | 502 | 17.2 | 1.84 | 35.6 | 2.8 | 46.8 |
| NA | 378 | 22 | 12.1 | 35.4 | 2.2 - 2.8 | 0.69 | 524 | 18.2 | 1.87 | 34.8 | 2.1 | 47.9 |
| MN | 378 | 25 | 10.9 | 33.4 | 2.2 - 2.8 | 0.69 | 540 | 18.2 | 1.89 | 34.0 | 1.5 | 49.1 |
| NA | 378 | 20 | 11.9 | 32.4 | 2.8 - 3.3 | 0.35 | 273 | 19.6 | 1.79 | 23.0 | 14.3 | 54.1 |
| MN | 378 | 20 | 11.8 | 31.7 | 2.8 - 3.3 | 0.35 | 352 | 18.9 | 1.78 | 24.7 | 13.3 | 52.9 |
| NA | 378 | 20 | 10.9 | 31.8 | 1.7 - 2.2 | 0.69 | 495 | 19.8 | 1.94 | 29.8 | 1.9 | 53.6 |
| MN | 378 | 20 | 10.4 | 31.9 | 1.7 - 2.2 | 0.69 | 590 | 18.7 | 1.93 | 31.2 | 1.9 | 52.3 |
| NA | 378 | 20 | 11.6 | 32.4 | 1.7 - 2.2[b] | 0.69 | 389 | 20.9 | 1.97 | 24.4 | 4.4 | 58.9 |
| MN | 378 | 20 | 10.9 | 30.1 | 1.7 - 2.2 | 0.69 | 453 | 17.9 | 1.87 | 29.5 | 5.6 | 51.9 |

a) Prepolymer formulation end cap abbreviation

b) Temperature held at 408°K (275°F) for 20 minutes and 435°K (325°F) for 20 minutes.

TABLE XXXIII

GLASS PREPREG VOLATILE MATTER CONTENT STUDY

| | Samples | | | |
|---|---|---|---|---|
| | 1 | 2 | 3 | 4 |
| Prepreg Drying Cycle | | | | |
| Min/°K — a | 5/378 | 5/378 | 5/378 | 5/378 |
| Min/°K — b | 15/378 | 20/378 | 10/378 | 20/378 |
| Prepreg Properties | | | | |
| Volatile Matter Content, % w/w | 12.1 | 10.5 | 13.5 | 10.9 |
| Resin Solids Content, % w/w | 34.3 | 30.7 | 30.6 | 31.0 |
| Laminate Properties | | | | |
| Flexural Strength, $MN/m^2$ | 544 | 382 | 118 | 510 |
| Flexural Modulus, $GN/m^2$ | 21.0 | 22.7 | -- | 17.6 |
| Density, $g/cm^3$ | 1.92 | 1.84 | 1.72 | 1.89 |
| Resin Content, % w/w | 32.2 | 33.9 | 20.8 | 32.0 |
| Void Content, % v/v | 1.5 | 4.1 | 18.7 | 2.9 |
| Fiber Content, % v/v | 51.1 | 47.9 | 53.7 | 50.1 |

[a]First Dip

[b]Second Dip

### 6.4.3 Reproducibility Studies

Four panels were molded from the Style 181 A1100 E-glass fabric/1000 FMW MN/80MDA:20TDA/PMDA prepreg in order to define inter-panel property variances. Processing conditions were those selected in Section 6.4.1 (0.69 $MN/m^2$ pressure and 1.7 - 2.2°K/min heat-up rate).

These panels provided good values for all properties tested as shown in Table XXXIV. The pooled percent standard deviations for a single panel were 5.35 $MN/m^2$ shear strength, 10.3 $MN/m^2$ flexural strength and 0.5 $GN/m^2$ flexural modulus. The individual value range for room temperature flexural

TABLE XXXIV

RESULTS OF AUTOCLAVE REPRODUCIBILITY GLASS REINFORCED LAMINATES[a]

| | Properties | Panel 19 | | Panel 34 | | Panel 35 | | Panel 46 | |
|---|---|---|---|---|---|---|---|---|---|
| | | Value | Std. Dev. | Value | Std. Dev. | Value | Std. Dev. | Value | Std. Dev. |
| Physical Properties | Resin Content, % w/w | 31.2 | 0.3 | 31.3 | 0.4 | 33.8 | 0.0 | 30.9 | 0.3 |
| | Density, g/cm$^3$ | 1.92 | 0.00 | 1.90 | 0.01 | 1.88 | 0.01 | 1.92 | 0.01 |
| | Void Content, % v/v | 1.9 | | 2.9 | | 2.1 | | 2.1 | |
| | Fiber Content, % v/v | 52.0 | | 51.4 | | 49.0 | | 52.3 | |
| Shear Properties | Strength, 297°K, MN/m$^2$ | 49.2 | 0.7 | 55.2 | 2.6 | 46.0 | 5.8 | 54.3 | 12.0 |
| | Strength, 589°K, MN/m$^2$ | 29.9 | 2.1 | 33.2 | 4.2 | 30.9 | 3.2 | 34.1 | 4.1 |
| | % Strength Retention[(b)] | 60.7 | | 60.0 | | 67.1 | | 62.8 | |
| Flexural Properties | Strength, 297°K, MN/m$^2$ | 599 | 12 | 578 | 10 | 519 | 15 | 529 | 14 |
| | Strength, 589°K, MN/m$^2$ | 410 | 8 | 433 | 8 | 435 | 3 | 420 | 6 |
| | % Strength Retention[(b)] | 68.4 | | 74.9 | | 83.7 | | 79.4 | |
| | Modulus @ 297°K, GN/m$^2$ | 23.0 | 0.4 | 22.8 | 0.6 | 19.7 | 0.3 | 20.8 | 0.7 |
| | Modulus @ 589°K, GN/m$^2$ | 19.7 | 0.4 | 19.7 | 0.7 | 18.1 | 0.7 | 18.8 | 0.5 |
| | % Retention[(a)] | 85.5 | | 85.8 | | 91.6 | | 90.7 | 0.6 |

(a) Style 181 E Glass Fabric with A1100 Finish

(b) $\frac{\text{Property at 589°K}}{\text{Property at 297°K}} \times 100$

strength for all four panels was 503 - 610 $MN/m^2$ which indicates good reproducibility of the best values reported in Tables XXXII and XXXIII. Overall, it is concluded from this study that good reproducibility is obtained with autoclave molded glass laminates containing the P10P-A resin system.

## 6.5 AUTOCLAVE MOLDING OF GRAPHITE PREPREGS

Prepregs were prepared from Courtaulds HMS graphite fiber tows and P10P-A amide-acid varnish. Processing studies were performed in order to establish processing conditions for autoclave molding flat panels. Composite shear strengths for the resultant panels were substantially lower than values previously obtained with A-type polyimides in graphite composites, therefore, a brief feasibility demonstration with sized fiber was performed.

### 6.5.1 Prepreg Volatile Matter Content Studies

Courtaulds HMS high modulus graphite fiber tows were impregnated with the P10P-A amide-acid varnish and collimated by drum winding at 31 to 32 tows per meter. Impregnation of the fibers was performed using a spray-gun mounted on the drum winding equipment. Resin content control was maintained by monitoring the quantity of resin deposited by the spray-gun. Winding rate was 12.7 cm/sec on a 76.2 cm diameter drum.

The prepreg tapes were removed from the drum on the Mylar backing film, cut to a convenient length (30-cm approximately), and dried in an air circulating oven. Drying cycles evaluated and the resultant prepreg volatile matter contents are reported in Table XXXV.

These prepregs were cut into 7.6 x 10.1-cm pieces and stacked 12-ply thick. All panels were molded identically by the process selected in Section 6.4.1 for glass prepregs. The resultant laminate data shown in Table XXXV indicated that horizontal shear strengths for all panels were considerably lower than obtained with P13N resin composites. Also, large variations in volatile matter contents of the prepregs were observed at identical drying cycles, *e.g.*, 20 minutes at 378°K provided 12.3 and 14.5% w/w, 50 minutes at 378°K provided 10.7 and 13.9% w/w. A possible explanation for this wide variability in resin and volatile matter contents could be preferential absorption into the graphite fiber. Consequently, it was decided to study the effect fiber sizing provides in control of these variables (See Section 6.5.4).

TABLE XXXV

GRAPHITE PREPREG VOLATILE MATTER STUDY

| | Samples | | | | | | |
|---|---|---|---|---|---|---|---|
| | 1 | 2 | 3 | 4 | 5 | 6 | 7 |
| **Prepreg Drying Cycle** | | | | | | | |
| °K/Min | 378/20 | 378/20 | 378/80 | 378/50 | 378/50 | 378/50 | 378/30 |
| Resin Batch | 5112-18 | 5112-18 | 5112-19 | 5112-19 | 5112-19 | 5112-22 | 5112-22 |
| **Prepreg Properties** | | | | | | | |
| Volatile Content, % w/w | 12.3 | 14.5 | 12.5 | 10.7 | 13.9 | 12.1 | 15.5 |
| Resin Solids Content, % w/w | 36.1 | 37.7 | 43.5 | 43.9 | 44.8 | 44.2 | 42.6 |
| **Laminate Properties** | | | | | | | |
| Flexural Strength, $MN/m^2$ | 583 | 584 | a | a | 490 | 402 | 508 |
| Flexural Modulus, $GN/m^2$ | 171 | 174 | a | a | 97 | 118 | 136 |
| Shear Strength, $MN/m^2$ | 36.7 | 24.9 | a | a | 30.4 | 40.5 | 43.4 |
| Density, $g/cm^3$ | 1.59 | 1.55 | 1.55 | 1.41 | 1.52 | 1.58 | 1.59 |
| Resin Content, % w/w | 30.0 | 22.6 | 43.1 | 43.3 | 45.1 | 44.7 | 40.50 |
| Void Content, % v/v | 4.7 | 9.9 | 2.2 | 11.0 | 3.4 | 0.9 | 0.7 |
| Fiber Content, % v/v | 58.6 | 63.1 | 46.4 | 42.1 | 43.9 | 46.0 | 49.8 |

[a]No test data

### 6.5.2 Reproducibility Study

Graphite prepreg tapes were prepared in the same manner as discussed above and molded into composite panels. The properties of these panels are provided in Table XXXVI. It is observed from these results that although a large data scatter is present between the flexural strengths of panels, the strength retention at 589°K for all three panels is excellent. Shear strengths for these panels again are low and demonstrate poor elevated temperature retention.

### 6.5.3 Fiber Sizing Feasibility Study

TRW P13N amide-acid varnish was applied to the graphite fiber tows and thermally treated for two minutes at 561°K (550°F). The P10P-A amide-acid varnish then was applied and the prepregs were press-molded by the standard procedure. Comparison between shear strengths obtained from press-molded composites containing sized and unsized fibers in the P10P-A resin matrix and unsized fibers in MN and NA/MDA/PMDA resin matrices are given in Table XXXVII. It is shown by these data that a) P10P-A resin provides lower shear strengths than other A-type polyimides in graphite composites, and b) the P13N sizing provides higher shear strengths with this resin than obtained with unsized fibers. It was concluded from the results of this and the preceding three studies discussed in this section that graphite composites containing P10P-A resin can be satisfactorily autoclave molded but considerably more developmental effort is required in order to optimize composite end-properties. The concept of pre-sizing fibers appears to be a sound approach to obtain good properties. It is believed that this approach will permit precise control of the prepreg volatile matter level as well as improving resin adhesion to the fibers.

## 6.6 DEMONSTRATION COMPONENT

A demonstration component was designed and then autoclave molded that represented an aerofoil leading edge section with an integrally molded vertical stiffening strut. Fiber orientations were a combination of plies at 0°, +30° and -30° to the aerofoils horizontal axis. Fabrications of two glass fiber and six graphite fiber reinforced parts were attempted. Design and fabrication details are provided below.

TABLE XXXVI

RESULTS OF AUTOCLAVE STUDY GRAPHITE COMPOSITES

| | Properties | Panel 23 | | Panel 36 | | Panel 37 | |
|---|---|---|---|---|---|---|---|
| | | Value | Std. Dev. | Value | Std. Dev. | Value | Std. Dev. |
| Physical Properties | Resin Content, % w/w | 30.0 | 0.4 | 44.7 | 0.5 | 40.5 | 0.9 |
| | Density, $g/cm^3$ | 1.59 | 0.00 | 1.58 | 0.00 | 1.59 | 0.01 |
| | Void Content, % v/v | 4.7 | | 0.9 | | 0.7 | |
| | Fiber Content, % v/v | 58.6 | | 46.0 | | 49.8 | |
| Shear Properties | Strength @ 297°K, $MN/m^2$ | 36.7 | 17.2 | 39.9 | 8.3 | 44.4 | 15.8 |
| | Strength @ 589°K, $MN/m^2$ | 23.6 | 23.4 | 23.0 | 59.9 | 24.0 | 20.7 |
| | % Retention | 62.5 | | 58.6 | | 54.0 | |
| Flexural Properties | Strength @ 297°K, $MN/m^2$ | 483 | 48 | 393 | | 424 | 19 |
| | Strength @ 589°K, $MN/m^2$ | 55 | 8 | 396 | 19 | 395 | 67 |
| | % Retention | 110 | | 101 | | 93.0 | |
| | Modulus @ 297°K, $GN/m^2$ | 15.0 | 1.3 | 10.1 | | 14.7 | 0.1 |
| | Modulus @ 589°K, $GN/m^2$ | | | 11.9 | 0.6 | 11.9 | 0.3 |
| | % Retention | | | 111. | | 81.0 | |

TABLE XXXVII

COMPARISON BETWEEN SIZED AND NON-SIZED GRAPHITE FIBER COMPOSITES

| Fiber Sizing Resin | Resin Formulation | Resin Content % w/w | Density $g/cm^3$ | Fiber Content % v/v | Void Content % v/v | Shear Strength $MN/m^2$ |
|---|---|---|---|---|---|---|
| None | MN/MDA/PMDA | 42.2 | 1.56 | 47.5 | 1.9 | 52.8 |
| None | NA/MDA/PMDA | 41.9 | 1.59 | 48.6 | 0.1 | 59.1 |
| None | MN/80MDA:20TDA/PMDA | 40.4 | 1.53 | 48.0 | 4.5 | 39.2 |
| P13N | MN/80MDA:20TDA/PMDA | 43.9 | 1.57 | 46.5 | 0.4 | 48.0 |

### 6.6.1 Component Design

The component contour was designed to simulate the leading edge of an air foil section. Fiber orientations were selected to provide maximum stiffness for resisting loads along the horizontal axis and also with sufficient fiber angulation to accomodate transverse loads. Continuous fibers were used through the reinforcing strut and into the outer skin so that loads were distributed efficiently. The design employed a balanced pattern of 0°, +30° and -30° fiber orientation to the aerofoils horizontal axis in order to minimize excessive residual stresses and warpage. Sketches of the component are provided in Figures 30 and 31.

During the design study, engineering estimates were made of the residual stresses resulting from differential thermal expansions during cure at the interfaces of different ply orientations. These estimates showed that residual stresses in the cured component would not be high enough to cause cracks or delaminations.

### 6.6.2 Mold Design

The mold design for the demonstration component utilized a welded construction of stainless steel alloy AISI-304 as shown in Figure 32. Stainless steel alloy AISI-304 was selected because it has a relatively low coefficient of thermal expansion and can be machined and welded easily. The importance of a low coefficient of thermal expansion is to prevent formation of gaps between adjacent bundles of graphite fibers during heat-up to the resin cure temperature (561 to 589°K). Mold construction consisted of a mold saddle (Figure 32) and a mold insert. The saddle was designed to the component's inside

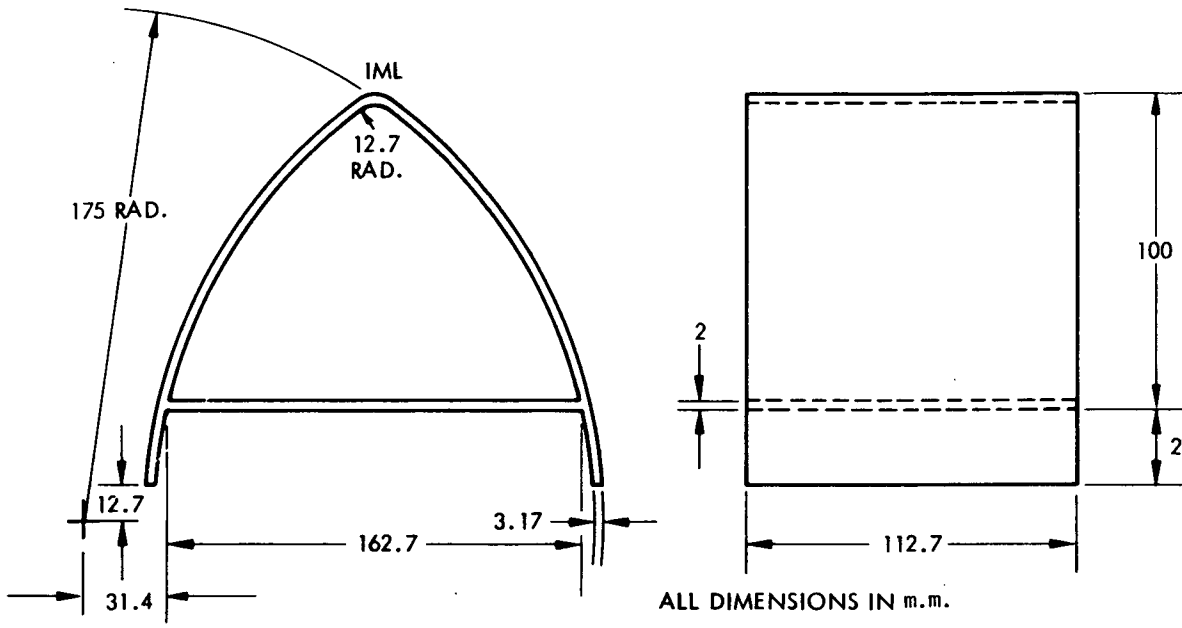


Figure 30. Graphite Composite, Autoclave Molded, Demonstration Component

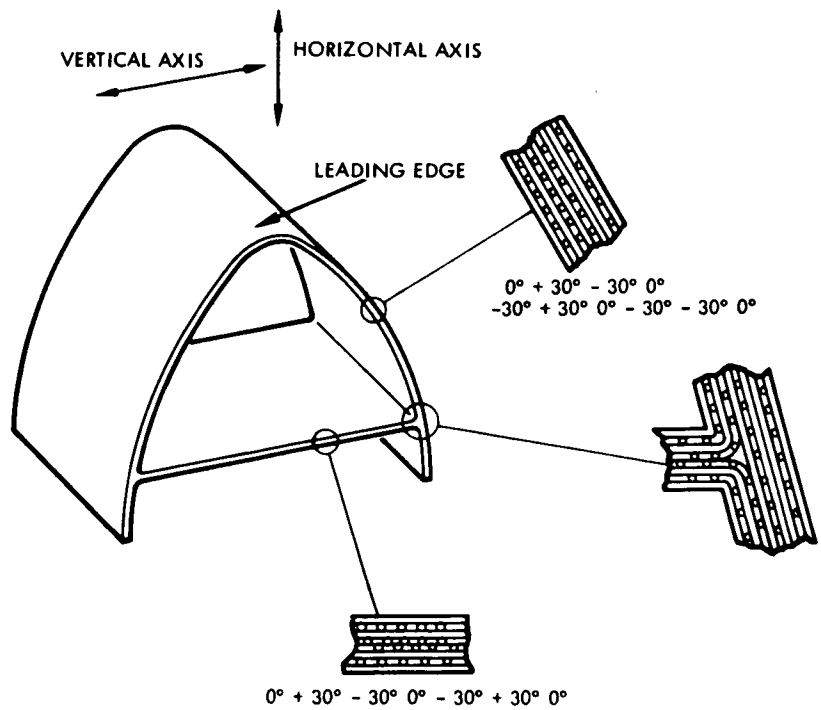


Figure 31. Demonstration Component

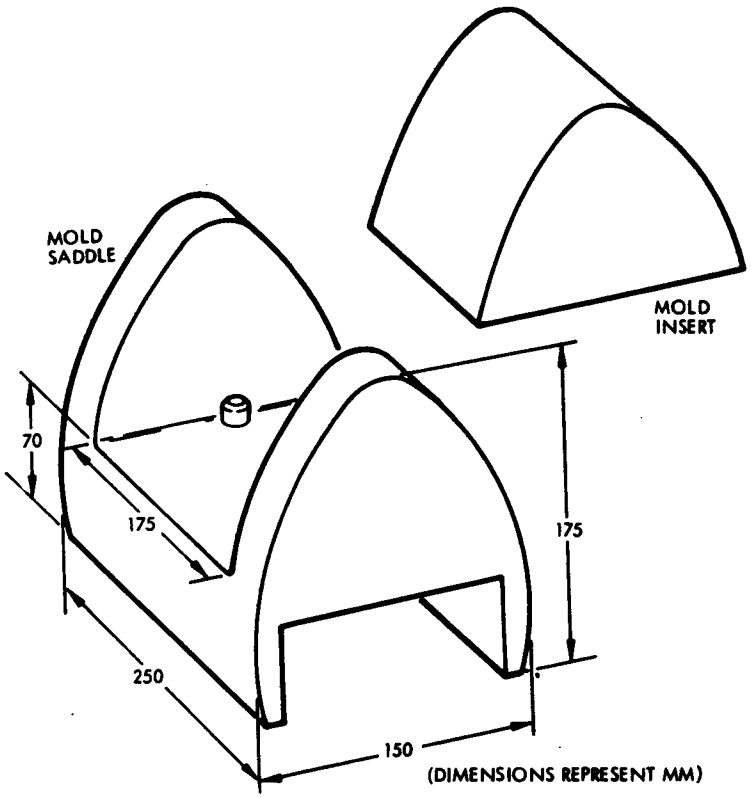


Figure 32. Lay-up Mold Design

mold line below the reinforcing strut and included end-plates contoured to the overall inside mold line. These plates were incorporated to provide a sealing surface for the flexible pressure membrane which is used while autoclave molding the component. This feature was necessary in order to minimize folds and creases in the flexible pressure membrane. The insert was contoured to the component's inside mold line above the reinforcing strut.

Fabrication of the saddle proceeded by welding two longitudinal "legs" underneath a flat plate and two transverse end plates on top of this plate. The mold insert was a solid piece of stainless steel alloy which was bolted to the saddle and then machined to the design contour simultaneously with the saddle. After machining, the insert was removed from the saddle and 0.203-cm was machined from the bottom surface. All tooling holes in both pieces were filled with weld.

### 6.6.3 Fabrication Process Development

Two glass fiber reinforced components were fabricated prior to venturing into the manufacture of the actual high modulus graphite fiber-reinforced component. The glass structure fabrication was conducted to provide experience with lay-up and molding techniques. The first component utilized prepreg prepared by drumwinding 20-end E-glass roving and then impregnating with P10P-A varnish by spray gun. In order to achieve suitable handleability of this prepreg for lay-up of the demonstration component it was necessary to retain a higher volatile matter content than used for flat panel lay-up (See Section 6.2.2). The volatile matter content selected as the most suitable was ∿18% w/w. Lay-up of this first component proceeded by plying one each 0°, +30°, -30° and 0° over the mold saddle and around the mold insert (See Figure 33 ,Steps A and B). Because the volatile matter content of this prepreg was high, the partial lay-up was staged in an air-circulating oven for 50 minutes at 378°K (220°F), 30 minutes at 394°K (250°F) and 60 minutes at 408°K (275°F).

The insert then was placed into the saddle (See Step C), and the remaining plies were laid-up overall (See Step D). These also were dried in the same manner as above after which a vacuum bag was installed over the lay-up prior to location of the assembly into the autoclave. Because the lay-up had been heated to 408°K during the pre-drying operation thus causing a size differential between mold and preform, it was decided to heat the mold up to this temperature under vacuum pressure before applying augmented pressure in order to minimize wrinkling. The part was autoclave cured under 1.38 $MN/m^2$ (200 psig) at 580°K (600°F) for one hour. Upon completion of the cure cycle, pressure was released prior to cool down in order to prevent unnecessary loading of the part during thermal contraction of the mold. No problems were encountered in removing the part from the mold because there were no restraints in lifting the part complete with mold insert from the mold-base (Step E) after which the mold insert slipped easily out of the part (Step F).

Examination of this first part showed that the glass fibers were not wetted thoroughly which apparently was caused by the prepregging method. Therefore, a second glass fiber part was fabricated using prepreg that had been impregnated by a dip tank process rather than the spray gun process.

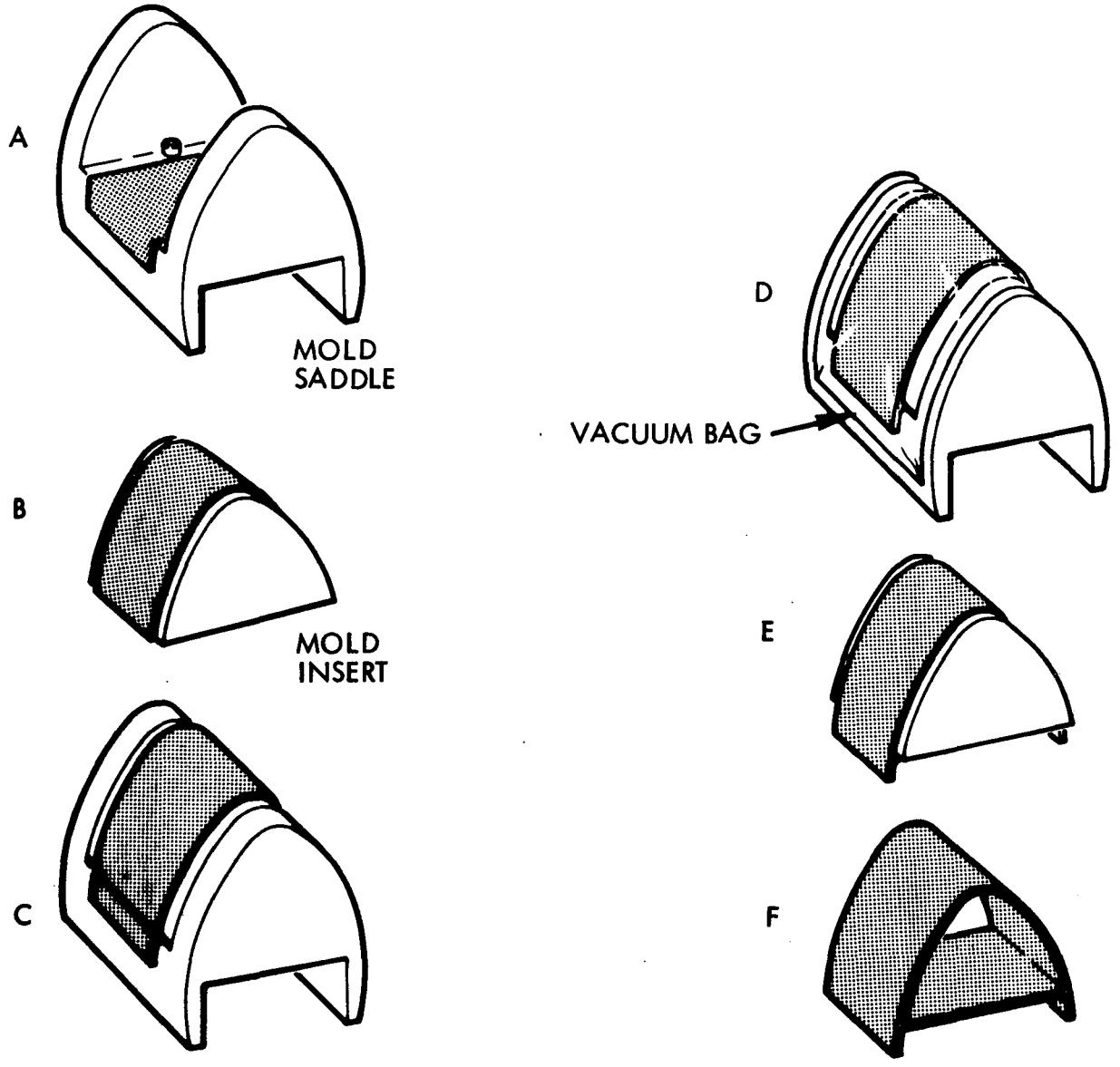


Figure 33. Fabrication Sequence

This second cured part had good fiber wetting throughout but had severe wrinkles along the leading edge. Since no problems were encountered in part lay-up nor in part removal from the mold, it was decided to proceed with the fabrication development studies using high modulus graphite fiber reinforcement.

The first graphite fiber reinforced part was fabricated by the same method as the glass fiber reinforced parts except that a 0.5-mm thick aluminum alloy overlay was used over the outside surface in an attempt to avoid wrinkling along the leading edge. Prepreg was prepared from Courtaulds HMS graphite fiber tow and P10P-A varnish by drumwinding and spray-gun impregnation. After the oven pre-drying cycles, it was observed that a large size-differential existed between the pre-form and the mold which resulted in severe contour distortion of the cured part (See Figure 34).

Therefore, a single step lay-up sequence was tried for the second graphite fiber reinforced part. (No intermediate drying operations were performed on the saddle and insert lay-ups). The resultant part did not cure fully which apparently was caused by excessive entrapped solvent (DMF).

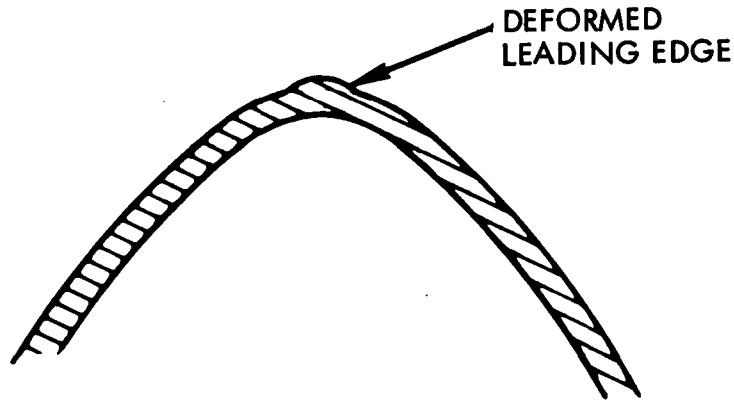


Figure 34. Deformed Leading Edge

For the third part, the intermediate drying operations were performed again but perforated Hi-Shrink Mylar tape was wrapped around the preforms during the drying cycles. The outer aluminum alloy sheet overlay was not used on this part. This third part had wrinkles along the leading edge which apparently were caused by insufficient debulking during lay-up.

For the fourth part, a perforated aluminum alloy overlay was used under the Mylar shrink tape during the final staging operation. After cure, this part appeared to suffer from pre-cure resulting in poor adhesion between

plies. Also, there was a slight distortion on both sides of the leading edge which apparently was propagated by mismatch between the staged preforms at the reinforcing strut interface.

It appeared that the pre-cure condition in the fourth part was caused by a decrease in heat-up rate at about the 522°K (480°F) point in the cure cycle. Therefore, for the fifth part, it was decided to overshoot the cure temperature in the autoclave in order to maintain the heat-up rate up to 561°K (550°F). Also, in order to circumvent the mis-match between preform interfaces, both preforms were staged with the insert and saddle together and a 1.5-mm shim to hold the faces apart. After one hour at 408°K (275°F), the faces were opened and the preforms were staged open face for an additional one hour at 408°K. This part appeared to be well cured, had good contour compliance and was well consolidated except for a small area along the leading edge. Apparently the aluminum alloy sheet overlay prevented molding pressure from being applied to the prepreg in this area.

It was concluded from these results that the final part fabricated during this program should utilize the same process as used for the fifth part except an aluminum alloy sheet overlay would not be used.

### 6.6.4 Detailed Fabrication Process

The detailed fabrication process used for the sixth and final demonstration part for this program was as follows:

6.6.4.1 Prepreg Preparation - Courtaulds HMS high modulus graphite fiber tows were impregnated with the PIOP-A amide-acid varnish and collimated at 31 to 32 tons per meter of width. Impregnation of the fibers was performed using a spray gun mounted on the drum winding equipment. Resin solids content was controlled to 40% w/w by monitoring the quantity of resin deposited by the spray gun. Winding rate was 12.7 cm/sec on a 76-cm diameter drum, width of the prepreg tape was 56-cm. After completion of winding, the prepreg tapes were dried to a volatile matter level of 18% w/w by rotating the drum for six hours under two heat lamps located approximately 20-cm from the prepreg surface. The tapes then were removed from the drum on the Mylar backing sheet and covered with polyethylene film.

TABLE XXXVIII. PREPREG CUTTING PATTERNS

| QUANTITY | SIZE (cm) | FIBER ORIENTATION |
|---|---|---|
| 2 | 14 X 21.6 | 0° |
| 1 | 14 X 21.6 | +30° |
| 1 | 14 X 21.6 | -30° |
| 2 | 14 X 43.2 | 0° |
| 1 | 14 X 43.2 | +30° |
| 1 | 14 X 43.2 | -30° |
| 2 | 14 X 33 | 0° |
| 2 | 14 X 33 | +30° |
| 2 | 14 X 33 | -30° |

6.6.4.3 Saddle Preform Lay-up and Staging (See Figure 33, Step A) - One each 0°, +30°, -30° and 0°, 14.0-cm wide by 21.6-cm long pieces of prepreg were stacked and laid on the mold saddle. Removal of Mylar and polyethylene films were facilitated by chilling with "dry-ice." The mold insert was placed on top of the prepreg lay-up and 1.5-mm thick shims were placed between the mold surfaces. Perforated Mylar shrink tape was wrapped around the mold saddle and insert and then this assembly was placed into a preheated oven at 378°K (220°F). The prepreg then was staged as follows:

50 minutes at 378°K (220°F)
30 minutes at 394°K (250°F)
60 minutes at 408°K (275°F)

Upon completion of this cycle, the mold insert was removed from the saddle and the prepreg then was staged for a further 60 minutes at 408°K.

6.6.4.4 Insert Preform Lay-up and Staging (See Figure 33 , Step B) - One each 0°, +30° and 0°, 14-cm wide by 43.2-cm long pieces of prepreg were laid-up around the mold insert. Staggered butt joints were used throughout the lay-up. This lay-up then was placed into the mold saddle with the saddle preform removed and 1.5-mm thick shims were placed between the mold surfaces. Perforated Mylar shrink tape was wrapped around this assembly and the prepreg was oven-staged in the same manner as the saddle preform.

6.6.4.5 Final Lay-up and Staging (See Figure 33, Step C) - The saddle preform was located on the mold saddle and then the mold insert and preform were placed into the saddle. One each +30°, -30°, 0°, -30° and 0°, 14-cm wide by 33-cm long pieces of prepreg were laid-up over the two preform subassemblies. A piece of aluminum alloy sheet, 0.5-mm thick, perforated with 4.76-mm diameter holes on 2.5-cm centers, was placed over the lay-up. This was wrapped with perforated Mylar shrink tape and then oven staged as follows:

50 minutes at 278°K (220°F)
30 minutes at 394°K (250°F)
60 minutes at 408°K (275°F)

6.6.4.6 Vacuum Bag Installation - The Mylar shrink tape and perforated aluminum alloy sheet were removed from the preform and surface irregularities from the perforations were removed with a scraper. A 6.4-mm wide bead of Stauffer-Wacker 7220 uncatalyzed silicone rubber gum stock was laid around the mold saddle's periphery. Primer SWS-401 was coated onto the faying surfaces of 0.05-mm thick Kapton film and air dried. A valve-stem vacuum line connector was installed in the Kapton film (See Figure 35) and Style 181 glass fabric, 4-ply thick, was placed around the edges of the preform and beneath the vacuum line connector. A thermo-couple was installed between the mold surfaces at the vertical strut. The Kapton film then was layed over the preform, sealed to the silicone rubber gum stock and air was evacuated down to provide a pressure of 6.9 $kN/m^2$. A bead of RTV 106 was extruded around the peripheral seal and over the Kapton film at the preform's edge (see Figure 29). The RTV 106 was cured for 16 hours at room temperature (~294°K).

This assembly (see Figure 36) was placed into the autoclave and a stainless steel sheathed bellows flexible vacuum hose was connected to the valve stem.

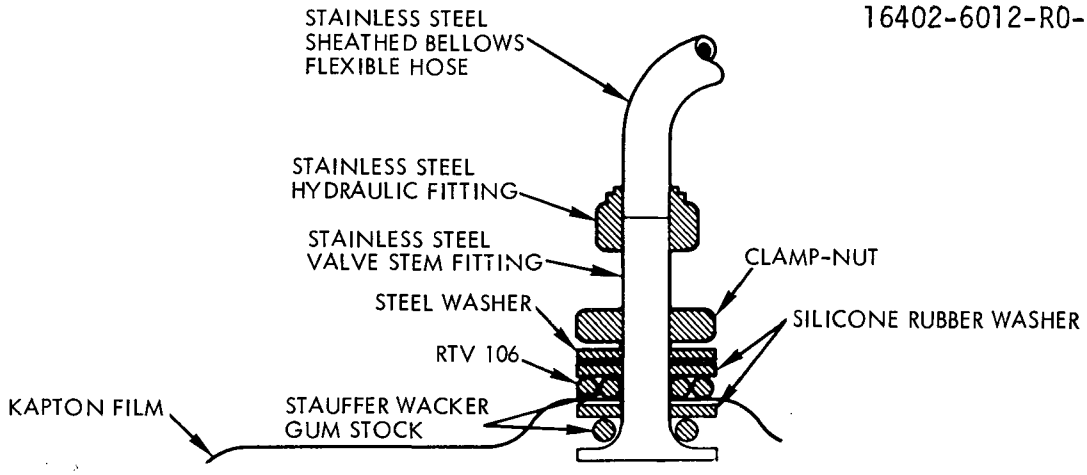


Figure 35. Schematic of Valve Stem Vacuum Hose Connector

6.6.4.7 Molding Cycle - The part was molded in accordance with the profile shown in Figure 37.

6.6.4.8 Part Removal - After completion of the molding cycle, pressure was released prior to cool-down of the mold and part to room temperature. The molded part and insert were removed from the saddle and then the insert was slipped out of the molded part.

6.6.5 Demonstration Component Final Inspection

Examination of the final part shown in Figure 38, was made in order to define the success of this effort. It appeared that a successful demonstration of the autoclave processability of P1OP-A resin system resulted from this work.

There was an inherent problem identified in the demonstration part configuration which precluded molding a wrinkle free exterior surface to the part. The main feature of the part associated with this problem was the reinforcing strut which, due to consolidation during cure, permitted the mold insert to move downwards thus providing slack in the outer fibers. These loose fibers subsequently wrinkled and remained along the leading edge of the cured final part. Consolidation of the prepreg tape was good, there was some transfer of the angled fibers pattern through to the outer surface.

Dimensionally the inside surfaces of the cured part complied very closely with the mold (see Table XXXIX). Thickness per ply of the laminate was 0.33-mm which was greater than the anticipated 0.25-mm per ply. Further detailed evaluations of the composite (e.g., resin content) will be performed after structural testing. A detailed structural testing plan is being prepared by NASA Lewis Research Center.

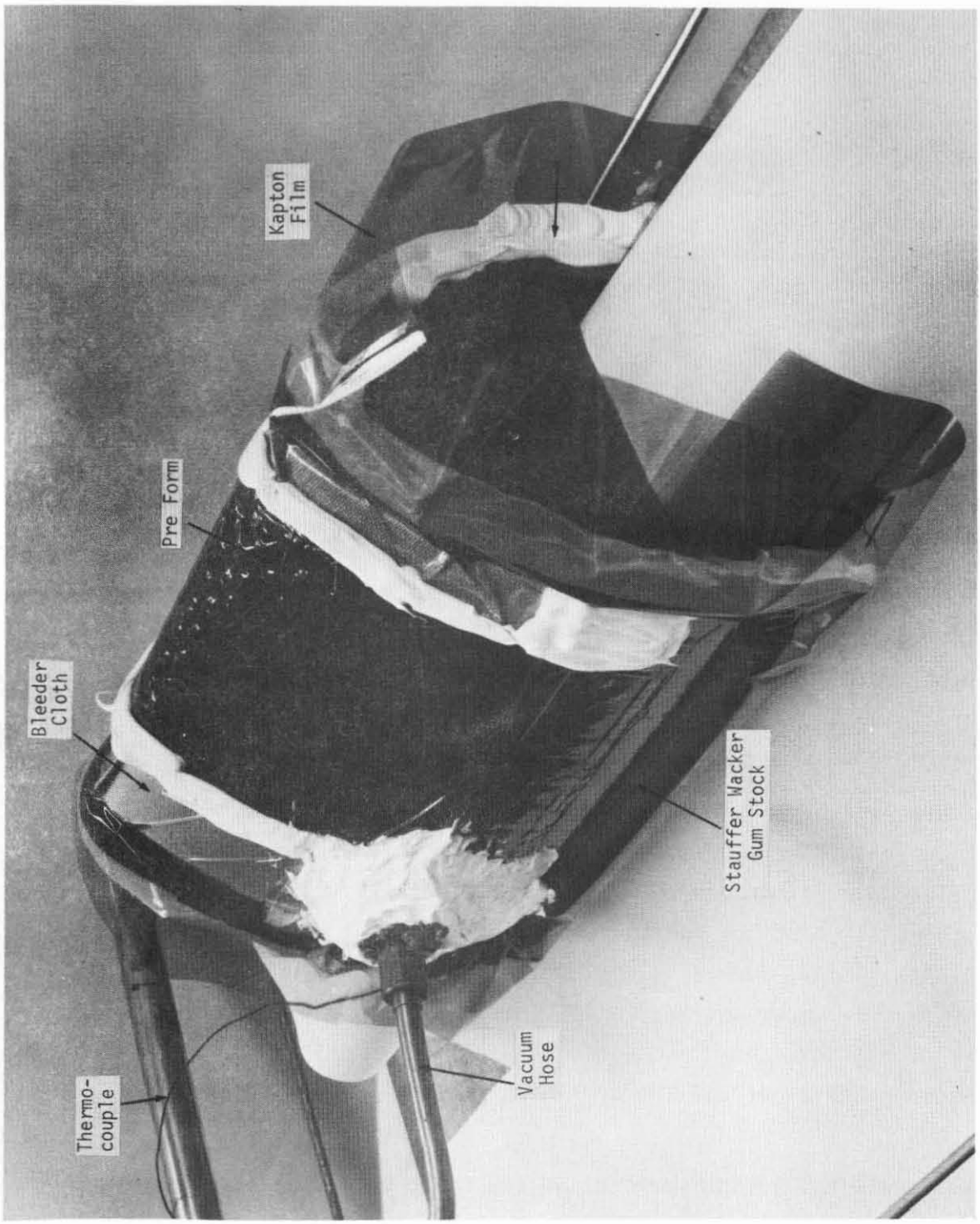


Figure 36. Demonstration Part Ready for Molding

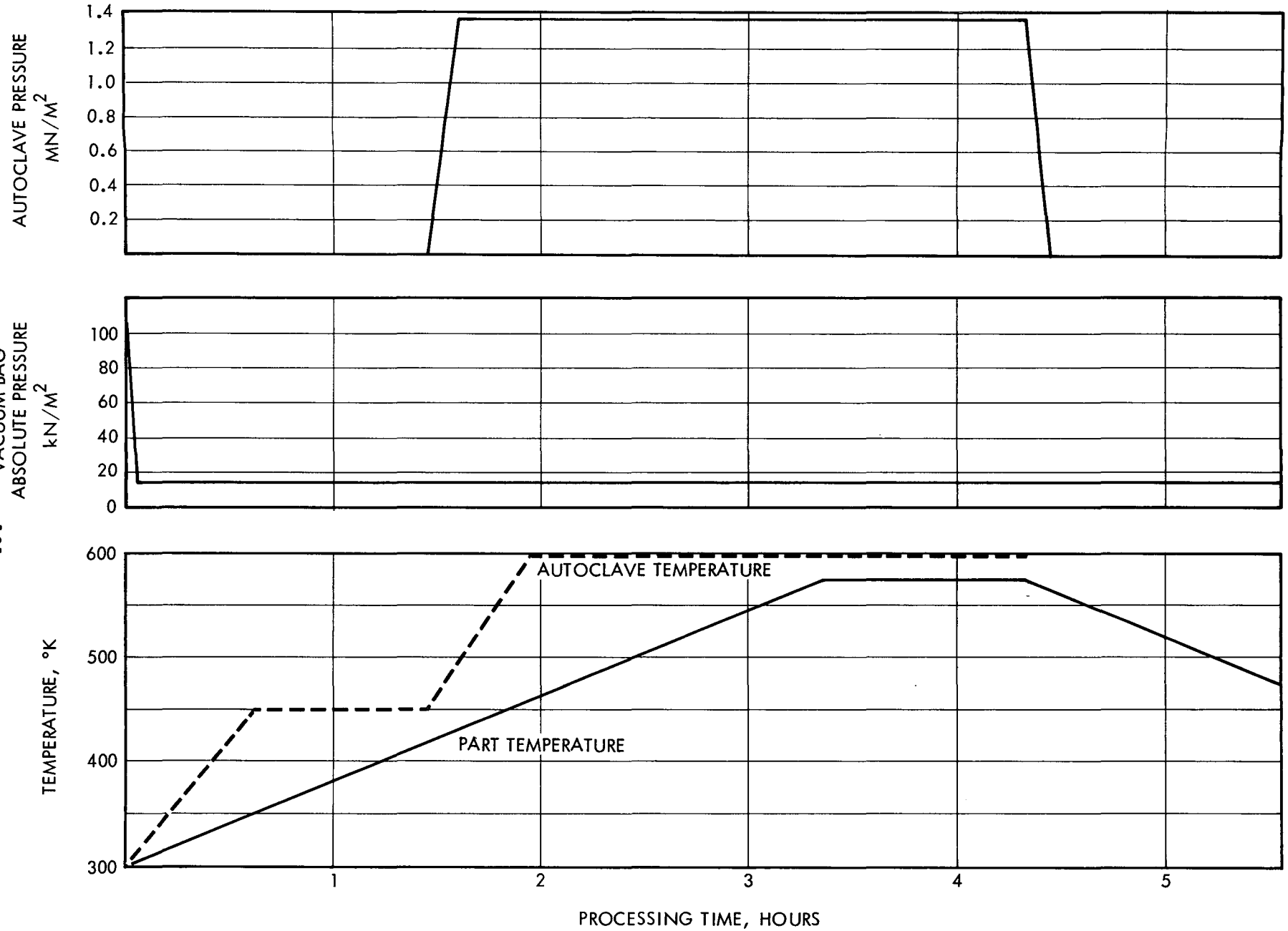


Figure 37. Autoclave Molding Cycle



CR 72984
16402-6012-RO-00

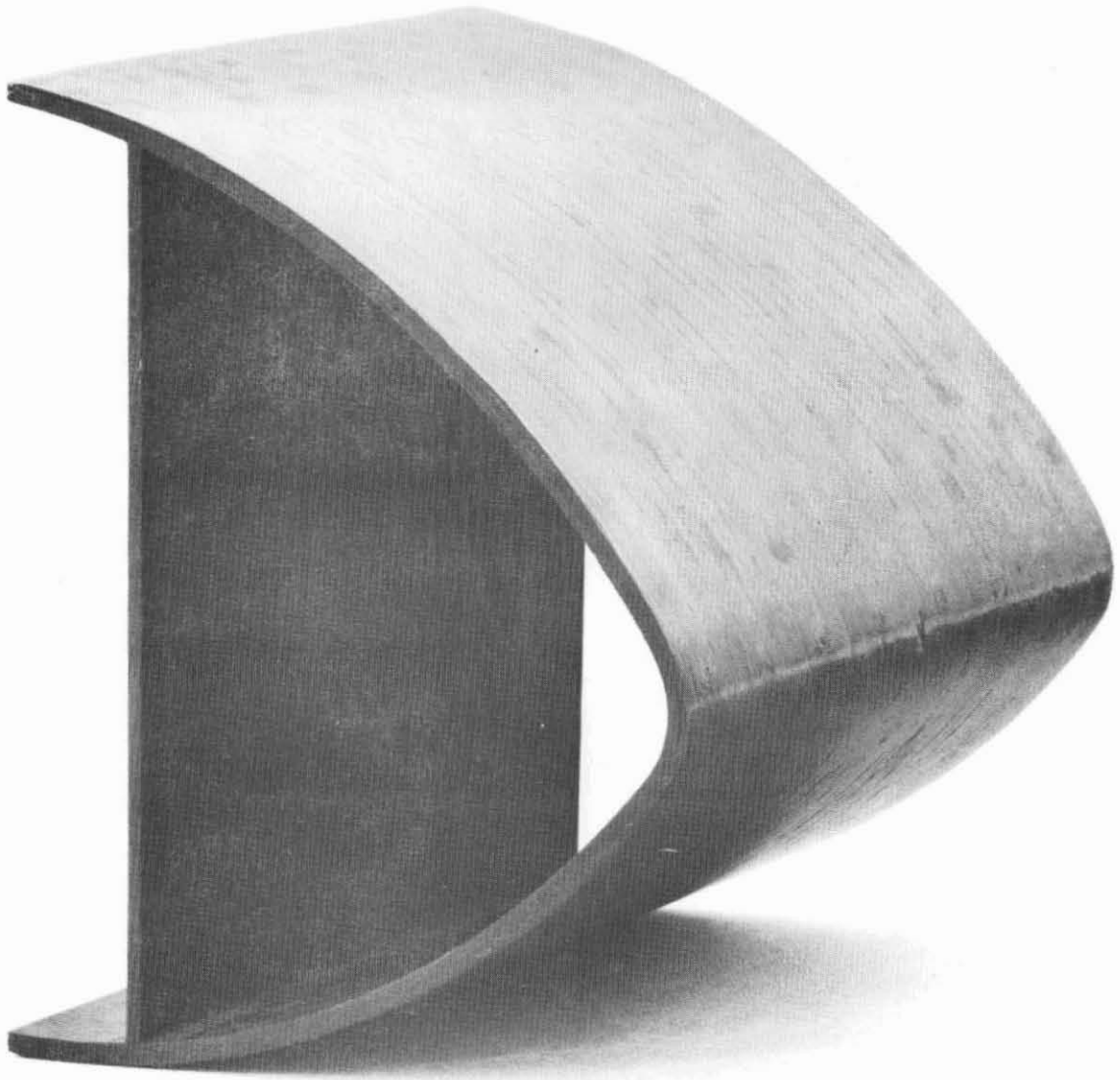

Figure 38. Final Simulated Air Foil Section

TABLE XXXIX
DIMENSIONS OF MOLDED COMPONENT

| Source of Measurement | Dimension[a] | |
|---|---|---|
| | A | B |
| Mold | 14.117 | 10.071 |
| Part | 14.135 | 10.074 |
| Variation | 0.018 | +0.003 |

(a)

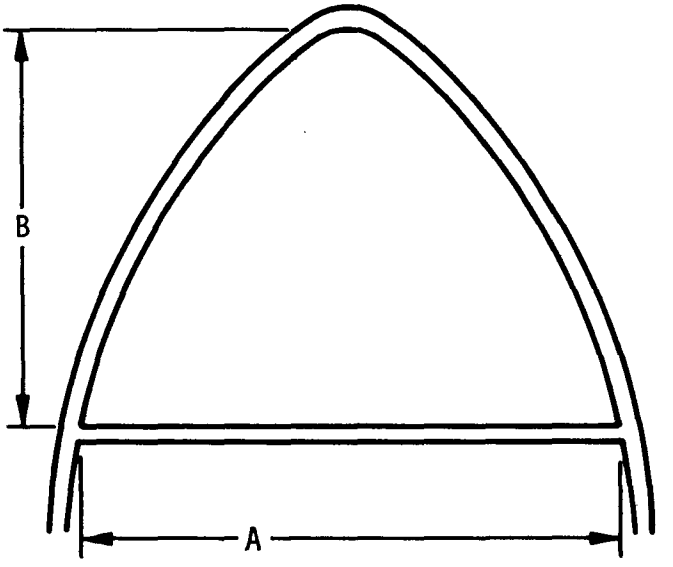

# 7. CONCLUSIONS AND RECOMMENDATIONS

Summarized below are the conclusions reached during this experimental study to improve A-type polyimide laminating resins. Based on the findings, recommendations are given for further material and process improvement studies.

## 7.1 CONCLUSIONS

1. Based on experimental studies with model compounds, the previously elucidated mechanism of pyrolytic polymerization has been substantiated. This mechanism, involving a partial reverse Diels-Alder reaction of the reactive end groups followed by a linear extension and crosslinking reaction of the components present, is valid in both reduced and applied pressure environments.
2. Model compound studies identified Lewis acids to be effective pyrolytic polymerization catalysts to reduce both cure time and temperature.
3. Comparison of nadic anhydride and nadic/maleic anhydride blends as reacting alicyclic prepolymer end groups identified nadic anhydride as the best endocyclic material for preparation of polymers by pyrolytic polymerization based on processing and thermo-oxidative stability characteristics.
4. A specific Lewis acid catalyst, tin tetrachloride, provided a significant reduction in the cure time required for prep- of thermo-oxidatively stabile P10P moldings.
5. Processing studies indicated that P10P resin can provide high modulus graphite fiber reinforced composites having excellent mechanical properties. However, it was observed that property scatter within and between panels is high.
6. A flexural creep phenomena was observed in P101P/Courtaulds HMS graphite fiber reinforced composites at elevated temperatures. It appears that the creep occurs in the resin matrix and is influenced jointly by both test temperature and stress level.
7. It was demonstrated that P10P-A resin is suited ideally as a laminating resin for use in autoclave processable glass fabric and high modulus graphite fiber prepregs. Processing studies demonstrated that composites can be autoclave molded at pressures in the range of 0.69 $MN/m^2$ to 1.38 $MN/m^2$ and with heat-up rates in the range of 1 to 6°K/minute.
8. Preliminary studies indicated that P10P-A resin matrix adhesion to Courtaulds HMS high modulus graphite fibers is weak. The feasibility of sizing the graphite fiber with another A-type polyimide resin (e.g., P13N) was demonstrated and was shown to improve composites interlaminar shear strength.

## 7.2 RECOMMENDATIONS

1. Additional study of model compounds is warranted toward achieving still further reduced processing conditions. Specific emphasis should be placed on modification of end cap chemical composition and further utilization of catalysts in order to reduce required cure temperature requirements to 500°K (450°F) temperatures.

2. Polymer synthesis and characterization studies should be conducted to confirm that the conclusions reached with model compound studies are valid for polymerization reactions.

3. Further autoclave processing development studies should be conducted on polyimide polymers that show promise for improved autoclavability to yield composites possessing high composite and thermo-oxidative stability properties.

4. It is recommended that detailed processing studies be performed to improve the adhesion of the new autoclavable resin to graphite fibers to include evaluation of sizing systems for the fibers; it is recommended that in-depth studies be performed on A-type polymers to determine mode and extent of flexural creep in high modulus composites.

# 8. NEW TECHNOLOGY

This section provides discussions of catalyst systems for promoting pyrolytic polymerization identified in this program and the technology associated with development of the autoclavable A-type polyimide resin, P10PA. These concepts are believed to be of sufficient novelty that new technology disclosures have been submitted to the TRW Patent Office. The subject matter of these disclosures are listed below:

| Docket No. | Title |
|---|---|
| 71-234 | Catalysts for Promoting Pyrolytic Polymerization |
| 71-264 | Autoclavable A-type Polyimide Resin and Process |
| 72-013 | Method for Improving Adhesion of P10PA Resin to Graphite Fibers |

A separate report covering these disclosures has been submitted to the NASA LeRC Technical Utilization Officer. Brief discussions of these disclosures, their novelty, features and applications are presented below.

## 8.1 CATALYSTS FOR PROMOTING PYROLYTIC POLYMERIZATION

During model compound catalyst screening studies in this program, it was observed that Lewis acids as a general class lowered both the cure time and duration necessary to prepare thermo-oxidatively stable polymers. Further efforts defined that a specific Lewis acid, tin tetrachloride ($SnCl_4$), demonstrated highly promising catalyst activity. The catalyst and methodology developed in model studies were applied to molding investigations on P10P polyimide powder. The results of this screening study showed that $SnCl_4$ effectively reduces the required cure time at 589°K (600°F) for P10P from 60 minutes to 10 minutes with very little sacrifice of long term (336 hour) thermo-oxidative stability in flowing air at 589°K.

## 8.2 AUTOCLAVABLE A-TYPE POLYIMIDE RESIN AND PROCESS

During resin screening studies in this program for A-type polyimides demonstrating chemical and physical behavior of reasonable cure temperature (<589°K), high gel time, high flow and high thermo-oxidative-stability, a specific prepolymer formulated molecular weight and chemical composition was identified that showed high promise for autoclave processability. The

resin modification selected for further process studies was a 1000 FMW combination of methyl nadic anhydride (MN), methylene dianiline (MDA), thiodianiline (TDA), and pyromellitic dianhydride (MN/80 MDA:20 TDA /PMDA), dubbed P10PA due its similarity in composition to the promising press laminating and molding formulation P10P (1000 FMW NA/MDA/PMDA). Development studies on P10PA demonstrated that low void content, high strength structural P10PA composites can be molded by autoclave processing. Composite reinforcements evaluated during these studies were Style 181 E-glass fabric and Courtaulds HMS high modulus graphite fibers. Autoclave processing conditions and techniques employed were compatible with commercial equipment *e.g.*, <1.38 $MN/m^2$ pressure, <589°K cure temperature and 1.0°K to 7.5°K minute heat-up rates. Flexural strengths of autoclave molded P10PA composites were equivalent to press molded P10P composites *e.g.*, autoclave molded P10PA resin, Style 181 glass fabric reinforced laminates provided 600 $MN/m^2$ flexural strength and P10PA resin, Courtaulds HMS graphite fiber reinforced composites provided 483 $MN/m^2$ flexural strength.

## 8.3 METHOD OF IMPROVING ADHESION OF P10PA RESIN TO GRAPHITE FIBERS

A process for sizing graphite fibers with P13N resin in order to improve the adhesion of P10PA resin to the fibers was demonstrated. Courtaulds HMS high modulus graphite fiber tows were impregnated by 1) immersing in diluted P13N varnish and then 2) treating thermally. These sized fibers then were coated with P10PA varnish and autoclave molded into flat panels. Shear strengths of the resultant panels were higher than previously obtained from panels containing non-sized fibers (approximately 15% improvement was obtained). With improved processing methodology, it is believed that further property improvements can be attained.

# APPENDIX A
## SYNTHESIS AND CHARACTERIZATION OF MODEL COMPOUNDS

The two model imides utilized throughout the model compound pyrolysis study were prepared and characterized as described below.

### A.1 MODEL COMPOUND SYNTHESIS

#### A.1.1 Synthesis of N-phenyl Nadimide

The synthesis of N-phenyl nadimide (I) in sufficient quantity to complete Task I model compound pyrolysis studies was accomplished by the following reaction:

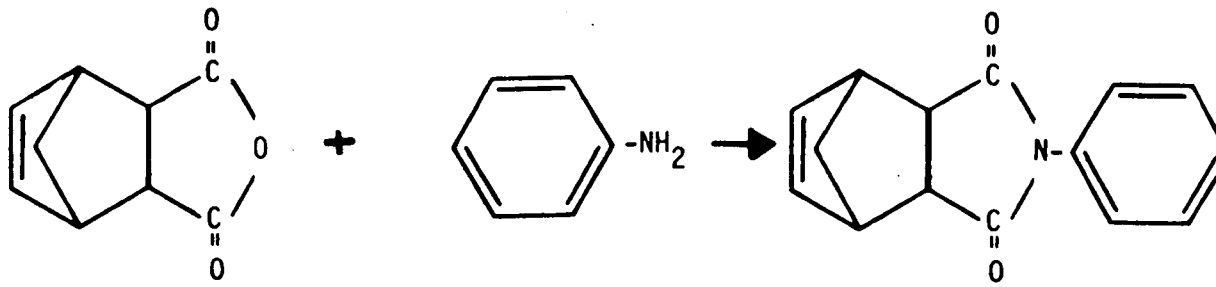


Nadic Anhydride Aniline N-Phenyl Nadimide (I)

The following quantities of ingredients were added to a four-liter round bottom flask fitted with a stirring apparatus, thermometer, modified Dean Stark trap and reflux condensor in the order and method described below:

| | |
|---|---|
| Nadic anhydride | 492.6 g (3.0 moles) |
| Aniline | 293.8 g (3.1 moles) |
| Toluene | 900 ml |
| Dimethylformamide | 450 ml |

The anhydride was dissolved in the mixed solvent followed by the slow addition of the aniline. The reaction mixture was refluxed at 391°K overnight, then 700 ml of solvent was distilled from the reaction vessel, and the remaining material was placed in a refrigerator for ten hours. The material that precipitated was collected by vacuum filtration, then redissolved in 1500 ml of hot methanol. The hot methanol solution was treated with activated carbon, filtered and placed in a refrigerator overnight. The recrystallized material was filtered and dried in a vacuum oven at 393°K until a constant weight was obtained. This procedure afforded 500 g (70%) of white crystals; m.p. = 415°K (DSC - see Section A.2.1)

The material was assessed for correct structure and purity as described in Section A.2.

A.1.2 Synthesis of N-phenyl Maleimide

The other model imide required for Task I pyrolysis studies, N-phenyl maleimide (II), was prepared by the following reaction:

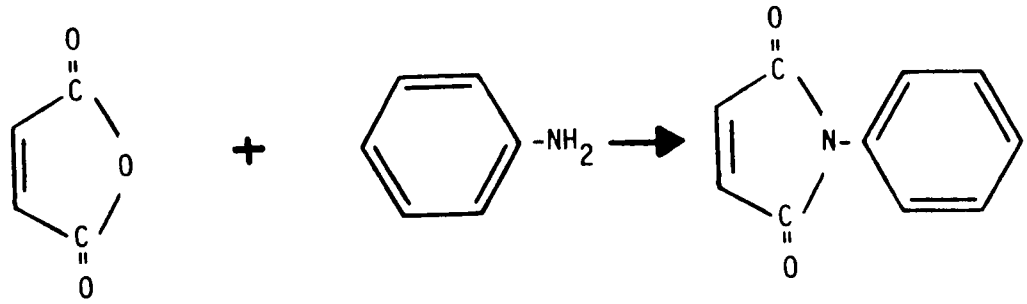


Maleic Anhydride Aniline N-phenyl Maleimide

The experimental procedure used to prepare (II) is given below:

> In a four-liter round bottom blask, fitted with a mechanical stirrer, thermometer, and reflux condensor, was placed a solution of 392.2g (4.0 moles) of maleic anhydride dissolved in 1000 ml of dimethyl formamide. Stirring was initiated and 372.5g (4.0 moles) of aniline was slowly added as a solid while maintaining the temperature below 323°K with the aid of an external ice-bath. This was followed by the addition of 36.8g (0.4 mole) of anhydrous sodium acetate and 448.8g (4.4 moles) of acetic anhydride under the same experimental conditions. The resulting mixture was stirred for one hour at 323°K, then the contents of the flask was poured into 6000 ml of water. The precipitate that formed was collected by vacuum filtration and washed with two successive 6000 ml portions of water. The yellow crude product was dissolved in 3000 ml of methanol and allowed to stand at room temperature. The yellow crystalline product that precipitated was collected by vacuum filtration, then dried at 343°K under vacuum overnight to give 690g (80%) of the desired N-phenyl maleimide; m.p. 364°K (DSC - see Section A.2.1).

The N-phenyl maleimide product was characterized as described below.

A.2 CHARACTERIZATION OF MODEL IMIDES

The N-phenyl nadimide and N-phenyl maleimide model compounds were characterized to have acceptable purity and correct structure by the methods described below.

A.2.1 Melting Point by Differential Scanning Calorimetry (DSC) Analysis

The N-phenyl mono-imides were assessed for melting point by DSC analysis. Each product gave a sharp 2°K melting point range and no discernible peaks indicative of significant impurities. These data are as follows:

| | M.P. (DSC) | M.P. (Literature) | Reference |
|---|---|---|---|
| N-phenyl Nadimide | 415°K | 417°K | 10 |
| N-phenyl Maleimide | 364°K | 364°K | 11 |

A.2.2 Infrared Analysis

The model imides were characterized for structure by infrared analysis. The spectra for N-phenyl nadimide and N-phenyl maleimide are given in Figures A.1 and A.2, respectively. Each matches identically the spectra determined and reported under Contract NAS3-12412 and were held to be of desired structure.

A.2.3 Nuclear Magnetic Resonance Analysis

The two model imides were analyzed by nuclear magnetic resonance (nmr) spectroscopy to substantiate the findings of the infrared analysis described above. the n.m.r. spectra of the model imides, N-phenyl nadimide and N-phenyl maleimide, are shown in Figures A.3 and A.4, respectively. The spectra are identical to those determined for (I) and (II) previously as reported in Contract NAS3-12412. These results complimented those given in Sections A.2.1 and A.2.2 and the combined information gave sufficient evidence that the two model imides were of high purity and suitable for undertaking the pyrolyses studies described in Section 2.2 and Appendix B.

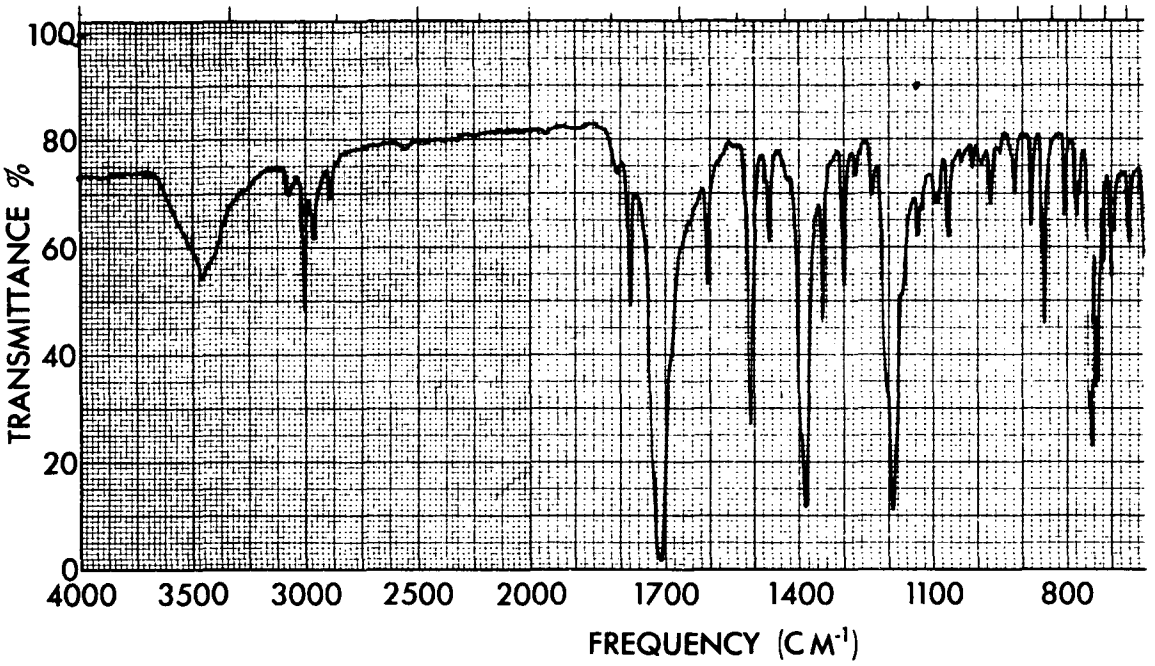


Figure A.1. Infrared Spectrum of N-Phenyl Nadimide (KBr)
Concentration: 3.3 mg/g KBr

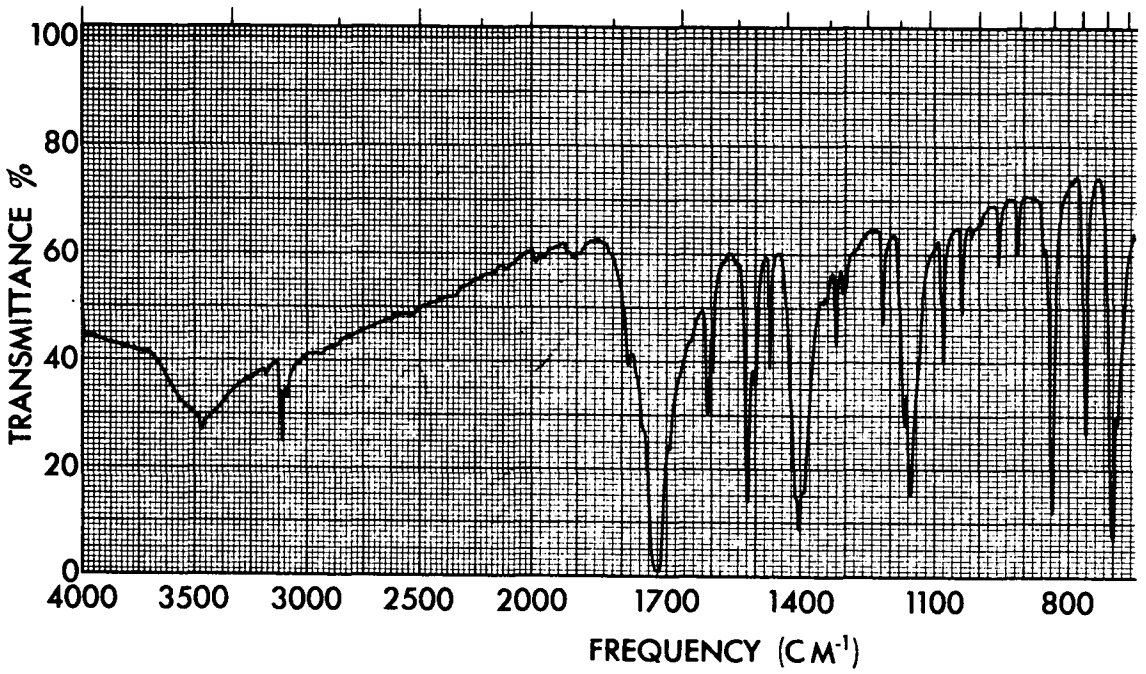


Figure A.2. Infrared Spectrum of N-Phenyl Maleimide (KBr)
Concentration: 3.7 mg/g KBr

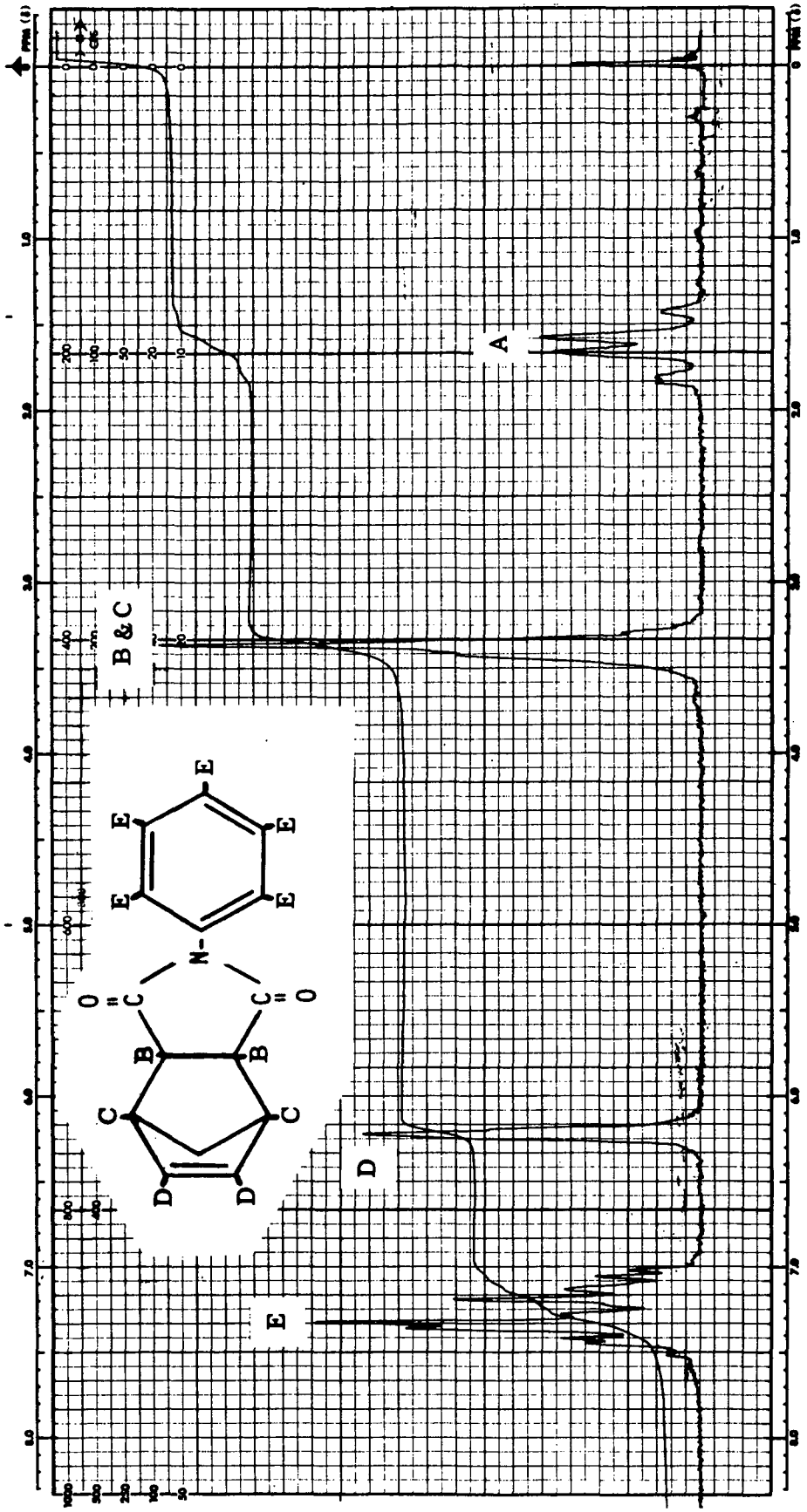


Figure A.3. Nuclear Magnetic Resonance Spectrum of N-phenyl Nadimide
Solvent: $CDCl_3$

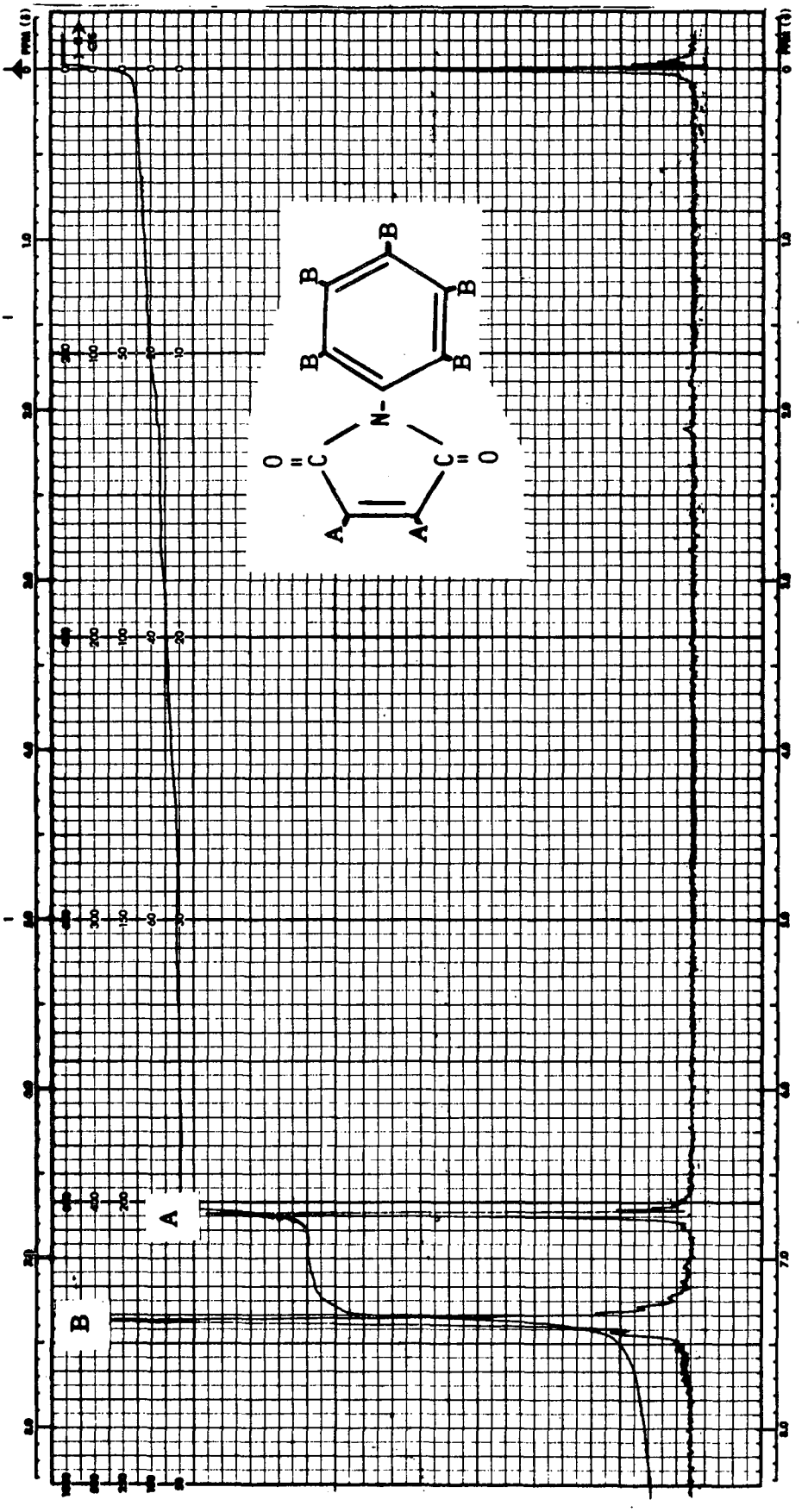


Figure A.4. Nuclear Magnetic Resonance Spectrum of N-phenyl Maleimide
Solvent: $CDCl_3$

# APPENDIX B
# CHARACTERIZATION OF MODEL COMPOUND PYROLYSIS RESIDUES

This appendix provides the results of characterization of the pyrolysis residues obtained in Task I - Model Compound Synthesis and Characterization Studies as described in Section 2. The data documented were determined on samples selected most promising from vacuum, pressure and pressure plus catalyst experiments on the basis of high (>589°K) initial thermo-oxidative stability as obtained by TGA screening as described in Sections 2.2.1, 2.2.2 and 2.2.3, respectively. Prior to proceeding with a detailed presentation of the characterization results, the most promising samples are reviewed and a code is assigned each for ease of reference.

## B.1 DESCRIPTION OF SELECTED SAMPLES AND CODE DESIGNATION

A total of eleven samples were selected as most promising and worthy of detailed analysis from vacuum, pressure and pressure plus catalyst pyrolyses studies on the basis of $\geq$589°K (600°F) initial thermo-oxidative stability by TGA screening. In order to simplify the total picture of 1) blend level of N-phenyl maleimide (II) in N-phenyl nadimide (I), 2) pyrolysis temperature, 3) pyrolysis duration, 4) pyrolysis environment (pressure or vacuum), and 5) $SnCl_4$ catalyst presence for each sample, a code has been devised which describes each of the five parameters. The code is as follows:

- The first Roman numeral(s) digit refer to use of N-phenyl nadimide I alone as a model compound or a 5% blend level of N-phenyl maleimide in N-phenyl nadimide I/II
- The second numeral refers to the pyrolysis temperature employed in °K
- The third numeral refers to the pyrolysis duration employed in hours
- The fourth denotation in the code refers to which environment the pyrolysis was conducted (V = vacuum condition and P = applied pressure of 1.38 $MN/m^2$
- The fifth denotation, if present, refers tothe use of a 1% w/w level of $SnCl_4$ catalyst, C, in the pyrolysis.

Examples of the code are as follows: 1) a blend level of 5% N-phenyl maleimide in N-phenyl nadimide pyrolyzed at 589°K for two hours at a pressure of

1.38 $MN/m^2$ in the absence of $SnCl_4$ is denoted as I/II-589-2-P; 2) a sample of N-phenyl nadimide alone, pyrolyzed at the identical conditions, but in the presence of $SnCl_4$, is denoted as I-589-2-P-C.

A complete tabulation of samples selected by TGA screening for detailed analysis are presented in Table B.I along with the code notation for each. This table should be employed for reference, if required, to aid in understanding the characterization data determined on the samples as detailed below.

TABLE B.I
REVIEW OF PYROLYSIS CONDITIONS EMPLOYED ON
SAMPLES SELECTED FOR DETAILED ANALYSIS

| Sample No. | Blend Level of (II) in (I) (% w/w) | $SnCl_4$ Catalyst Level (% w/w) | Pyrolysis Conditions Temperature (°K) | Pressure ($MN/m^2$) | Time (Hr) | Code Assigned |
|---|---|---|---|---|---|---|
| 1 | 0.0 | 0.0 | 589 | Vacuum | 2.0 | I-589-2-V |
| 2 | 0.0 | 0.0 | 589 | Vacuum | 1.0 | I-589-1-V |
| 3 | 5.0 | 0.0 | 589 | Vacuum | 1.0 | I/II-589-1-V |
| 4 | 0.0 | 0.0 | 589 | 1.38 | 2.0 | I-589-2-P |
| 5[a] | 0.0 | 0.0 | 589 | 1.38 | 2.0 | I-589-2-P |
| 6 | 5.0 | 0.0 | 589 | 1.38 | 2.0 | I/II-589-2-P |
| 7[b] | 5.0 | 0.0 | 589 | 1.38 | 2.0 | I/II-589-2-P |
| 8 | 0.0 | 1.0 | 561 | 1.38 | 2.0 | I-561-2-P-C |
| 9[c] | 0.0 | 1.0 | 561 | 1.38 | 2.0 | I-561-2-P-C |
| 10 | 0.0 | 1.0 | 561 | 1.38 | 1.1 | I-561-1-P-C |
| 11 | 0.0 | 1.0 | 575 | 1.38 | 1.0 | I-575-1-P-C |

[a]Repeat of Sample 4
[b]Repeat of Sample 6
[c]Repeat of Sample 8

## B.2 INFRARED SPECTROSCOPIC ANALYSIS

The infrared spectrum of each of the pyrolysis residues was determined employing a Perkin Elmer Model 621 spectrophotometer. The infrared analysis of each sample was used as a screening tool for gross structural characteristics. No discernible difference is present in the spectra between N-phenyl

nadimide pyrolyzed in the three environments (vacuum, pressure and pressure plus catalyst). Three representative spectra, one from each environment are presented in Figures B.1, B.2 and B.3 for samples I-589-1-V, I-589-2-P, and I-561-2-P-C, respectively.

In each of the samples of pyrolyzed N-phenyl nadimide (I) there was definite appearance of 1630 $cm^{-1}$ olefinic unsaturation band ascribed by Bellamy (Reference 11 ) to *cis*-unsaturation in a five-membered ring. It was experimentally established that (I) does not absorb bromine, presumably because of steric interference by the methylene bridge (Reference 1). The 1630 $cm^{-1}$ band present in the spectra is not present in the spectrum of model compound (I) given in Figure A.1.

Similarly, the spectrum for a representative 5% w/w blend of N-phenyl maleimide in I, sample I/II-589-2-P, does not show any discernible differences between those of (I). This spectrum is presented as Figure B.4 and gives credence to the mechanistic interpretation presented in Section 2.3.2.1 that maleic entities are most probably an integral part of the model polymers and hence, most probably occur during cure of A-type polyimide polymers.

## B.3 NUCLEAR MAGNETIC RESONANCE MEASUREMENTS (n.m.r.)

Each of the pyrolysis products listed in Table B.I was subjected to n.m.r. analysis employing a Varian Model A-60 spectrometer. Samples from each of the three environments employed in the pyrolysis study all gave equivalent n.m.r. spectra, which were identical to those determined in NAS3-12412 studies (Reference 1).

Each spectrum contains principal absorptions peaks at approximately 2.60$\tau$ assigned to phenyl protons and at 7.30$\tau$ characteristic of methinyl protons. Representative spectra for pyrolysis residue samples I-589-1-V, I-589-2-P, I-561-2-P-C, and I/II-589-2-P are presented in Figures B.5, B.6, B.7 and B.8, respectively. The broad region of proton absorption in the range of approximately 6.0-8.5$\tau$ is once again assigned to protons deemed present in the model compound polymers as shown in Section 2.3. Details of the assignment of protons was presented in a prior study (Reference 1) in NAS3-12412. Representative absorptions for protons deemed present in the model polymers are presented in Table B.II.

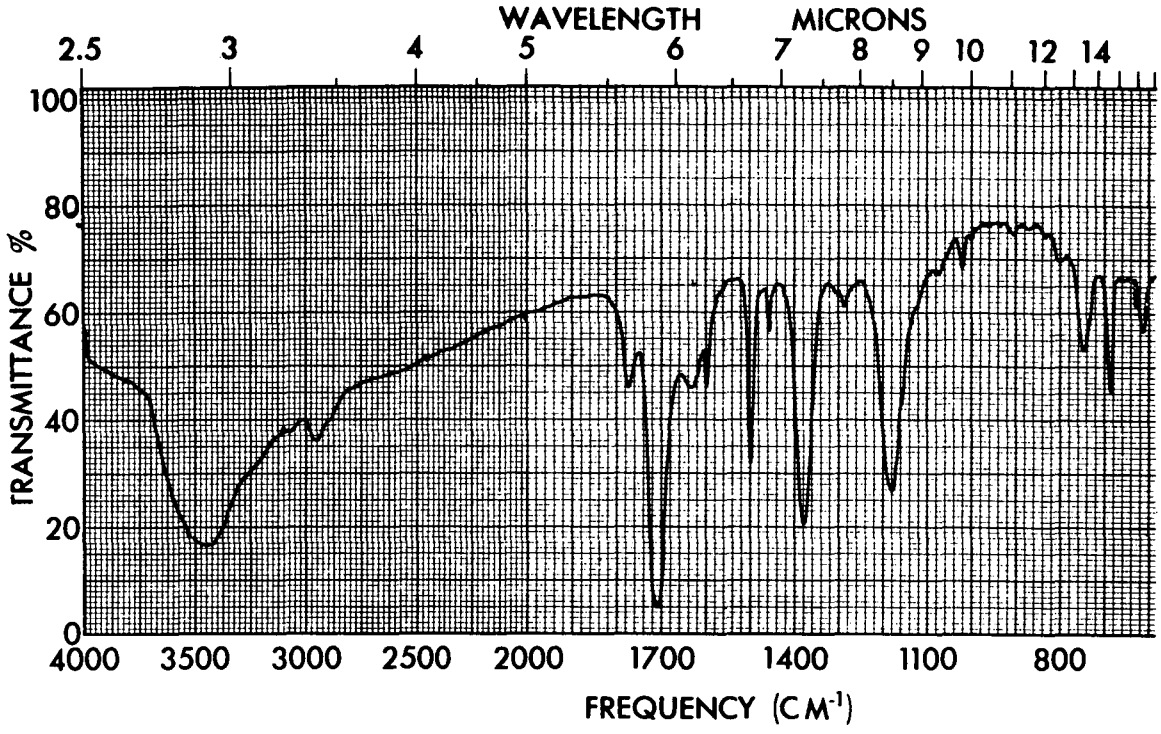


Figure B.1. Infrared Spectrum of Pyrolysis Residue
I-589-1-V (KBr)
Concentration: 3.3 mg/g KBr

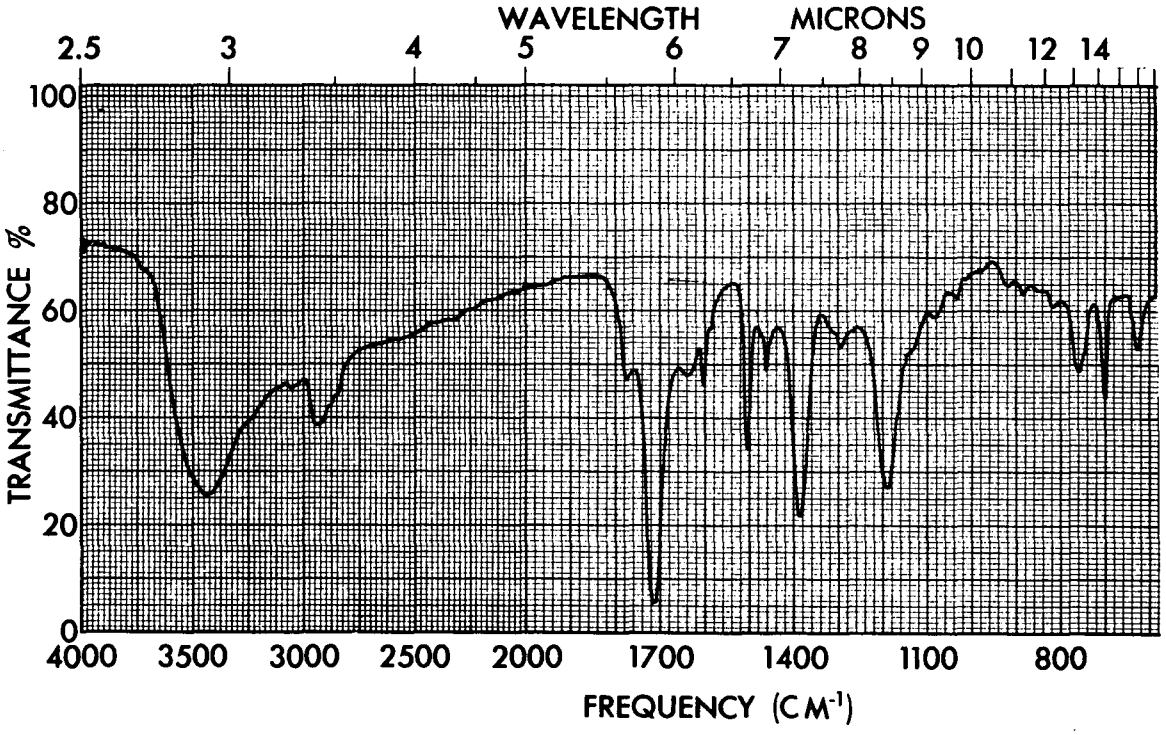


Figure B.2. Infrared Spectrum of Pyrolysis Residue
I-589-2-P (KBr)
Concentration: 3.3 mg/g KBr

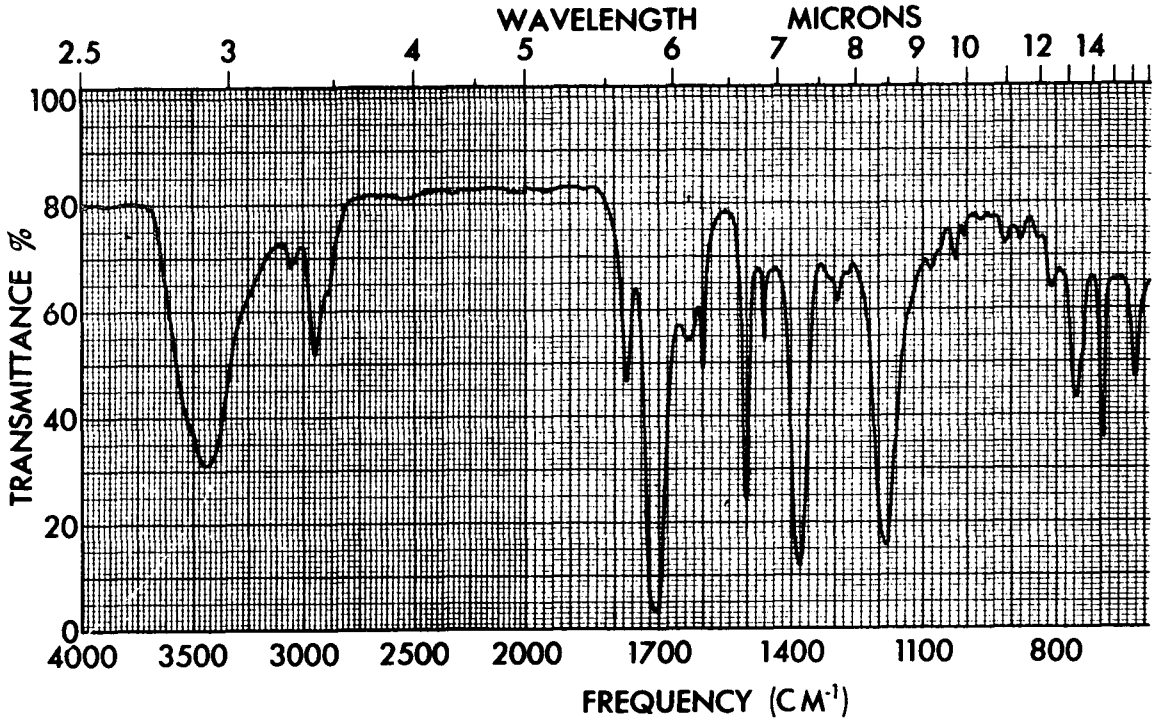


Figure B.3. Infrared Spectrum of Pyrolysis Residue
I-561-2-P-C (KBr)
Concentration: 3.3 mg/g KBr

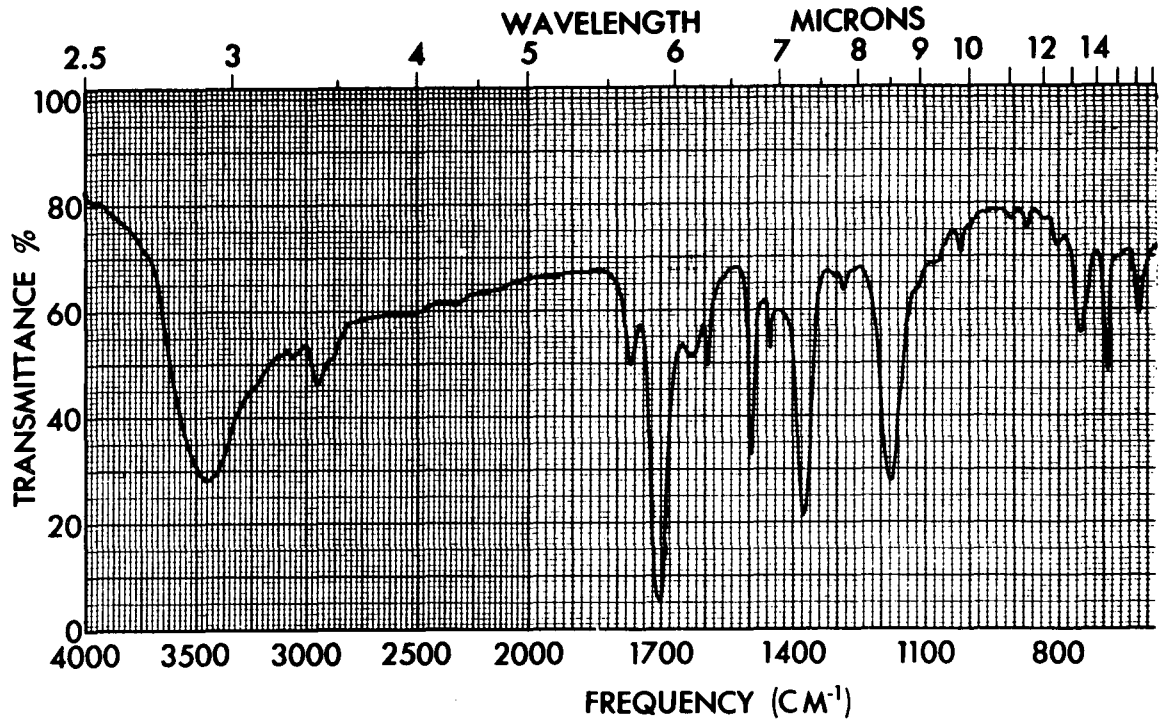


Figure B.4. Infrared Spectrum of Pyrolysis Residue
I/II-589-2-P (KBr)
Concentration: 3.3 mg/g KBr

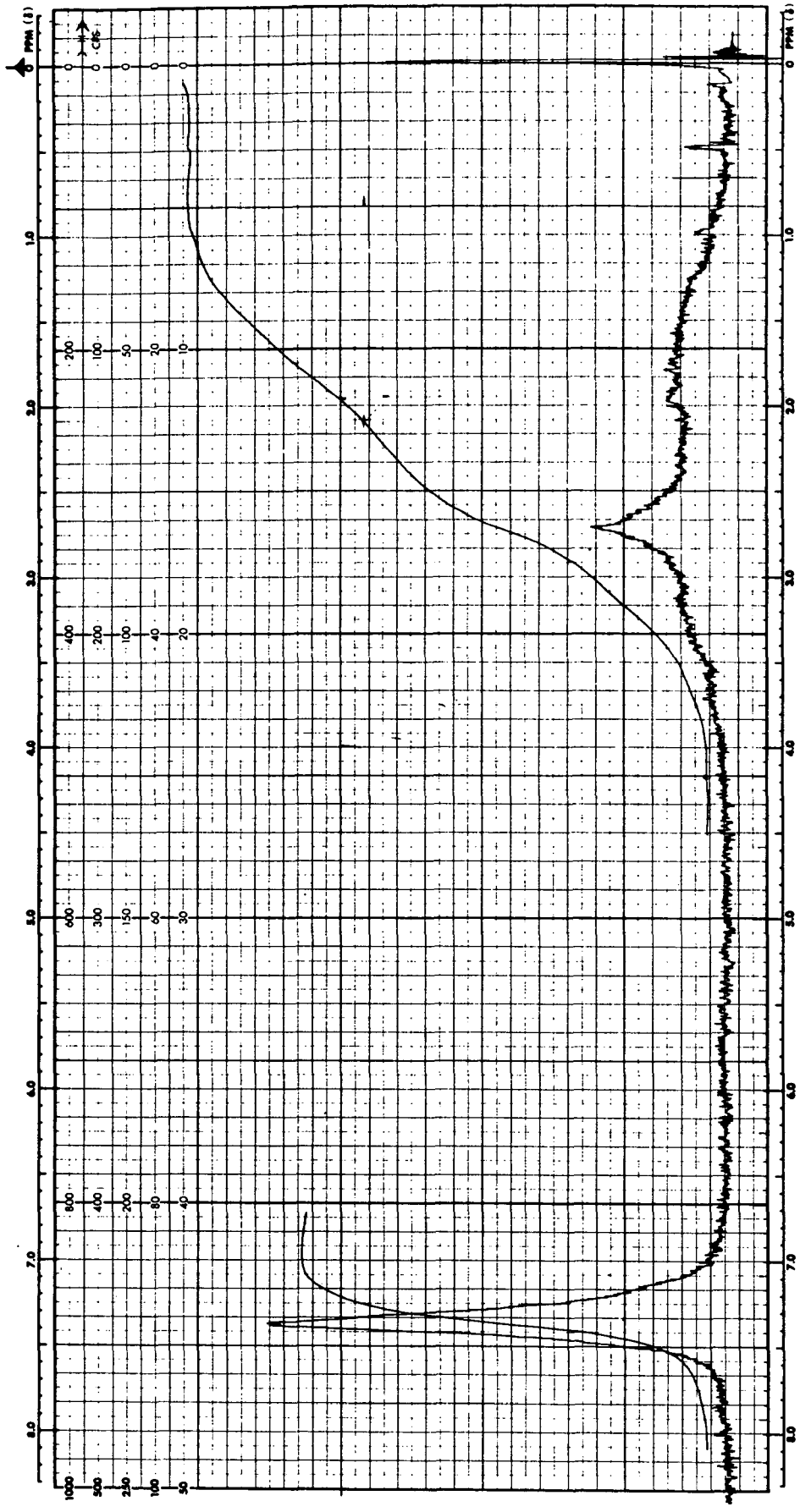

Figure B.5. Nuclear Magnetic Resonance Spectrum of Pyrolysis Residue I-589-1-Y
Solvent: $CDCl_3$

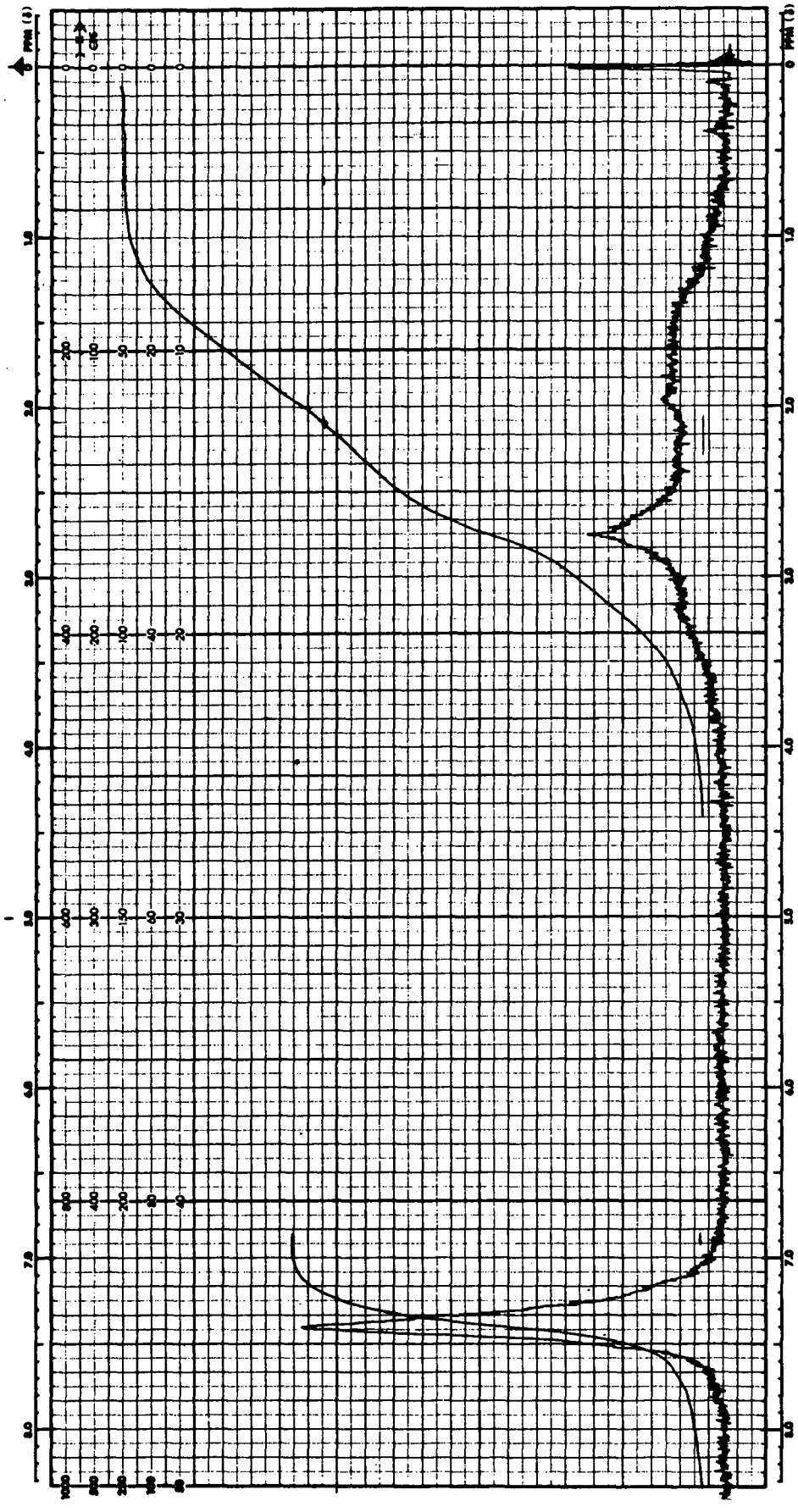

Figure B.6. Nuclear Magnetic Resonance Spectrum of Pyrolysis Residue I-589-2-P
Solvent: $CDCl_3$

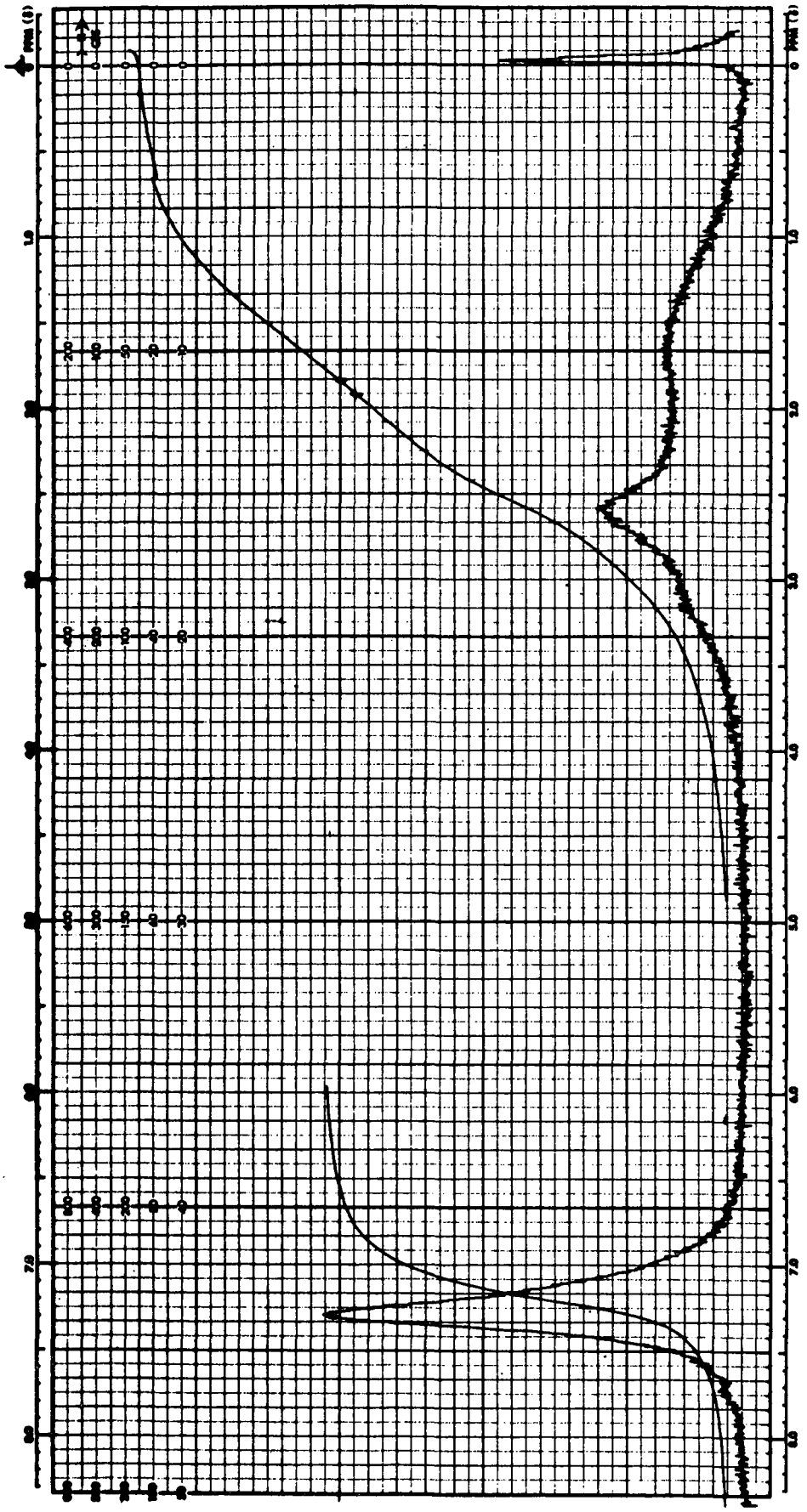

Figure B.7 Nuclear Magnetic Resonance Spectrum of Pyrolysis Residue I-561-2-P-C
Solvent: $CDCl_3$

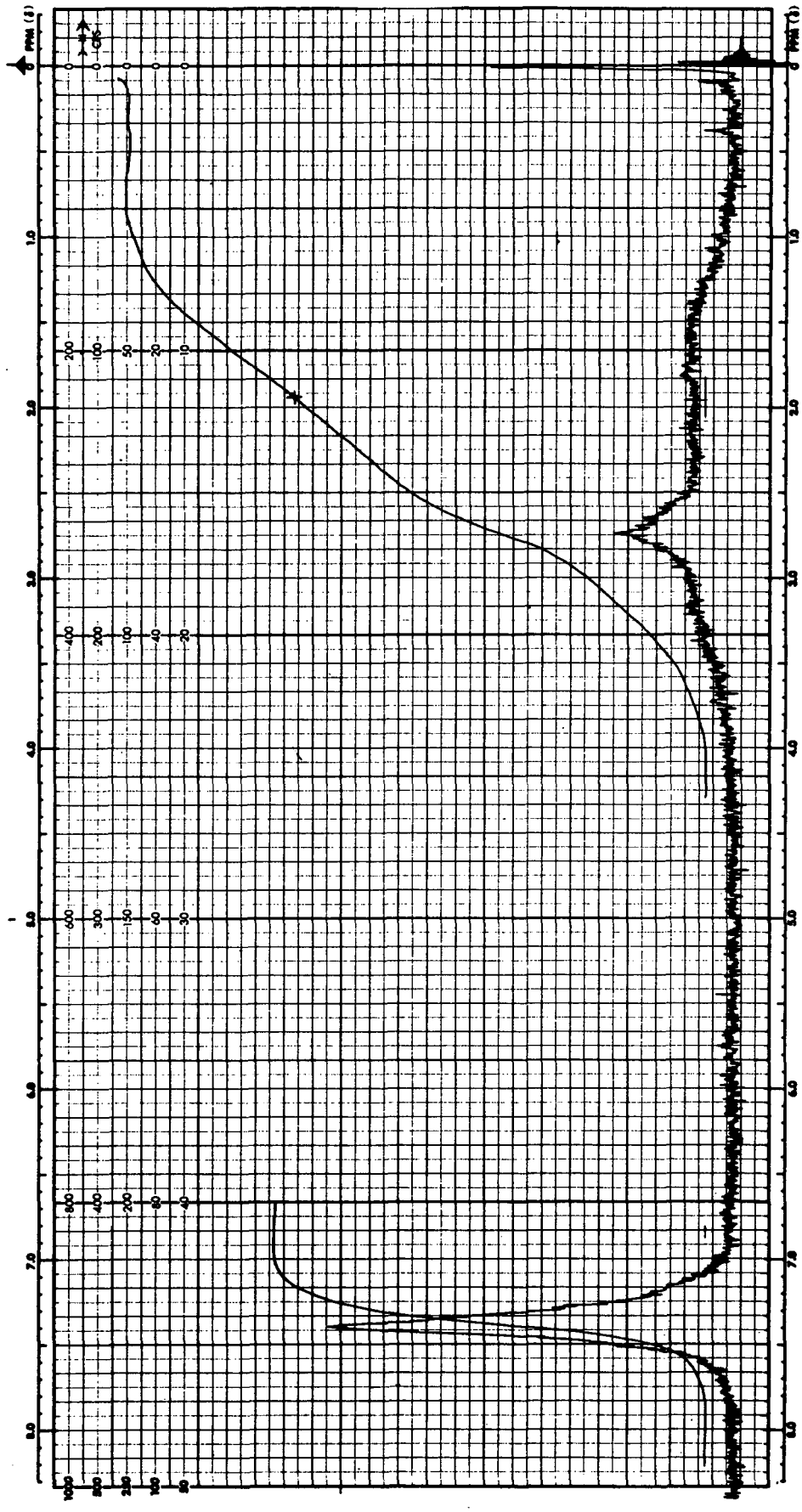

Figure B.8. Nuclear Magnetic Resonance Spectrum of Pyrolysis Residue I/II-589-2-P
Solvent: $CDCl_3$

TABLE B.II

SUMMARY OF OTHER PROTONS POSSIBLE IN MODEL POLYMERS

| Compound | Proton Absorption Peaks ($\tau$) | Source |
|---|---|---|
| N-phenyl Nadimide | 8.40 (bridge methylene A) | Reference 13 |
| Cyclopentene | 7.72 (methylene 2) | Reference 13 |
| | 8.10 (methylene 3) | |
| Cyclopentane | 8.49 (methylene) | Reference 14 |
| Norbornane | 7.81 (methylene) | Reference 15 |

The n.m.r. structural elucidation of the model polymers gives strong evidence, in addition to the infrared spectral results presented in Section B.1, that the same gross polymer backbone structure results from pyrolysis of nadic and nadic/maleic end capped polymers. Because 1) the combined infrared and n.m.r. data, strongly suggest that the same structure results regardless of the pyrolysis environment used in this program, and 2) these findings correlate identically with those determined previously in NAS3-12412 (Reference 1), it is strongly believed that the mechanistic interpretations presented in Section 2 represent a best fit for the model imide studies and therefore, most probably apply directly to the cure phenomena occurring in A-type polyimide polymers.

## B.4 MOLECULAR WEIGHT DETERMINATIONS

The experimental results of the number average molecular weight ($\overline{M}_n$) determinations for the most promising pyrolysis runs are summarized in Table B.III. These data were obtained using standard VPO methodology and dimethyl formamide (DMF) solvent at a temperature of 283°K.

The results reported in Table B.III are grouped according to the particular pyrolysis environment employed (i.e., vacuum, pressure or pressure plus catalyst), and the code designated in Table B.I is used to indicate particular pyrolysis conditions for each sample. The $\overline{M}_n$'s when grouped in this manner show that a clear trend toward a particular molecular weight average occurring in each experimental environment studied. Each of these $\overline{M}_n$'s ranges fits nicely for incorporation of approximately four, five and

TABLE B.III
VAPOR PHASE OSMOMETRY MOLECULAR WEIGHT DATA

| Sample Code | Environment | $\overline{M}_n$ |
|---|---|---|
| I-589-2-V | Vacuum (See Section 2.2.1) | 810 |
| I-589-1-V | | 890 |
| I/II-589-1-V | | 950 |
| I-589-2-P | Pressure, uncatalyzed | 1130 |
| I-589-2-P (Repeat of above) | (See Section 2.2.2) | 1040 |
| I/II-589-2-P | | 1040 |
| I/II-589-2-P (Repeat of above) | | 1000 |
| I-561-2-P-C | Pressure, $SnCl_4$ catalyzed | 730 |
| I-561-2-P-C (Repeat of above) | (See Section 2.2.3) | 730 |
| I-575-1-P-C | | 720 |
| I-561-1-P-C | | 760 |

three model compound units into the polymer structure for a vacuum, pressure and pressure plus catalyst pyrolysis environments, respectively. A mechanistic interpretation of these data is presented in Section 2.3.

## B.5 UNSATURATION CONTENT BY BROMINE TITRATION

The relative unsaturation content of key pyrolysis residues were determined by a standard bromine titration method described previously in NAS3-12412 (Reference 1). A summary of these results is presented in Table B.IV. The data are, again, grouped in a manner according to the pyrolysis environment employed as was used for the $\overline{M}_n$ results described in the previous section.

The bromine absorption of the most promising pyrolysis residues, again, tend to group themselves according to the pyrolytic environment employed. The experimentally determined abosrption of bromine indicates that a relatively low level of titratable olefinic linkages (ascribed to a cyclopentene entity in the polymer backbone) are present in the total pyrolytic mass isolated. These data were mechanistically correlated with the infrared

TABLE B.IV
BROMINE ABSORPTION DATA

| Sample Code | Environment Employed | Experimental Bromine Absorption (meg/g) | Approximate Mass of Samples Required to Absorb 1 Mole of $Br_2$ |
|---|---|---|---|
| I-589-1-V | Vacuum (See Section 2.2.1) | 1.7 | 2600 |
| I/II-589-1-V | | 1.3 | 3500 |
| I-589-2-P | Pressure (See Section 2.2.2) | 1.8 | 2500 |
| I-589-2-P | | 1.8 | 2500 |
| I/II-589-2-P | | 1.6 | 2800 |
| I/II-589-2-P | | 1.8 | 2500 |
| I-561-2-P-C | Pressure, $SnCl_4$ Catalyst (See Section 2.2.3) | 0.9 | 4700 |
| I-561-2-P-C | | 1.1 | 4200 |
| I-575-1-P-C | | 1.0 | 4500 |
| I-561-1-P-C | | 1.2 | 3700 |

and n.m.r. structural data as well as $\overline{M}_n$ results as presented in Section 2.3. The bromine absorption of key samples, when correlated with structural and $\overline{M}_n$ data, strongly indicate that a large proportion of the model compounds studied undergo homolytic vinyl polymerization in addition to a reverse Diels-Alder recombination mechanism. Homolytic polymerization appears to be particularly facile in the presence of the $SnCl_4$ catalyst investigated. It is interesting to note that when maleic/nadic blends are employed there was a consistent trend to have lower residual unsaturation which is directly relatable to the amount of maleic end cap employed.

# APPENDIX C
# SYNTHESIS AND CHARACTERIZATION OF MODIFIED A-TYPE POLYIMIDE RESIN CANDIDATES

This appendix provides details on methodology used to synthesize, mold and characterize candidate modified A-type polyimide resins investigated during this program. The resin candidates included those described in Sections 3 and 6.

## C.1 VARNISH PREPARATION

The methodology used to prepare 1000 formulated molecular weight (FMW) nadic anhydride (NA)/methylene dianiline (MDA)/pyromellitic dianhydride (PMDA) as a varnish in dimethyl formamide was modified over that employed previously in Contract NAS3-12412 to reflect use of the controlled procedures implemented in the latter phases of Contract NAS3-13203. The varnish ingredients were carefully analyzed prior to resin preparation and varnish synthesis variables were carefully controlled. These more precise experimental controls gave a 40% w/w solids loaded amide-acid (A-A) varnish in DMF of viscosity ~300% greater than that obtained in Contract NAS3-12412 (Reference 1). Experimental details are given below.

### C.1.1 Monomer Purification and Analyses

The NA, MDA, and PMDA monomers used in the preparation of 1000 FMW NA/MDA/PMDA (P1OP) varnishes were purified by recrystallization. Additional monomers, thiodianiline (TDA), methyl nadic anhydride (MN), maleic anhydride (MA) used in the autoclave studies were also purified during the program. The method of purification and analysis data for each monomer are given in Table C.I. It is believed that the >94% purity determined for each ingredient is sufficient for reproducible preparation of high quality A-type formulation modifications.

Each batch of DMF (J. T. Baker reagent grade) used in the program was determined to be acceptable for low water content. The DMF contained $\leq$0.02% w/w water (Karl-Fischer titration).

### C.1.2 Varnish Synthesis Methodology

All varnish batches of 1000 FMW NA/MDA/PMDA prepared to date from the ingredients discussed above were of considerably higher viscosity (ca.,

TABLE C.I
MONOMER PURIFICATION DATA

| Monomer | Method of Purification[a] | Purity[d] Determined by Analysis |
|---|---|---|
| NA | Recrystallization from benzene | 95%[c] |
| MN | Distillation | 94%[c] |
| MA | Recrystallization from isopropanol | 95%[c] |
| MDA | Recrystallization from isopropanol | 97%[d] |
| TDA | Recrystallization from isopropanol | 99%[b] |
| PMDA | Recrystallization from acetone/ benzene | 98%[c] |

[a]Each purification was carried out by one recrystallization or distillation

[b]Non-aqueous titration in acetonitrile using perchloric acid in acetonitrile/acetic acid as the titrant

[c]Difference between methanolysis and basic hydrolysis

[d]Average of replicate determinations

300%) than those prepared previously. The synthesis methodology, including close control of experimental variables and atmospheric exposure, used for all varnish preparations in this program is described below for a representative P10P run.

A 5-l round bottomed flask equipped with mechanical stirrer, nitrogen, inlet dropping funnel, and a thermocouple, was purged with nitrogen then 725 g of recrystallized MDA in 1400 ml of DMF (dissolved under nitrogen) was added as a solution through the dropping funnel. The temperature was adjusted to $\leq$298°K, then 513 g of NA, slurried in 400 ml of DMF was added with stirring over a period of 12 minutes, during which time the temperature was controlled between 293°K and 298°K by external cooling with an ice bath. After this addition, the reaction mixture was allowed to stir under nitrogen for 22 minutes at 297°K, then 456 g of recrystallized PMDA, slurried in 896 ml of DMF was carefully added over a period of 38 minutes, during which time the temperature was controlled between 293°K and 298°K by external cooling. After this addition, the mixture was allowed to stir at 298°K for two hours under nitrogen. The resulting 40% w/w solids loaded varnish product from this procedure was light brown in color and had a Brookfield viscosity of 0.325 $Ns/m^2$. The varnish was carefully bottled and stored under nitrogen prior to use.

The experimental procedure detailed for P10P was utilized to prepare all candidate A-type polyimide formulation modifications from purified ingredients at a 40% w/w solids loading in DMF. The specific varnish formulation synthesized and experimental viscosity data obtained are given in Table E.II.

TABLE C.II
VARNISH DATA ON A-TYPE RESIN CANDIDATES

| Formulation | Formulated Molecular Weight (FMW) | Viscosity[a] ($Ns/m^2$) |
|---|---|---|
| NA/MDA/PMDA | 1000 | 0.295 @ 296°K |
| | 1150 | 0.810 @ 297°K |
| MN/MDA/PMDA | 1000 | 0.278 @ 295°K |
| | 1150 | 0.443 @ 295°K |
| NA/80MDA:20TDA/PMDA | 1000 | 0.325 @ 295°K |
| | 1150 | 0.429 @ 295°K |
| MN/80MDA:20TDA/PMDA | 1000 | 0.225 @ 296°K |
| | 1150 | 0.353 @ 296°K |
| 95NA:5MA/MDA/PMDA | 1000 | 0.270 @ 297°K |

[a]Determined by a Brookfield Viscometer

The viscosities of the eight candidates demonstrated no significant deviations other than the expected trend toward higher viscosity as the FMW as increased from 1000 to 1150. The varnishes were converted to prepolymer molding powders as described in Section C.2.

## C.2 MOLDING POWDER SYNTHESIS

The varnishes listed in Table C.II were converted into polyimide prepolymer molding powders by stripping the DMF at 413°K under reduced pressure on a rotary evaporator and subsequently drying at 403°K in a forced air oven until the volatile matter content determined by a 589°K (600°F) burnoff for 0.5-hour in air gave a reading of approximately 3% w/w. Complete imidization was confirmed by infrared analyses. The infrared spectrum (Figure C.1) obtained from the 1150 FMW MN/MDA/PMDA imidized powder

displays the strong imide absorption at 1720 and 1780 $cm^{-1}$ and the absence of any amide-acid absorption at 1620- 1640 $cm^{-1}$. This spectrum is representative of all prepolymer molding powders prepared in this program.

## C.3 CHARACTERIZATION OF MOLDED (CURED) RESINS

In addition to specific characterization data given in Sections 3 and 6, concerning cured A-type polyimide resin modifications (e.g., thermo-oxidative stability; Barcol hardness), each cured resin was analyzed as follows:

### C.3.1 Infrared Analysis

Each cured resin was assessed for gross structural characteristics by infrared analysis. A representative spectrum is shown in Figure C.2 for the 1150 FMW MN/MDA/PMDA cured neat resin. This spectrum is similar to that observed for the other resins and shows very little deviation from the imidized uncured prepolymer (see Figure C.1). Important absorption bands present in the spectrum are the 1780 $cm^{-1}$ to 1710 $cm^{-1}$ bands indicative of retention of imide linkages and the absorption at $\sim$2940 $cm^{-1}$ are indicative of retention of the carbon-hydrogen elements of methyl nadic anhydride (MN).

Similar infrared determinations were made on four key 1000 FMW NA/MDA/PMDA (P10P) resin samples molded in Task II studies as described in Section 3. Figures C.3 through C.5 show the spectra obtained for P10P containing varying amounts of $SnCl_4$ catalysts (0.0, 1.0 and 2.5% w/w) molded for a period of sixty minutes for comparison purposes. Figure C.6 shows the spectrum of P10P containing 1.0% $SnCl_4$ which had been molded for ten minutes. Each of the four spectra are similar in all respects to each other and also contain absorptions at approximately the same frequencies as the cured 1150 NA/MDA/PMDA given in Figure C.2.

This shows that the $SnCl_4$ catalyst apparently functions to only accelerate and not radically change the pyrolytic cure mechanism of actual A-type polymers, as was preliminarily assessed to be the case in model compound studies discussed in Section 3.

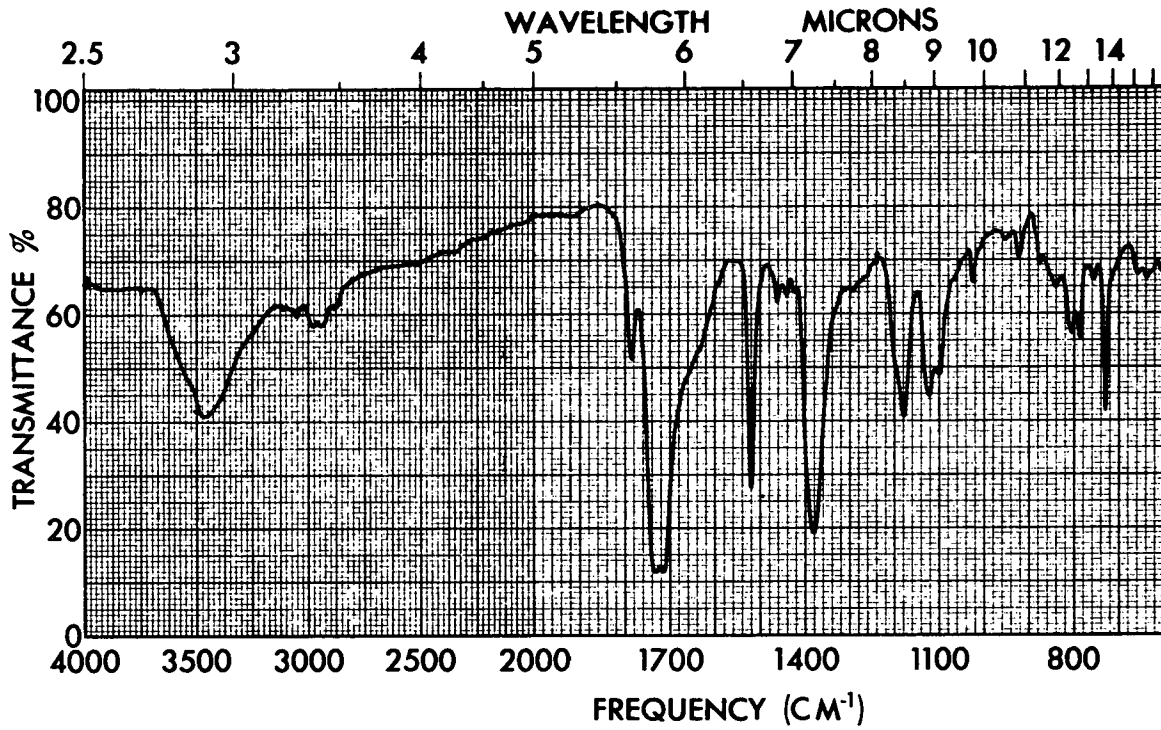


Figure C.1. Infrared Spectrum of 1150 FMW MN/MDA/PMDA Imidized Prepolymer Powder (KBr)
Concentration: 3.3 mg/g KBr

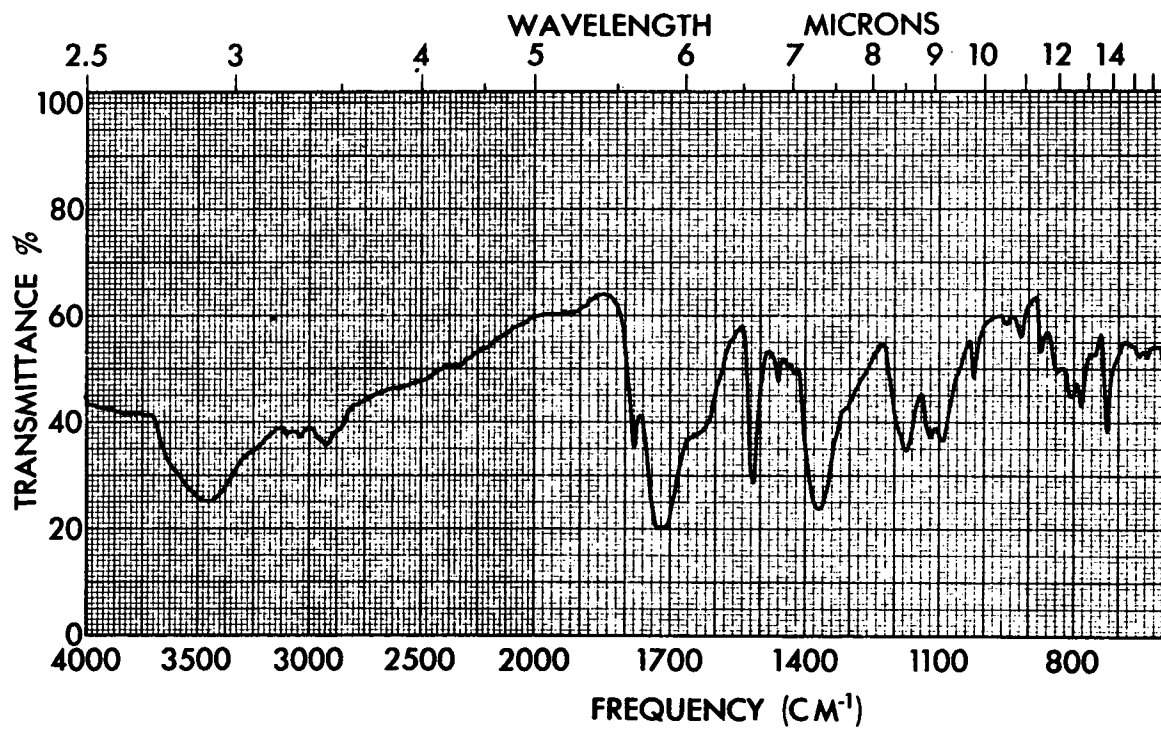


Figure C.2. Infrared Spectrum of 1150 FMW MN/MDA/PMDA Cured Polymer (KBr)
Concentration: 6.6 mg/g KBr

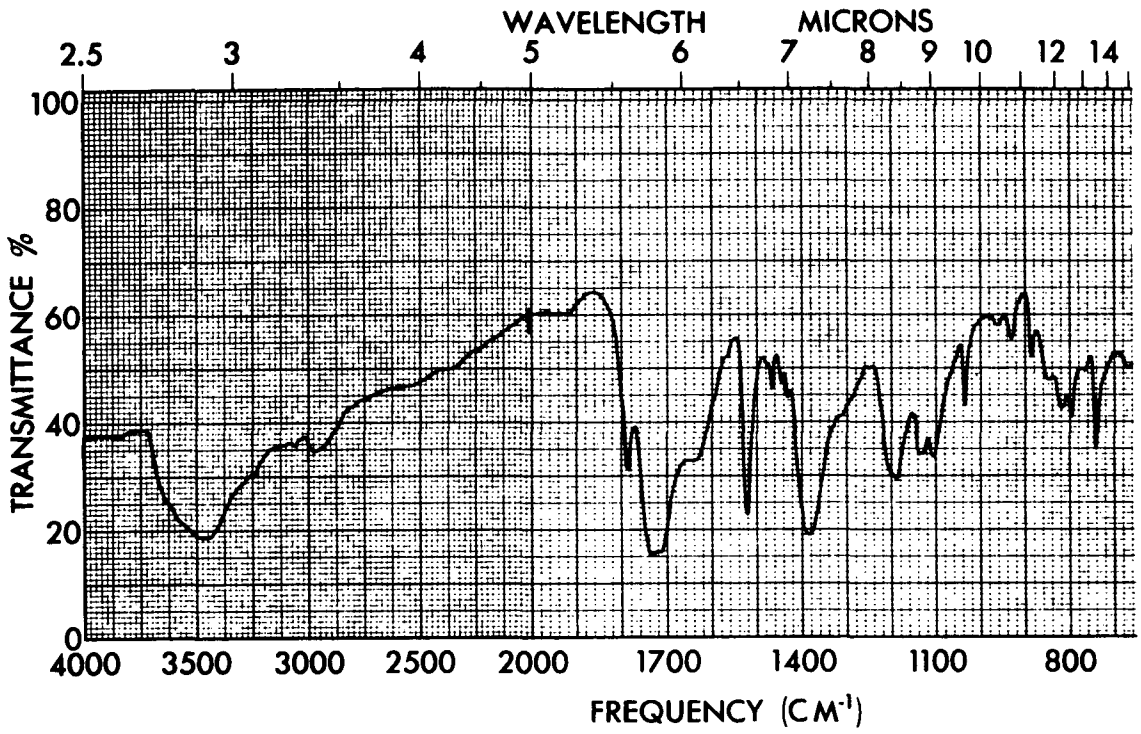


Figure C.3. Infrared Spectrum of P10P Cured in the Absence of $SnCl_4$ for 1.0 Hour (KBr)
Concentration: 3.3 mg/g KBr

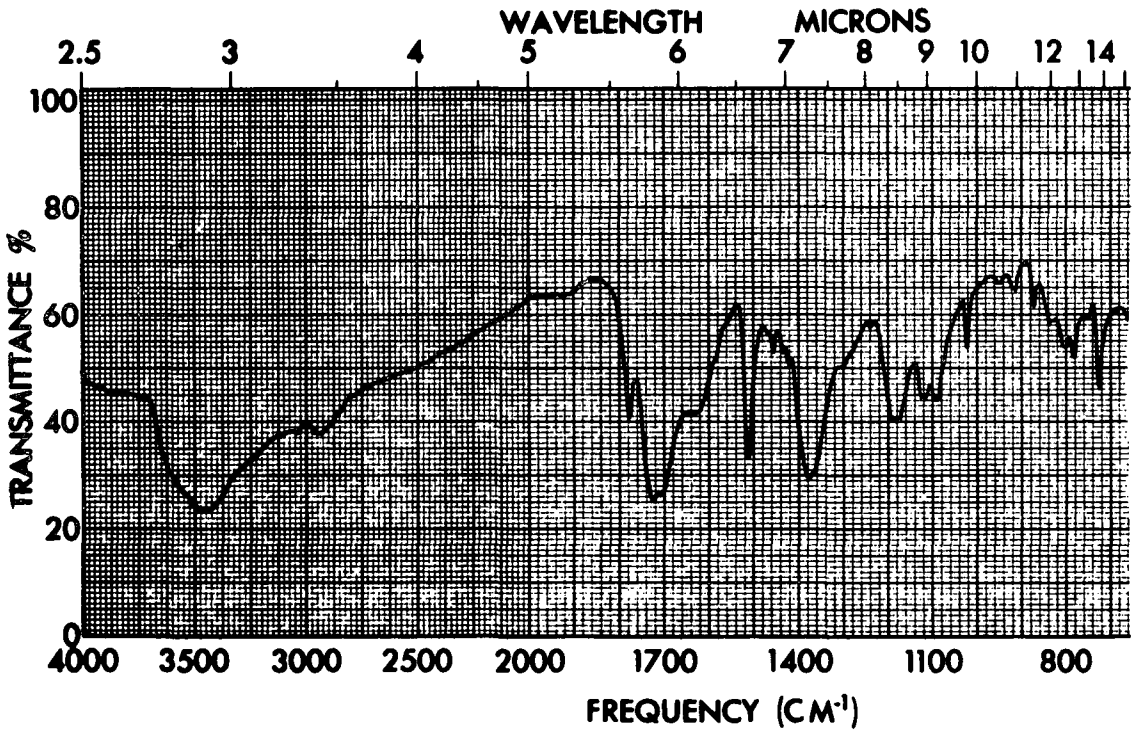


**Figure C.4. Infrared Spectrum of P10P Cured in the Presence of 1.0% $SnCl_4$ for 1.0 Hour (KBr)
Concentration: 3.3 mg/g KBr**

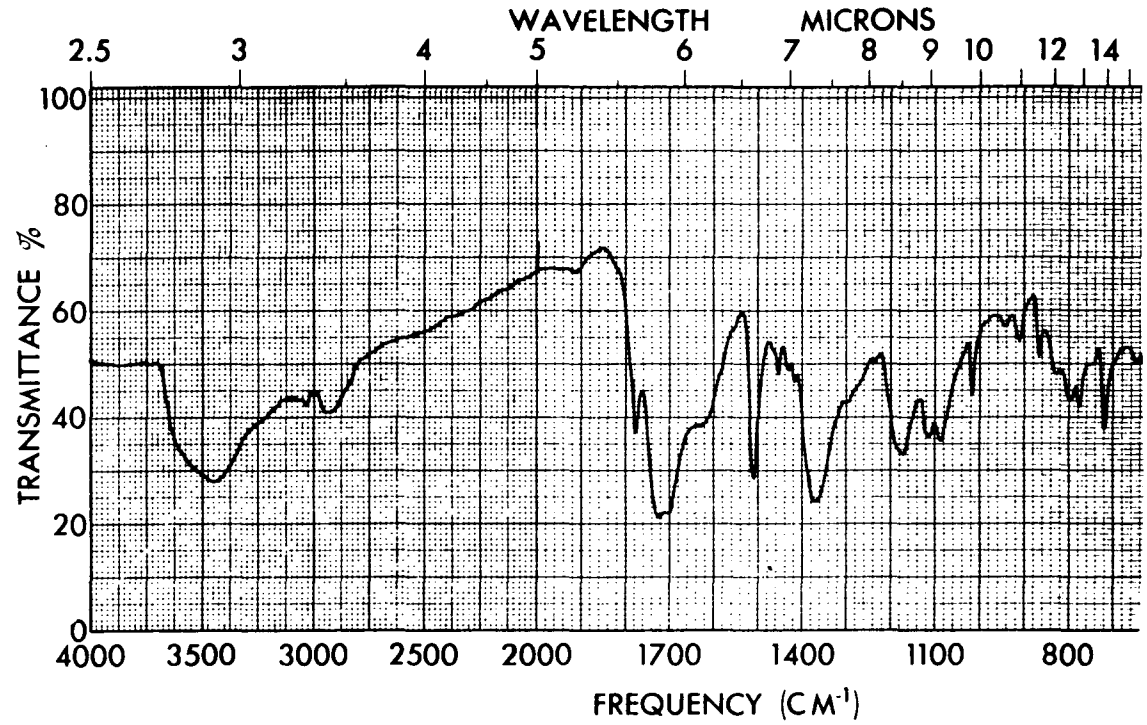


Figure C.5. Infrared Spectrum of P10P Cured in the Presence of 2.5% w/w $SnCl_4$ for 1.0 Hour (KBr)
Concentration: 3.3 mg/g KBr

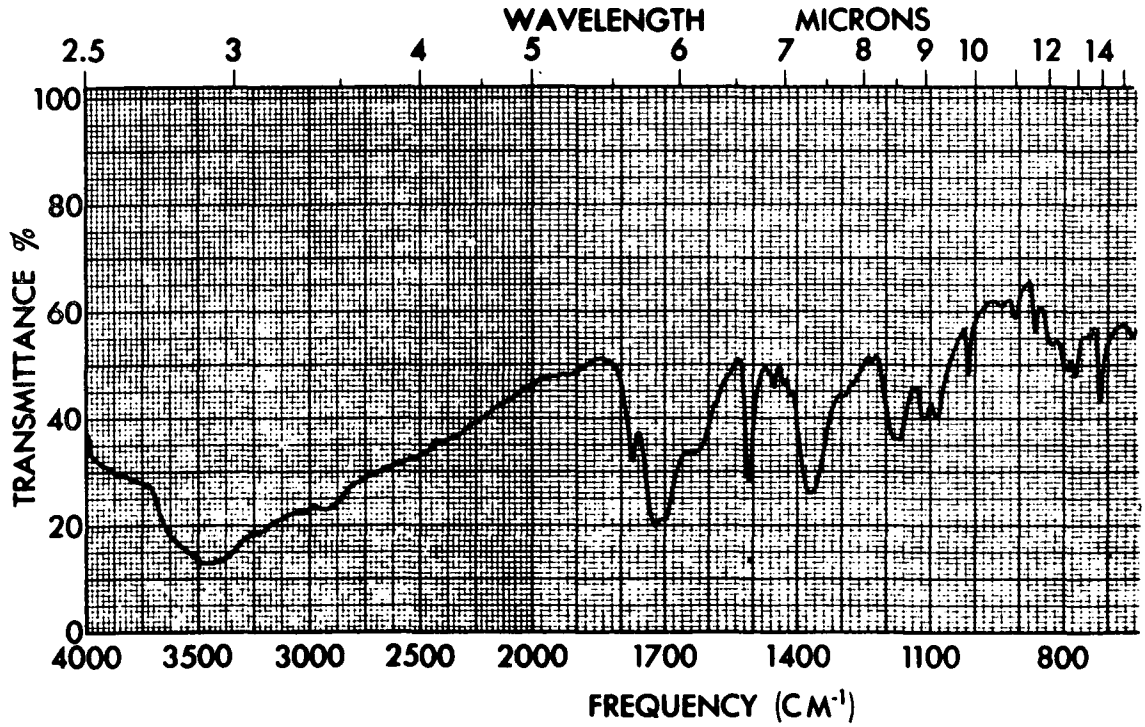


Figure C.6. Infrared Spectrum of P10P Cured in the Presence of 1.0% w/w $SnCl_4$ for 0.17 Hour (KBr)
Concentration: 3.3 mg/g KBr

### C.3.2 Thermo-oxidative Stability Methodology

Each of the A-type resins were screened for thermo-oxidative stability by isothermally aging in air at appropriate temperatures as discussed in Section 3 and 6. The aging experiments were conducted with a Linberg Heavy Duty crucible furnace, Model 56311, connected to a temperature controller manufactured by the same company. The samples were aged in a half-circle form of approximately 4 mm thickness and 12.5 mm diameter after accurately weighing the specimens to the nearest tenth of a milligram. The samples were arranged on a tree-type set-up and placed in the furnace. Air at a 100 $cm^3$/min flow (monitored by a bubble-type indicator) was introduced through a capillary tube into the bottom of the furnace and allowed to flow upward through the furnace, exiting through the top. The temperature was monitored by a thermometer calibrated against an NBS standard. The thermometer bulb was inserted into the furnace to a point approximating the center of the sample array. During the aging experiments, the resin weight loss was monitored by removing the samples every 72-96 hours, allowing them to equilibrate at 298°K, then weighing them to the nearest tenth of a milligram. After each weighing, the samples were rotated from bottom to top on the tree to ensure that each was adequately exposed to the air current at the desired temperature.

After the isothermal aging periods, the samples displayed many microcracks in all surface edges and some had warped slightly toward the center.

# APPENDIX D

## RAW OXIDATIVE DEGRADATION DATA

This appendix provides the raw oxidative degradation data used in Section 5.0 for elucidating thermal degradation modes of P10P HMS graphite fiber compositer in various oxygen level environments and temperatures. Flexural properties of randomly selected specimens from all of the compositer test panels are provided in Table D.I. Weight retention data for thermo-oxidatetively aged specimens are provided in Tables D.II through D.III and flexural properties of these specimens are provided in Tables D.IX through D.XIII. The gaseous effluent analysis data are provided in Tables D.XIV through D.XX.

TABLE D.I

FLEXURAL PROPERTIES OF PIOP/GRAPHITE PANELS

Panel Number 66

| Specimen Number | Width mm | Thickness mm | Load Kg | Stress $MN/m^2$ | M Kg/mm | Modulus[a] $GN/m^2$ | Type of Failure |
|---|---|---|---|---|---|---|---|
| 2 | 12.52 | 3.26 | 54.9 | 616 | 45.4/1.867 | 144 | T |
| 9 | 12.55 | 3.16 | 46.3 | 550 | 45.4/2.026 | 145 | T |
| 15 | 12.57 | 3.28 | 49.9 | 550 | 45.4/1.867 | 140 | S |

Average Stress = 572 $\pm$ 38 $MN/m^2$ Average Modulus = 143 $\pm$ 3 $GN/m^2$

Panel Number 67

| | | | | | | | |
|---|---|---|---|---|---|---|---|
| 3 | 12.52 | 3.23 | 59.4 | 681 | 45.4/1.803 | 154 | T |
| 4 | 12.55 | 3.28 | 63.5 | 703 | 45.4/1.791 | 147 | T |
| 6 | 12.52 | 3.12 | 58.5 | 716 | 45.4/1.994 | 153 | T |
| 10 | 12.57 | 3.14 | 57.6 | 692 | 45.4/1.753 | 170 | T |
| 14 | 12.55 | 3.12 | 54.0 | 662 | 45.4/1.930 | 159 | T |
| 15 | 12.55 | 3.13 | 58.1 | 706 | 45.4/1.994 | 152 | T |

Average Stress = 693 $\pm$ 19 $MN/m^2$ Average Modulus = 156 $\pm$ 8 $GN/m^2$

Panel Number 70-1

| | | | | | | | |
|---|---|---|---|---|---|---|---|
| 4 | 12.67 | 3.35 | 72.6 | 802 | 45.4/2.000 | 142 | T |
| 7 | 12.67 | 3.28 | 73.5 | 845 | 45.4/2.178 | 139 | T |
| 14 | 12.67 | 3.33 | 79.4 | 887 | 45.4/1.975 | 146 | T |

Average Stress = 845 $\pm$ 43 $MN/m^2$ Average Modulus = 142 $\pm$ 4 $GN/m^2$

Panel Number 70-2

| | | | | | | | |
|---|---|---|---|---|---|---|---|
| 2 | 12.70 | 3.33 | 82.6 | 921 | 45.4/1.981 | 145 | T |
| 10 | 12.70 | 3.35 | 74.4 | 821 | 45.4/1.969 | 144 | T |
| 14 | 12.62 | 3.28 | 73.9 | 855 | 45.4/2.146 | 141 | T |

Average Stress = 866 $\pm$ 51 $MN/m^2$ Average Modulus = 143 $\pm$ 2 $GN/m^2$

Panel Number 71

| | | | | | | | |
|---|---|---|---|---|---|---|---|
| 3 | 12.67 | 3.20 | 67.6 | 780 | 45.4/2.057 | 137 | T |
| 8 | 12.62 | 3.18 | 65.3 | 767 | 45.4/2.057 | 140 | T |
| 15 | 12.45 | 3.19 | 62.1 | 732 | 45.4/2.064 | 139 | T |

Average Stress = 760 $\pm$ 25 $MN/m^2$ Average Modulus = 139 $\pm$ 1 $GN/m^2$

[a]Tested at Room Temperature

[b]T = Tensile, S = Shear

TABLE D.I (CONT.)

FLEXURAL PROPERTIES OF P10P/GRAPHITE PANELS

Panel Number 73-1

| Specimen Number | Width mm | Thickness mm | Load Kg | Stress $MN/m^2$ | M Kg/MM | Modulus[a] $GN/m^2$ | Type of[b] Failure |
|---|---|---|---|---|---|---|---|
| 5 | 12.60 | 3.23 | 63.0 | 710 | 45.4/1.803 | 150 | T |
| 10 | 12.60 | 3.26 | 73.0 | 817 | 45.4/1.797 | 149 | T |
| 15 | 12.65 | 3.19 | 67.6 | 783 | 45.4/1.867 | 152 | T |

Average Stress = 770 $\pm$ 54[a] $MN/m^2$ Average Modulus = 150 $\pm$ 1[a] $GN/m^2$

Panel Number 73-2

| | | | | | | | |
|---|---|---|---|---|---|---|---|
| 5 | 12.70 | 3.24 | 65.8 | 736 | 45.4/1.842 | 146 | T |
| 6 | 12.73 | 3.20 | 66.2 | 758 | 45.4/1.772 | 157 | T |
| 14 | 12.70 | 3.20 | 58.1 | 667 | 45.4/1.899 | 148 | T |

Average Stress = 721 $\pm$ 48[a] $MN/m^2$ Average Modulus = 150 $\pm$ 6 $GN/m^2$

Panel Number 74-1

| | | | | | | | |
|---|---|---|---|---|---|---|---|
| 2 | 12.67 | 3.08 | 72.6 | 905 | 45.4/1.905 | 166 | T |
| 4 | 12.67 | 3.18 | 75.7 | 886 | 45.4/1.835 | 157 | T |
| 6 | 12.65 | 3.14 | 70.3 | 843 | 45.4/1.835 | 163 | T |
| 10 | 12.67 | 3.17 | 69.9 | 821 | 45.4/1.835 | 158 | T |
| 11 | 12.70 | 3.11 | 73.5 | 893 | 45.4/1.848 | 165 | T |
| 12 | 12.62 | 3.14 | 74.8 | 896 | 45.4/1.867 | 159 | T |

Average Stress = 874 $\pm$ 34 $MN/m^2$ Average Modulus = 161 $\pm$ 4 $GN/m^2$

Panel Number 74-2

| | | | | | | | |
|---|---|---|---|---|---|---|---|
| 1 | 12.62 | 3.23 | 69.4 | 786 | 45.4/1.911 | 143 | T |
| 10 | 12.67 | 3.12 | 76.2 | 924 | 45.4/1.874 | 162 | T |
| 14 | 12.67 | 3.11 | 63.5 | 776 | 45.4/1.949 | 157 | T |

Average Stress = 829 $\pm$ 83 $MN/m^2$ Average Modulus = 154 $\pm$ 10 $GN/m^2$

Panel Number 65

| | | | | | | | |
|---|---|---|---|---|---|---|---|
| 4 | 12.55 | 3.20 | 57.6 | 671 | 45.4/1.886 | 150 | T |
| 5 | 12.55 | 3.13 | 49.0 | 594 | 45.4/2.305 | 131 | T |
| 9 | 12.52 | 3.31 | 67.1 | 729 | 45.4/1.727 | 148 | T |
| 10 | 12.55 | 3.19 | 59.0 | 689 | 45.4/1.848 | 154 | T |
| 13 | 12.55 | 3.30 | 56.2 | 614 | 45.4/1.803 | 143 | T |
| 14 | 12.52 | 3.18 | 57.6 | 680 | 45.4/1.956 | 148 | T |

Average Stress = 662 $\pm$ 50 $MN/m^2$ Average Modulus = 146 $\pm$ 8 $GN/m^2$

[a]Tested at Room Temperature

[b]T = Tensile, S = Shear

TABLE D.I (CONT.)
FLEXURAL PROPERTIES OF P1OP/GRAPHITE PANELS

Panel Number 72-1

| Specimen Number | Width mm | Thickness mm | Load Kg | Stress $MN/m^2$ | M Kg/mm | Modulus $GN/m^2$ | Type of Failure |
|---|---|---|---|---|---|---|---|
| 5 | 12.65 | 3.14 | 68.5 | 818 | 45.4/1.867 | 159 | T |
| 9 | 12.65 | 3.23 | 69.4 | 788 | 45.4/1.822 | 151 | T |
| 11 | 12.65 | 3.19 | 56.7 | 657 | 45.4/1.975 | 143 | T |

Average Stress = 754 $\pm$ 85 $MN/m^2$ Average Modulus = 151 $\pm$ 8 $GN/m^2$

Panel Number 72-2

| | | | | | | | |
|---|---|---|---|---|---|---|---|
| 1 | 12.60 | 3.30 | 61.7 | 671 | 45.4/1.816 | 141 | T |
| 6 | 12.70 | 3.18 | 58.1 | 676 | 45.4/1.873 | 152 | T |
| 11 | 12.65 | 3.15 | 64.9 | 772 | 45.4/1.829 | 161 | T |

Average Stress = 706 $\pm$ 57 $MN/m^2$ Average Modulus = 152 $\pm$ 10 $GN/m^2$

TABLE D.II

WEIGHT RETENTION OF UNSTRESSED GRAPHITE P10P COMPOSITES MAINTAINED AT 505°K IN FLOWING 20% OXYGEN ENVIRONMENT

| Coupon Code | Accumulated Exposure Time, Hours | | | | | | | | | | | | | |
|---|---|---|---|---|---|---|---|---|---|---|---|---|---|---|
| | 23 | 69 | 163 | 257 | 327 | 427 | 521 | 585 | 653 | 745 | 809 | 903 | 995 | 1283 |
| 74-2-3 | 99.5 | 99.4 | 99.0 | 98.5 | 98.0 | 97.5 | 95.6 | | | | | | | |
| 67-13 | 99.5 | 99.3 | 98.8 | 98.2 | 97.6 | 97.0 | 94.8 | | | | | | | |
| 65-15 | 99.4 | 99.3 | 98.9 | 98.2 | 97.7 | 97.0 | 94.7 | 93.1 | 92.0 | 91.6 | 91.3 | 90.8 | 90.5 | |
| 66-6 | 99.5 | 99.4 | 99.1 | 98.7 | 98.5 | 98.2 | 97.2 | 96.1 | 95.5 | 95.3 | 95.1 | 94.8 | 94.6 | 93.7 |
| 67-5 | 99.5 | 99.4 | 99.1 | 98.7 | 98.3 | 98.0 | 96.7 | 95.5 | 94.8 | 94.6 | 94.3 | 93.9 | 93.7 | 92.6 |
| 72-1-15 | 99.6 | 99.4 | 98.9 | 98.2 | 97.7 | 97.1 | 94.8 | | | | | | | |
| 71-14 | 99.4 | 99.3 | 99.1 | 98.9 | 98.8 | 98.5 | 97.8 | 97.1 | 96.5 | 96.3 | 96.1 | 95.8 | 95.7 | 94.9 |
| 73-2-10 | 99.5 | 99.3 | 98.8 | 98.1 | 97.5 | 96.8 | 94.4 | 92.6 | 91.4 | 91.0 | 90.7 | 90.1 | 89.6 | |
| 73-2-1 | 99.5 | 99.2 | 97.6 | 95.9 | 94.6 | 93.4 | 90.2 | 88.0 | 86.8 | 86.5 | 86.2 | 85.9 | 85.7 | |

TABLE D.III

WEIGHT RETENTION OF UNSTRESSED GRAPHITE P10P COMPOSITES MAINTAINED AT 589°K IN FLOWING 20% OXYGEN ENVIRONMENT

| Coupon Code | Accumulated Exposure Time, Hours | | | | | | | |
|---|---|---|---|---|---|---|---|---|
| | 17.5 | 39 | 107 | 127 | 147.5 | 191.5 | 284 | 375.5 |
| 66-11 | 98.7 | 98.2 | 96.9 | 96.7 | 96.5 | 96.1 | 95.2 | |
| 65-7 | 98.8 | 98.4 | 97.4 | 97.1 | 96.8 | 96.4 | 95.3 | |
| 70-2-6 | 98.9 | 98.5 | 97.5 | 97.3 | 97.1 | 96.8 | 95.6 | 94.4 |
| 70-1-6 | 98.9 | 98.5 | 97.5 | 97.3 | 97.1 | 96.8 | 95.3 | 93.5 |
| 65-2 | 98.8 | 98.5 | 97.4 | 97.2 | 96.9 | 96.5 | 95.1 | 93.4 |
| 71-12 | 98.9 | 98.6 | 97.4 | 97.0 | 96.6 | 95.8 | 93.6 | 90.8 |
| 70-1-10 | 98.9 | 98.6 | 97.6 | 97.3 | | | | |
| 72-1-7 | 98.7 | 98.1 | 96.6 | 96.2 | | | | |
| 74-1-15 | 98.9 | 98.3 | 96.8 | 96.3 | | | | |
| 72-1-14 | 98.7 | 98.1 | 96.4 | 96.0 | 95.6 | 94.9 | 92.7 | |
| 73-2-8 | 98.6 | 98.0 | 96.2 | 95.7 | | | | |
| 73-1-14 | 98.4 | 97.5 | 94.6 | 93.8 | 93.1 | 91.9 | 89.5 | |

TABLE D.IV

WEIGHT RETENTION OF UNSTRESSED GRAPHITE P10P COMPOSITES MAINTAINED AT 589°K IN FLOWING 60% OXYGEN ENVIRONMENT

| Coupon Code | Accumulated Exposure Time , Hours | | | | | |
|---|---|---|---|---|---|---|
| | 17.5 | 39 | 107 | 127 | 147.5 | 191.5 |
| 70-2-3 | 98.5 | 97.9 | 96.1 | 95.5 | 95.0 | 93.8 |
| 70-1-9 | 98.5 | 97.9 | 95.9 | | | |
| 65-3 | 98.5 | 97.7 | 94.8 | | | |
| 73-1-4 | 98.2 | 97.1 | 93.7 | | | |
| 72-1-10 | 98.0 | 96.9 | 93.6 | | | |
| 73-1-3 | 98.1 | 96.9 | 93.3 | 92.1 | 91.1 | 89.2 |
| 70-2-11 | 98.2 | 96.9 | 91.8 | 90.2 | 88.9 | 86.8 |
| 72-2-7 | 97.1 | 94.7 | 87.5 | 85.8 | 84.4 | 82.2 |

TABLE D.V

WEIGHT RETENTION OF UNSTRESSED GRAPHITE P10P COMPOSITES MAINTAINED AT 505°K IN FLOWING 100% OXYGEN ENVIRONMENT

| Coupon Code | Accumulated Exposure Time, Hours | | | | | | | |
|---|---|---|---|---|---|---|---|---|
| | 23 | 69 | 163 | 257 | 327 | 427 | 521 | 585 |
| 66-1 | 99.4 | 99.1 | 97.5 | 95.3 | | | | |
| 71-13 | 99.3 | 98.9 | 96.9 | 94.2 | | | | |
| 72-2-4 | 99.5 | 98.5 | 94.7 | 91.4 | | | | |
| 73-2-2 | 99.5 | 98.9 | 96.9 | 94.1 | 91.8 | 90.2 | | |
| 74-2-5 | 99.4 | 98.9 | 96.8 | 93.6 | 91.1 | 89.6 | | |
| 67-2 | 99.5 | 99.3 | 98.1 | 96.7 | 95.1 | 93.6 | | |
| 73-1-1 | 99.2 | 98.1 | 95.4 | 92.9 | 91.1 | 89.7 | 86.9 | 84.3 |
| 66-3 | 99.5 | 99.2 | 98.2 | 96.7 | 95.0 | 93.3 | 90.0 | 86.8 |
| 74-2-6 | 99.5 | 99.1 | 97.4 | 94.7 | 92.6 | 91.1 | 88.0 | 85.4 |

TABLE D.VI

WEIGHT RETENTION OF UNSTRESSED GRAPHITE P10P COMPOSITES MAINTAINED AT 589°K IN FLOWING 100% OXYGEN ENVIRONMENT

| Coupon Code | Accumulated Exposure Time, Hours | | | | |
|---|---|---|---|---|---|
| | 30 | 40.5 | 60.5 | 80.5 | 101.5 |
| 70-1-13 | 98.5 | 97.9 | 97.1 | 96.5 | 95.9 |
| 67-12 | 98.1 | 97.2 | 96.2 | 95.3 | 94.5 |
| 74-1-8 | 97.8 | 96.6 | 95.4 | 93.9 | 92.8 |
| 72-1-2 | 96.4 | 94.0 | 91.6 | 89.4 | 87.9 |

TABLE D.VII

WEIGHT RETENTION OF STRESSED GRAPHITE P10P COMPOSITES MAINTAINED AT 505°K IN FLOWING 20% OXYGEN ENVIRONMENT

| Coupon Code | Accumulated Exposure Time, Hours | | | | | | | |
|---|---|---|---|---|---|---|---|---|
| | 162 | 208 | 302 | 372 | 466 | 536 | 630 | 724 |
| 72-2-2 | 99.9 | 98.6 | 95.9 | 93.2 | 91.8 | 91.8 | 91.2 | 91.2 |
| 73-2-11 | 97.3 | 96.0 | 92.6 | 90.6 | 89.9 | 89.9 | 89.9 | 89.9 |
| 73-1-6 | 99.3 | 98.7 | 98.0 | 96.7 | 94.7 | 94.7 | 94.7 | 94.7 |
| 71-7 | 99.3 | 98.7 | 97.4 | 96.0 | 94.7 | 94.1 | 94.1 | 94.1 |
| 73-1-8 | 99.3 | 98.0 | 96.0 | 94.0 | 92.7 | 92.7 | 92.7 | 92.7 |
| 74-2-2 | 99.3 | 98.6 | 98.0 | 95.9 | 95.3 | 95.3 | 95.3 | 95.3 |
| 72-1-4 | 99.3 | 98.7 | 97.3 | 96.0 | 96.0 | 96.0 | 96.0 | 96.0 |
| 67-4 | 99.3 | 98.7 | 98.0 | 97.3 | 96.0 | 96.0 | 96.0 | 96.0 |
| 73-1-11 | 98.6 | 98.0 | 96.0 | 94.7 | 93.4 | 92.7 | 92.7 | 92.7 |

TABLE D.VIII

WEIGHT RETENTION OF STRESSED GRAPHITE P10P COMPOSITES MAINTAINED AT 589°K IN FLOWING 20% OXYGEN ENVIRONMENT

| Coupon Code | Accumulated Exposure Time, Hours | | |
|---|---|---|---|
| | 23 | 95 | 141 |
| 72-1-6 | 0 | 97.1 | 96.7 |
| 74-2-15 | 0 | 97.1 | 96.4 |
| 71-6 | 0 | 97.4 | 95.9 |

TABLE D.IX

FLEXURAL PROPERTIES AFTER AGING AT 505°K
IN 20% v/v OXYGEN ATMOSPHERE

| Specimen Identification | Original[a] Nominal Flexural Strength $MN/m^2$ | Aging Duration Hours | Flexural Strength $MN/m^2$ | Strength[b] Retention % | Flexural Modulus $GN/m^2$ |
|---|---|---|---|---|---|
| 67-13 | 889 | 521 | 582 | 66 | 137 |
| 72-1-15 | 986 | 521 | 666 | 67 | 153 |
| 74-3 | 998 | 521 | 759 | 83 | 159 |
| 73-2-10 | 963 | 995 | 624 | 65 | 138 |
| 73-2-1 | 963 | 995 | 586 | 61 | 151 |
| 65-16 | 613 | 995 | 613 | 100 | 128 |

[a] Nominal flexural strength = $\bar{x} - 3\sigma$ (See Table 3.3.1-1)

[b] $\frac{\text{Flexural strength after aging}}{\text{Nominal flexural strength}} \times 100 = \left(\frac{F_{ua}}{F_{un}} \times 100\right)$

TABLE D.X

FLEXURAL PROPERTIES AFTER AGING AT 589°K
IN 20% v/v OXYGEN ATMOSPHERE

| Specimen Identification | Original[a] Nominal Flexural Strength $MN/m^2$ | Aging Duration Hours | Flexural Strength $MN/m^2$ | Strength[b] Retention % | Flexural Modulus $GN/m^2$ |
|---|---|---|---|---|---|
| 70-1-10 | 974 | 127 | 652 | 67 | 148 |
| 72-1-7 | 986 | 127 | 697 | 71 | 154 |
| 74-1-15 | 998 | 127 | 775 | 77 | 159 |
| 73-2-8 | 963 | 127 | 665 | 69 | 153 |
| 72-1-14 | 986 | 285 | 675 | 68 | 152 |
| 66-11 | 568 | 284 | 614 | 108 | 153 |
| 65-5 | 613 | 284 | 707 | 116 | 151 |
| 73-1-14 | 1032 | 284 | 558 | 54 | 139 |
| 70-2-6 | 949 | 375-5 | 719 | 76 | 131 |
| 65-2 | 613 | 375-5 | 651 | 106 | 155 |
| 71-12 | 864 | 375-5 | 672 | 78 | 148 |
| 70-1-6 | 973 | 375-5 | 855 | 88 | 161 |

[a] Nominal flexural strength = $\bar{x} - 3\sigma$ (See Table 3.3.1-1)

[b] $\frac{\text{Flexural strength after aging}}{\text{Nominal flexural strength}} \times 100 = \left(\frac{F_{ua}}{F_{un}} \times 100\right)$

TABLE D.XI

FLEXURAL PROPERTIES AFTER AGING AT 589°K
IN 60% v/v OXYGEN ATMOSPHERE

| Specimen Identification | Original[a] Nominal Flexural Strength $MN/m^2$ | Aging Duration Hours | Flexural Strength $MN/m^2$ | Strength[b] Retention % | Flexural Modulus $GN/m^2$ |
|---|---|---|---|---|---|
| 65-3 | 613 | 107 | 694 | 120 | 150 |
| 70-1-4 | 974 | 107 | 816 | 84 | 140 |
| 73-1-4 | 1032 | 107 | 683 | 67 | 150 |
| 72-1-10 | 986 | 107 | 823 | 83 | 152 |
| 73-1-3 | 1032 | 191.5 | 681 | 66 | 149 |
| 70-2-11 | 949 | 191.5 | 450 | 48 | 155 |
| 72-2-7 | 936 | 191.5 | 407 | 47 | 167 |
| 70-2-3 | 939 | 191.5 | 561 | 59 | 144 |

[a]Nominal flexural strength = $\bar{x} - 3\sigma$ (See Table 3.3.1-1)

[b]$\frac{\text{Flexural strength after aging}}{\text{Nominal flexural strength}} \times 100 = \left(\frac{F_{ua}}{F_{un}} \times 100\right)$

TABLE D.XII

FLEXURAL PROPERTIES AFTER AGING AT 505°K
IN 100% v/v OXYGEN ATMOSPHERE

| Specimen Identification | Original[a] Nominal Flexural Strength $MN/m^2$ | Aging Duration Hours | Flexural Strength $MN/m^2$ | Strength[b] Retention % | Flexural Modulus $GN/m^2$ |
|---|---|---|---|---|---|
| 71-13 | 864 | 257 | 560 | 65 | 146 |
| 66-1 | 568 | 257 | 722 | 127 | 150 |
| 72-2-4 | 936 | 257 | 583 | 62 | 159 |
| 73-2-2 | 963 | 427 | 352 | 37 | 143 |
| 74-2-5 | 769 | 427 | 456 | 60 | 150 |
| 67-2 | 889 | 427 | 533 | 60 | 143 |
| 74-2-6 | 769 | 585 | 502 | 65 | 164 |
| 73-1-1 | 1032 | 585 | 583 | 57 | 148 |
| 66-3 | 568 | 585 | 626 | 110 | 146 |

[a]Nominal flexural strength = $\bar{x} - 3\sigma$ (See Table 3.3.1-1)

[b]$\frac{\text{Flexural strength after aging}}{\text{Nominal flexural strength}} \times 100 = \left(\frac{F_{ua}}{F_{un}} \times 100\right)$

TABLE D.XIII

FLEXURAL PROPERTIES AFTER AGING AT 589°K
IN 100% OXYGEN ATMOSPHERE

| Specimen Identification | Original[a] Nominal Flexural Strength $MN/m^2$ | Aging Duration Hours | Flexural Strength $MN/m^2$ | Strength[b] Retention % | Flexural Modulus $GN/m^2$ |
|---|---|---|---|---|---|
| 70-1-13 | 974 | 101.5 | 822 | 85 | 145 |
| 72-1-2 | 986 | 101.5 | 551 | 56 | 141 |
| 74-1 | 998 | 101.5 | 779 | 78 | 156 |
| 67-12 | 889 | 101.5 | 681 | 77 | 153 |

[a]Nominal flexural strength = $\bar{x} - 3\sigma$ (See Table 3.3.1-1)

[b]$\frac{\text{Flexural strength after aging}}{\text{Nominal flexural strength}} \times 100 = \left(\frac{F_{ua}}{F_{un}} \times 100\right)$

TABLE D.XIV

GASEOUS EFFLUENT ANALYSIS AT 505°K AT 20% OXYGEN UNSTRESSED

| Gaseous Effluent | Time of Sampling After Initiation (Hrs) | | | | | |
|---|---|---|---|---|---|---|
| | 0.25 | 1.0 | 3.5 | 6.5 | 23 | 275 |
| $CO_2$ % v/v | 0.53 | 0.36 | 0.22 | 0.21 | 0.21 | 0.21 |
| CO % v/v | ND[a] | ND | ND | ND | ND | ND |
| $H_2O$ % v/v | 0.06 | 0.31 | 0.54 | 0.46 | 0.38 | 0.46 |

[a]Code: ND = None detected

TABLE D.XV

GASEOUS EFFLUENT ANALYSIS AT 589°K AND 20% V/V OXYGEN UNSTRESSED

| Gaseous Effluent | Time of Sampling After Initiation (Hrs) | | | |
|---|---|---|---|---|
| | 1.0 | 17.5 | 39 | 127 |
| $CO_2$ % v/v | 2.2 | 0.82 | 0.50 | 0.14 |
| CO % v/v | 1.2 | ND[a] | ND | ND |
| $H_2O$ % v/v | 0.41 | 0.52 | 0.41 | 0.32 |

[a]Code: ND = None detected

TABLE D.XVI

GASEOUS EFFLUENT ANALYSIS AT 589°K AND 60% V/V OXYGEN UNSTRESSED

| Gaseous Effluent | Time of Sampling After Initiation (Hrs) | | | | |
|---|---|---|---|---|---|
| | 1.0 | 17.5 | 39 | 107 | 127 |
| $CO_2$ % v/v | 2.2 | 1.1 | 1.1 | 0.76 | 0.62 |
| CO % v/v | 1.3 | ND[a] | ND | ND | ND |
| $H_2O$ % v/v | 0.21 | 0.50 | 0.46 | 0.36 | 0.30 |

[a]Code: ND = None detected

TABLE D.XVII

GASEOUS EFFLUENT ANALYSIS AT 505°K AT 100% OXYGEN UNSTRESSED

| Gaseous Effluent | Time of Sampling After Initiation (Hrs) | | | | | |
|---|---|---|---|---|---|---|
| | 0.25 | 1.0 | 3.5 | 6.5 | 23 | 257 |
| $CO_2$ % v/v | 0.71 | 0.59 | 0.60 | 0.71 | 0.60 | 0.56 |
| CO % v/v | 0.20 | ND | ND | ND | ND | <0.1 |
| $H_2O$ % v/v | 0.26 | 0.46 | 0.64 | 0.47 | 0.47 | 0.47 |

[a]Code: ND = None detected

TABLE D.XVIII

GASEOUS EFFLUENT ANALYSIS AT 589°K AND 100% V/V OXYGEN UNSTRESSED

| Gaseous Effluent | Time of Sampling After Initiation (Hrs) | | | |
|---|---|---|---|---|
| | 1.0 | 30 | 40.5 | 60.5 |
| $CO_2$ % v/v | 1.1 | 0.59 | 0.51 | 0.58 |
| CO % v/v | 0.23 | ND[a] | ND | ND |
| $H_2O$ % v/v | 0.45 | 0.47 | 0.41 | 0.45 |

[a]Code: ND = None detected

TABLE D.XIX

GASEOUS EFFLUENT ANALYSIS AT 505°K, AT 20% OXYGEN AND AT 50% STRESS LEVEL

| Gaseous Effluent | Time of Sampling After Initiation (Hrs) | | | |
|---|---|---|---|---|
| | 0.5 | 1.5 | 6.0 | 22 |
| $CO_2$ % v/v | 0.16 | 0.62 | 0.51 | 0.51 |
| CO % v/v | ND | ND | ND | ND |
| $H_2O$ % v/v | 0.94 | 0.68 | 0.47 | 0.46 |

[a]Code: ND = None detected

TABLE D.XX

GASEOUS EFFLUENT ANALYSIS AT 589°K, AT 20% OXYGEN AND AT 50% STRESS LEVEL

| Gaseous Effluent | Time of Sampling After Initiation (Hrs) | |
|---|---|---|
| | 0.25 | 16 |
| $CO_2$ % v/v | 0.49 | 0.21 |
| CO % v/v | ND | ND |
| $H_2O$ % v/v | 0.47 | 0.43 |

[a]Code: ND = None detected

# APPENDIX E

## RAW FLEXURAL CREEP DATA

This appendix provides the raw flexural creep data used in Section 5.5 for calculating normalized values, as well as the best fit curves used for plotting flexural deflection creep curves. The measured deflections of flexural test coupons at two stress levels and four air temperatures are presented in Table E.I. These data were plotted to show deflection vs. temperature at two stress levels for five specific time intervals from the commencement of the creep tests. Wild data were expelled and the best fit curves shown in Figures E.1 through E.5 were drawn.

TABLE E.I. RAW FLEXURAL CREEP DATA

| Test Temperature OK | Flexural Load % | Deflection, mm. Time at Test Temperature, Min. 0 | 15 | 30 | 60 | 120 | 240 | 450 | 1350 |
|---|---|---|---|---|---|---|---|---|---|
| 558 | 50 | 1.189 | 1.295 | 1.334 | 1.361 | 1.382 | 1.397 | 1.409 | 1.478[b] |
| | 75 | 1.953 | 2.062 | 2.083 | 2.133 | 2.205 | 2.359 | 2.441 | 2.807 |
| 566 | 50 | 1.285 | 1.458 | 1.524 | 1.554 | 1.575 | 1.595 | 1.603 | 1.651 |
| | 75 | 1.775 | 1.803 | 1.829 | 1.854 | 1.854 | 1.885 | 1.902 | 1.943 |
| 577 | 50 | 1.577 | 1.950 | 2.123 | 2.209 | 2.271 | 2.304 | 2.362 | 2.438 |
| | 75 | 1.892 | 2.051 | 2.098 | 2.146 | 2.164 | 2.189 | 2.209 | 2.261 |
| 589 | 50 | 1.140 | 1.389 | 1.448 | 1.486 | 1.506 | 1.527 | 1.544 | 1.600 |
| | 75 | 1.684 | 1.956 | 2.027 | 2.085 | 2.187 | 2.540 | 2.788 | c |

[a]Stress level; % of ultimate flexural strength at test temperature

[b]1.478 mm deflection after 2700 minutes of test

[c]4.064 mm deflection after 1600 minutes of test; specimen failed

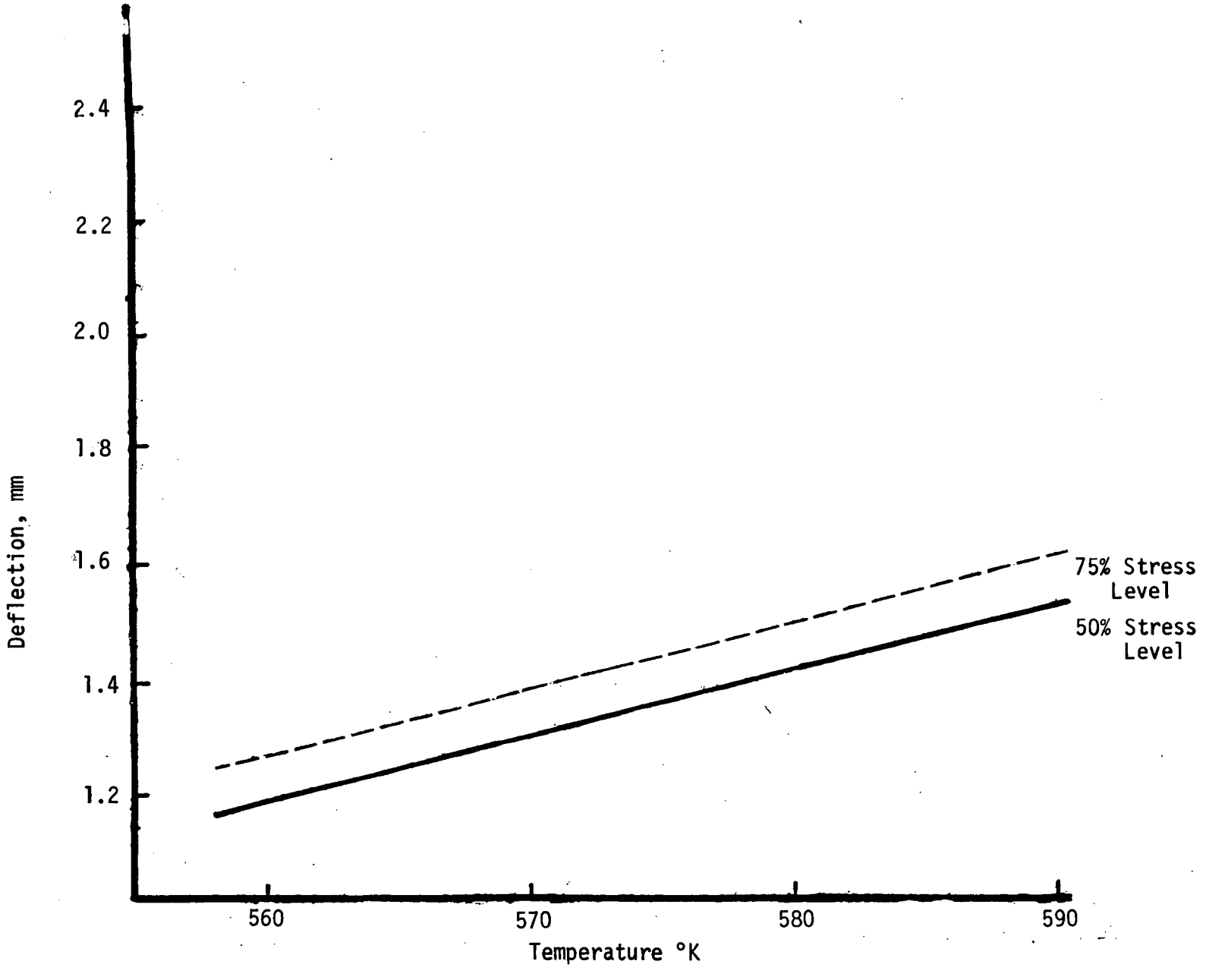


Figure E.1. Deflection *vs* Temperature at Start

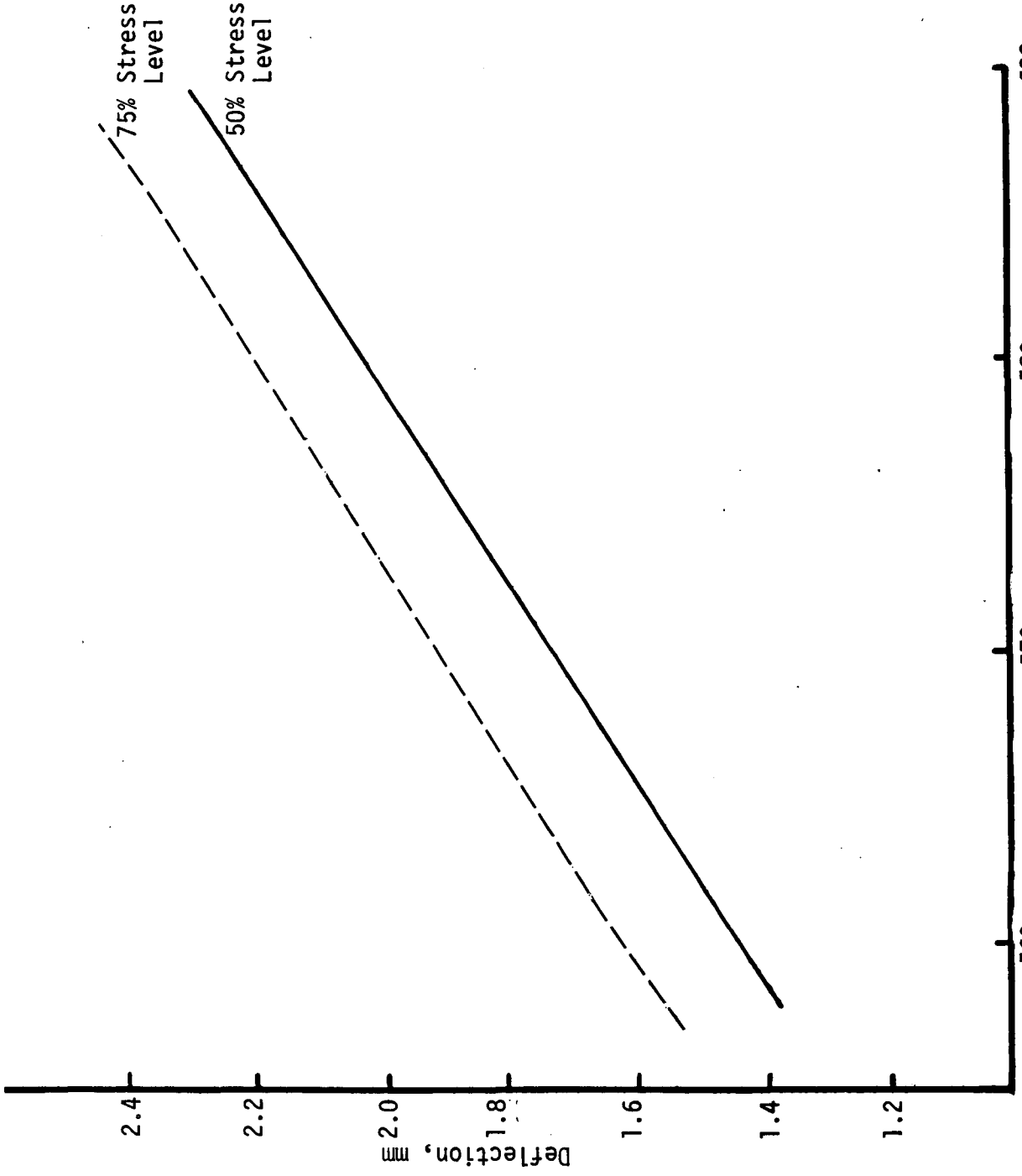


Figure E.2. Deflection *vs* Temperature After 60 Minutes

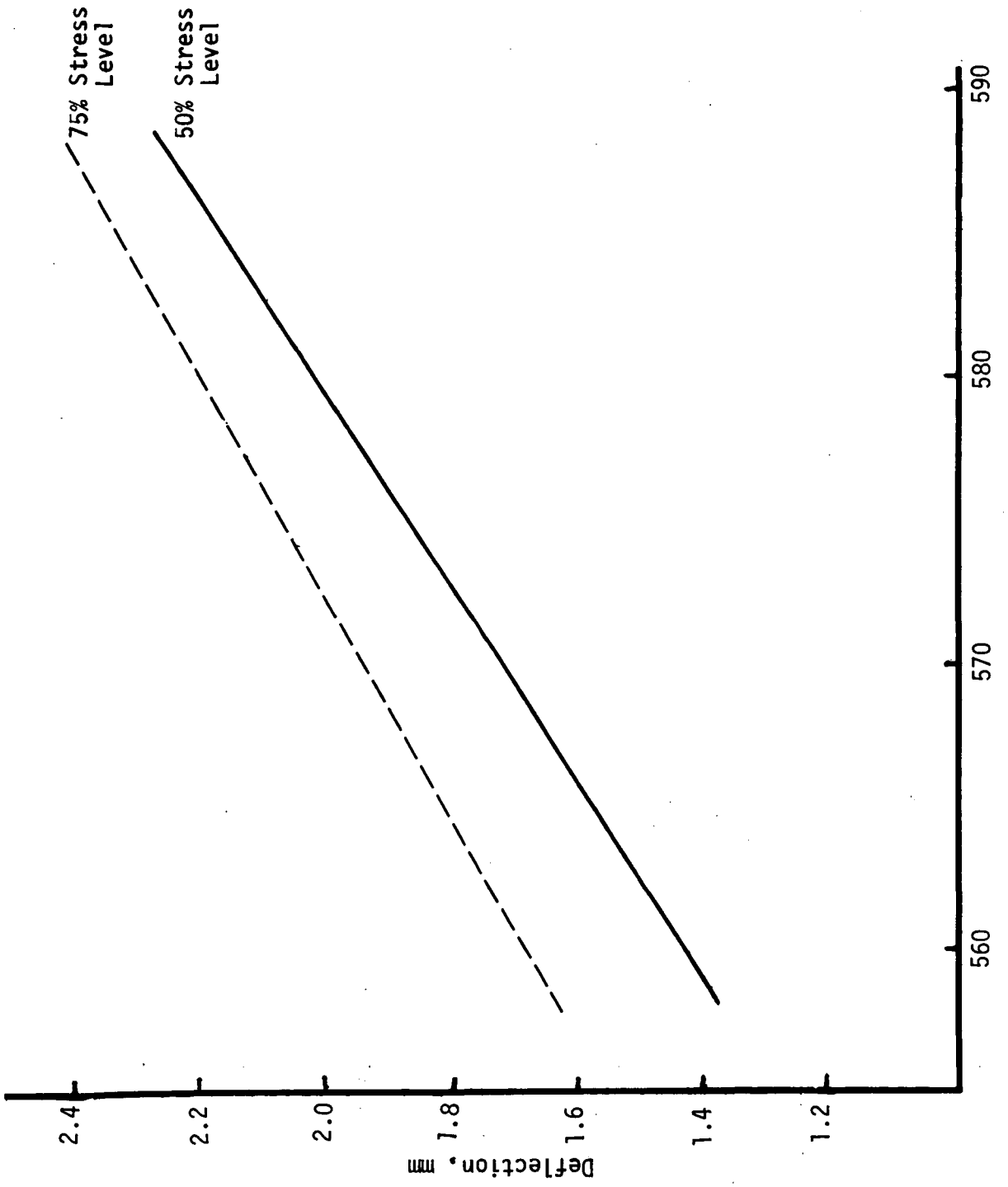


Figure E.3. Deflection *vs* Temperature After 240 Minutes

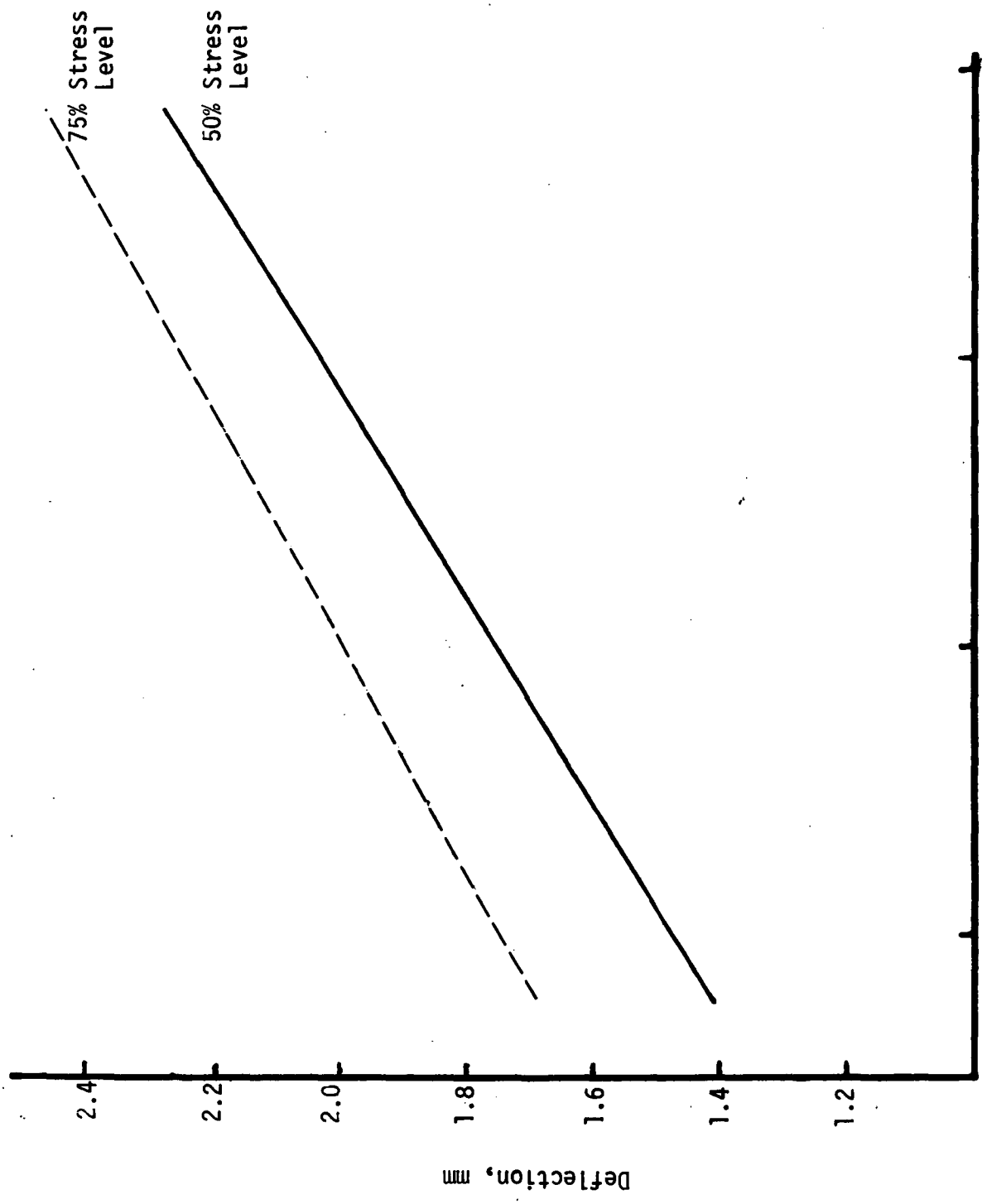


Figure E.4. Deflection *vs* Temperature After 450 Minutes

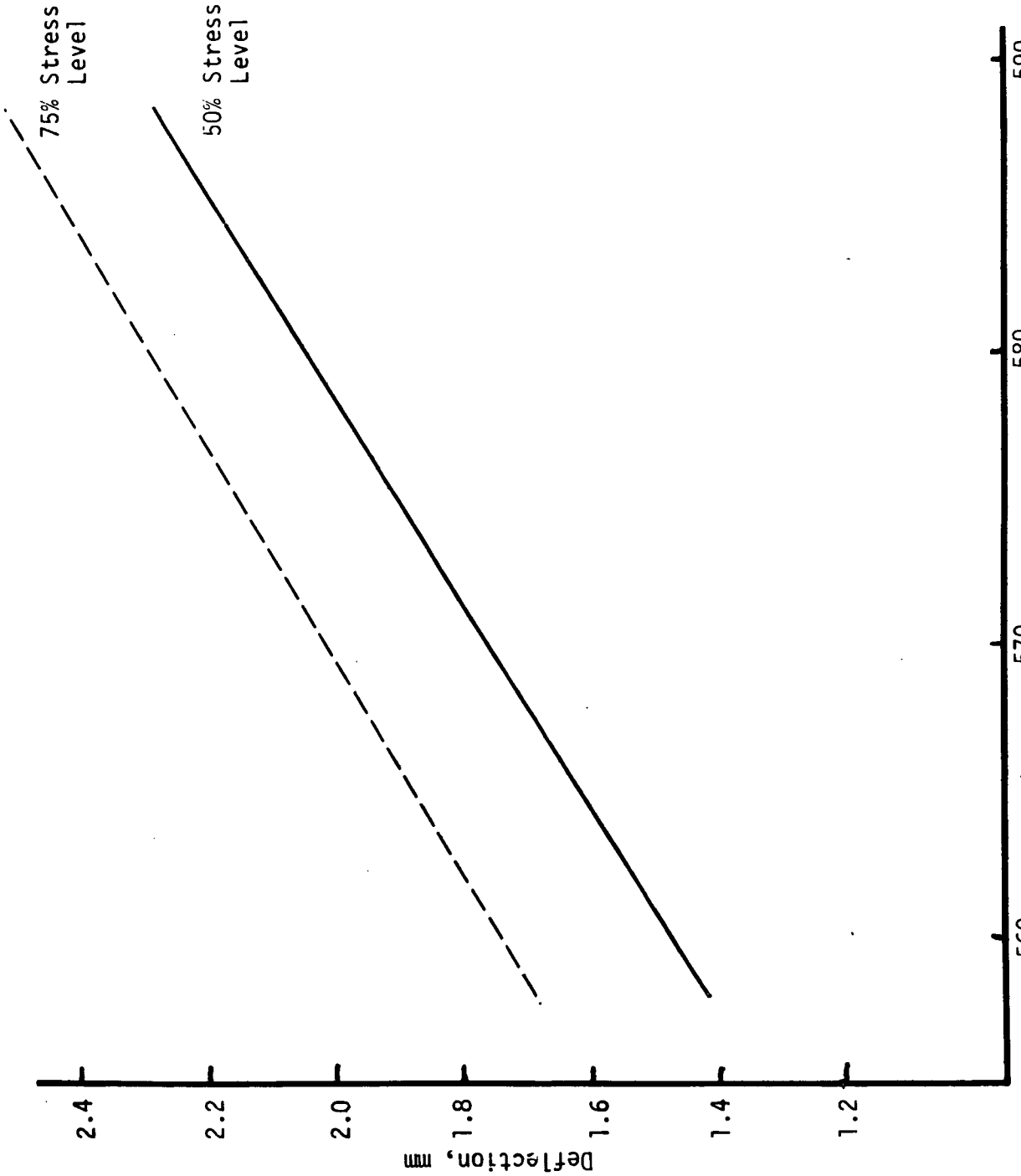


Figure E.5. Deflection *vs* Temperature After 1350 Minutes

# APPENDIX F

# TEST PROCEDURES FOR CHARACTERIZATION OF PREPREG AND COMPOSITES

## F.1 RESIN CONTENT BY BURN-OFF

Samples of cured composite or prepreg were weighed in a tarred crucible and then placed into an 830°K muffle furnace. After constant weight was attained (usually after one hour for prepreg and four hours for composite) the resin content was calculated:

$$W_r = \frac{(W_1 - W_2)}{W_1} \quad 100$$

Where:

$W_r$ = Weight content of resin solids, %
$W_1$ = Weight of original sample, g
$W_2$ = Weight of specimen after burn-off, g

## F.2 RESIN CONTENT BY ACID DIGESTION

The resin was digested from the cured sample by pouring concentrated sulfuric acid (120 ml) onto the sample in a glass beaker and then heating the acid for a minimum of 20 minutes until it turned black. At this point, 30% hydrogen peroxide solution was added dropwise to the acid until it turned clear again. The acid was reheated for a minimum of one hour. During this period, further drops of hydrogen peroxide solution were added to clear the acid whenever the acid turned black. Upon completion of this cycle, the acid was cooled to room temperature and an additional 2 ml of hydrogen peroxide solution was added. The solution was heated again until white fumes appeared after which it was cooled to room temperature. The acid was decanted from the filaments using a fritted glass filter, washed firstly in distilled water and then in acetone, after which the filaments were dried for 15 minutes in a 450°K air circulating oven. Resin solids contents were calculated:

$$W_r = \frac{(W_1 - W_2)}{W_1} \quad 100$$

Where:

$W_r$ = Weight content of resin solids, % w/w

$W_1$ = Weight of cured composite sample

$W_2$ = Weight of filaments after acid digestion of the resin matrix

F.3 VOLATILE MATTER CONTENT

Volatile matter contents were determined by weight loss after exposure of a 0.5 g prepreg sample in an air circulating oven at 590°K for 30 minutes.

F.4 DENSITY OF COMPOSITES

Density of composites was determined from measured volumes (air pycnometer) and weights of specimens.

F.5 COMPOSITE FIBER VOLUME

Fiber volume percent of the composites was calculated by the formula:

$$V_f = 100\ (1\text{-}K)\ \frac{D_c}{D_f}$$

Where:

$V_f$ = Volume percent fiber, ml

$D_c$ = Measured density of composite, g/ml

$D_f$ = Density of fiber, g/ml

K = Weight fraction, resin

The specific gravity of the Courtaulds HMS fiber is 1.90 $g/cm^3$ and of the cured PIOP polyimide resin is 1.30 $g/cm^3$.

F.6 COMPOSITE VOID CONTENT

Void contents of the composites were calculated using the formula:

$$V_v = 100 - D_c \left[ \frac{W_r}{D_r} + \frac{W_f}{D_f} \right]$$

Where:

$V_v$ = Volume of voids, % v/v

$D_c$ = Measured density of composite, $g/cm^3$

$D_r$ = Density of resin, $g/cm^3$

$D_f$ = Density of fiber, $g/cm^3$

$W_r$ = Weight content of resin, percent

$W_f$ = Weight content of fiber, percent

## F.7 PERCENT RESIN FLOW OF PREPREGS

Percent resin flow was determined by weight loss determinations on molded prepreg flow specimens (six-ply prepreg, 45° bias, 10-cm x 10-cm square) after removal of the resin flash.

Flow properties were calculated:

$$F_w = \frac{W_1 - W_3}{W_1} \quad 100$$

and

$$F_d = \frac{W_2 - W_3}{W_2} \quad 100$$

Where:

$F_w$ = Percent wet resin flow, % w/w

$F_d$ = Percent dry resin flow, % w/w

$W_1$ = Initial weight of prepreg specimen, g

$W_2$ = Weight of prepreg sample after molding, g

$W_3$ = Weight of prepreg sample after molding and with resin flash removed, g

## F.8 SHEAR STRENGTH OF COMPOSITES

The cured composites were machined into short beam shear specimens 0.63-cm wide x 1.78-cm long and tested in flexure at a mid-span loading point using a 4:1 span to depth ratio. Loading rate was 1.3 mm/minute.

Shear strengths were calculated using the simple formula:

$$S_u = \frac{0.75V}{tb}$$

Where:

$S_u$ = Ultimate shear strength, $MN/m^2$

V = Load at failure, N

t = Specimen thickness, mm

b = Specimen width, mm

## F.9 FLEXURAL PROPERTIES OF COMPOSITES

The cured composites were machined into flexural specimens 1.3 cm wide by 13-cm long and tested in flexure at a single mid-span loading point using a 32:1 span-to-depth ratio. Loading rate was 1.3 mm/minute.

Flexural strengths and moduli were calculated using the formuli:

$$F_u = \frac{3\ PL}{2Bd^2}$$

and

$$E_b = \frac{L^3\ m}{4bd^3}$$

Where:

$F_u$ = Stress in the outer fiber at mid-span, $MN/m^2$

$E_b$ = Modulus of elasticity in bending, $GN/m^2$

P = Load at failure, N

L = Span, inch

b = Width of specimen, mm

d = Thickness of specimen, mm

m = Slope of the tangent to the initial straightline portion of the load deflection curve, N/mm

## REFERENCES

1. E. A. Burns, R. J. Jones, R. W. Vaughan and W. P. Kendrick, "Thermally Stable Laminating Resins," Final Report Contract NAS3-12412, NASA CR-72633, dated 17 January 1970.

2. E. A. Burns, H. R. Lubowitz, and J. F. Jones, "Investigation of Resin Systems for Improved Ablative Materials," Contract NAS3-7949, NASA Report No. CR-72460, Lewis Research Center, Cleveland, Ohio, 10 October 1968.

3. H. A. Brunson and H. Standinger, Ind. Eng. Chem., 18, 381 (1926)..

4. C. Aso, T. Kunitake, and Y. Ishimoto, J. Polymer Sci., Pt. A-1, 6, 1163 (1968).

5. A. G. Davies and A. Wassermann, J. Polymer Sci., 6, 1887 (1966).

6. C. Aso, T. Kunitake, K. Ito, and Y. Ishimoto, Polymer Letters, 4, 701 (1966).

7. W. L. Truett, D. R. Johnson, I. M. Robinson and B. A. Montague, J. Am. Chem. Soc., 82, 2337 (1960).

8. R. J. Jones, R. W. Vaughan, and E. A. Burns, "Resin/Graphite Fiber Composites," Final Report on Subcontract to NASA Contract NAS3-13203 Report No. 12909-6008-RO-00, dated 31 December 1970.

9. O. L. Davies, "Design and Analysis of Industrial Experiments," 2nd Edition, Hafner Publishing Company, New York, 1963.

10. I. Heilbron, Editor, "Dictionary of Organic Compounds," 4th Ed., Oxnard University Press, A65, p. 395.

11. R. C. Weast, Editor, "Handbook of Chemistry and Physics," 50th Ed. The Chemical Rubber Co., 1969, p. C-359.

12. L. J. Bellamy, "The Infrared Spectra of Complex Molecules," Methuen and Co. Ltd., Suffolk, England, 1962, p. 34.

13. F. A. Bovey, "NMR Data Tables for Organic Compounds," Interscience Publishers, 1967, p. 96.

14. Ibid., p. 104.

15. Ibid., p. 183.

FOLDOUT FRAME 1

FOLDOUT FRAME 2

PRECEDING PAGE BLANK NOT FILMED

CR 72984

16402-6012-R0-00

## ENGLISH - INTERNATIONAL UNITS CONVERSION

The conversion graphs presented here are to facilitate understanding of the international units used in this report throughout those parts of the materials and process industry in which they have not yet been adopted. The two conversion graphs for pressure can be used for ranges outside those covered by simple power of ten multipliers (e.g., 1.38 $MN/m^2$ can be converted to psi using upper portion of the far left graph which shows 138 $GN/m^2$ is equivalent to 20 Msi. Dividing these numbers by $10^5$ converts 138 $GN/m^2$ to 1.38 $MN/m^2$ and 20 Msi to 200 psi).

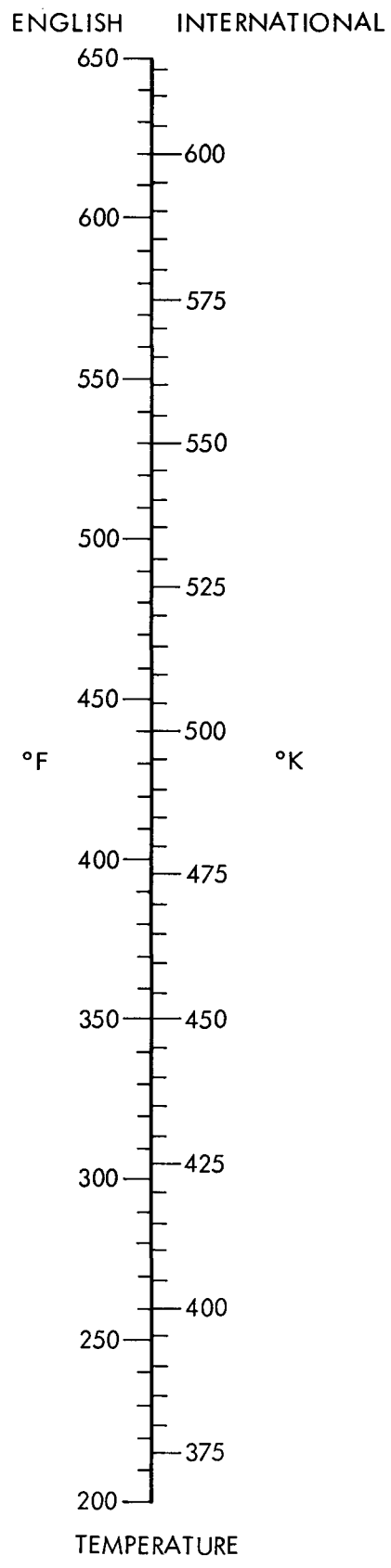


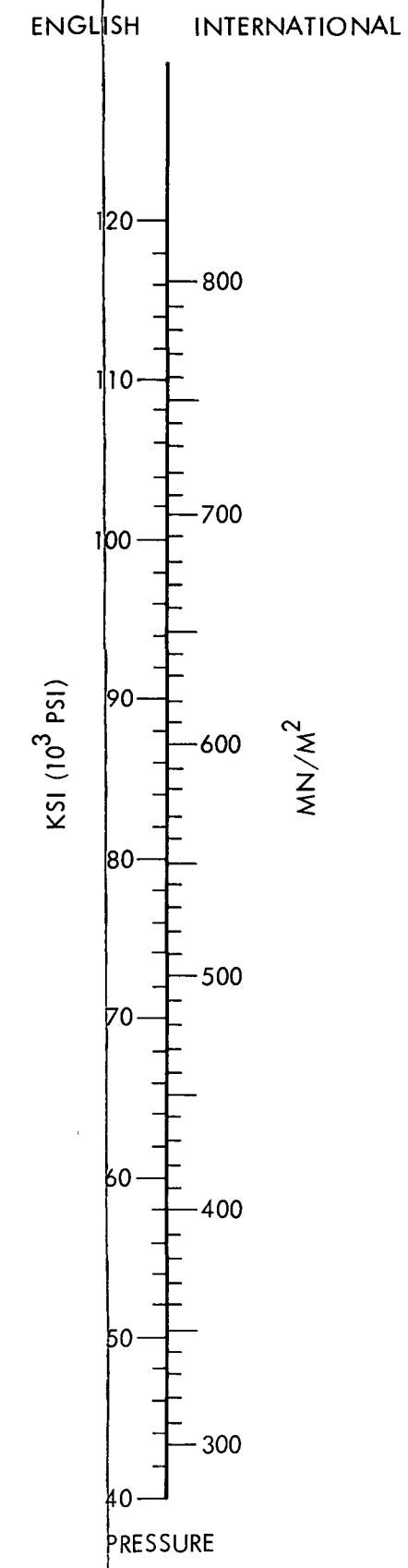


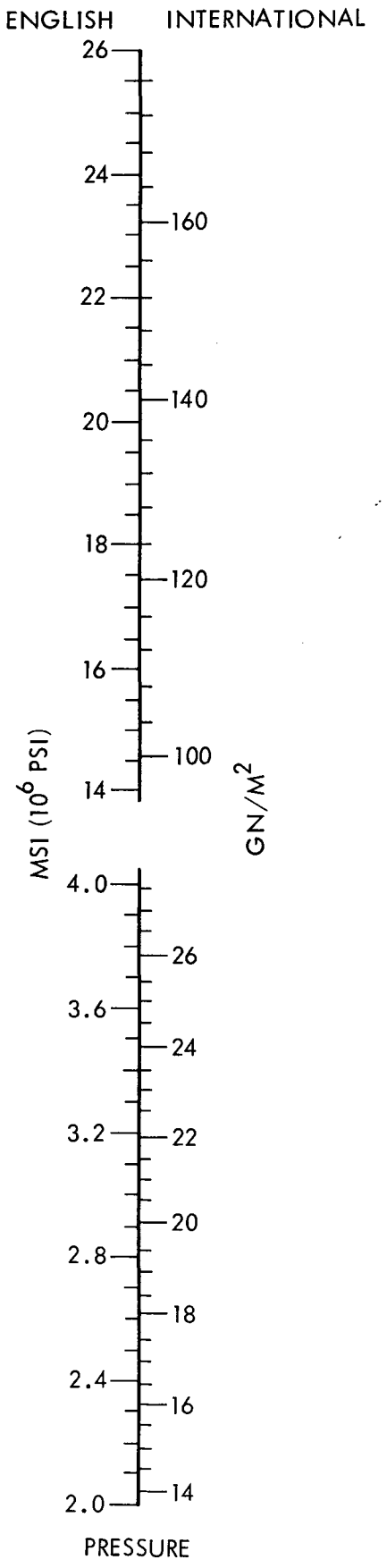

THE FOLLOWING PAGES ARE DUPLICATES OF ILLUSTRATIONS APPEARING ELSEWHERE IN THIS REPORT. THEY HAVE BEEN REPRODUCED BY A DIFFERENT METHOD SO AS TO FURNISH THE BEST POSSIBLE DETAIL TO THE USER.

DISTRIBUTION LIST

| | COPIES |
|---|---|
| National Aeronautics and Space Administration<br>Lewis Research Center<br>21000 Brookpark Road<br>Cleveland, Ohio 44135 | |
| Attn: Contracting Officer, MS 77-3 | 1 |
| Technical Report Control Office, MS 5-5 | 1 |
| Technology Utilization Office MS 3-16 | 1 |
| AFSC Liaison Office, MS 4-1 | 2 |
| Library, MS 60-3 | 2 |
| Office of Reliability & Quality Assurance, MS 500-111 | 1 |
| G. M. Ault MS3-13 | 1 |
| R. H. Kemp MS 49-1 | 1 |
| Polymer Section MS 49-1 | 15 |
| National Aeronautics and Space Administration<br>Washington D.C. 20546 | |
| Attn: RW | 3 |
| National Technical Information Service<br>Springfield, Virginia 22151 | 40 |
| National Aeronautics and Space Administration<br>Ames Research Center<br>Moffett Field, California 94035 | |
| Attn: John Parker | 1 |
| National Aeronautics and Space Administration<br>Flight Research Center<br>P. O. Box 273<br>Edwards, California 93523 | |
| Attn: Library | 1 |
| National Aeronautics and Space Administration<br>Goddard Space Flight Center<br>Greenbelt, Maryland 20771 | |
| Attn: Library | 1 |

| | COPIES |
|---|---|
| National Aeronautics and Space Administration<br>John F. Kennedy Space Center<br>Kennedy Space Center, Florida 32899 | |
| Attn: Library | 1 |
| National Aeronautics and Space Administration<br>Langley Research Center<br>Langley Station<br>Hampton, Virginia 23365 | |
| Attn: V. L. Bell | 1 |
| N. Johnston | 1 |
| National Aeronautics and Space Administration<br>Manned Spacecraft Center<br>Houston, Texas 77001 | |
| Attn: Library | 1 |
| Code EP | 1 |
| National Aeronautics and Space Administration<br>George C. Marshall Space Flight Center<br>Huntsville, Alabama 35812 | |
| Attn: J. Curry | 1 |
| J. Stuckey | 1 |
| Jet Propulsion Laboratory<br>4800 Oak Grove Drive<br>Pasadena, California 91103 | |
| Attn: Library | 1 |
| Office of the Director of Defense<br>Research and Engineering<br>Washington D. C. 20301 | |
| Attn: H. W. Schulz, Office of Assistant Director (Chem. Technology) | 1 |
| Defense Documentation Center<br>Cameron Station<br>Alexandria, Virginia 22314 | 1 |
| Research and Technology Division<br>Bolling Air Force Base<br>Washington D. C. 20332 | |
| Attn: RTNP | 1 |

COPIES

Air Force Materials Laboratory
Wright-Patterson Air Force Base
Dayton, Ohio 45433

| | | |
|---|---|---|
| Attn: | MANP/ R. L. Van Deusen | 1 |
| | MANC/ D. L. Schmidt | 1 |
| | MANC/ T. J. Reinhart | 1 |
| | MANE/ J. K. Sieron | 1 |
| | MAAA/ W. M. Scardino | 1 |

Office of Aerospace Research (RROSP)
1400 Wilson Boulevard
Arlington, Virginia 22209

Attn: Major Thomas Tomaskovic 1

Arnold Engineering Development Center
Air Force Systems Command
Tullahoma, Tennessee 37389

Attn: AEOIM 1

Air Force Systems Command
Andrews Air Force Base
Washington, D. C. 20332

Attn: SCLT/Capt. S. W. Bowen 1

Air Force Rocket Propulsion Laboratory
Edwards, California 93523

Attn: RPM 1

Air Force Flight Test Center
Edwards Air Force Base, California 93523

Attn: FTAT-2 1

Air Force Office of Scientific Research
Washington, D. C. 20333

Attn: SREP, J. F. Masi 1

Commanding Officer 1
U. S. Army Research Office (Durham)
Box GM, Duke Station
Durham, North Carolina 27706

| | COPIES |
|---|---|
| U. S. Army Missile Command<br>Redstone Scientific Information Center<br>Redstone Arsenal, Alabama 35808 | |
| Attn: Chief, Document Section | 1 |
| Bureau of Naval Weapons<br>Department of the Navy<br>Washington, D. C. 20360 | |
| Attn: DLI-3 | 1 |
| Commander<br>U. S. Naval Missile Center<br>Point Mugu, California 93041 | |
| Attn: Technical Library | 1 |
| Commander<br>U. S. Naval Ordnance Test Station<br>China Lake, California 93557 | |
| Attn: Code 45 | 1 |
| Director (Code 6180)<br>U. S. Naval Research Laboratory<br>Washington D. C. 20390 | |
| Attn: H. W. Carhart | 1 |
| Picatinny Arsenal<br>Dover, New Jersey | |
| Attn: SMUPA-VP3 | 1 |
| Aerojet-General Corporation<br>P. O. Box 296<br>Azusa, California 91703 | |
| Attn: Ira Petker | 1 |

COPIES

Aeronautic Division of Philco Corporation
Ford Road
Newport Beach, California 92600

Attn: L. H. Linder, Manager 1
Technical Information Department

Aeroprojects, Inc.
310 East Rosedale Avenue
West Chester, Pennsylvania 19380

Attn: C. D. McKinney 1

Aerospace Corporation
P. O. Box 95085
Los Angeles, California 90045

Attn: Library-Documents 1

Aerotherm Corporation
800 Welch Road
Palo Alto, California 94304

Attn: Roald Rindal 1

Allied Chemical Corporation
General Chemical Division
P. O. Box 405
Morristown, New Jersey 07960

Attn: Security Office 1

American Cyanamid Company
1937 West Main Street
Stamford, Connecticut 06902

Attn: Security Officer 1

ARO, Incorporated
Arnold Engineering Development Center
Arnold Air Force Station, Tennessee 37389

Attn: B. H. Goethert, Chief Scientist 1

Atlantic Research Corporation
Shirley Highway and Edsall Road
Alexandria, Virginia 22314

Attn: Security Office for Library 1

| | COPIES |
|---|---|
| AVCO Corporation<br>Space Systems Division<br>Lowell Ind. Park<br>Lowell, Massachusetts 01851 | |
| Attn: Library | 1 |
| Battelle Memorial Institute<br>505 King Avenue<br>Columbus, Ohio 43201 | |
| Attn: Report Library, Room 6A | 1 |
| Bell Aerosystems, Inc.<br>Box 1<br>Buffalo, New York 14205 | |
| Attn: T. Reinhardt | 1 |
| The Boeing Company<br>Aero Space Division<br>P. O. Box 3707<br>Seattle, Washington 98124 | |
| Attn: Ruth E. Peerenboom (1190) | 1 |
| Celanese Research Company<br>Morris Court<br>Summit, New Jersey | |
| Attn: J. R. Leal | 1 |
| Chemical Propulsion Information Agency<br>Applied Physics Laboratory<br>8621 Georgia Avenue<br>Silver Spring, Maryland 20910 | 1 |
| University of Denver<br>Denver Research Institute<br>P. O. Box 10127<br>Denver, Colorado 80210 | |
| Attn: Security Office | 1 |
| Dow Chemical Company<br>Security Section<br>Box 31<br>Midland, Michigan 48641 | |
| Attn: R. S. Karpiuk, 1710 Building | 1 |

COPIES

E. I. duPont deNemours and Company
Product Development
Industrial Products Division
Fabrics and Finishes Department
Wilmington, Delaware

Attn: J. R. Courtwight 1

Dynamic Science
Division of Marshall Industries
2400 Michelson Drive
Irvine, California 92664

Attn: K. Paciorek
R. Kratzer 1

Esso Research & Engineering Company
Government Research Laboratory
P. O. Box 8
Linden, New Jersey 07036

Attn: J. A. Brown 1

Ethyl Corporation
Research Laboratories
1600 West Eight Mile Road
Ferndale, Michigan 48220

Attn: E. B. Rifkin, Assistant Director
Chemical Research 1

Geigy Industrial Chemicals
Ardsley, New York 10502

Attn: S. Durrel 1

General Dynamics/Astronautics
P. O. Box 1128
San Diego, California 92112

Attn: Library & Information Services (128-00) 1

General Electric Company
Re-Entry Systems Department
P. O. Box 8555
Philadelphia, Pennsylvania 19101

Attn: Library 1

| | COPIES |
|---|---|
| General Electric Company<br>Aircraft Engine Group<br>Cincinnati, Ohio | |
| Attn: M. Grande | 1 |
| General Technologies Corporation<br>708 North West Street<br>Alexandria, Virginia | |
| Attn: H. M. Childers | 1 |
| Hercules Powder Company<br>Allegheny Ballistics laboratory<br>P. O. Box 210<br>Cumberland, Maryland 21501 | |
| Attn: Library | 1 |
| Hughes Aircraft Company<br>Culver City, California | |
| Attn: N. Bilow | 1 |
| Institute for Defense Analyses<br>400 Army-Navy Drive<br>Arlington, Virginia 22202 | |
| Attn: Classified Library | 1 |
| ITT Research Institute<br>Technology Center<br>Chicago, Illinois 60616 | |
| Attn: C. K. Hersh, Chemistry Division | 1 |
| Lockheed-Georgia Company<br>Marietta, Georgia | |
| Attn: W. S. Cremens | 1 |
| Lockheed Missiles & Space Company<br>Propulsion Engineering Division (D.55-11)<br>1111 Lockheed Way<br>Sunnyvale, California 94087 | 1 |
| Lockheed Propulsion Company<br>P. O. Box 111<br>Redlands, California 92374 | |
| Attn: Miss Belle Berlad, Librarian | 1 |

COPIES

McDonnell Douglas Aircraft Company
Santa Monica Division
3000 Ocean Park Boulevard
Santa Monica, California 90406

Attn: J. L. Waisman 1

Minnesota Mining & Manufacturing Company
900 Bush Avenue
St. Paul, Minnesota 55106

Attn: Code 0013 R&D 1
Via: H. C. Zeman, Security Administrator

Monsanto Research Corporation
Dayton Laboratory
Station B, Box 8
Dayton, Ohio 45407

Attn: Library 1

North American Rockwell Corporation
Space & Information Systems Division
12214 Lakewood Boulevard
Downey, California 90242

Attn: Technical Information Center 1
D/096-722 (AJ01)

Northrop Corporate Laboratories
Hawthorne, California 90250

Attn: Library 1

Rocket Research Corporation 1
520 South Portland Street
Seattle, Washington 08108

Rocketdyne, A Division of
North American Rockwell Corporation
6633 Canoga Avenue
Canoga Park, California 91304

Attn: Library, Dept. 596-306 1

Rohm and Haas Company
Redstone Arsenal Research Division
Huntsville, Alabama 35808

Attn: Library 1

| | COPIES |
|---|---|
| Sandia Corporation<br>Livermore Laboratory<br>P. O. Box 969<br>Livermore, California 94551 | |
| Attn: Technical Library (RPT) | 1 |
| Thiokol Chemical Corporation<br>Alpha Division, Huntsville Plant<br>Huntsville, Alabama 35800 | |
| Attn: Technical Director | 1 |
| TRW, Inc.<br>TRW Equipment Laboratories<br>Cleveland, Ohio | |
| Attn: W. E. Winters | 2 |
| United Aircraft Corporation<br>United Aircraft Research Laboratories<br>East Hartford, Connecticut 06118 | |
| Attn: D. A. Scola | 1 |
| United Aircraft Corporation<br>Pratt and Whitney Aircraft<br>East Hartford, Connecticut | |
| Attn: Library | 1 |
| United Aircraft Corporation<br>United Technology Center<br>P. O. Box 358<br>Sunnyvale, California 94088 | |
| Attn: Library | 1 |
| Westinghouse Electric Corporation<br>Westinghouse Research Laboratories<br>Pittsburgh, Pennsylvania | |
| Attn: Library | 1 |
| Whittaker Corporation<br>Research & Development/San Diego<br>3540 Aero Court<br>San Diego, California 92123 | |
| Attn: R. Gosnell | 1 |